



<https://theses.gla.ac.uk/>

Theses Digitisation:

<https://www.gla.ac.uk/myglasgow/research/enlighten/theses/digitisation/>

This is a digitised version of the original print thesis.

Copyright and moral rights for this work are retained by the author

A copy can be downloaded for personal non-commercial research or study, without prior permission or charge

This work cannot be reproduced or quoted extensively from without first obtaining permission in writing from the author

The content must not be changed in any way or sold commercially in any format or medium without the formal permission of the author

When referring to this work, full bibliographic details including the author, title, awarding institution and date of the thesis must be given

Enlighten: Theses

<https://theses.gla.ac.uk/>
research-enlighten@glasgow.ac.uk

STUDIES ON CYCLIC AMP PHOSPHODIESTERASES

**A thesis submitted to the University of Glasgow
for the degree of Doctor of Philosophy in
the Faculty of Science**

by

SUAT ERDOGAN BVSc, MSc

**Division of Biochemistry and Molecular Biology
Institute of Biomedical and Life Science (IBLS)
University of Glasgow**

August 1997

© Suat Erdogan

ProQuest Number: 10391366

All rights reserved

INFORMATION TO ALL USERS

The quality of this reproduction is dependent upon the quality of the copy submitted.

In the unlikely event that the author did not send a complete manuscript and there are missing pages, these will be noted. Also, if material had to be removed, a note will indicate the deletion.



ProQuest 10391366

Published by ProQuest LLC (2017). Copyright of the Dissertation is held by the Author.

All rights reserved.

This work is protected against unauthorized copying under Title 17, United States Code
Microform Edition © ProQuest LLC.

ProQuest LLC.
789 East Eisenhower Parkway
P.O. Box 1346
Ann Arbor, MI 48106 – 1346

GLASGOW
UNIVERSITY
LIBRARY

Kenis 11051 (copy 2)

GLASGOW UNIVERSITY
LIBRARY

*This thesis is dedicated to
my parents*

CONTENTS

	Page
List of Tables	viii
List of Figures	ix
List of Abbreviations	xiii
Acknowledgements	xvi
Abstract	xvii
CHAPTER 1	
INTRODUCTION	1-54
1 Introduction	1
1.1 Adenosine-3',5'-cyclic monophosphate (cAMP) signalling	2
1.1.2 Generation of cAMP	2
1.1.3 G-proteins	4
1.1.4 Adenylate cyclases	5
1.1.5 cAMP-dependent protein kinase	8
1.1.6 Protein kinase A anchoring proteins	9
1.1.7 The nuclear response to cAMP	10
1.2 The effects of cAMP in the immune system	11
1.3 The effects of cAMP in various systems	14
1.3.1 cAMP in the central nervous system (CNS)	14
1.3.2 cAMP in platelets	14
1.3.3 cAMP in the heart	15
1.3.4 cAMP in smooth muscle	15
1.3.5 cAMP as a hormonal second messenger	16
1.4 Degradation of cAMP	17
1.5 Cyclic nucleotide phosphodiesterases (PDEs)	17
1.5.1 Nomenclature	20
1.5.2 Primary structure of PDEs	20
1.5.3 PDE1: Ca ²⁺ / calmodulin-stimulated PDEs	22
1.5.4 PDE2: cyclic GMP-stimulated PDEs (cGS-PDE)	25
1.5.6 PDE3: cyclic GMP-inhibited PDEs (cGI-PDE)	27
1.5.7 PDE4: cyclic AMP-specific PDEs (cAMP PDE)	30
1.5.7.1 Background	30

1.5.7.2	Molecular cloning of PDE4 isoforms	32
1.5.7.3	The structural features of the PDE4 isoforms	32
1.5.7.4	PDE4A	36
1.5.7.5	PDE4B	41
1.5.7.6	PDE4C	43
1.5.7.7	PDE4D	44
1.5.7.8	Regulation of PDE4 enzymes	45
1.5.7.9	Phosphorylation of PDE4 isoforms	45
1.5.7.10	Regulation of PDE4 expression	46
1.5.7.11	Regulation of PDE4 by phosphatidic acid	47
1.5.7.12	Interaction of PDE4 with SH3 domains	48
1.5.7.13	Therapeutic role of PDE4 inhibitors	49
1.5.8	PDE5: cyclic GMP-specific PDEs (cGMP PDE)	50
1.5.9	PDE6: photoreceptor PDEs	52
1.5.10	PDE7: cAMP-specific rolipram-insensitive PDEs	53

CHAPTER 2

MATERIAL AND METHODS 55-86

2.1	Materials	56
2.1.1	Radiochemicals	56
2.1.2	Tissue culture plastic ware	56
2.1.3	Tissue culture medium	56
2.1.4	General reagents	57
2.1.4.1	Chemical compounds	57
2.1.4.2	Biochemical reagents	58
2.1.5	Molecular Biology reagents	60
2.1.6	Equipment	60
2.1.7	Cell lines	61
2.1.7.1	COS7 cells	61
2.1.7.2	Human leukaemic T-cell line Jurkat (J6)	61
2.2	Methods	62
2.2.1	Treatment of Jurkat T-cells with vehicles	62
2.2.1.1	Determination of cell number and viability	62
2.2.1.2	Cell lysis and homogenisation of Jurkat T-cells	63
2.2.2	Antibody preparation	64
2.2.3	SDS-PAGE electrophoresis	64

2.2.4	Western blotting	65
2.2.5	Cyclic AMP phosphodiesterase assay	66
2.2.5.1	Preparation of reagents	68
2.2.5.2	Assay procedure	69
2.2.5.3	Calculation of specific activities	69
2.2.6	Determination of kinetic constants	70
2.2.7	Determination of IC ₅₀ values	70
2.2.8	Relative V _{max} determinations	71
2.2.9	Cyclic AMP determination	71
2.2.9.1	Assay principle	71
2.2.9.2	Preparation of cyclic AMP binding protein	72
2.2.9.3	Assessing intracellular cAMP concentrations	72
2.2.9.4	Preparation of reagents for assay	73
2.2.9.5	Assay procedure	73
2.2.10	Protein determination	74
2.2.11	Immunoprecipitation	75
2.2.12	Expression of the PDE cDNAs in COS7 cells	75
2.2.12.1	DEAE dextran method of transient transfection	75
2.2.12.2	Disruption of transfected COS7 cells	76
2.2.12.3	Subcellular fractionation	76
2.2.12.4	Treatment of membranes with high salt concentration	77
2.2.12.5	Solubilisation of membranes with Triton X-100	77
2.2.13	Lactate dehydrogenase assay	77
2.2.14	Precipitation of oligonucleotides	78
2.2.14.1	Quantitation of oligonucleotides	78
2.2.15	RNA extraction by Tri-Reagent	79
2.2.15.1	Determination of RNA concentration	80
2.2.16	First-strand cDNA synthesis	80
2.2.17	The Polymerase Chain Reaction (PCR)	80
2.2.18	Agarose gel electrophoresis	81
2.2.19	Purification of DNA from PCR products	81
2.2.20	Competent cell preparation	82
2.2.21	Transformation of plasmid vector into competent cells	83
2.2.22	Storage of E. coli cells	83
2.2.23	Plasmid DNA purification	83
2.2.24	Estimation of DNA concentration	84
2.2.25	Storage of plasmid DNA	85
2.2.26	Analysis of data and statistics	85

CHAPTER 3
INVESTIGATION OF THE EFFECT OF cAMP
ELEVATING AGENTS ON PHOSPHODIESTERASE
ACTIVITIES IN HUMAN JURKAT T-CELLS **87-147**

3.1	Introduction	88
3.1.1	Aim of the study	93
3.2	Results	93
3.2.1	Characterisation of the phosphodiesterase isoforms of Jurkat T-cells	93
3.2.2	Effect of cyclic AMP-elevating agents on phosphodiesterases of Jurkat T-cells	97
3.2.3.	Determination of PDE4 subtype gene expressions and the effect of elevated cyclic AMP	102
3.3	Conclusions and Discussion	107

CHAPTER 4
CHARACTERISATION OF FIVE HUMAN PDE4D
ISOFORMS **148-195**

4.1	Introduction	149
4.1.1	Aim of the study	151
4.2	Results	151
4.2.1	Expression and subcellular distribution of human PDE4D1, PDE4D2, PDE4D3, PDE4D4 and PDE4D5 cDNAs in COS7 cells	151
4.2.2	Immunological detection of human PDE4D1, PDE4D2, PDE4D3, PDE4D4 and PDE4D5 cDNAs expressed in COS7 cells	152
4.2.3	Solubilisation of particulate fractions of the human PDE4D3, PDE4D4 and PDE4D5 by Triton X-100 and NaCl	154
4.2.4	Kinetics of cAMP hydrolysis by five human PDE4D isoforms	154

4.2.5	Inhibition of particulate and cytosolic forms of the five human PDE4D enzymes by rolipram	156
-------	---	-----

4.3.	Conclusion and Discussion	157
------	---------------------------	-----

CHAPTER 5

ANALYSIS OF CHIMERIC SPECIES FORMED BETWEEN N- AND C-TERMINAL REGION OF INACTIVE HUMAN PDE4A SPLICE VARIANT 2EL	196-217
--	----------------

5.1	Introduction	197
-----	--------------	-----

5.1.2	Aim of the study	200
-------	------------------	-----

5.2.	Results	200
------	---------	-----

5.2.1	Sequence alignments of 2EL, HYB1, HYB2, Delta-1, PDE46 and h6.1	200
-------	---	-----

5.2.2.	Expression and subcellular distribution of HYB1, HYB2, Delta-1 cDNAs in COS7 cells	201
--------	--	-----

5.2.3	Immunological detection of HYB1 and Delta-1	202
-------	---	-----

5.2.4	Transcriptional analysis of HYB1 and HYB2 chimeras	203
-------	--	-----

5.2.5	Kinetics of cAMP hydrolysis by HYB1	203
-------	-------------------------------------	-----

5.2.6	Dose-dependent inhibition of HYB1 by rolipram	204
-------	---	-----

5.3	Conclusion and Discussion	205
-----	---------------------------	-----

CHAPTER 6

FINAL DISCUSSION	218-227
-------------------------	----------------

REFERENCES	228-246
-------------------	----------------

PUBLICATIONS	247
---------------------	------------

LIST OF TABLES

Table 1.1	Cyclic nucleotide phosphodiesterase families and their properties	19
Table 1.2	Properties of PDE4 enzymes expressed in various tissues	37
Table 3.1	Assessment of cAMP phosphodiesterase activities in Jurkat T-cells	111
Table 3.2	The effect of actinomycin D on the increase in Jurkat T-cell PDE3 and PDE4 activities induced upon activation of adenylate cyclase by forskolin and cholera toxin	112
Table 3.3	The enhancement of forskolin-stimulated cAMP accumulation in Jurkat T-cells by PDE inhibitors	113
Table 3.4	Summary of forskolin mediated induction of PDE4 splice variants	114
Table 4.1	cDNA clones corresponding to transcripts from the human PDE4D isoforms	161
Table 4.2	Subcellular distribution of human PDE4D activities, as expressed in COS7 cells	162
Table 4.3	Properties of human PDE4D proteins expressed in COS7 cells	163
Table 4.4	Solubilisation of membrane-associated human PDE4D proteins by detergents or high salt concentrations	164
Table 4.5	K_m values for cAMP for human PDE4D isoforms transfected in COS7 cells	165
Table 4.6	V_{max} values for cAMP for human PDE4D isoforms transfected in COS7 cells	166
Table 4.7	Inhibition of human PDE4D isoforms from COS7 transfected cells by rolipram	167
Table 4.8	Hill coefficients for the inhibition of human PDE4D isoforms by rolipram	168
Table 5.1	The human PDE4A splice variants	208
Table 5.2	Properties of the chimeric PDE4A species HYB1	209

LIST OF FIGURES

Figure 1.1	Diagram illustrating the synthesis of cAMP by adenylate cyclase and its degradation by cAMP phosphodiesterase	3
Figure 1.2	Schematic representation of cyclic nucleotide phosphodiesterases (PDEs)	21
Figure 1.3	Schematic structure of full-length human PDE4 forms	33
Figure 1.4	Sequence alignment of four human PDE4 family enzymes	35
Figure 2.1	The principle of the cyclic AMP phosphodiesterase assay	67
Figure 2.2	Standard curve for a Bradford protein assay	86
Figure 3.1	RT-PCR analysis of PDE1 'generic' transcripts in Jurkat T-cells	115
Figure 3.2	Alignment of PDE1 transcript RT-PCR products from human Jurkat T-cells	116
Figure 3.3	Identification of PDE3 activity in Jurkat T cells: Inhibition by cGMP	117
Figure 3.4	Identification of PDE3 activity in Jurkat T cells: Inhibition by cilostimide	118
Figure 3.5	Identification of PDE2 activity in Jurkat T cells: Inhibition by EHNA	119
Figure 3.6	Identification of PDE4 activity in Jurkat T cells: Inhibition by rolipram	120
Figure 3.7	The effect of forskolin on the accumulation of intracellular cAMP concentrations in Jurkat T-cells	121
Figure 3.8	Time course of total PDE activity in the presence of forskolin	122
Figure 3.9	Time course of cholera toxin activated total PDE activity	123
Figure 3.10	Time course of forskolin activated PDE1 activity	124
Figure 3.11	Time course of forskolin activated PDE2 activity	125
Figure 3.12	Time course of forskolin activated PDE3 activity over first two hours	126
Figure 3.13	Time course of forskolin activated PDE3 activity	127
Figure 3.14	Time course of forskolin activated PDE4 activity	128
Figure 3.15	Time course of cholera toxin activated PDE3 activity	129
Figure 3.16	Time course of cholera toxin activated PDE4 activity	130
Figure 3.17	Total PDE activity in the Jurkat T-cell line upon stimulation with anti-CD3 antibodies	131

Figure 3.18	Time course of total PDE and PDE4 activities in the presence of PHA	132
Figure 3.19	Time course of total PDE and PDE1 activities in the presence of PMA	133
Figure 3.20	Schematic representation of primers used to analyse human PDE4 transcripts by RT-PCR	134
Figure 3.21	RT-PCR analysis of hormone effects on PDE4A 'generic' transcripts in Jurkat T-cells	135
Figure 3.22	RT-PCR analysis of hormone effects on PDE4D 'generic' transcripts in Jurkat T-cells	136
Figure 3.23	RT-PCR analysis of hormone effects on PDE4B 'generic' transcripts in Jurkat T-cells	137
Figure 3.24	RT-PCR analysis of hormone effects on PDE4C 'generic' transcripts in Jurkat T-cells	138
Figure 3.25	RT-PCR analysis of Jurkat T-cells using PDE4B1, PDE4B2 and PDE4B3 specific primers	139
Figure 3.26	Immunoblot analysis of PDE4A immunoreactivity in Jurkat T-cells	140
Figure 3.27	RT-PCR analysis of Jurkat T-cells using PDE46 specific primers	141
Figure 3.28	RT-PCR analysis of Jurkat T-cells using PDE4D3 specific primers	142
Figure 3.29	RT-PCR analysis of Jurkat T-cells using PDE4D4 specific primers	143
Figure 3.30	RT-PCR analysis of Jurkat T-cells using PDE4D5 specific primers	144
Figure 3.31	RT-PCR analysis of Jurkat T-cells using PDE4D1 specific primers	145
Figure 3.32	RT-PCR analysis of Jurkat T-cells using PDE4D1/2 specific primers	146
Figure 3.33	Immunoblot analysis of PDE4D immunoreactivity in Jurkat T-cells	147
Figure 4.1	Alignment of the amino acid sequences of the human PDE4D isoforms	169
Figure 4.2	Linearity of detection of various cytosolic PDE4D proteins	170
Figure 4.3	Linearity of detection of various membrane PDE4D proteins	171

Figure 4.4	Immunoblotting of COS7 cells transfected with the cDNA for human PDE4D1	172
Figure 4.5	Immunoblotting of COS7 cells transfected with the cDNA for human PDE4D2	173
Figure 4.6	Immunoblotting of COS7 cells transfected with the cDNA for human PDE4D3	174
Figure 4.7	Immunoblotting of COS7 cells transfected with the cDNA for human PDE4D4	175
Figure 4.8	Immunoblotting of COS7 cells transfected with the cDNA for human PDE4D5	176
Figure 4.9	Solubilisation of human PDE4D5 protein from membranes using high salt and non-ionic detergent treatments	177
Figure 4.10	Solubilisation of human PDE4D3 protein from membranes using high salt and non-ionic detergent treatments	178
Figure 4.11	Solubilisation of human PDE4D4 protein from membranes using high salt and non-ionic detergent treatments	179
Figure 4.12	Effect of cAMP concentration on the velocity of soluble hPDE4D1 activity	180
Figure 4.13	Effect of cAMP concentration on the velocity of soluble hPDE4D2 activity	181
Figure 4.14	Effect of cAMP concentration on the velocity of soluble hPDE4D3 activity	182
Figure 4.15	Effect of cAMP concentration on the velocity of soluble hPDE4D4 activity	183
Figure 4.16	Effect of cAMP concentration on the velocity of soluble hPDE4D5 activity	184
Figure 4.17	Effect of cAMP concentration on the velocity of particulate hPDE4D3 activity	185
Figure 4.18	Effect of cAMP concentration on the velocity of particulate hPDE4D4 activity	186
Figure 4.19	Effect of cAMP concentration on the velocity of particulate hPDE4D5 activity	187
Figure 4.20	Dose-dependent inhibition of soluble hPDE4D1 activity by rolipram	188
Figure 4.21	Dose-dependent inhibition of soluble hPDE4D2 activity by rolipram	189

Figure 4.22	Dose-response curve for the inhibition of soluble hPDE4D3 activity by rolipram	190
Figure 4.23	Dose-response curve for the inhibition of soluble hPDE4D4 activity by rolipram	191
Figure 4.24	Dose-response curve for the inhibition of soluble hPDE4D5 activity by rolipram	192
Figure 4.25	Dose-response curve for the inhibition of particulate hPDE4D3 activity by rolipram	193
Figure 4.26	Dose-response curve for the inhibition of particulate hPDE4D4 activity by rolipram	194
Figure 4.27	Dose-response curve for the inhibition of particulate hPDE4D5 activity by rolipram	195
Figure 5.1	Alignment of the amino acid sequences of PDE46, h6.1, 2EL, HYB1, HYB2 and Delta-1	210
Figure 5.2	Schematic representation of human PDE4A forms, HYB1 and HYB2 chimeras and Delta-1 truncated forms	211
Figure 5.3	Immunoblot of HYB1 and Delta-1 expressed in COS7 cells	212
Figure 5.4	Transcriptional analysis of HYB1 chimera by RT-PCR	213
Figure 5.5	Transcriptional analysis of HYB2 chimera by RT-PCR	214
Figure 5.6	Determination of K_m for the cytosolic HYB1 fraction	215
Figure 5.7	Linearity of detection of various concentrations of cytosolic h6.1 and HYB1	216
Figure 5.8	Dose-response curve for the inhibition of cytosolic HYB1 activity by rolipram	217

LIST OF ABBREVIATIONS

A ₂₆₀	absorbance at 260 nm
AKAP	PKA anchor proteins
ATF	activation transcription factor
ATP	adenosine triphosphate
BSA	bovine serum albumin
[Ca ²⁺] _i	intracellular calcium concentration
°C	degrees celcius
CaM	calmodulin
CaMPK	calmodulin-dependent protein kinase
cAMP	adenosine-3',5'-cyclic monophosphate
CAT	chloramphenicol acetyl transferase
cDNA	complementary deoxyribonucleic acid
cGMP	guanosine-3',5'-cyclic monophosphate
CHO	chinese hamster ovary cell line
Cilostimide	[4,5-dihydro-6[4-(1H-imadazol-1-yl)phenyl]-5-methyl 3(2H)-pyrazone]
C-terminal	carboxy-terminal of a protein
CRE	cAMP response element
CREB	cAMP response element binding protein
CREM	cAMP response element modulator
DMSO	dimethyl sulphoxide
DNA	deoxyribonucleic acid
DTT	dithiothreitol
EDTA	ethylenediaminetetra-acetic acid
EGTA	ethylene glycolbis(β-aminoethylether)-N,N,N',N'- tetra-acetic acid
EHNA	erythro-9-(2-hydroxy-3-nonyl)-adenine
ERK	Extracellular signal regulated kinase
FBS	foetal bovine serum
FSH	follicle stimulating hormone
GDP	guanosine diphosphate
g	gram
g _{av}	average gravitational force
G _i	inhibitory G-protein to adenylate cyclase activity
G _s	stimulatory G-protein to adenylate cyclase activity
G-protein	GTP binding protein
GST	glutathione S-transferase

GTP	guanine trisphosphate
h6.1	human PDE4A
h	hour
Hepes	N-2-Hydroxyethylpiperazine-N'-2-ethane-sulphonic acid
IBMX	1-isobutylmethyl-3-xanthine
IC ₅₀	concentration at which 50 % inhibition ensues
IL	interleukin
kDa	kilodaltons
K _m	Michaelis constant, equal to the substrate concentration at which the reaction rate is half the maximum value
LH1/2	Linker Region 1/2
MAPK	mitogen-activated protein kinase
Milrinone	[1,6-Dihydro-2-methyl-6-oxo-(3,4'-bipyridine)-5-carbonitrile]
mg	milligram
min	minute
ml	millilitre
NF-AT	nuclear factor of activated T cells
N-terminus	amino terminus of protein
PAGE	polyacrylamide gel electrophoresis
PBS	phosphate buffered saline
PCR	polymerase chain reaction
PDE	phosphodiesterase
pH	$-\log_{10}[\text{H}^+]$
PHA	phytohaemagglutinin
PI3K	phosphatidylinositol-3'-kinase
PKA	protein kinase A
PKC	protein kinase C
PKG	cGMP dependent protein kinase
PMA	phorbol-12-myristate, 13-acetate
PMSF	phenylmethylsulphonyl fluoride
PTK	protein tyrosine kinase
RD1	rat <i>dunce</i> -like 1 (PDE4A)
RNA	ribonucleic acid
Ro 20-1724	[4-(Butoxy-4-methoxybenzyl)-2-imidazolidinone]
Rolipram	[4-{3-(cyclopentoxyl)-4-methoxyphenyl}-2-pyrrolidone]
RT-PCR	reverse transcriptase-polymerase chain reaction
s	second
SD	standard deviation
SDS	sodium dodecyl sulphate

SH2/3	Src homology domain 2/3
TBS	Tris buffered saline
TCR	T cell antigen receptor
TEA	triethanolamine
TEMED	N,N,N',N'-tetramethylethylene diamine
TPA	12-O-tetradecanoylphorbol 13-acetate
Tris	Tris(hydroxymethyl)methylamine
TNF α	tumor necrosis factor-alpha
TSH	thyroid stimulating hormone
V	volts
V_{\max}	maximum reaction rate
UCR1/2	Upstream Conserved Region 1/2

ACKNOWLEDGEMENTS

I would like to express my sincere thanks to my supervisors, Professor Miles Houslay and Dr. Margaret Harnett, for their generous support, understanding, patience and friendly supervision throughout the course of this study and for their constructive comments and criticism in the preparation of this thesis. I am grateful to Professors Gordon Lindsay and Charles Fewson for allowing me to work in the the Division of Biochemistry and Molecular Biology for the use of their facilities throughout my period of study. Many thanks also to The Mustafa Kemal University in Turkey for financial support, without their help this study would never have been possible.

I am indebted to all the members of the 'Gardiner Lab' who have helped me in any way during my PhD.

My appreciation is also extended to Drs. Sandra Spence and Moira Wilson for their friendship and giving up their valuable time to read this thesis.

I am grateful to the Medical Illustrations Unit for the preparation of a poster demonstration and slides used for presentations.

I am totally indebted to my wife Dr. Zeynep Erdogan for her support and tolerance and my two sons Emre (<1) and F. Mert (3¹/₂) who both were born during this study.

My final thanks go to my parents, brother and sisters in Turkey for their moral support and understanding over the past three years.

ABSTRACT

The second messenger cyclic AMP plays a pivotal role in the control of cell function through the transduction of extracellular signals into intracellular activation. However, this cyclic nucleotide negatively modulates the synthesis and release of inflammatory mediators and the proliferation of lymphocytes. The sole mechanism for degradation of cAMP is achieved through the action of cyclic AMP phosphodiesterases (PDEs). This activity is provided by a multigene family which produces a variety of enzymes. The PDE4 isoforms appear to be the predominant cAMP-metabolising enzymes in essentially all pro-inflammatory and immune cells implicated in the pathogenesis of asthma, arthritis and atopic dermatitis. With respect to the development of novel drugs to treat such diseases, an understanding of the regulation and the function of PDE4 enzymes has been identified as crucial.

In this thesis, three different, but related, studies were carried out. The first study was an investigation of the expression and the regulation of cAMP phosphodiesterases in human Jurkat T lymphocytes. In the second study, the properties of the proteins encoded by five different mRNA transcripts from the human PDE4D gene were analysed after transient expression in COS7 cells. These included the PDE4D1 and PDE4D2 forms which I had shown to become induced in Jurkat T-cells with chronically elevated cAMP levels. Finally, the role of the N- and C-terminal regions of the inactive human PDE4A splice variant, 2EL originally cloned from a Jurkat T-cell library, was investigated.

The Jurkat T-cell PDE activity was determined using selective PDE activators and inhibitors. Although a small amount of PDE1, PDE2 and PDE7 enzymes were present, PDE3 and PDE4 enzymes were shown to provide the major Jurkat T-cell PDE activity. Chronic elevation of intracellular cAMP levels achieved either by direct stimulation of adenylate cyclase or via stimulation of G_s or using a cell-

permanent cAMP analogue increased PDE3 and PDE4 activities but did not affect PDE1, PDE2 and PDE7 activities. Despite the fact that the major PDE activity in quiescent Jurkat T-cells was contributed by PDE3 enzymes, PDE4 activity appeared to play a key role in the control of intracellular cAMP levels. Analyses done using RT-PCR and immunoblotting demonstrated that forskolin-elevated intracellular cAMP levels induced the 'short' form of PDE4D isoforms, PDE4D1 and PDE4D2, but did not induce any other PDE4 isoforms. However, chronic elevation of cAMP levels also led to the down-regulation of the novel 118 kDa PDE4A species found in resting Jurkat T-cells.

The two human 'short' forms (PDE4D1 and PDE4D2) and the three 'long' forms (PDE4D3, PDE4D4 and PDE4D5) of human PDE4D isoforms were transiently expressed in COS7 cells. The 'short' PDE4D forms exhibited similar properties and were exclusively expressed in cytosol. In contrast, the 'long' forms showed different enzyme kinetics and were found in both particulate and cytosol fractions. It was suggested that the unique N-terminal regions of the PDE4D3, PDE4D4 and PDE4D5 proteins, which are derived from alternatively spliced regions of their mRNAs, are important in determining their enzyme activity, inhibitor sensitivity and subcellular localisation.

The inactive human PDE4A species 2EL was cloned from resting Jurkat T-cells. However, it was not known that the inactivity is due to the premature truncation of either N- or C-terminal putative catalytic domain. This was investigated using chimeras and truncated PDE forms. It was shown that the C-terminal premature truncation terminates the 2EL's catalytic activity.

CHAPTER 1

INTRODUCTION

1. Introduction

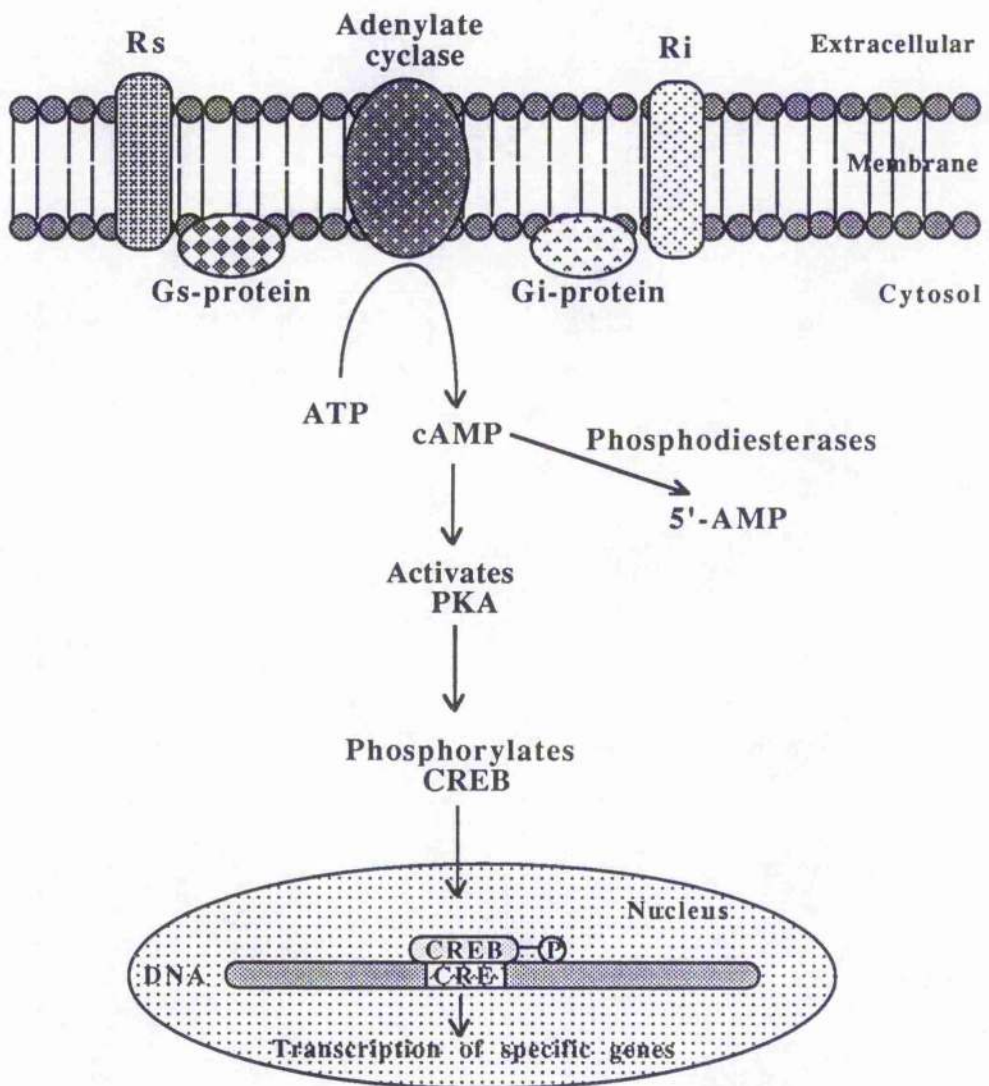
1.1. Adenosine-3',5'-cyclic monophosphate (cAMP) signalling

The second messenger cAMP is an important mediator which is found ubiquitously in mammalian cells. The interaction between various extracellular ligands such as hormones, growth factors, cytokines and neurotransmitters with their cell surface receptors can lead to the activation of plasma membrane bound adenylate cyclase (Macphee et al., 1988, Manganiello, et al., 1995). This activation of adenylate cyclase is mediated by the action of the stimulatory GTP-binding protein (G-proteins) called G_s . Various other receptors can cause inhibition of adenylate cyclase through the inhibitory G_i G-proteins (Milligan & Green, 1991). Adenylate cyclase catalyses the conversion of intracellular ATP to cAMP (Sutherland et al., 1968). cAMP mediates many important physiological responses and metabolic processes such as exocytosis, platelet aggregation and neurotransmission (Bourne et al., 1974, Omburo et al., 1997), for example, as well as having long term effects on key processes such as cell growth and differentiation (Kammer, 1988). These actions are all mediated by cAMP-dependent protein kinase A (PKA), which serves to phosphorylate key target proteins and thus alter their functioning (Scott, 1991, Houslay et al., 1995). Intracellular cAMP homeostasis is maintained not only by regulating its synthesis by adenylate cyclase (Taussig & Gilman, 1995), but also by control of its degradation through the action of the cyclic nucleotide phosphodiesterases (PDEs) (Houslay & Kilgour, 1990, Beavo, 1995, Conti et al., 1995b) (Figure 1.1).

1.1.2. Generation of cAMP

The receptor-adenylate cyclase complex consist of three components: the receptor, G-protein and the catalytic subunit of the adenylate cyclase (Figure 1.1). The binding of an effector to a cell surface receptor leads to the formation of an active conformation of the effector-receptor complex.

Figure 1.1. Diagram illustrating the synthesis of cAMP by adenylate cyclase and its degradation by cAMP phosphodiesterase



This complex catalytically activates the heterotrimeric GTP-binding proteins (G-proteins) by accelerating the exchange of bound GDP with GTP. The GTP-bound G-protein α -subunit then interacts with adenylate cyclase, either leading to its activation, in the case of G_s , or inhibition, in the case of G_i . Inactivation of the G-protein results from the hydrolysis of the bound GTP to GDP by the intrinsic GTPase activity of the α -subunit. The reactivation of the G-protein requires a further replacement of GDP by GTP. Thus, the level of adenylate cyclase activity depends on the distribution between active and inactive G-protein units, which is, in turn, regulated by the relative rates of activation and inactivation of receptor through association-dissociation of agonist.

1.1.3. *G-proteins*

All of the G-protein-coupled receptors consist of a single polypeptide chain with seven putative transmembrane domains. Upon agonist binding to the receptor, it is thought that the conformation of receptor changes, allowing the association of the G-protein with cytoplasmic regions of the receptor. Heterotrimeric G-proteins are a group of membrane-associated proteins that bind GTP with high affinity (Neer, 1995). Each G-protein consists of three subunits called α , β and γ and such G-proteins are generally defined on the molecular identity of the α -subunit within the heterotrimer (Gilman, 1987, Milligan, 1995). In the complex, the α -subunit binds and hydrolyses GTP and the $\beta\gamma$ -dimer serves as a functional monomer, in part by anchoring the α -subunit to the membrane. To date, about twenty α -subunits, five β -subunits and twelve γ -subunits have been demonstrated (Milligan, 1995).

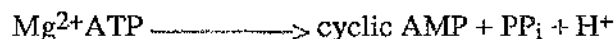
In the resting state, the α , β and γ -subunits are complexed together with GDP bound to the α -subunit. Receptor activation results in the activation of the G-protein complex and release of the GDP from the α -subunit, which is in turn replaced by GTP. Upon binding GTP, the α -subunit dissociates from the $\beta\gamma$ -dimer and diffuses along the inner surface of the plasma membrane and couples

with an effector molecule such as adenylate cyclase (Gilman, 1984). This active state is 'switched off' via the GTP hydrolysing activity of the α -subunit. Once inactivated the α -subunit reassociates with the $\beta\gamma$ -dimer and the complex returns to its resting state (Casey & Gilman, 1988, Houslay, 1992).

Inhibition of adenylate cyclase by G-inhibitory (G_i) family of G-proteins is less well understood. G_i is a guanine-nucleotide binding protein(s) defined originally by its ability to mediate inhibition of adenylate cyclase by agonists and other agents (Katada et al., 1984). Three forms of G_i -proteins have now been cloned, G_i -1, G_i -2 and G_i -3 (Milligan & Green, 1991), all of which are subjected to ADP-ribosylation by pertussis toxin which prevents coupling of α_i to appropriate inhibitory receptors. Current theories suggest that G_i can inhibit adenylate cyclase in two ways. One involves the release of $\beta\gamma$ from G_i attenuating G_s dissociation and activation by a Mass Activation process. Another suggests a direct inhibition of adenylate cyclase by GTP-bound $G_{i\alpha}$. However, modulation is likely to depend upon adenylate cyclase isoform and G_i isoforms present in cells.

1.1.4. Adenylate cyclases

Adenylate cyclases (EC 4.6.1.1) are a group of enzymes that are responsible for the synthesis of cAMP from intracellular ATP (Figure 1.1). The reaction catalysed by this enzyme can be represented by :



Their activity is controlled dynamically by a variety of hormones, neurotransmitters and other regulatory molecules. At least eight genetically distinct adenylate cyclase encoding cDNAs have been cloned: six of these (types I-VI) are from mammalian sources, one is from *Drosophila* and one is from *Dictyostelium* (Tang & Gilman, 1992). Their molecular mass ranges from 120 to 165 kDa with a complex topology within the membrane (Cali et al., 1996). Adenylate cyclase consists of a single polypeptide which has a short cytoplasmic N-terminus and is

followed by a six transmembrane spanning region (M1), a large (40 kDa) cytoplasmic domain (C1), and a second set of six transmembrane spans (M2) and finally a second cytoplasmic domain (C2) (Tang & Gilman, 1992). This structure is highly similar to that of certain ion channels and ATP-dependent transporters, particularly the P glycoprotein and cystic fibrosis transmembrane conductance regulator (Taussig & Gilman, 1995). Although, there is little evidence to suggest that various adenylate cyclases may also serve as ion channels or transporters, one interesting observation from studies in *Paramecium* suggest that the adenylate cyclase form expressed there can also serve as a K^+ channel. However, the structure of this one-form is not yet known (Schultz et al., 1992).

Among the different isoforms of adenylate cyclase, the amino acid sequence homology is about 50 % (Tang & Gilman, 1992). However, the two large cytoplasmic loops, $C_{1\alpha}$ and $C_{2\alpha}$, show significant homology (>90 % identity) between family members whereas the two groups of putative transmembrane helices (M_1 and M_2) are quite distinct (Houslay & Milligan, 1997). The cytoplasmic regions of adenylate cyclase provide the active site(s) and their expression allows for the reconstitution of enzyme activity (Sunahara et al., 1996).

All adenylate cyclase isoforms are stimulated by both forskolin and the α -subunit of G_s ($G_{s\alpha}$) and all are inhibited by certain adenosine (P-site inhibitors) analogues. However, it is unclear whether the same is true for a range inhibitory effects upon adenylate cyclase where each enzyme family displays different properties of regulation by Ca^{2+} , PKC, G_i form and $\beta\gamma$ -subunits of G-proteins (Houslay & Milligan, 1997, Milligan, 1995, Taussig & Gilman, 1995). Changes in intracellular Ca^{2+} have profound effects on type I, III and VIII adenylate cyclase activity, being stimulated by nanomolar concentrations of Ca^{2+} / calmodulin, thus causing an increase in intracellular cAMP levels. Although type V and VI activities are inhibited by Ca^{2+} at low micromolar concentrations, these and type II and IV

are insensitive to micromolar concentrations of calmodulin (Pieroni et al., 1993). Indeed inhibition of cAMP production resulting from elevations in Ca^{2+} has been correlated with the expression of type V or type VI adenylate cyclases in some intact cells (Ishikawa et al., 1992, Yoshimura & Cooper, 1992).

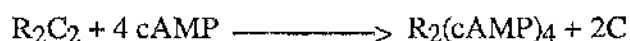
Adenylate cyclase isoforms are differently regulated by $\beta\gamma$ -subunits of G_s -proteins in a type-specific fashion. $\beta\gamma$ -subunits inhibit solely the type I isoform activity. In contrast, $\beta\gamma$ -subunits can synergistically activate type II (Tang & Gilman, 1991) and type IV (Gao & Gilman, 1991) adenylate cyclases; in the presence of $G_{s\alpha}$, activity is enhanced by 5-10-fold (Pieroni et al., 1993). Stimulation of these cyclases requires substantially higher concentrations of $\beta\gamma$ than of $G_{s\alpha}$ and the source of these subunits in physiological states is thought to be derived from G_i or G_o .

The uncoupling of receptors from G_s stimulation appears to be a process that is mediated via receptor phosphorylation rather than G-protein phosphorylation or internalisation. The kinases that are involved in the phosphorylation are PKA and PKC and a variety of receptor-specific kinases that view the agonist-bound forms of receptors as preferential substrates (Houslay, 1992). However, inhibition of adenylate cyclase by PKA-mediated phosphorylation may also provide a key route in specific cell types. Type VI adenylate cyclase is found in S49 lymphoma cells and contains two PKA phosphorylation sites. Phosphorylation of these sites *in vitro* causes inhibition of this enzyme (Premont et al., 1992). PKA phosphorylation of type V also inhibits this enzyme activity as shown in heart (Iwami et al., 1995). In contrast to PKA, PKC phosphorylation stimulates certain types of adenylate cyclases. It has been shown that PKC phosphorylation of the type V enzyme *in vitro* demonstrated a marked increase in enzymatic activity (Kawabe et al., 1994). This effect is specific to the PKC isoforms α and ξ (Jacobowitz et al., 1993). PKC also can stimulate type III

(Jacobowitz et al., 1993). In addition, the inhibition of type II adenylate cyclase activity mediated by G_i , has been noted to be suppressed by phorbol ester treatment (Chen & Iyengar, 1993).

1.1.5. cAMP-dependent protein kinase

The intracellular receptor system for cAMP is provided by cAMP-dependent protein kinase (PKA). This has been shown to be the only protein, apart from the PDEs, that binds cAMP with high affinity in eukaryotic cells. PKA exists as a tetrameric conformation and comprises a family of enzymes within which each member consists of two regulatory (R) and two catalytic (C) subunits (R_2C_2) which form an inactive holoenzyme (Tang & Gilman, 1992). In the absence of cAMP PKA is tightly regulated and maintained in an inactive state. Activation of PKA is mediated by cAMP binding with a high affinity to the R-subunits, which results in the dissociation of the complex and the release of the free and active monomeric catalytic subunits (Taylor et al., 1990). Activation can be shown by :



Indeed the released and activated catalytic subunits can even migrate from the cytoplasm to the nucleus. These subunits are able to phosphorylate target proteins with target serine residues in the context X-Arg-Arg-X-Ser-X. Such functional motifs are found within a large number of cytoplasmic and nuclear proteins (Lalli & Sassone-Corsi, 1994, Meinkoth et al., 1990).

Two classes of PKA have been identified, type-I and type-II, that differ with respect to their regulatory (R) subunits, as indicated by their different molecular masses, amino acid sequences and affinity for cAMP analogues (Clegg et al., 1988, Oyen et al., 1989). Type-I holoenzymes were originally classified by the presence of a high affinity binding site for $Mg^{2+}ATP$ in the regulatory subunit (RI) (Taylor et al., 1990). Type-II were distinguished by autophosphorylation of the

regulatory subunits (RII) (Taylor et al., 1990). Isoforms of RI (α and β) and RII (α and β) subunits, as well as the catalytic (C) (α , β and γ) subunit have also been isolated. These species all differ in their subcellular and tissue distribution. Thus RI α is expressed in most tissues, whereas the RI β is a tissue-specific isoform (Clegg et al., 1988). RII α is found in a wide variety of cells, however, RII β is expressed in only certain restricted cells (Luo et al., 1990). Intracellular localisation also varies. The RI isoforms are found primarily in the cytosolic compartment of the cell, although a fraction has been found associated with the membranes of erythrocytes (Rubin et al., 1972). In contrast to this, the RII isoforms are generally particulate, with up to 75 % of the cellular RII pool being associated with the plasma membrane and cytoskeletal components, secretory granules or the nuclear membrane (Nigg et al., 1985, Salavatori et al., 1990).

1.1.6. Protein kinase A anchoring proteins

PKA is a multifunctional enzyme with a broad substrate specificity. It has been suggested that hormones and other agents able to increase intracellular cAMP levels may permit a preferential phosphorylation of certain specific target substrates. For such a scenario to occur, different G_s-coupled receptors are presumed to be located at spatially distinct sites on cells together with appropriate adenylate cyclase isoforms, again located at specific regions of the cell surface. The production of cAMP from such sites may produce distinct concentration gradients within the cell. These can be detected by PKA isoforms which must be localised in specific cell areas. Indeed, it has been demonstrated that association of the type-II PKA with the plasma and other membranes is determined by association with members of a large family of anchoring proteins (AKAPs) (Carr et al., 1992, Faux & Scott, 1996). This localisation involves protein-protein interaction between regulatory RII subunits and specific RII-anchoring proteins (Carr et al., 1991). The binding of cAMP to the inactive PKA holoenzyme, much of which is anchored in the perinuclear region of the cytoplasm through

membrane-associated anchoring proteins (Scott & Carr, 1992), releases the active C subunit, which is then competent to phosphorylate substrates.

A number of AKAPs have been demonstrated, each compartmentalising PKA to specific subcellular regions and often showing tissue specific expression (Carr et al., 1993, Carr et al., 1992). Intriguingly, it is now known that at least one anchoring protein binds more than one enzyme at a time. For example, AKAP79 not only binds PKA but also the protein phosphatase, calcineurin (Coghlan et al., 1995), as well as the α and β isoforms of PKC (Klauck et al., 1996). It appears that AKAPs contain at least two functional domains (Faux & Scott, 1996): an enzyme binding site and a targeting site which is responsible for anchoring to subcellular structures such as DNA binding domains (Coghlan et al., 1994) and cytoskeletal binding domains (Glantz et al., 1993). The first 5 amino acids of each RII unit, particularly the isoleucines at positions 3 and 5, are critical for AKAP interaction (Hausken et al., 1994).

1.1.7. The nuclear response to cAMP

The released, active catalytic subunits of PKA can translocate to the nucleus. The nuclear targets for activated PKA are transcription factors which bind to the DNA sequences present in the promoter regions of cAMP-inducible genes (Figure 1.1). Most of these genes contain one or a few cAMP-responsive elements (CREs) (Comb et al., 1986). The consensus CRE is a short palindromic core sequence (5'-TGACGTCA-3') (Montminy et al., 1986) which mediates cAMP-dependent stimulation of transcription. The CRE-binding factors can be divided into activators and repressors. The transcription activation factors are CRE-binding protein (CREB) and different members of the activation transcription (ATF-1) family and CRE-modulator (CREM τ) (Meyer & Habener, 1993, Weng et al., 1993, Yamamoto et al., 1988). The repressors include CREM α , - β and - γ (Laoide et al., 1993).

CREB is a dimeric protein (Gonzalez et al., 1989, Hoeffler et al., 1988) which contains three major structural elements: a DNA-binding domain rich in basic amino acids that recognise the CRE site, a leucine zipper responsible for dimerisation and a highly acidic transactivation region which contains a cluster of potential phosphorylation sites (for PKA, PKC, casein kinase I and II). The two other regions within the transactivation region are now known to be important for the stimulation of transcription by CREB. The first of these is the α peptide which interacts co-operatively with the PKA phosphorylation site and is important for maximal cAMP-dependent induction (Yamamoto et al., 1990). The second subdomain, which is required for full transcriptional activity, lies within the phosphorylation (P-box) region (Lee et al., 1990).

Activated PKA leads to phosphorylation of serine residue 133 of CREB (de Groot & Sassone-Corsi, 1992). This phosphorylation event is thought to activate CREB by inducing a conformational change in the protein which, in turn, allows transcriptional activation from CRE-containing promoters (Gonzalez et al., 1991). Attenuation or inhibition of cAMP-stimulated gene transcription requires dephosphorylation of transcription factors to occur, representing a key mechanism in the negative regulation of CREB activity. It appears that protein phosphatase-2A (PP2A) and PP1 can oppose the action of PKA (Hagawara et al., 1992).

1.2. The effects of cAMP in the immune system

Early researches suggested that cAMP can exert positive modulatory effects on lymphocyte activation (Rochette-Egly & Kempf, 1981, Wang et al., 1978). However, there is now general agreement that cAMP can serve as a negative regulator of mammalian immune system activation and cellular functions. The sustained elevation of cAMP can inhibit platelets responses to agonists including shape change, aggregation, adhesion and release of granule contents (Omburo et

al., 1997). An increased cAMP levels in leukocytes also results in the inhibition of specific differentiated cellular functions such as release of histamine (Bourne et al., 1974). Also *in vitro* studies on neutrophils have shown that elevated intracellular cAMP levels can inhibit superoxide production in response to stimulation with the chemotactic peptide fMLP (Nielson, 1987, Nielson et al., 1990). A similar inhibition was also apparent in eosinophils with a reduction of respiratory burst, lipid mediator production, infiltration and adhesion functions as well as the release of pro-inflammatory mediators having been noted (Souness et al., 1994, Teixeira et al., 1996). Furthermore, enhanced cAMP can suppress synthesis of the pro-inflammatory mediator TNF- α via blocking of the cytokine pathway from human monocytes (Greten et al., 1995) and can also inhibit release of inflammatory mediators histamine and leukotriene C₄ from basophils (Peachell et al., 1992).

cAMP is known to suppress lymphocyte proliferative responses and immune effector functions by acting at early points as well as at more distal steps of the response (Anastassiou et al., 1992, Bourne et al., 1974, Kammer, 1988, Vercammen & Ceuppens, 1987). Intracellular levels of cAMP in such cells have been manipulated using forskolin (a direct activator of adenylate cyclase), cyclic AMP PDE inhibitors and cell permeable cAMP analogues (Erdogan & Houslay, 1997, Kelley et al., 1990, Marcoz et al., 1993b, Novak & Rothenberg, 1990). Additionally, agonists to receptors which are coupled to G_s proteins, such as prostaglandins E₂ or isoproterenol as well as cholera toxin, (which by covalent modification (ADP-ribosylation) activates G_s) have also been used to increase cAMP levels (Alava et al., 1992, Anastassiou et al., 1992, Mary et al., 1989, Wacholtz et al., 1991). The resultant increase in cAMP suppresses various functional indices of T-cell activation including exocytosis (Takayama et al., 1988), proliferation (Krause & Deutsch, 1991, Link et al., 1990), cytokine (IFN γ , IL-2 and IL6) induction (Anastassiou et al., 1992, Snijdwint et al., 1993,

Wacholtz et al., 1991) and expression of CD7 and IL2 receptors (Krause & Deutsch, 1991, Rincon et al., 1988).

Increased cAMP levels also inhibits TCR-coupled early activation events such as PIP₂ breakdown (Alava et al., 1992, Lerner et al., 1988), tyrosine phosphorylation (Anastassiou et al., 1992, Klausner et al., 1987), [Ca²⁺]_i elevations and PKC activation (Chouaib et al., 1987, O'Shea et al., 1987, Paliogianni et al., 1993), raf-1 activation (Whitehurst et al., 1995) and K⁺ conductance (Bastin et al., 1990, Payet & Dupuis, 1992).

The molecular mechanism underlying the late cAMP inhibition of nuclear activation events in T cells is as yet poorly understood. However, in this system, the main target of T cell inhibition by cAMP appears to be at the level of IL-2 production (Anastassiou et al., 1992, Lerner et al., 1988, Paliogianni et al., 1993). It has recently been shown that cAMP inhibits the growth of fibroblasts, adipocytes and muscle cells by activation of PKA. The activation of PKA is believed to inhibit the activation of mitogen-activated protein (MAP) kinase by eliciting the phosphorylation and activation of c-Raf (Cook & McCormick, 1993, Wu et al., 1993). However, other MAP kinase isoforms are resistant to cAMP inhibition because they do not have a PKA phosphorylation site (Hsueh & Lai, 1995). Indeed, cAMP elevations does not inhibit MAPK activation in T-cells, but rather elevated cAMP levels serve to inhibit c-Jun N-terminal kinase (JNK) (Hsueh & Lai, 1995). As T-cell activation, including interleukin-2 gene activation, requires the integration of the Raf-1 and JNK pathways, then a block in either will lead to an inhibitory effect. Indeed, transfection of constructs encoding competitive inhibitors of c-Jun phosphorylation by JNK serves to inhibit IL-2 promoter activation (Su et al., 1994).

1.3. The effects of cAMP in various systems

1.3.1. cAMP in the central nervous system (CNS)

cAMP has major role in the biochemistry of learning, memory and neurotransmission regulation in the central nervous system (CNS) (Byers et al., 1981, Nighorn et al., 1991). Investigations with two invertebrates, sea snail (*Aplysia californica*) and fruit fly (*Drosophila melanogaster*) have demonstrated that cAMP is important in this system. Indeed, numerous genetic mutations have been associated with alterations of the cAMP signalling pathway including *dunce*, which encodes a cAMP-specific PDE and *rutabaga* (*rut*) which encodes a Ca^{2+} / CaM stimulated adenylate cyclase (Dudai, 1988, Levin et al., 1988, Qui et al., 1991). These studies have shown alterations in olfactory learning (Byers et al., 1981) caused by loss of the *dunce* PDE activity (Nighorn et al., 1991). The functional role of cAMP in the mammalian CNS is not well understood yet. However, inhibitors selective for certain cAMP PDEs (PDEs), such as rolipram have clinical activity as antidepressants (Wachtel, 1983). This suggests that cAMP PDEs may play a direct and active role in the biochemistry of learning and memory, by controlling cAMP levels.

1.3.2. cAMP in platelets

Platelets play a central role in thrombosis and homeostasis. The stimulated response of platelets involves adhesion to the vessel wall, secretion of secretory granule components and aggregation. This sequence of events leads to the final platelet plug found in normal homeostatic events and the inappropriate increase in platelet mass in thrombosis. These stimulatory events are dependent on both intra and extra cellular calcium. cAMP itself, and agents which elevate intracellular cAMP levels, inhibit these responses by regulation of the free calcium level in the platelet, or by the control of calcium-dependent reactions which are essential for these responses. It may be considered that platelet responsiveness depends on a

critical balance between agents that alter cytosolic free calcium and cAMP (Beltman et al., 1993, Feinstein et al., 1981). Therefore, an increase in cAMP phosphodiesterase activity may play an important role in the desensitisation of platelets to further exposure to adenylate cyclase agonists.

1.3.3. cAMP in the heart

cAMP has been shown to be crucial in the control of cardiac contraction and diastolic relaxation. The force of contraction in heart muscle is generated by the interaction between two proteins, actin and myosin, which can form cross-bridges. This interaction is regulated by the binding of Ca^{2+} to the protein complex troponin C (Wetzel & Haeufel, 1988). Thus, the developed force ultimately depends on either the increase in intracellular free Ca^{2+} ions or the increase in the calcium sensitivity of the contractile elements or both. The other important positive inotropic agents in the heart is cAMP. cAMP activation of PKA leads to the phosphorylation of cardiac voltage dependent Ca^{2+} channels, resulting in an increase of Ca^{2+} release from the sarcoplasmic reticulum (Schmitz et al., 1987). Indeed it has been shown that both PDE inhibitors and β -adrenergic agents, which elevate intracellular levels of cAMP, are therapeutically useful as positive inotropic agents (Beavo et al., 1994, Schmitz et al., 1987).

1.3.4. cAMP in smooth muscle

The intracellular second messenger cAMP is an important regulator of airway smooth muscle tone and vascular smooth muscle relaxation. Elevation of cAMP levels is associated with agonist-induced relaxation of bovine, canine and guinea pig tracheal smooth muscle (Torphy & Cieslinski, 1989). These actions are mediated by PKA that phosphorylates and consequently alters the activity of physiologically relevant substrates. Several mechanisms have been demonstrated for the inhibitory action of cAMP on smooth muscle contraction. Relaxation of smooth muscle occurs when there is a significant reduction in sarcoplasmic Ca^{2+}

concentrations (Gunts & Stropp, 1988, Scheid et al., 1979) or when there is a suppression of actin-myosin interaction due to phosphorylation of myosin light chain kinase (Adestein et al., 1978). Selective inhibitors of either PDE3 or PDE4 enzymes inhibit the proliferation of rat vascular smooth muscle cells following injury (Polson & Strada, 1996). Inhibition of PDE4 activity in vascular smooth muscle has also implicated in the treatment of pulmonary arterial hypertension (Polson & Strada, 1996). However, the exact role of PDEs in this disorder has not been determined.

1.3.5. cAMP as a hormonal second messenger

cAMP is the important second messenger that mediates the hormonal regulation of blood glucose and fatty acid levels. Lipolysis and glycogenolysis in adipocytes and hepatocytes, respectively are promoted by agents that increase intracellular cAMP levels and are antagonised by agents that decrease intracellular cAMP (Beebe et al., 1985). Stimulation of cAMP PDE activities by insulin (Heyworth et al., 1983, Pyne et al., 1989) contributes to the mechanism by which this hormone can lower cAMP in adipocytes and hepatocytes.

Lipolysis in adipocytes is promoted by hormones such as catecholamines, corticotrophin and glucagon which increase intracellular cAMP levels (Stralfors et al., 1984). Conversely, lipolysis is completely or partially prevented by a number of antilipolytic agents, including insulin which activate PDEs and may also inhibit adenylate cyclase. The precise mechanism(s) of the antiglycogenolytic action of insulin is not well known (see section 1.5.6). Recent studies have demonstrated insulin inhibition of cellular responses and not only suggested a central role for activation of cAMP PDE in the antiglycogenolytic action of insulin but also showed that these actions did not require inhibition of adenylate cyclase (Beebe et al., 1985).

1.4. Degradation of cAMP

The termination of second messenger cAMP is mediated by the heterologous family of enzymes known as the cyclic nucleotide PDEs (Beavo, 1995, Conti et al., 1995b). The degradation of cAMP through the action of PDEs (Figure 1.1) presents a physiological function the modulation of which may usefully be manipulated in the control of disease states. However, it has been established that cAMP is also excreted in substantial quantities in urine in human and animals (Ashman et al., 1963). Renal clearance of cAMP represents about 20 % of total body clearance depending on the species studied (Jard et al., 1975, Murad, 1973) suggesting an active extrusion of cAMP from kidney cells. Indeed, kidney MDCK cells appear to pump out both cAMP and cGMP (Woods & Houslay, 1991). cAMP is also actively extruded from pigeon erythrocytes (Muir & Murray, 1987) and Dictyostelium (Pitt et al., 1992).

1.5. Cyclic nucleotide phosphodiesterases (PDEs)

Cyclic nucleotide phosphodiesterases (PDEs) (EC 3.1.4.17) catalyze the hydrolysis of the 3'-phosphodiester bond of cAMP (Figure 2.1) and cGMP to form 5'-nucleoside monophosphate products (5'-AMP, -GMP respectively) which are unable to activate PKA. Therefore, breakdown of cAMP plays a pivotal role in terminating cAMP signal transduction.

Cyclic nucleotide PDE family isoforms represents a family of enzymes with a wide range of properties that are exemplified by their different sensitivities to specific inhibitors, cofactor requirements, tissue and subcellular distributions, hormonal regulation, phosphorylation by kinases and interaction with other proteins. PDEs can be divided into at least seven identified classes that are categorised on the basis of their primary sequence (Table 1.1). PDE1 enzymes hydrolyse both cAMP and

cGMP and have activities which are stimulated by Ca^{2+} / calmodulin at physiological concentrations (Beltman et al., 1993, Conti et al., 1995b, Wang et al., 1990) (Figure 1.2). PDE2 isoforms similarly hydrolyse both cAMP and cGMP but their activity is stimulated by micromolar concentrations of cGMP (Table 1.1, Figure 1.2). This is because cGMP binds to a distinct regulatory site on the PDE2 enzymes which is found towards the amino-terminus (Beavo, 1995, Pyne et al., 1986, Stroop et al., 1989). PDE3 enzymes specifically hydrolyse cAMP however, in this instance, cGMP can inhibit cAMP hydrolysing activity at lower, micromolar concentrations (Manganiello et al., 1995b) (Table 1.1). PDE4 isoforms are cAMP specific and are insensitive to cGMP and Ca^{2+} / calmodulin (Table 1.1). They are specifically inhibited by the antidepressant drug, rolipram (Beavo, 1995, Bolger, 1994). PDE5 and PDE6 both specifically hydrolyse cGMP but differ in structure and tissue distribution (Table 1.1). Indeed, PDE6 is found only in photoreceptor cells where it plays a pivotal role in visual signal transduction (Beavo, 1995, Pyne et al., 1996). PDE7 isoforms specifically hydrolyse cAMP and are insensitive to inhibition by all known PDE inhibitors including the non-selective PDE inhibitor isobutylmethylxanthine (IBMX) (Manganiello et al., 1995a, Michaeli et al., 1993) (Table 1.1).

Table 1.1. Cyclic nucleotide phosphodiesterase families and their properties

Family	Number of Genes	Regulatory properties	Selective inhibitors IC ₅₀ (μM)	K _m cAMP (μM)	K _m cGMP (μM)	References
PDE1	3	Ca ²⁺ , calmodulin; phosphorylation by PKA, CaM-kinase	nifedipine (1-3) vinpocetine (20)	10-113	1-5	(1, 2, 3)
PDE2	1	stimulated by low (μM) cGMP	EHNA (1-3)	30	15	(4, 5, 6)
PDE3	2	inhibited by low (μM) cGMP; phosphorylation by PKA, insulin activated kinase	cilostimide (0.005) milrinone (0.3) cGMP (0.1)	0.1-0.8	0.1-0.8	(7, 8, 9, 10, 11)
PDE4	4	cAMP specific	rolipram (0.1-5) Ro 20-1724 (1.5) IBMX (15)	1-6	>300	(6, 12, 13, 14, 15)
PDE5	2	cGMP specific phosphorylation by PKG	zaprinast (0.8) dipyridamole (0.9)	>100	4-5	(1, 6)
PDE6	3	cGMP specific	unknown	>100	5-20	(6)
PDE7	1	cAMP specific	unknown	0.2		(16)

1; (Beavo, 1995), 2; (Charbonneau et al., 1986), 3; (Wang et al., 1990), 4; (Mery et al., 1995), 5; (Michie et al., 1996), 6; (Conti et al., 1995b), 7; (Beavo & Reifsnnyder, 1990), 8; (Manganiello et al., 1990), 9; (Manganiello et al., 1995), 10; (Hidaka & Endo, 1984), 11; (Degerman et al., 1996), 12; (Bolger et al., 1993), 13; (Bolger et al., 1996), 14; (Giembycz et al., 1996), 15; (Conti et al., 1995a), 16; (Michaels et al., 1993)

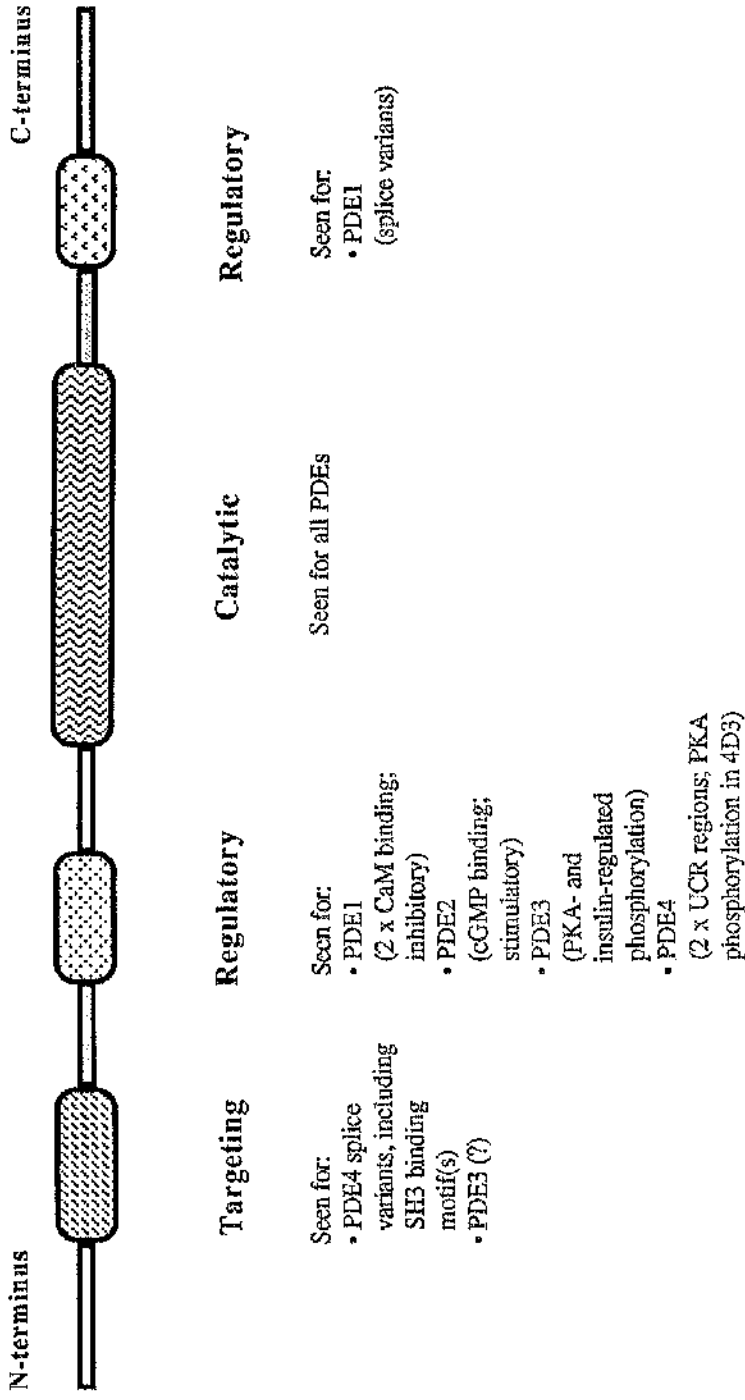
1.5.1. Nomenclature

It has become clear that the PDE superfamily is a large and complex gene family. Initially, PDEs were classified into cGMP and cAMP PDEs simply on the basis of their substrate hydrolysing activities. However, with the realisation that multiple forms of each class existed it was necessary to develop a more sophisticated system. The new classification system is based on both the primary sequence and the way in which the enzymes are regulated (Beavo et al., 1994). The standard nomenclature for describing products of the PDE4 genes is as follows (i) the first two letters represent species (e.g. HS for *homo sapiens*; RN for *rattus norvegicus*), (ii) the designator 'PDE' for cyclic nucleotide phosphodiesterase, (iii) an arabic numeral for the gene family, (iv) a single letter represents individual gene product (A/B/C/D for each of the four PDE4 gene families), (v) an arabic numeral represents splice variant and (vi) a single letter for the report, for example HSPDE4A4B belongs to a homo sapiens PDE, from the PDE4 gene.

1.5.2. Primary structure of PDEs

All mammalian PDEs contain a core of about 300 amino acids that are highly conserved (with ~30 - 40 % amino acid identity) and are likely to make up the catalytic domain of the enzyme (Charbonneau, 1990, Manganiello et al., 1995a). Most of the individual types of PDE have closely related subfamilies. They are products of distinct but highly homologous genes, which give rise to alternatively spliced mRNAs. The amino acid identity of the core catalytic region rises up to 70 - 90 % within a PDE family. Outside the catalytic domain, there is no region of sequence common to all PDEs. However, the members of each class often share additional motifs (Figure 1.3). For example, two highly conserved regions are located in the N-terminal region of the PDE4 proteins which are called UCR1 and UCR2 (Upstream Conserved Region 1 and 2) (Bolger, 1994).

Figure 1.2. Schematic representation of cyclic nucleotide phosphodiesterases (PDEs)



Adapted from Houslay & Milligan (1997)

1.5.3. PDE1: Ca^{2+} / calmodulin-stimulated PDEs (CaM-PDE)

This PDE was first described in bovine and rat brain (Cheung, 1967, Kakiuchi & Yamazaki, 1970). It was shown that PDE1 activity was stimulated by Ca^{2+} in a manner that required a small protein-activator factor (Cheung, 1967, Cheung, 1971, Kakiuchi & Yamazaki, 1970, Kakiuchi et al., 1970). Later, it was demonstrated that the PDE activity which was prepared from bovine heart, was dependent on the presence of both Ca^{2+} and a binding protein (Teo et al., 1973). This activator protein was later named calmodulin (Cheung, 1978). PDE1 appears to be widely distributed in mammalian tissues with the exception of human monocytes (Wang et al., 1990) and rat splenic lymphocytes (Hait & Weiss, 1977).

PDE1 subfamily possesses a great diversity in apparent molecular weight, substrate specificity, tissue distribution, kinetic properties and affinity for calmodulin (Beavo, 1988, Rybalkin & Beavo, 1996, Sharma & Kalra, 1994). Different isoforms were distinguished by direct protein sequencing and cDNA cloning studies (Bentley et al., 1992, Charbonneau et al., 1991). To date, three different genes have been identified in the Ca^{2+} / CaM-stimulated PDE family: PDE1A, PDE1B and PDE1C. Alternative splicing of these genes is believed to lead to production of more than one protein from each locus (Beavo, 1995).

Two splice variants of the *PDE1A* gene, PDE1A1 and PDE1A2, have been isolated from bovine heart and brain, respectively (Sonnenburg et al., 1993, Sonnenburg et al., 1995). Bovine heart PDE1A1 (59 kDa) and bovine brain PDE1A2 (61 kDa) are identical in amino acid sequences apart from their extreme N-termini which contain unique sequences (Beltman et al., 1993, Yan et al., 1996). This suggests that these two isoforms are generated from alternatively spliced genes (Novack et al., 1991, Sonnenburg et al., 1993).

The 63 kDa PDE1B1 was first described in bovine brain and only one mRNA product has been isolated so far (Sharma et al., 1984). The amino acid sequences of PDE1B1 and the 59/61 kDa PDE1A isoforms whilst similar, are not identical (Beavo, 1995, Beltman et al., 1993) thus PDE1B1 is a product of a different but homologous gene (Bentley et al., 1992). PDE1B1 has been cloned from bovine (Bentley et al., 1992), rat (Repaske et al., 1992) and mouse (Polli & Kincaid, 1992) brain cDNA libraries. In the present study is described the derivation of a partial sequence of the human form of PDE1B (see chapter 3) obtained by RT-PCR analyses done on RNA from a human Jurkat T-cell line (Spence et al., 1997). However, recently, the cDNA encoding the complete open reading frame of human PDE1B was cloned from a human leukemic B-cell line (Jiang et al., 1996).

The *PDE1C* gene family is the largest and most diverse of the CaM-stimulated enzymes within the PDE1 family. Five PDE1C isoforms have been identified from human brain and heart, called PDE1C1 and PDE1C3 (Loughney et al., 1996); rat olfactory epithelia, PDE1C2 (Yan et al., 1995); mouse brain and testis, PDE1C4 and PDE1C5 (Yan et al., 1996). The predicted molecular weights of the *PDE1C* gene products are about 75 kDa (Beavo, 1995) which is higher than other PDE1 gene products shown so far. The PDE1C1, PDE1C3, PDE1C4 and PDE1C5 proteins have the same N-termini but different C-termini. However, they differ from the PDE1C2 protein sequence at both the N- and C-terminal regions (Yan et al., 1996). These five distinct types of cDNAs appear to be alternative splice variants of the *PDE1C* gene.

The *PDE1* gene products require both Ca²⁺ and CaM for activity (Table 1.1). Ca²⁺/CaM increases the activity of all of the PDE1s by at least 6 - 20-fold (Wang et al., 1990). However, they show different responses to Ca²⁺ stimulation. Although the PDE1A2 and PDE1B enzymes are encoded by different genes, they have similar affinities for Ca²⁺/CaM, whereas the PDE1A1, which differs from the

PDE1A2 only in the N-terminal region, has a higher affinity for Ca^{2+} (Charbonneau et al., 1991). PDE1C2 also shows more sensitivity to Ca^{2+} stimulation than PDE1C1, PDE1C4 and PDE1C5 isoforms (Yan et al., 1996). This suggests that the different N-terminal region or perhaps the distinct region found in the C-terminus in PDE1C2 are responsible for altering/determining/influencing the Ca^{2+} stimulation. All of the *PDE1C* gene products have similar K_m values and approximately the same maximum velocity (V_{max}) for cAMP and cGMP hydrolysis (Table 1.1) (Yan et al., 1996). PDE1C variants have similar kinetic properties, however, they have higher affinity for both substrates whereas PDE1A and PDE1B hydrolyse cGMP preferentially (Manganiello et al., 1995a, Rybalkin & Beavo, 1996).

It has been shown that at least three of the PDE1 enzymes are regulated *in vitro* by phosphorylation/dephosphorylation (Table 1.1). Both bovine brain PDE1A1 and PDE1A2 are phosphorylated by PKA (Hashimoto et al., 1989, Sharma & Wang, 1985). The 63 kDa PDE1B isoform found in brain can be phosphorylated by Ca^{2+} / CaM dependent kinase II (Hashimoto et al., 1989, Sharma & Wang, 1986, Zhang et al., 1993). Phosphorylation of these enzymes does not alter the catalytic properties, but it does cause a decrease in the affinity of the PDE for calmodulin and requires increased levels of calcium for optimal stimulation of activity (Sharma & Wang, 1985, Sharma & Wang, 1986). Phosphorylation of both enzymes can be blocked by Ca^{2+} / CaM (Sharma & Wang, 1985). Calcineurin, a Ca^{2+} / CaM-sensitive phosphatase, can dephosphorylate these enzymes (Sharma & Wang, 1985, Sharma & Wang, 1986) and this restores the initial CaM affinity and Ca^{2+} sensitivity.

It has been shown that PKC induces PDE1 activity both rapidly and transiently in CHO cells following treatment with PMA (Spence et al., 1995). This is due to the specific production of transcripts from the *PDE1B* gene (Spence et al., 1997).

Such an action appears to be mediated specifically by PKC- α and PKC- ϵ isoforms and identifies a novel PKC isoform-specific effect on cAMP signalling processes.

1.5.4. PDE2: cyclic GMP-stimulated PDEs (cGSPDE)

PDE2 activity was initially described in rat liver supernatant fraction (Beavo et al., 1970) and in the crude particulate fraction of several other rat tissues such as brain (Beavo et al., 1971). This enzyme was purified initially from bovine heart tissues and adrenal glands (Martins et al., 1982) and also from liver (Yamamoto et al., 1983a) as well as having been identified in a number of other tissues and cell types (Erdogan & Houslay, 1997, Michie et al., 1996, Pyne et al., 1986). PDE2 efficiently hydrolyses both cAMP and cGMP with positively co-operative kinetics for cGMP as an effector. cGMP, however, is the preferred substrate and also serves at low concentrations (μM) as an activator of cAMP hydrolysis (Table 1.1) (Manganiello et al., 1990b, Moss et al., 1977) where it can stimulate the hydrolysis of cAMP by ~50-fold (Beavo et al., 1971).

The native cGMP-stimulated PDE2 is a homodimer with apparent molecular mass of ~240 kDa (Martins et al., 1982, Yamamoto et al., 1983a). The purified bovine adrenal and heart tissue PDE2 appears to be composed of a single 105 kDa species (Martins et al., 1982). The first PDE2 to be cloned was from bovine adrenal cortex (Sonnenburg et al., 1991) and then, subsequently, from rat brain (Yang et al., 1994) and liver (Repaske et al., 1993). Two distinct PDE2 splice variants have been described, the PDE2A1 cytosolic isoform identified in bovine heart/adrenal (Martins et al., 1982) and membrane-associated PDE2A2 form identified in liver (Yamamoto et al., 1983a). RNAase protection assays (Sonnenburg et al., 1991) and sequence analysis done on rat brain PDE2 (Epstein et al., 1994) are consistent with generation of soluble, cytosolic and membrane-associated PDE2 isoforms by alternative mRNA splicing. The sequence of these

isoforms show homology to segments of other PDEs. A comparison of this region of homology shows it to be comprised of ~260 residues and is thought to contain the catalytic site (Charbonneau et al., 1986, Sonnenburg et al., 1991).

PDE2 takes the form of a chimeric molecule having two distinct regions forming an allosteric regulatory site and a catalytic domain (Charbonneau et al., 1986). This allosteric domain, which is near to the N-terminal region, consists of about 360 residues that shows similarity to a region found in the retinal rod PDE5 and photoreceptor PDE6 (Charbonneau et al., 1989, Sonnenburg et al., 1991) and represents a putative cGMP binding domain. The degree of homology in this region is reasonably good (30 %) between PDE2 and PDE6 (Stroop & Beavo, 1991, Stroop & Beavo, 1992). cGMP binds to PDE2 with high affinity via this allosteric regulatory domain so as to cause stimulation of activity when cAMP is the substrate (Charbonneau et al., 1986, Erneux et al., 1985, Yamamoto et al., 1983b). The resultant cGMP activity increase is transient unless cGMP synthesis is constantly elevated, since the PDE2 hydrolyses both cAMP and cGMP.

Soluble and particulate forms of PDE2A1 and PDE2A2 have similar kinetic properties (Murashima et al., 1990). However, specificity of PDE2s for hydrolysis of cGMP are about 3-fold higher than hydrolysis of cAMP (Moss et al., 1977, Wada et al., 1987). One of the PDE2 isoforms has been shown to be phosphorylated both *in vitro* and *in vivo* by PKA. This is the particulate 105 kDa brain enzyme. However, this modification appears not to alter the kinetic properties of the enzyme (Whalin et al., 1988).

Only one PDE2 specific inhibitor has recently been found, namely EHNA (erythro-9-(2-hydroxyl-3-nonyl)-adenine) which was originally called MEP-1 (Mery et al., 1995, Michie et al., 1996, Podzuweit et al., 1995). EHNA exerts selective inhibition of PDE2 activity with an IC₅₀ of 1-3 μM compared to an IC₅₀

of more than 100 μM for other PDE forms (Mery et al., 1995, Michie et al., 1996, Podzuweit et al., 1995) (Table 1.1).

1.5.6. PDE3: cyclic GMP-inhibited PDEs (cGIPDE)

PDE3 isoforms are found in a large array of tissues, including bovine and rat adipose tissues, human platelets and T-cells, rat liver and epididymal tissues, human and bovine heart (Degerman et al., 1987, Erdogan & Houslay, 1997, Giembycz et al., 1996, Grant & Coleman, 1984, Kasuya et al., 1995, Taira et al., 1993). The subcellular distribution of PDE3 species varies, with the enzyme present in the cytosol (Grant & Coleman, 1984) as well as membrane-associated (Anderson et al., 1989, Giembycz et al., 1996, Pyne et al., 1987). The distribution between membrane and cytosol fraction appears to vary in different cell types. The basis of the differences in distribution is not understood, however, such PDE3 activity is encoded by two genes, PDE3A and PDE3B (Meacci et al., 1992, Taira et al., 1993). Recombinant PDE3A and PDE3B proteins exhibit high affinities for both cAMP and cGMP, with K_m values in the range of 0.1 - 0.8 μM (Table 1.1) and the V_{max} values for cAMP greater (4-10-fold) than those for cGMP (Degerman et al., 1987, Degerman et al., 1994, Manganiello et al., 1990a). Low (μM) concentrations of cGMP serve as a competitive inhibitor of cAMP hydrolysis by PDE3s (Table 1.1). Another characteristic of PDE3s is their sensitivity to inhibition by certain drugs that augment myocardial contractility, inhibit platelet aggregation and relax smooth muscle. These include cilostimide ($\text{IC}_{50} = 0.005 \mu\text{M}$), milrinone ($\text{IC}_{50} = 0.3 \mu\text{M}$) and enoximone ($\text{IC}_{50} = 1 \mu\text{M}$) (Beavo & Reifsnnyder, 1990, Manganiello et al., 1990a, Manganiello et al., 1995b) (Table 1.1). Such compounds have IC_{50} values at least 10-100-fold lower for PDE3s than for other PDE enzymes, indicating a profound selectivity.

In situ hybridisation studies have showed that PDE3A transcripts are most abundant in white and brown adipose tissue and in hepatocytes, whereas PDE3B transcripts occur at high levels in the gastrointestinal and cardiovascular systems in rats (Reinhardt et al., 1995). This suggests that PDE3 forms exhibit cell-specific differences in properties. Primary sequence analysis indicates that the PDE3 forms contain the conserved catalytic domain found among all PDEs. PDE3A and PDE3B catalytic regions are highly conserved and are followed by a hydrophilic C-terminal region. The N-terminal region is distinct and contains putative hydrophobic membrane-association domains and several consensus PKA phosphorylation sites (Figure 1.2). Within the conserved domain of the PDE3s is a unique insertion of 44 amino acids which is not present in the conserved domains of other PDE families (Manganiello et al., 1995b, Taira et al., 1993).

Some variation has been found in the analysis of the molecular masses of PDE3 isoforms. It has been shown that PDE3A and PDE3B cDNAs encode proteins of ~125 kDa. However, PDE3s are particularly sensitive to endogenous proteolysis producing fragments of around ~110 kDa from human platelets and bovine cardiac tissues (Rascon et al., 1992, Smith et al., 1993). Indeed, a 62 kDa 'dense-vesicle' rat liver PDE has also been purified (Marchmont et al., 1981, Pyne et al., 1987) although it is unclear as to whether this is a proteolysed species or splice variant.

Platelets have a central role in thrombosis and homeostasis where cAMP plays an inhibitory role in platelet action and aggregation. PDE3A is a major PDE in these cells and probably serves as a principal homeostatic regulator of basal cAMP in platelets. Treatment of intact rat or human platelets with prostaglandin E₁ or cAMP elevating agents, such as forskolin, stimulates PDE3 activity (Alvarez et al., 1981). This was shown to be due to PDE3A becoming phosphorylated by PKA. This can be expected to occur in response to anti-aggregatory signalling molecules (such as the prostaglandins) in human platelets (Macphee et al., 1988). The

increase in PDE activity may play an important role in the desensitisation of platelets to further exposure to adenylate cyclase agonists.

The purified heart PDE3 can also serve as a substrate for PKA *in vitro* (Harrison et al., 1986). This phosphorylation may mediate a negative feed back mechanism which co-operates with in the restoration of resting cAMP levels within the system (Manganiello et al., 1990a). The inhibition of PDE3s causes a substantial increase in cardiac contractility. There are several inhibitors of this family of PDEs, including the cardiotonic agents cilostimide, milrinone and amrinone as well as cGMP (Reeves & England, 1990).

Incubation of intact adipocytes and hepatocytes with agents that increase cAMP leads to activation of PDE3 (Beltman et al., 1993). This activation is thought to be important in 'feedback' regulation of intracellular cAMP levels and the activation state of PKA phosphorylation.

There is considerable evidence that PDE3s are important regulators of the effects of insulin on lipid and carbohydrate metabolism (Houslay & Kilgour, 1990, Manganiello et al., 1990a). Incubation of intact rat adipocytes and hepatocytes with insulin results in rapid phosphorylation and activation of the membrane-bound (or dense-vesicle) PDE3B (Gettys et al., 1987, Heyworth et al., 1983, Smith et al., 1991). Activation of PDE3B by insulin results in reduction in cAMP levels, PKA activation, net dephosphorylation and decreased activity of hormone-sensitive lipase and reduced hydrolysis of triglyceride (Degerman et al., 1996). A possible route for the insulin-stimulated PDE3B phosphorylation of Ser³⁰² may involve an insulin-stimulated protein serine kinase (PDE3IK) (Rahn et al., 1994). Insulin-induced activation of PDE3IK leading to the phosphorylation and activation of PDE3B can be blocked by the phosphatidylinositol 3-kinase (PI3-K) inhibitor wortmannin (Rahn et al., 1994). This suggests that the antilipolytic signal cascade is mediated via receptor activation of PI3-K.

Further studies have been carried out with cAMP-mediated activation of PDE3s by lipolytic hormones and agents. In adipocytes, lipolysis can be promoted by hormones such as adrenaline via beta adrenoceptor stimulation (Anderson et al., 1989) resulting in the elevation of intracellular cAMP levels. Isoproterenol rapidly activates adenylate cyclase and increases the concentration of cAMP, resulting in the phosphorylation by PKA, of Ser³⁰² and activation of PDE3B in rat adipocytes (Degerman et al., 1990, Smith & Manganiello, 1989). This PKA-mediated phosphorylation of PDE3B causes the activation of the enzyme, resulting in a short-term negative feedback (Manganiello et al., 1990a). Conversely, stimulation of adipocytes by insulin, prostaglandin E₁ and adenosine causes an antilipolytic effect by reduction of cAMP levels within the cell (Manganiello et al., 1990a). These antilipolytic agents also mediate an effect by inhibiting adenylate cyclase via G_i. Thus, there is a fine balance between cAMP production by adenylate cyclase and cAMP degradation by PDE3s.

1.5.7. PDE4: cyclic AMP-specific PDEs (cAMP PDE)

1.5.7.1. Background

The PDE4 enzymes are a large multi-gene family consisting over 13 different isoforms seen in both humans and rodents (Bolger, 1994, Conti et al., 1995b). Four different genes encode mRNAs for PDE4 isoforms in mammals with a great similarity between species. These are called PDE4A, PDE4B, PDE4C and PDE4D (Table 1.2). The first gene was cloned in rats (Bolger, 1994, Davis et al., 1989, Swinnen et al., 1989a) and later in humans (Bolger et al., 1993, Engels et al., 1995, Horton et al., 1995, Livi et al., 1990, McLaughlin et al., 1993, Sullivan et al., 1994) and in mice (Milatovich et al., 1994). The four genes are distributed on three chromosomes. The gene for PDE4A is localised on the short arm of human chromosome 19 as is that for PDE4C (Horton et al., 1995, Milatovich et al., 1994). However, PDE4B is found on chromosome 1 (Milatovich et al., 1994,

Szpirer et al., 1995) and PDE4D on chromosome5 (Milatovich et al., 1994, Szpirer et al., 1995). Each of these four genes appear to produce multiple mRNA transcripts involving 5'-domain swopping, yielding isoforms with distinct N-terminal domains (Bolger, 1994) (Figure 1.3). In contrast the C-terminal domain of each particular PDE4 gene family is unique and is thus common to all active isoforms produced from a particular PDE4 gene. The four rat and four human genes show a one to one homology, in that each of the four human PDE4 genes is more closely related to one specific rat gene than to any other human gene (Bolger, 1994, Bolger et al., 1994).

The enzymes of the PDE4 multigene family are characterised by their high and specific affinity for cAMP, selective and specific inhibition by the anti-depressant drug rolipram (Table 1.1), and insensitivity to the cGMP and Ca^{2+} / CaM (Beavo, 1995, Beavo & Reifsnnyder, 1990, Conti et al., 1991, Conti et al., 1995b, Thompson, 1991). This group of PDEs are the closest mammalian homologues to the *dunce* gene of *Drosophila melanogaster* (Figure 1.4), which was first isolated as a mutation effecting a phenotypic learning defect (Qiu & Davis, 1993, Qui et al., 1991). It was shown that mutation within this locus also led to a variety of behavioural defects, disturbed cAMP metabolism and caused sterility in adult females (Tulley & Quinn, 1986). The abnormal cAMP metabolism was due to a mutation in a PDE gene, leading to an absence or greatly reduced PDE activity and an enhanced cAMP level within the cell (Byers et al., 1981, Davis & Kiger, 1981). Analyses subsequently showed that *dunce* was the structural gene for a cAMP-specific PDE (Davis & Kauvar, 1984). Indeed, defects in memory and learning in *dunce* flies can be rescued by the expression of a mammalian PDE4 cDNA *Drosophila* (Dauwalder & Davis, 1995). Such experiments demonstrate the close functional homology between the *Drosophila* and mammalian PDE4 enzymes.

1.5.7.2. Molecular cloning of PDE4 isoforms

Three approaches have been used to clone members of the PDE4 enzymes. The *Drosophila dunce* gene was isolated by a chromosome walking technique before cDNAs were isolated for any of the mammalian PDE4 genes (Davis & Davidson, 1986). Subsequently the *dunce* cDNA was used to probe mammalian cDNA libraries (Davis et al., 1989). A second strategy was to isolate cDNA clones whose expression would suppress the heat-shock sensitive phenotype of *Saccharomyces cerevisiae* having mutations in the RAS-cAMP pathway (Colicelli et al., 1989). RAS proteins are regulators of adenylate cyclase and consequently involved in cAMP production in yeast. Activating mutations of this pathway produce their phenotype by elevating cAMP levels as a consequence of acute sensitivity to heat-shock. Selection was performed on the basis of rescue of heat-shock sensitivity, by a lowering of cAMP levels. PCR is another approach which has also been employed, using oligonucleotide primers designed to amplify DNA sequences with homology to both the *dunce* gene and previously isolated mammalian PDE4 clones (Bolger et al., 1994).

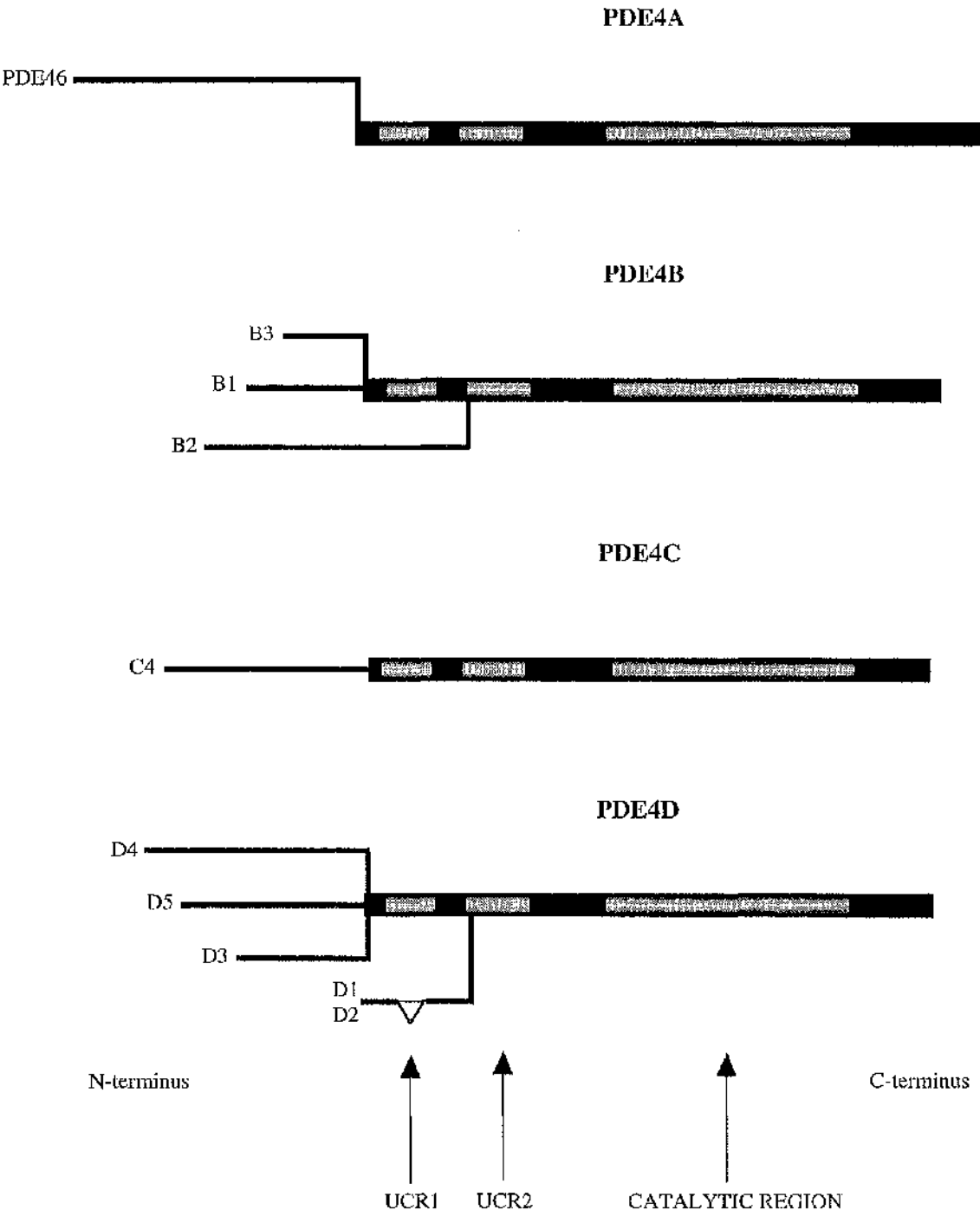
1.5.7.3. The structural features of the PDE4 isoforms

The human and *Drosophila dunce* PDE4 amino acid sequences demonstrate regions of strong conservation within their coding sequences. Alignment of the full length sequences of both human (Figure 1.4) and rat PDE4s shows that there are three distinct conserved regions. The core region is, of course, that which shows similarity with all other PDE enzyme classes and which forms the putative catalytic region (Jin et al., 1992). The catalytic core region of PDE4s shows ~30-40 % similarity with various PDE proteins (Houslay et al., 1997). The other two regions which are found upstream of the catalytic region, that is towards the N-terminal region of these proteins, are called UCR1 and UCR2 (Upstream Conserved Region 1 and 2) (Figure 1.3, 1.4).

Figure 1.3. Schematic structure of full-length human PDE4 forms

Shown is the schematic representation of the four human PDE4 mRNAs. Black areas denote regions of lower or absent sequence homology. Regions of the strongest sequence conservation (UCR1, UCR2 and catalytic; shown by arrows) are shown in the light areas. Regions of sequence unique to an individual alternatively spliced mRNA is shown by thin branched lines. The triangle in the PDE4D2 cDNA indicates lacking 86 bp sequence, as compared to the PDE4D1 clone.

Figure 1.3. Schematic structure of full-length human PDE4 forms



UCR1 and UCR2 appear to be distinct features of the PDE4 family, as these regions, although strongly conserved between organisms as evolutionary divergent as *Drosophila melanogaster* and humans (Figure 1.4), have no close homologues in any other sequences in the GenBank or EMBL database (Bolger, 1994, Bolger et al., 1993). The comparison between the three conserved regions of the mammalian PDE4s shows >80 % sequence identity and greater than 95 % homology to both each other and to the corresponding regions in the *Drosophila melanogaster dunce* PDE. However, UCR1 and UCR2 are distinct in that they lack homology to each other and are separated by relatively low homology regions that have been called LR1 and LR2 (Linker Region 1 and 2) (Houslay et al., 1997) (Figure 1.4). LR1 region, is formed from ~33 residues, and shows no homology between isoforms, whereas LR2 region, a ~76 residues, exhibits loose similarity between the various PDE4 classes. The functions of UCR1/UCR2 and LR1/LR2 regions are unknown. However, UCR1, but not UCR2, is affected by alternative mRNA splicing in that 'short' PDE4 forms lack UCR1. Whilst the short forms of PDE4B/C/D all possess an intact UCR2 region together with a unique N-terminal region, the splice junction is different for the PDE4A gene, resulting in a disruption of UCR2. It would seem that these conserved regions are likely to be important in the functioning or regulation of members of the PDE4 isoforms. Whilst, however, this is poorly understood, the phosphorylation of PDE4D3 (Sette & Conti, 1996) within UCR1 leads to a marked increase in catalytic activity. Furthermore a yeast-two hybrid system study has been used to show that UCR1 may interact directly with UCR2 region (Bolger, unpublished work).

Figure 1.4. Sequence alignment of four human PDE4 family enzymes

The peptide sequences of human PDE4 isoforms and the PDE4B splice product of the *Drosophila melanogaster dunce* gene (exons 3 to 13, excluding exon 4) have been aligned. The specific cDNA clones are: PDE4A species: PDE46, PDE4B species: PDE4B1, PDE4C species: PDE4C1B, PDE4D species: PDE4D4. Horizontal lines indicate the positions of UCR1, UCR2 and the catalytic region of the proteins. • denoted an identical amino acid residue in both sequences.

Figure 1.4. Sequence alignment of four human PDE4 family enzymes



350
 |
 |..*.....|..*.....*.....*.....|..*.....|
 HSPDE4A LSEMSRSGNQVSEYISTTFLDKQNEVEIPSPMTKEREKQQAPRPRPSQP
 HSPDE4B LSEMSRSGNQVSEYISNTFLDKQNDVEIPSPQKDKREKKKKQ-----
 HSPDE4C LSETSRSGNQVSEYISRTFLDQQTEVELPKVTAAE-----AP-----
 HSPDE4D LSEMSRSGNQVSEFISNTFLDKQHEVEIPSPQKEKEKKKKRP-----
 dunce FSESSRSGNOISEYICSTFLDKQOEFDLPSLRVEDNPVELVAANAAAGQQ

UCR2 ends

400
 |
 .||*||*.....*.....*.....|..*.....|..*.....|..*.....|..*.....|
 HSPDE4A PP-----PPVPHLQPMQITGLKK-IMHSNSLNNSNIPRFGVKTDQEEL
 HSPDE4B -----QLMTQISGVKK-IMHSSSLNNTSISRFGVNTENEDH
 HSPDE4C -----QPMRISGLHG-LCHSASLSSATVPRFGVQTDQEEQ
 HSPDE4D -----MSQISGVKK-IMHSSSLTNSSIPRFGVKTEQEDV
 dunce SAGQYARSRSRGPMSQISGVKRLSHTNSFTGERLPTFGVETPRENE

Catalytic begins

450
 |
 .|.....*.....|..*.....|..*.....|..*.....|..*.....|..*.....|..*.....|..*.....|..*.....|
 HSPDE4A LAQELLENLKWGLNIFCVSDYAGGRSLTCIMYMFQERDILLKFRIPVD
 HSPDE4B LAKELEDLNKWGLNIFNVAGYSHNRPLTCIMYAFQERDILLKTFRISSD
 HSPDE4C LAKELEDTNKWGLDVFKVADVSGNRPLTAIFSIQERDILLKTFQIPAD
 HSPDE4D LAKELEDVNKWGLHVFRIAEELSGNRPLTVIMHTIFQERDILLKTFKIPVD
 dunce LGTLGELDWTWGIQIFSIGEFVNRPLTCVAYTIFOSRELLTSLMIPPK

500
 |
 .||.....*.....|..*.....|..*.....|..*.....|..*.....|..*.....|..*.....|..*.....|..*.....|
 HSPDE4A TMVT-YMLTLEDHYHADVAYHNSLHAADVLOQSTHVLLATPALDAVFTDL
 HSPDE4B TFLIT-YMMLTLEDHYHSDVAYHNSLHAADVAQSTHVLLSTPALDAVFTDL
 HSPDE4C TLAT-YLLMLEGHYHANVAYHNSLHAADVAQSTHVLLATPALEAVFTDL
 HSPDE4D TLIT-YLMTLEDHYHADVAYHNNIHAADVQSTHVLLSTPALEAVFTDL
 dunce TFLNNEMSTLEDHYVKDNPFHNSLHAADVTOSTNVLNTPALEGVFTPL

550
 |
 .|.....*.....|..*.....|..*.....|..*.....|..*.....|..*.....|..*.....|..*.....|..*.....|
 HSPDE4A EILAAALFAAAIHDVDHPGVSNOFLINTNSEALALMYNDESVLENHHLAVG
 HSPDE4B EILAAIFAAAIHDVDHPGVSNOFLINTNSEALALMYNDESVLENHHLAVG
 HSPDE4C EILAAALFAAAIHDVDHPGVSNOFLINTNSDVALMYNDASVLENHHLAVG
 HSPDE4D EILAAIFASAIHDVDHPGVSNOFLINTNSEALALMYNDSVLENHHLAVG
 dunce EVGGALFAACIHDVDHPGLTNOFLVNSSSELALMYNDESVLENHHLAVA

600
 |
|.....*.....|..*.....|..*.....|..*.....|..*.....|
 HSPDE4A FKLLQEDNCDIFQNLKQRQSLRKMVIDMVLATDM-----
 HSPDE4B FKLLQEEHCDIFMNLTKKQRQTLRKMVIDMVLATDM-----
 HSPDE4C FKLLQAENCDIFQNLKQRQSLRKMVIDMVLATDM-----
 HSPDE4D FKLLQEENCDIFQNLTKKQRQSLRKMVIDMVLATDM-----
 dunce FKLLONOGCDIFCNMOKKOROTLRKMVIDIVLSTDM

800
 |
*.....|
 HSPDE4A FQFELTLEEEEEIEISMAQIPCTAQEALTAQGLSGVEEALDA-----
 HSPDE4B FQFELTLEEDSEGEPEKE-----G-----EGHSYFSSSTKTLCV-----
 HSPDE4C FQFELTLEEAEEEEEEEE-----EEGEETA-----
 HSPDE4D FQFELTLEEDGESDTEKD-----SGSQVEEDTSCSDSKTLCT-----
 dunce ..FOVTLSESDOEN

Catalytic ends

1.5.7.4. *PDE4A*

The human *PDE4A* gene is localised between the genes for TYK2 and the LDL receptor in the p13.2 region on the short arm of human chromosome 19 (Olsen, A., Sullivan, M. and Houslay, M.D. unpublished data). It has been demonstrated that this gene family consists of at least three catalytically active and two catalytically inactive isoforms which are produced by alternate splicing (Table 5.1). Active products of the *PDE4A* gene, like other active PDE4s, have identical catalytic sites and C-terminal regions but exhibit highly distinct N-terminal regions. Catalytically active PDE4A isoforms are; PDE46 (HSPDE4A4B) (Bolger et al., 1993), hPDE-IV_A-h6.1 (h6.1, HSPDE4A4C) (Sullivan et al., 1994) and hPDE-IV_A-Livi (hPDE-1, HSPDE4A4A) (Livi et al., 1990). However, resequencing of the hPDE-1 clone showed that errors were made in the original sequence and that h6.1 provided the correct one (Jacobitz et al., 1996) (h6.1 and hPDE-1 properties are discussed in chapter 5). Catalytically inactive products are; 2EL (HSPDE4A8) (Horton et al., 1995) and TM73 (HSPDE4A5?) (Bolger et al., 1993) (Table 1.2). It is possible that more PDE4A isoforms will be isolated in the future. Indeed, this study shows that a novel, active human PDE4A species to exist in human Jurkat T-cells (see chapter 3).

PDE46 reflects a full-length 'long' isoform of human *PDE4A* gene which is analogous to the rat PDE4A splice variant RPDE6 (Bolger, 1994, Bolger et al., 1996, McPhee et al., 1995). PDE46 consists of 886 amino acids as deduced from the cDNA sequence. Expression of the cDNA for PDE46 in COS7 cells produced a ~125 kDa species which reflects a similar form seen in human monocytes and U937 cells (Huston et al., 1996, Manning et al., 1996, Torphy et al., 1995). The h6.1 isoform was cloned from a cDNA library of human T-cells using a PDE specific probe (Sullivan et al., 1994) which was generated by PCR using primers based on the reported h-PDE-1 (Livi et al., 1990).

Table 1.2. Properties of human (h) and rat (r) PDE4 enzymes

Clone name	Source	Accession numbers	Amino acids	K _m for cAMP	Rel-V _{max} cytosolic	IC ₅₀ rolipram (μM) cytosolic	particulate	Mw (kDa) on SDS/PAGE	References
PDE4A:									
hPDE46	h	L20965	886	2	(1)	1.6	0.2	125	(1, 2, 3, 4, 5)
h6.1	h	U18087	686	6	11.5	0.6	n/a	99	
h-PDE1	h	M37744	686	3	-	-	-	98	
TM3	h	L20967	800	inactive					
2EL	h	U18088	323	inactive					
PDE4B:									
RD1	r	M26715	610	4	n/a	n/a	0.5	79	(6, 7, 8)
RPDE6	r	L27057	844	2	(1)	0.2	1.2	109	
RPDE39	r	L36467	763	3	1	1	0.5	98	
PDE4B:									
TM72 (B1)	h	L20966	736	2	(1)	0.08	0.05	104	(4, 9)
PDE32 (B2)	h	L20971	564	3	4	0.02	0.21	80	
PDE4B3 (B3)	h	U85048	721	1.5	2	0.05	0.1	103	
DPD (B1)	r	J04563	562	4.8		0.7		64	(9, 10, 11, 20)
ratPDE4 (B2)	r	M25350	564	4		0.7		64	
pRPDE74 (B3) r			721	no data available					

Table 1.2. Properties of human (h) and rat (r) PDE4 enzymes (continued)

Clone name	Source	Accession numbers	Amino acids		K _m for cAMP	Rel-V _{max}		IC ₅₀ rolipram (μM)	M _w (kDa)		References
			acids	for		cytosolic	cytosolic particulate		SDS/PAGE	on	
PDE4C:											
PDE4C1A	h	L20968	251		no data available						(4, 12, 13, 14)
PDE4C1B	h	Z46632	712		1.5		6.6				
PDE4C2A	h	U88712	605		0.6					80	
PDE4C3A	h	U88713	699		no data available						
PDE4C4A	h	U66346	791		no data available						
RPDE36											
ratPDE1	r	L27061	536		no data available						(7, 15)
PDE4D:											
ratPDE3.1	r	M25349	584		1.9		0.6			71	
ratPDE3.2	r	U09456	505							67	
ratPDE3.3	r	U09457	672							93	

References: 1; (Huston et al., 1996), 2; (Sullivan et al., 1994), 3; (Livi et al., 1990), 4; (Bolger et al., 1993), 5; (Horton et al., 1995), 6; (Davis et al., 1989), 7; (Bolger et al., 1994), 8; (Bolger et al., 1996), 9; (Huston et al., 1997), 10; (Colicelli et al., 1989), 11; (Swinnen et al., 1991), 12; (Engels et al., 1995), 13; (Obermolte et al., 1997), 14; (Owens et al., 1997), 15; (Swinnen et al., 1989a), 16; (Swinnen et al., 1989b), 17; (Jin et al., 1992), 18; (Sette et al., 1994), 19; Swinnen et al., 1991, 20; Lobban et al., 1994.

The amino acid alignment shows that h6.1 is an N-terminally truncated form of PDE46 and the identical region is from the amino acid residue at position 210 of PDE46 to the extreme C-terminus of PDE46. However, the first 9 amino acids of h6.1 are non-native and were engineered to reflect the sequence of h-PDE1, which is now known to be artefactual.

2EL was cloned from resting a human Jurkat T-cell library. It exhibits no apparent PDE activity (Horton et al., 1995). This inactive PDE4A is a 323 residue protein which differs markedly from PDE46 or h6.1 in two aspects (Figure 5.2). In 2EL, the catalytic 'core' region is truncated at both its N- and C-terminal ends, leaving a portion of the 'core' region which reflects residues 365 and 643 in PDE46 (Bolger et al., 1993). It also has a novel sequence of 33 amino acids at its N-terminus (Figure 5.1) and due to a 34 bp insert within the catalytic region, is prematurely terminated as a result of the frameshift of the 2EL open reading frame (ORF) leading to a unique sequence of 14 amino acids which forms its novel C-terminus (Horton et al., 1995). It is possible that loss of either or both the N- and C-terminal regions found in active PDE46 and h6.1 might account for 2EL being catalytically inactive. Neither the functional significance of producing such a protein, nor the molecular basis for lack of catalytic function is known.

On a subcellular level, PDE46 is found both in the cytosol and also associated with membranes, where it is preferentially located in cortical areas of the cell (Huston et al., 1996, Houslay et al., 1997). In contrast, h6.1 does not show any association with the cell plasma membrane (Huston et al., 1996). The particulate PDE46 activity and immunoreactivity were not solubilised by either high salt concentrations nor by the non-ionic detergent, Triton X-100. From kinetic studies, the particulate form of PDE46 exhibited a relative V_{max} value which was approximately half of that of the cytosolic form, suggesting that particulate association altered enzyme conformation. However, truncated form h6.1

demonstrated a ~11-fold higher catalytic activity than PDE46 (Huston et al., 1996) suggesting again that the N-terminal region of PDE46 can modulate the conformation and activity of the catalytic unit. Particulate PDE46 also showed a ~60-fold higher affinity for rolipram than cytosolic PDE46 (Huston et al., 1996). Interestingly, both PDE46 and h6.1 were inhibited by rolipram in a simple competitive fashion with h6.1 showing a ~2-fold higher affinity for rolipram than cytosolic PDE46 (Huston et al., 1996, Wilson et al., 1994) (Table 1.2).

In rats, *PDE4A* gene encodes three splice variants, which are called RD1 (RNPDE4A1A), RPDE6 (RPDE4A5) (McPhee et al., 1995) and RPDE39 (RPDE4A8) (Bolger et al., 1996). RD1 was the first mammalian *PDE4A* transcript to be described. The cDNA clone encodes an enzyme of 610 amino acids that is expressed primarily in the brain, particularly the cerebellum (Bolger et al., 1994, Shakur et al., 1993, Shakur et al., 1995). Native RD1 which lacks the UCR1 region and the N-terminal portion of UCR2 (Davis et al., 1989) is found associated predominantly with membranes (93 %) in cerebellum (Shakur et al., 1995). RPDE6 is expressed in a number of different tissues, although it is highly expressed in the brain and encodes a protein of 844 amino acids which is present in both particulate (25 %) and soluble (75 %) forms (Bolger et al., 1994, MCPhee et al., 1995). Another alternatively spliced form RPDE39 (763 amino acids) is found distributed between the membrane (15 %) and cytosol (85 %) in transfected COS7 cells (Bolger et al., 1996) and appear to be exclusively expressed in the testis (Bolger et al., 1996) and hepatocytes (Zeng, L. and Houslay, M.D., unpublished data).

Products of each of the PDE4 loci appear to have distinct tissue distributions, suggesting that these alternatively spliced transcripts have specific and subtle differences in function, regulation and subcellular targeting. For example, the unique amino terminal region of RD1 encodes a membrane association motif.

Thus, whilst RD1 is exclusively membrane-associated an N-terminally truncated RD1 species, which lacks the first 25 amino acids (met²⁶RD1) forming the alternatively spliced region, was found as a cytosol species when expressed in COS7 cells (Shakur et al., 1993). It was shown that the unique N-terminal splice region of RD1 encodes a structure able to target an essentially soluble core PDE to the membrane fraction (Scotland & Houslay, 1995). This was confirmed by forming a chimera of the N-terminal first 23 amino acids of RD1 fused to the N-terminus of the normally soluble bacterial enzyme, chloramphenicol acetyltransferase (CAT). Whilst CAT alone is normally expressed in the soluble fraction, chimeric protein was associated with membranes (Scotland & Houslay, 1995). Further deletion studies demonstrated that the membrane-association of RD1 was determined by the distinct tryptophan-rich region (Smith et al., 1996). RD1 protein can be released from the membrane by non-ionic detergent Triton X-100 but not high salt treatments (Shakur et al., 1993). This suggests that membrane-association occurs by virtue of hydrophobic interactions (McPhee et al., 1995). A relative V_{\max} study showed that the N-terminal domain also profoundly reduces catalytic activity. Indeed, experimentally truncated form met²⁶RD1 is catalytically 2-fold more active than RD1 and RD1 exhibits ~3-fold higher activity than long forms (Bolger et al., 1996). This indicates that N-terminal portions of RPDE4A not only regulate membrane-association but also regulate catalytic activity.

1.5.7.5. PDE4B

Three catalytically active human PDE4B splice variants have been cloned (Table 1.2 and Figure 1.3). These reflect alternate mRNA splicing of products of the *PDE4B* gene. These various PDE4B isoforms have distinct N-terminal regions where PDE4B1 (Bolger et al., 1993) and PDE4B3 (Huston et al., 1997), contain both UCR1 and UCR2, whereas PDE4B2 (McLaughlin et al., 1993) contains only the UCR2 region. The 721 residue PDE4B3 is the largest protein migrating

as a ~104 kDa species on SDS-PAGE when expressed in transfected COS7 cells (Huston et al., 1997) (Table 1.2). All the three PDE4B splice variants compartmentalised between cytosol and particulate fractions of transfected COS7 cells. Treatment either with the detergent Triton X-100 or high salt concentrations released both the PDE4B1 and PDE4B2 membrane PDE proteins. This may reflect the association of PDE4B1 and PDE4B2 to a particulate component via either integral membrane interactions or binding through hydrophobic interactions. However, particulate PDE4B3 was not solubilised by using any of the previous procedures. This may suggest binding of this isoform with cytoskeletal components associated with the P2 pellet fraction.

The K_m values for cAMP of all the isoforms were similar (Table 1.2) with the relative V_{max} value of PDE4B2 being ~4-fold higher than that of the long forms (Table 1.2) (Huston et al., 1997).

Immunoblotting and mRNA transcription studies have shown that PDE4B isoforms are present in most circulating human and rat blood cells except T-cells (Engels et al., 1994, Erdogan & Houslay, 1997, Manning et al., 1996).

As for the human *PDE4B* gene, three rat PDE4B splice variants have been described. These are DPD (RNPDE4B1A) (Colicelli et al., 1989), ratPDE4 (RNPDE4B2A) (Swinnen et al., 1989a) and the novel pRPDE74 (RNPDE4B3) (Bolger, G.B. unpublished work). However, it is unclear whether the DPD cDNA represents a distinct isoform or an N-terminally truncated form. Indeed, the human homologue of this species TM72 appears to encode a rather larger protein suggesting that DPD is N-terminally truncated.

The distribution of rat PDE4 and DPD has been characterised in rat brain (Lobban et al., 1994) and showed distinct localisation patterns in various brain areas. The

cerebellum, mid brain and brain stem did not contain DPD but expressed ratPDE4, whereas the hypothalamus, the striatum, hippocampus and cortex expressed both species. Transcription analysis showed that rat PDE4B isoforms are also found in liver, lung, kidney, heart (Engels et al., 1994) and Sertoli cells (Monaco et al., 1994).

1.5.7.6. *PDE4C*

Products of the *PDE4C* gene are the least well characterised compared with those of other PDE4 genes. Two rat and four human partial PDE4C clones have been reported which are now believed to be the result of cloning artefacts or incomplete clones (Table 1.2). The rat clones are RNPDE4C1A (Swinnen et al., 1989b) and RNPDE4C1B (Bolger et al., 1994). The human partial PDE4C clones are HSPDE4C1A (Bolger et al., 1993), HSPDE4C1B (Engels et al., 1995), HSPDE4C2A and HSPDE4C3A (Owens et al., 1997). However, one human full length PDE4C (HSPDE4C4A) splice variant from foetal lung library has recently been cloned (Oberholte et al., 1997) (Table 1.2).

The amino acid sequence of HSPDE4C1B and HSPDE4C2A showed the same identity in the catalytic domain with other PDE4 isoforms. These PDE4C enzymes also show low K_m for cAMP (Table 1.2) (Engels et al., 1995, Owens et al., 1997). However, in general, PDE4 inhibitors have little selectivity for PDE4 subtypes although most appear to be less potent against PDE4C compared with other subtypes (Engels et al., 1995). In contrast to the other PDE4A/B and D isoforms, the human PDE4C is absent in cells of the immune system and present at very low levels in brain (Engels et al., 1994, Erdogan & Houslay, 1997). RT-PCR analysis however, suggests that transcripts for this enzyme occur in rat liver, lung, kidney, brain and heart, and in human liver, kidney and heart (Engels et al., 1994).

1.5.7.7. *PDE4D*

PDE4D gene encodes a number of alternatively spliced isoforms in rats and humans (Bolger, 1994, Sette et al., 1994b). In humans, five variants are found. These are called PDE4D1, PDE4D2 (Nemoz et al., 1996), PDE4D3, PDE4D4 (Bolger et al., 1993) and PDE4D5 (Bolger et al., 1997). Each of these isoforms possesses identical C-terminal catalytic 'core' regions and have uniquely spliced N-terminal regions (Bolger et al., 1997, Jin et al., 1992, Nemoz et al., 1996) (Figure 1.3). Three of the PDE4 proteins contain both UCR1 and UCR2 regions; PDE4D3, PDE4D4 and PDE4D5, which are so-called 'long' forms. PDE4D1 and PDE4D2 are so-called 'short' forms that lack UCR1 (Figure 1.3) (Bolger, 1994). PDE4D2 differs from PDE4D1 by virtue of a small deletion (86 bp) in its N-terminal region (Figures 1.3 and 4.1).

Four different transcripts of the *PDE4D* gene have been demonstrated in rats (Table 1.2). These are called rat PDE4D1, rat PDE4D2, rat PDE4D3 (formerly known as ratPDE3.1, ratPDE3.2 and ratPDE3.3, respectively) (Swinnen et al., 1989b, Jin et al., 1992, Sette et al., 1994) and PDE4D4 (Vicini and Conti, unpublished data). The rat counterpart of human PDE4D5 has also been shown in rat brain by immunoblotting using an antibody generated to the common C-terminal region (Bolger et al., 1997). An alignment of the rat and human PDE4D1, PDE4D2 and PDE4D3 amino acid sequences shows highly conserved features. Each of the human proteins is nearly identical in length to its rat counterpart and has greater than 90 % amino acid identity. However, recent data suggests that each of the various isoforms may have a distinct function. For example, they differ in their ability to be induced by increased cAMP levels (Erdogan & Houslay, 1997, Sette et al., 1994a, Verghese et al., 1995) and in protein-protein interaction with SH3 domains (O'Connell & Houslay, unpublished data). The rat PDE4D1, PDE4D2 and PDE4D3 proteins also vary in their enzymologic properties and in their regulation by phosphorylation (Sette & Conti,

1996, Sette et al., 1994a). However, no comparative analyses have been done on all five PDE4D forms expressed in a single cell type.

1.5.7.8. Regulation of PDE4 enzymes

Differential regulation of PDE4 enzymes can be achieved by regulation of the level of cAMP. This may form part of a long-term adaptation process for PDE4 isoforms which is mediated via a cAMP-dependent mechanism. Such a process may result from hormonal or direct activation of adenylate cyclase and can also be achieved with cAMP analogues. Short-term regulation of specific PDE isoforms may also be achieved by cAMP-dependent phosphorylation.

1.5.7.9. Phosphorylation of PDE4 isoforms

Protein phosphorylation has been described as a physiological regulator of PDEs (Beltman et al., 1993). Thyroid-stimulating hormone (TSH) stimulation of rat FRTL-5 thyroid cells caused elevation of intracellular cAMP levels and results in a PKA mediated phosphorylation of PDE4D3 (Sette et al., 1994a). PDE4D3 has also been shown to be phosphorylated when the recombinant enzyme was transfected into both MA-10 cells (Sette & Conti, 1996) and Sf9 cells (Alvarez et al., 1995).

There are two potential sites for PKA mediated phosphorylation of PDE4D3 which are formed by serine/threonine residues within a RRxS/T motif (Sette & Conti, 1996). Ser¹³ and Ser⁵⁴ residues form potential phosphorylation sites and these are found in the N-terminal region of the protein. However, whilst both can be phosphorylated it has been shown that only the phosphorylation of Ser⁵⁴ leads to activation of PDE4D3 (Sette & Conti, 1996). Ser⁵⁴ is located in the UCR1 region which is found in all 'long' form PDE4 enzymes. However, to date, no other

PDE has been shown to be phosphorylated by PKA. This may reflect however, simply the lack of studies done or specificity effects.

Within the PDE4 family, the human PDE4B2 isoform has also shown to be phosphorylated by MAP kinase on Ser⁴⁸⁷ (Lenhard et al., 1996). This serine residue is found in the catalytic region of the enzyme. PDE4B2 when expressed *in vitro* by Sf9 cells and in yeast, but not in *E. coli*, was shown to be phosphorylated. However, the functional and physiological significance of this phosphorylation is as yet unclear.

1.5.7.10. Regulation of PDE4 expression

Long-term incubation of various cells with cAMP elevating agents have been shown to lead to an increase in PDE4 activity in certain cell types (Conti et al., 1991, Erdogan & Houslay, 1997, Manning et al., 1996, Verghese et al., 1995). In some cells, this up-regulation of PDE activity forms part of the general phenomenon of desensitisation, a homeostatic mechanism whereby cells reduce their responsiveness in the face of repeated or continuous stimulation with hormones or other agents that increase cAMP (Collins et al., 1992, Sette et al., 1994a). The PDE4 family plays an important role in this phenomenon. Exposure of rat FRTL-5 thyroid cells to TSH showed that PDE4D1 and PDE4D2 were up-regulated whilst, at the same time, PDE4D3 became phosphorylated (see above) (Sette et al., 1994b). This investigation demonstrated that splice variants from the same locus could be differentially regulated on stimulation of a cell by a particular hormone. Similarly, challenge of rat Sertoli cells with either follicle stimulating hormone (FSH) or dibutyryl cAMP led to the induction of the 'short' forms of the *PDE4D* gene; PDE4D1 and PDE4D2 (Swinnen et al., 1991b). Furthermore, prolonged exposure of human monocytes and Mono Mac 6 cells with cAMP elevating agents caused the up-regulation of PDE4D1 and PDE4D2 (Verghese et al., 1995). This is consistent with the suggestion that regulation of the

transcription of a specific subset of PDE4D transcripts, namely PDE4D1 and PDE4D2, is determined by cAMP. Thus, the 'short' forms of PDE4D appear to be under the control of a cAMP-sensitive promoter. Because no induction of the three 'long' form transcripts was apparent in such studies, it is likely that the long isoforms are under the control of one or more cAMP-insensitive promoter(s).

Prolonged exposure to the β -adrenoreceptor agonist salbutamol in both human monocytes (Manning et al., 1996) and U937 monocytic cell line (Torphy et al., 1995) caused an increase in PDE4A as detected by both transcript analysis and by immunoblotting. This PDE4A elevation appeared to be due to increases in the ~125 kDa PDE46 isoform.

Studies in human monocytes (Manning et al., 1996), monocytic cells (Verghese et al., 1995) and U937 cells (Torphy et al., 1995) have also shown that the ~74 kDa PDE4B2 isoform was increased upon chronic elevation of cAMP levels. This has also been noted to occur in rat Sertoli cells upon chronic cAMP elevation (Swinnen et al., 1991a).

1.5.7.11. Regulation of PDE4 by phosphatidic acid

It has been demonstrated that there is an interaction between lipid signalling and PDE4 regulation. Stimulation of lipid signalling pathways can produce phosphatidic acid (PA) and increased PDE4 activity has been seen in rat thymocytes in response to PA (Marcoz et al., 1993a). One of the PDE4 forms which could be separated biochemically from rat thymocyte homogenates was shown to be activated specifically by PA (Savany et al., 1996). Consistent with this, a partially purified PDE4 activity from human monocytic U937 cells was also shown to be activated ~2-fold by phosphatidic acid in a dose dependent fashion with an IC_{50} of ~40 μ g/ml (DiSanto & Heaslip, 1995). This suggests that PA may

be able to activate specific PDE4 species. The identity of such isoforms and the mechanism of activation remains to be determined, although recent work suggests that the long but not short PDE4D forms may be specifically activated by PA (Grance et al., 1997).

1.5.7.12. Interaction of PDE4 with SH3 domains

Src Homology 3 (SH3) domains are structurally distinct globular structures found in a variety of signalling and cytoskeletal proteins which can direct the formation of functionally important complexes (Mayer & Baltimore, 1993). These include tyrosyl protein kinases involved in cellular regulation, adapter proteins such as Grb2 which is involved in MAP kinase activation, phox proteins involved in macrophage activation, as well as various cytoskeletal proteins (Musacchio et al., 1992, Pawson & Gish, 1992). SH3 domains thus play a pivotal role in the assembly of important signalling complexes at functionally relevant intracellular locations. They interact with target proteins through proline-rich domains where the basic motif requirement for SH3 interaction is PxxP (Mayer & Baltimore, 1993, Pawson & Gish, 1992). Such a motif is found in the N-terminal splice regions of the rat PDE4A splice variant RPDE6 and its human counterpart PDE46 as well as PDE4D4. RPDE6 was the first specific PDE to be shown to interact with an SH3 domain, namely that of v-Src. This interaction occurred by virtue of its N-terminal splice region (O'Connell et al., 1996). The binding of RPDE6 to the SH3 domain of v-Src did not cause a change in PDE activity.

Such interactions may be important in targeting the expression of specific PDE4 isoforms to specific locations within the cell.

1.5.7.13. Therapeutic role of PDE4 inhibitors

A large number of compounds which can serve as selective PDE4 inhibitors have been described (rolipram, Ro 20-1724, CDP840, RP73401) and these compounds inhibit PDE4 enzymes with IC_{50} values in the nM - μ M range (Alvarez et al., 1995, Muller et al., 1996, Souness & Scott, 1993). To date, however, there is no compound which can potently and selectively discriminate between the various PDE4 isoforms.

Rolipram is a highly specific and selective inhibitor of PDE4s and has been reported to inhibit all known members of the PDE4 family to a relatively equal extent (Bolger et al., 1993, Muller et al., 1996). Rolipram is known to interact with PDE4s in at least two distinct fashions: either by binding to 'high-affinity' binding sites at very low concentrations ($K_d = 0.4 - 6$ nM) or by a 'lower-affinity' interaction ($K_i = 0.06 - 1$ μ M) which is presumed to occur at the enzyme catalytic domain (Schneider et al., 1986, Torphy et al., 1992).

PDE4s are the predominant cAMP hydrolysing enzymes family found in most, if not all, immune and inflammatory cells (Erdogan & Houslay, 1997, Manning et al., 1996, Thompson et al., 1976, Torphy & Udem, 1991, Torphy et al., 1995, Verghese et al., 1995). Investigations have revealed that many functions of the immune system and inflammatory responses are inhibited by agents that increase intracellular cAMP concentrations. Elevation of cAMP levels by rolipram can markedly inhibit the production of the pro-inflammatory mediator TNF- α but not other cytokines such as IL-1 and arachidonic acid metabolism in monocytes (Kelly et al., 1996, Souness et al., 1996). PDE4 inhibitors rolipram and RP 73401 suppress the functioning of eosinophils by reducing their superoxide generation, infiltration and adhesion functions (Kaneko et al., 1995, Souness et al., 1995, Underwood et al., 1993). Inhibition of PDE4s in T-lymphocytes causes a

profound decrease in exocytosis, proliferation, cytokine production (IFN- α , IL2, IL6) and expression of CD7 and IL2 receptors (Anastassiou et al., 1992, Averill et al., 1988, Giembycz et al., 1996, Krause & Deutsch, 1991, Takayama et al., 1988). Enhanced cAMP levels in neutrophils can inhibit both PLA₂ and PLD activities but not PLC responses (Nakashima et al., 1995). Due to the effect of selective PDE4 inhibitors on the reduction of pro-inflammatory cell functions, inhibitor development has focused on the central nervous system (CNS), with emphasis on depression (Krause et al., 1990, Scott et al., 1991), in disorders of the immune and inflammatory systems, vascular intimal proliferation and relaxation of airway smooth muscles (Francis et al., 1988, Pan et al., 1994). Experimental and clinical trials have been done to examine the role of such inhibitors in the treatment of atopic and inflammatory diseases including atopic dermatitis (Chan et al., 1993) and particularly asthma (Giembycz, 1996, Torphy & Udem, 1991) as well as in autoimmune diseases such as arthritis and multiple sclerosis (Tracey & Cerami, 1993), viral diseases such as AIDS (Fauci et al., 1991) and bacterial or parasitic infections like septic shock (Sekut et al., 1995). However, although PDE4 inhibitors promise to be useful in the treatment of certain diseases, it appears that they also have some unwanted side-effects. A particular contra-indication of PDE4 inhibitors is gastro-intestinal discomfort, mainly indicated by nausea and vomiting (Palfreyman & Souness, 1996).

1.5.8. PDE5: cyclic GMP-specific PDEs (cGMP PDE)

PDE5 enzymes have been purified from rat lung (Francis & Corbin, 1988) and are present in a variety of tissues including platelets (Hamet & Coquil, 1978), vascular smooth muscle, rat spleen (Coquil, 1983) and guinea pig lung (Burns et al., 1992, Davis & Kuo, 1977). To date, only one gene isoform has been cloned for this family, BTPDE5A (McAllister et al., 1993). Although, PDE5 and the other cGMP-specific PDE, PDE6 have similar kinetic properties, sequence alignment of

catalytic region indicates only around 60 % identity (Beavo, 1995). Therefore, this demonstrates that they represent different gene families.

PDE5 has a high affinity for cGMP and practically no hydrolysing activity for cAMP (Table 1.1). It forms a homodimer of native mass ~177 kDa from two, ~93 kDa subunits (Francis et al., 1990). PDE5 also has two Zn²⁺ binding sites which are found in the catalytic domain (Francis et al., 1994) and whose role has yet to be determined.

Intriguingly, as in PDE2, PDE5 contains two distinct binding sites for cGMP. One of these is the catalytic site where cGMP is enzymatically converted to 5'-GMP and the other is a non-catalytic binding site. The non-catalytic cGMP-binding site is found towards the N-terminal regulatory portion of the protein, thus resembling PDE2 and PDE6 (McAllister et al., 1993). Binding of cGMP to the non-catalytic site of PDE5 induces a conformational change in an N-terminal domain of 142 amino acids, the result of which is that Ser⁹² becomes a target for phosphorylation by PKG (Francis et al., 1990, Thomas et al., 1990). It has also been shown that PKA catalyses the phosphorylation of the same site, although PKG phosphorylated this site at a 10-fold faster rate (Thomas et al., 1990). Phosphorylation at this site did not appear to modulate activity in the purified enzyme analysed in this study. However, in contrast to this other studies have shown that PKA can catalyse a 10-fold increase in the catalytic activity of the guinea pig lung PDE5 and also decrease the sensitivity of PDE5 to inhibition by zaprinast (Burns & Pyne, 1992, Burns et al., 1992).

1.5.9. PDE6: photoreceptor PDEs (cGMP-specific PDE)

PDE6 enzymes play key roles in photoreceptor signal transduction. In retinal rod photoreceptor cells, visual signalling is triggered upon the absorption of photons by rhodopsin. Photoexcited rhodopsin leads to an activation of the retinal GTP-binding protein (transducin). Rapid hydrolysis of cGMP by activated PDE6 results in closure of the cGMP-dependent Na⁺ channel in the plasma membrane which is normally kept open by cGMP (Stryer, 1986).

Three distinct genes encode this PDE family (Table 1.1); one cone and two rod PDE genes. Rod PDE6 protein consists of α (88 kDa) and β (84 kDa) and two inhibitory γ (11 kDa) subunits (Lipkin et al., 1990, Miki et al., 1975, Pittler et al., 1990) as indicated by sequence comparison and DNA hybridisation. PDE6 α and PDE6 β contain two catalytic sites that are inhibited by the binding of PDE6 γ . The cone PDE6 consists of α homodimers (94 kDa) and 11- and 13 kDa inhibitory subunits (Gillespie, 1990). Both rod and cone PDE6s contain two internal repeats that make up the noncatalytic cGMP-binding domain conserved in PDE2, PDE5 and PDE6 families (Gillespie, 1990, McAllister et al., 1993, Sonnenburg et al., 1991, Stroop & Beavo, 1992).

Phosphorylation of rod PDE6s has been shown to occur within the catalytic (Udovichenko et al., 1993) and inhibitory subunits (Tsuboi et al., 1994) and this is achieved by different kinases. Phosphorylation of Thr³⁵ in the bovine PDE6 γ subunit by PKC increases the inhibitory activity of PDE6 γ , perhaps by increasing its affinity for PDE6 $\alpha\beta$ catalytic subunits (Udovichenko et al., 1994).

IBMX inhibits the bovine rod PDE6 with a K_i of 10 μ M in a similar way to all other PDE enzymes (except PDE7) (Baehr et al., 1979, Gillespie & Beavo, 1989).

1.5.10. PDE7: cAMP-specific rolipram-insensitive PDE

Only one member of the *PDE7* gene family has been cloned to date. This was from a human glioblastoma cDNA library (Michaeli et al., 1993) using a method similar to that used to isolate rat DPD (Colicelli et al., 1989). Northern blotting and transcript analyses have shown that PDE7 is highly abundant in human skeletal muscle with much lower levels noted in a number of other human tissues including kidney, brain, heart and some, but not all, T lymphocyte forms (Bloom & Beavo, 1994, Giembycz et al., 1996, Ichimura & Kase, 1993, Michaeli et al., 1993).

The PDE7 clone (HCP1) shows high homology in the presumed catalytic domain of ~300 amino acids to other cAMP PDEs. This PDE enzyme is most closely related to the PDE4 family (<60 %) in the catalytic region which is consistent with its specificity for cAMP and insensitivity to cGMP both as a substrate and inhibitor. However, PDE7 activity is not inhibited by PDE4 specific inhibitors such as Ro 20-1724 and rolipram (Table 1.1). HCP1 appears not to be a full-length cDNA and thus only this truncated form has been characterised to date. Recombinant PDE7 exhibits high affinity for cAMP ($K_m = 0.2 \mu\text{M}$) and is most similar to the K_m of PDE3 but it was not selectively inhibited by the PDE3 inhibitors milrinone and cGMP and, unlike PDE1, its activity was not affected by Ca^{2+} / CaM. Additionally, PDE7 family enzymes appear to be resistant to inhibition by the non-selective reversible PDE inhibitor, IBMX (Lavan et al., 1989, Michaeli et al., 1993).

In this thesis, I have investigated the catabolism of cAMP in human Jurkat cells, which serve as a model for human T lymphocytes. The research concentrated on the regulation of cAMP PDEs at the transcriptional and translational levels using cAMP-elevating agents. I then characterised the five human PDE4D isoforms

expressed in COS7 cells including the PDE4D1 and PDE4D2 forms which I had shown to become induced in Jurkat T-cells whose cAMP levels had been chronically elevated. I then studied the role of N- and C-terminal regions of the inactive human PDE4A splice variant, 2EL which was originally cloned from a Jurkat T-cell library.

CHAPTER 2

MATERIALS and METHODS

2.1 Materials

2.1.1. Radiochemicals:

Amersham PLC	[8- ³ H] Adenosine 3', 5'-cyclic
Amersham, Bucks., U.K.	monophosphate
	[5, 8- ³ H] Adenosine 3', 5'-cyclic
	monophosphate
	[¹²⁵ I]-labelled anti-mouse IgG
	[¹⁴ C]-labelled protein molecular weight
	markers

2.1.2. Tissue culture plastic ware:

Costar Co	Filters (0.22 μ m)
U.S.A.	Multiple cell plates
	50 ml centrifuge tubes
	Tissue culture pipettes

2.1.3. Tissue culture medium:

Gibco BRL	DMEM (Dulbecco's Modified Eagle
Paisley, U.K.	medium, 1 x)
	Foetal bovine serum
	Nuserum
	Glutamine (200 mM)
	Penicillin (10 000 IU/ml)
	RPME-1640 medium
	Sodium bicarbonate (7.5 %)
	Streptomycin (10 mg/ml)
	Trypsin/EDTA

Nunc	Cryotubes
InterMed, U.K.	25 and 80 cm ² tissue culture flasks
	6 well plates
Whatman Ltd.	Whatman 3 mm Paper
Maidstone, U.K.	Whatman 0.2 μM nitrocellulose paper

2.1.4. General reagents

2.1.4.1. Chemical compounds:

BDH, MERCK Ltd	β-Mercaptoethanol
Glasgow, U.K.	Charcoal (Norit Gsx)
	EDTA (Ethylenediaminetetraacetic acid)
	Glycine
	Glucose
	HEPES (N-2-Hydroxyethylpiperazine-N'-2-ethane-sulphonic acid)
	Methanol
	Peptone from casein (pancreatically digested)
	SDS (Sodium dodecyl sulphate)
	TEA (Triethanolamine hydrochloride)
	Universal indicator
	Yeast extract
Sigma	EGTA [Ethylene glycol-bis (β-aminoethyl ether) N,N,N',N'-tetraacetic acid]
Poole, Dorset, U.K.	Tris
	Triton X-100
	Tween-80

Fisons Scientific Equipment
Loughborough, U.K.

Dimethyl sulphoxide
Glycerol
Sodium Acetate
Sodium Citrate
Sucrose

Boehringer

Lewes, E. Sussex, U.K.

Dithiothreitol
Nicotinamid adenine dinucleotide
(reduced form)

2.1.4.2. Biochemical reagents:

Sigma

Poole, Dorset, U.K.

Actinomycin D
Ampicillin
Antipain
Aprotinin
Benzamidine hydrochloride
Bovine brain calmodulin
Bromophenol blue
BSA (Bovine serum albumin)
Chloroquine
Cholera toxin
Cyclic AMP
Cyclic GMP
Dextran T-500 (Mw 500 kDa)
Digitonin
Dowex 1X8-400 (chloride form; 200-
400 mesh)
8-bromo cAMP
PHA (Phytohaemagglutinin)

	IBMX (3-isobutyl-1-methylxanthine)
	Pepstatin A
	PMSF (Phenylmethylsulphonyl fluoride)
	Snake venom (<i>Hannah ophiophagus</i>)
	Sodium pyruvate
	TEMED (N,N,N',N'-Tetramethylethylene diamine)
	Trypan Blue (0.4 %)
	12-O-tetradecanoylphorbol 13-acetate (TPA/PMA)
Peptide Research Foundation London, U.K.	Leupeptin
Calbiochem Cambridge, U.K.	Forskolin Pansorbin
Bio-rad Laboratories Ltd Hertfordshire, U.K.	30 % Acrylamide/bis acrylamide mix (29:1) Bradford reagent
National Diagnostics Buckinghamshire, U.K.	Ecoscint scintillation fluid
M & B Dagenham, U.K.	Ammonium persulphate
Gibco BRL Paisley, Scotland	Pre-stained molecular weight markers

Amersham International Amersham, Buckinghamshire U.K.	Anti-mouse IgG conjugated to horseradish peroxidase ECL (enhanced chemiluminescence)
SAPU Scotland, U.K.	HRP conjugated anti-rabbit IgG
Gift from Aktiengesellschaft Berlin 65, Germany	Rolipram {4-[3-(cyclopentoxyl)-4- methoxyphenyl]-2-pyrrolidone }
Gift from Dr. T. Podzuweit Planck Institute, Bad Nauheim, Germany	EHNA [erythro-9-(2-hydroxy-3-nonyl)-Max adenine]
Pfizer Central Research Sandwich, Kent, U.K.	Cilostimide {4,5-dihydro-6[4-(1H- imidazol-1-yl)phenyl]-5-methyl-3(2H) pyrazone }

2.1.5. Molecular Biology reagents:

Pharmacia Biotech Herts, U.K.	First strand cDNA synthesis kit
Stratagene Cambridge, U.K.	pCRscript AMP cloning kit <i>Pfu</i> DNA polymerase
Sigma Poole, Dorset, U.K.	Agarose (low melting temperature) DEPC (Diethyl pyrocarbonate (1 %) in water) Ethidium bromide Tri-reagent

Promega Deoxyribonucleoside triphosphates
Southampton, U.K. MgCl₂
Phix174 DNA/Hae III Markers
Taq buffer
Taq polymerase
Wizard™ Mini, Maxi, PCR and Clean-up
preps (DNA purification system)

2.1.6. Equipment:

Progene PCR amplification machines
Cambridge, U.K.

2.1.7. Cell lines

2.1.7.1. COS7 cells

These are SV-40 immortalised kidney fibroblasts isolated from an African Green monkey. They express SV-40 large antigen and therefore permit the replication and expression of plasmids which contain an SV-40 origin and promoter region. They were cultured in DMEM (x1) medium supplemented with 1 % (v/v) penicillin/streptomycin, glutamine and 10 % (v/v) foetal bovine serum.

2.1.7.2. Human leukaemic T-cell line Jurkat (J6)

The Jurkat T-cell line was obtained from European Collection of Cell Cultures (ECACC), Centre for Applied Microbiology and Research, Salisbury, UK. This is a proliferating mature T-cell line which was isolated from a 14 year old boy suffering from acute lymphoblastic leukaemia and grown in suspension with a doubling time of 24 h. They were cultured in plastic flasks (80 cm²) in RPMI-1640 medium supplemented with 5 % (v/v) heat-inactivated foetal bovine serum, 1% (v/v) penicillin/streptomycin and 1 % (v/v) glutamine solution at 37 °C in a

humidified atmosphere of 95 % air, 5 % CO₂. Culture medium was changed twice a week. Cells were seeded at 1 in 5 dilution into fresh, pre-warmed medium under sterile conditions.

On removing cells from liquid nitrogen the medium was further supplemented with 5 % (v/v) FBS, 0.1 % (v/v) gentamycin and 0.1 % (v/v) ciproxin for the first week of culture. When freezing cells, they were first pelleted by centrifugation at 440 g_{av} for 5 min before being resuspended in the freezing medium at a density of 10⁷ cells/ml. This medium consisted of 90 % FBS (v/v) and 10 % (v/v) DMSO. After aliquoting into cryotubes the cells were frozen slowly overnight in a -80 °C freezer and then stored in liquid nitrogen until required.

2.2. Methods

2.2.1. Treatment of Jurkat T-cells with vehicles

The cells were split two days before treatment with any of the vehicles and on the day of incubation they were harvested. The cell pellets were then diluted with fresh medium at the densities of 1.0-1.5 x 10⁶ cells/ml. They were then incubated as indicated for the particular experimental procedure. At the end of the incubation the cells were washed twice with serum-free medium, counted and homogenised (section 2.2.1.2.).

2.2.1.1. Determination of cell number and viability

An aliquot of Jurkat T-cells in suspension was mixed with an equal volume of Trypan Blue solution (0.4 %) and the number and viability of the cells was determined. This was achieved by viewing the cells under a light microscope in a haemocytometer. The viability of cells was established as the percentage of cells that excluded the Trypan Blue dye, that is the proportion of total cells whose

membranes remained intact and appeared white under the microscope (>95 %) were determined to be viable. The cell number was calculated by using the grid on the slide which ensured that the same area was counted for each determination. 100 cells in 32 squares denoted 1×10^6 cells per ml thus the viable cell number could be calculated.

2.2.1.2. Cell lysis and homogenisation of Jurkat T-cells

Following incubation, cells were harvested by centrifugation (5 min, $440 g_{av}$, at room temperature), and then washed twice with serum-free RPMI-1640 medium under the same centrifugation conditions and resuspended in ice-cold homogenisation buffer. This buffer comprised 10 mM tris/HCl pH 7.4 containing 0.25 M sucrose, 25 mM $MgCl_2$, 1 mM EDTA, 0.5 mg/ml detergent digitonin, 0.1 mM dithiothreitol and protease inhibitors at a final concentration of 40 μ g/ml PMSF, 156 μ g/ml benzamidine, 1 μ g/ml each of aprotinin, leupeptin, pepstatin A and antipain. The protease inhibitors were initially dissolved as a 1000 x stock in 100 % DMSO before addition to the buffer. This extract was left on ice for 5-10 minutes prior to use. The disruption method was described previously (Harnett et al., 1991). Using digitonin released all (>98 %) of the lactate dehydrogenase activity (section 2.2.13) associated with these cells and also rendered soluble all (>98 %) cAMP phosphodiesterase activity. This method of cell disruption was employed rather than either homogenisation or sonication procedures as they not only failed to disrupt all the cells as indicated by Trypan Blue exclusion but caused disruption in a highly variable fashion. Samples were then taken either for immediate assay of PDE activity or were snap frozen in liquid nitrogen and stored at $-80^\circ C$ until use.

2.2.2. Antibody preparation

Polyclonal anti-PDE4A sera was used for immunoprecipitation and immunoblotting. It was developed against a C-terminal human PDEA fusion protein by using the a 300 bp DNA fragment which was cloned into the inducible bacterial expression vector pGEX-3X (Huston et al., 1996) and raised in New Zealand White rabbits. Immunoblotting was also carried out using monoclonal antibodies designed to be specific for particular PDE4 families. A glutathione-S-transferase (GST) fusion proteins formed from portions of the C-terminal ends found to be unique to each of the PDE4 families. They were generated using the vector pGEX2T. Mice were immunised, hybridomas were generated and the monoclonal antibodies were cloned using standard methods. Antibody names and peptides are listed below:

<u>Antibody code</u>	<u>PDE epitope</u>	<u>Antibody name</u>
PDE4A-GST (polyclonal)	788-886 in PDE46	PDE4A
66C12H (monoclonal)	800-810 in PDE46	PDE4A
96G7A (monoclonal)	529-558 in TM72	PDE4B
61D10E (monoclonal)	634-650 in PDE4D3	PDE4D

2.2.3. SDS-PAGE electrophoresis

Separation of proteins by electrophoresis was carried out on 8 % polyacrylamide gels as previously described (Laemmli, 1970). Samples (5-100 µg protein) were solubilised in a volume of Laemmli buffer containing 0.1 M Tris/HCl pH 6.8, 20 % (v/v) glycerol, 2 % (w/v) SDS, 0.02 % Bromophenol blue and 5 % (v/v) β-mecaptoethanol (which was added just prior to use) and immediately boiled for 3 min. An 8 % resolving gel containing 30 % acrylamide/bisacrylamide (29:1), 1.5 M Tris/HCl pH 8.8, 10 % (w/v) SDS, 10 % (w/v) ammonium persulphate and

0.06 % (v/v) TEMED was made up before being allowed to set to a final volume of 30 ml in 1.5 mm glass electrophoresis apparatus. Then 5 % stacking gel containing 30 % acrylamide/bisacrylamide (29:1), 1 M Tris/HCl (pH 6.8), 10 % (w/v) SDS, 10 % (w/v) ammonium persulphate and 0.1 % TEMED was made up to a final volume of 8 ml before being poured on the top of the resolving gel with a comb in place. Samples and prestained protein molecular weight standards (214.2 kDa, 111.4 kDa, 74.25 kDa, 45.5 kDa and 29.5 kDa) were loaded in the wells and electrophoretically separated in running buffer (0.2 M Glycine, 25 mM Tris, 0.1 % (w/v) SDS) at 8 mA/gel overnight or 60 mA/gel for 3-4 h with cooling. When the dye front reached the edge of the gel electrophoresis was stopped and proteins transferred to nitrocellulose paper by Western blotting.

2.2.4. Western blotting

Proteins were transferred from SDS gel to nitrocellulose paper using constant current and 90 volts for 90 min in a Bio-Rad transblot apparatus with blotting buffer (0.2 M Glycine, 25 mM Tris, 20 % Methanol). Non-specific binding to filters was blocked by incubation in 5 % non-fat dried milk powder/TBS buffer (500 mM NaCl, 20 mM Tris, pH 7.4) at room temperature for 90 min or overnight. The blot was washed briefly with distilled water before washing twice with TBS containing 0.2 % Tween-80 and twice with TBS, each for 5 min. The nitrocellulose was then immunoblotted with a 1:300 or 1:2000 dilution of the appropriate antisera with TBS containing 1 % dried milk powder for 2 h.

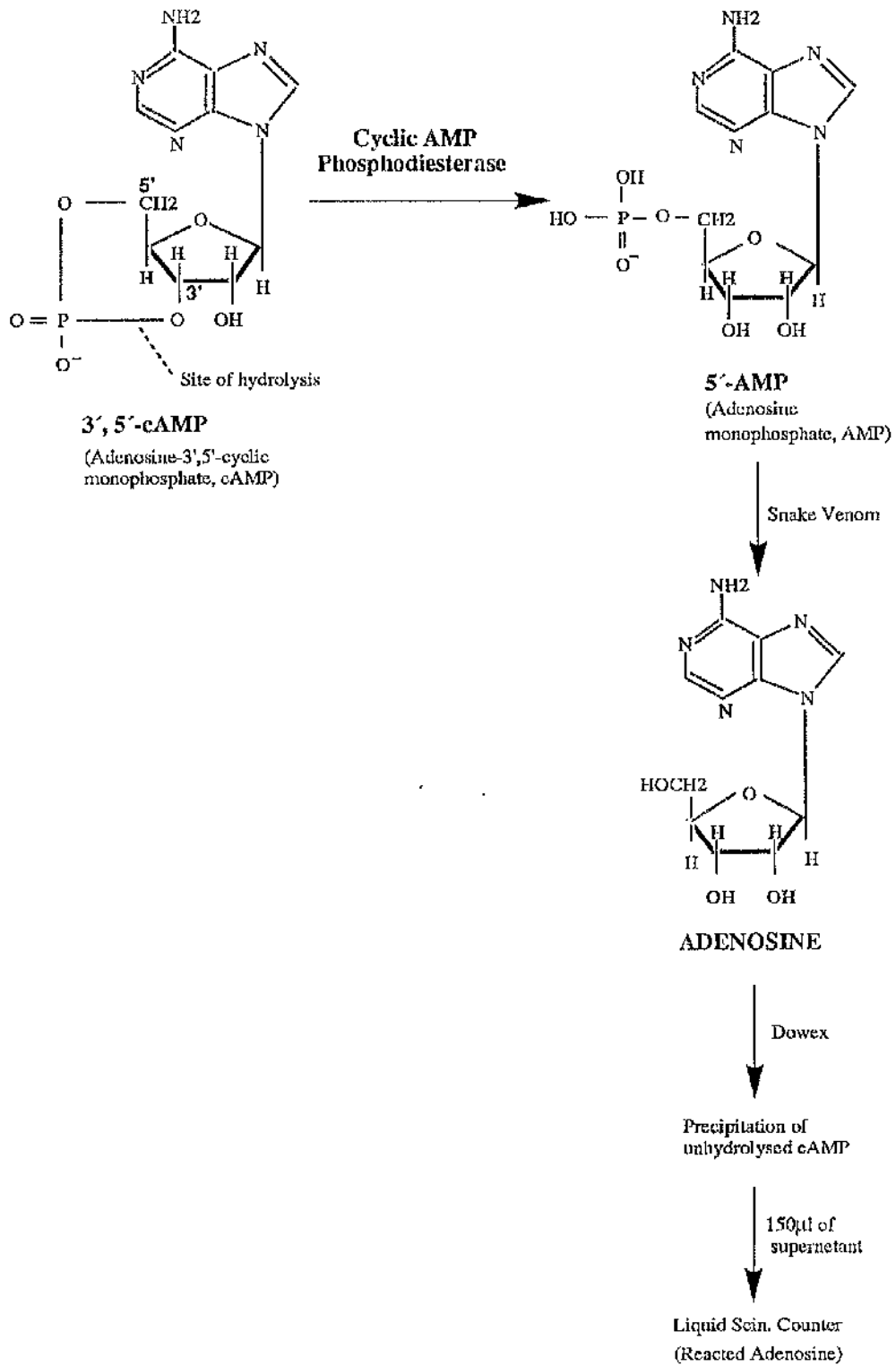
The blot was then washed as above and then incubated for 90 min at room temperature with a 1:1000-2000 (in TBS buffer containing 1 % non-fat dried milk powder) dilution of anti-rabbit peroxidase linked IgG, anti-mouse IgG or ¹²⁵I-labelled anti-mouse IgG. With anti-rabbit peroxidase linked IgG and anti-mouse IgG, the Amersham enhanced chemiluminescence (ECL) Western blotting

visualisation protocol was used to detect the bands, whilst ^{125}I -labelled bands were visualised by phosphoimaging. Quantification of the relative amounts of antigen present in each of the fractions was done in a variety of ways, in order to identify situations where a linear relationship held between the amount of antigen present and the magnitude of the signal detected. The densitometric scanning of the ECL experiments was done using both photosensitive Amersham film and Kodak X-ray film with various exposure times and a range of applied protein concentrations so as to identify a linear detection range. Confirmation was also obtained in selected instances using ^{125}I -labelled anti-mouse IgG with excision of the labelled bands identified by auto-radiography for counting.

2.2.5. Cyclic AMP phosphodiesterase assay

Cyclic nucleotide phosphodiesterase activity was determined by a modification of the two-step assay (Rutten et al., 1973, Thompson & Appleman, 1971) as previously described by (Marchmont & Houslay, 1980b) using [^3H]-cAMP and sufficient unlabelled cAMP to produce the desired substrate concentration. Briefly, [^3H]-cyclic nucleotide (8- ^3H -adenosine 3',5'-cyclic mono-phosphate) is hydrolysed to labelled nucleotide 5'-mono-phosphate by PDEs (Figure 2.1). The nucleotide mono-phosphate ring is then converted to the corresponding labelled nucleoside by incubation with snake venom which has 5'-nucleotidase activity. The conditions are such that complete conversion takes place within the incubation time. Unhydrolysed cyclic nucleotide is separated from the nucleoside by batch binding of the mixture to Dowex 1-chloride. This binds the charged nucleotides, but not the uncharged nucleosides.

Figure 2.1. The principle of the cyclic AMP phosphodiesterase assay



2.2.5.1. Preparation of reagents

(i) 3',5'-cyclic AMP: 1 mM stock solution was prepared and diluted in 20 mM Tris/HCl, 10 mM MgCl₂ pH of 7.4 (Tris/MgCl₂ buffer) and aliquots were frozen as stock. The concentration required for the assay was obtained by diluting the stock on the day of each assay. Mg²⁺ ions which were in dilution buffer are required as a cofactor for cAMP PDE activity.

(ii) Effectors: Rolipram, cilostimide and IBMX were dissolved in DMSO at concentrations such that the final DMSO concentration was 0.1 %. This was demonstrated to have no effect on PDE activities (Michie, 1995). All the ligands were stored at -20 °C. Cyclic GMP and EHNA were dissolved in distilled water. On the day of the assay, they were subsequently diluted in 20 mM Tris/HCL, pH 7.4 to the desired concentration .

(iii) Snake venom (*Hannah ophiophagus*): A 10 mg/ml stock solution was dissolved in distilled water and stored frozen in aliquots. This was diluted to 1 mg/ml in distilled water for use in the assay.

(iv) Dowex 1x8-400-chloride: This was prepared as described previously (Thompson et al., 1979). Briefly, at 4 °C, 400 g Dowex 1-chloride was washed with 1 M NaOH for 15 min. Resin was then washed extensively with distilled water, until the pH of the eluate fell to 7.0. After this time the resin was washed with 1 M HCl for 15 min, followed by more washing in distilled water until the eluate pH rose to 3.0. The dowex was stored at 4 °C with distilled water (1:1). For use in the assay, the Dowex was further diluted with ethanol, to a final ratio of Dowex:water:ethanol (1:1:1, by volume). Ethanol is used in order to prevent non-specific binding of adenosine to Dowex and to prevent adenosine deaminase converting adenosine to inosine, which can also bind to Dowex.

2.2.5.2. Assay procedure

Appropriate amounts of homogenate enzyme extracts were used to give linear time courses. These were incubated in a final volume of 100 μl containing 25 μl of phosphodiesterase effector maintained at 4 $^{\circ}\text{C}$ in 1.5 ml Eppendorf tubes. Blanks were included with every experiment by replacing the enzyme sample with 25 μl of the homogenisation buffer and the effector buffer. The reaction was initiated with the addition of 1 μM cAMP, unless stated otherwise. This substrate contained 50 μl of 0.15 μCi cAMP. The tubes were mixed by vortexing and incubated for 10 min at 30 $^{\circ}\text{C}$. The reaction was terminated by placing the tubes in a boiling water bath for 2 min. The samples were then allowed to cool to 4 $^{\circ}\text{C}$. 25 μg snake venom was added to the tubes and they were incubated for 10 min at 30 $^{\circ}\text{C}$. The tubes were then placed on ice and 400 μl of a freshly prepared slurry of Dowex:ethanol:water (1:1:1) was added. During this addition the Dowex was stirred gently in order to ensure a homogeneous suspension was being added. The tubes were left at 4 $^{\circ}\text{C}$ for 30 min, remixed and then centrifuged at 16 000 g_{av} for 3 min to sediment out the Dowex resin. A 150 μl aliquot of supernatant was removed and mixed with 2 ml Ecoscint and the amount of ^3H -adenosine was counted in a LKB scintillation counter for 60 s per sample.

2.2.5.3. Calculation of specific activities

The corrected cpm per sample was obtained by subtracting the blank value in each case. Determining the protein content (section 2.2.10.) of each sample allowed the results to be expressed in terms of specific activity. The results were then calculated as pmols cAMP hydrolysed/min/per mg of protein \pm SD.

2.2.6. Determination of kinetic constants

Value of K_m was determined by varying the amount of unlabelled cAMP ranging from 0.25 μM to 25 μM (unless stated otherwise) in the reaction cocktail in the presence of a fixed concentration of radiolabelled cyclic nucleotide tracer. In order to calculate K_m values the data from PDE assays were computer fitted to the hyperbolic form of the Michaelis-Menten equation where $V_{observed} = (V_{max} [S] / (K_m + [S]))$ using the Ultrafit (Levenberg-Marquardt algorithm with the KaleidaGraph package for the Apple Macintosh, experimental errors supplied; Biosoft, U.K.) graphical package. In each case, the 'robust weighting' facility was used and the 'goodness of fit' index was not less than 0.99 with each estimation.

2.2.7. Determination of IC_{50} values

Dose-effect studies were performed with 1 μM cAMP (unless stated otherwise) as substrate over a range of inhibitor concentrations as shown in the appropriate figures. Inhibitors were added at a volume of 25 μl , which was included in the assay volume of 100 μl . As such, a 4 times final inhibitor concentration was prepared, of which 25 μl was added to each reaction mixture. For each inhibitor study, a DMSO control was included in the assay which contained the highest DMSO concentration used. In each case, the DMSO concentration was shown to have no effect. The data analysed by curve-fitting to the appropriate equation using the Levenberg-Marquardt algorithm with the KaleidaGraph package for the Apple Macintosh in order to derive IC_{50} values with associated errors. The effector concentration used is described in the appropriate figure legends.

2.2.8. Relative V_{\max} determinations

Relative activity was done using a modification of the methodology described previously by others (Shakur et al., 1993, McPhee et al. 1995). Increasing concentrations of protein (5 to 50 μg) from COS7 cells, transfected with different PDE expressing-plasmids, were analysed by Western blotting either using ^{125}I -labelled second (anti-mouse) antibody as a detection system or an ECL procedure. For ^{125}I -labelling, quantitative data was obtained from phosphoimager analysis. For ECL, the blots were scanned. The appropriate signal absorbance (A) versus amount of protein (μg) was plotted in order to gauge the relative concentrations of PDE protein in each of the preparations. For the V_{\max} determinations, amounts of protein from transfected cells which would provide equal amounts of PDE protein were taken for PDE assay. Relative V_{\max} values could be calculated using the Michaelis equation and the experimentally derived K_m (see section 2.2.6.) values.

2.2.9. Cyclic AMP determination

2.2.9.1. Assay principle

Determination of cAMP content was based on the saturation assay of (Brown et al., 1972) as described (Kishihara et al., 1993). The binding protein utilised in the assay is cyclic AMP-dependent protein kinase (PKA) which has binding sites for cAMP. Following stimulation of the cells in the presence of the desired effectors for a fixed time the cells were lysed, thus releasing the cytosolic cyclic nucleotides. After neutralising, the cells were incubated with [^3H]-labelled cAMP (5- and 8-position of the adenine ring) and cAMP binding protein, allowing competition of labelled and unlabelled cAMP for a limited number of binding sites on the binding protein. A standard curve was obtained by incubating known concentrations of unlabelled cyclic AMP with fixed amounts of binding protein and radioactive cyclic AMP. Thus the unknown cAMP concentrations can be determined in samples by

comparison with the standard curve. After the incubation, activated charcoal was added to the sample to absorb unbound cyclic nucleotide from the solution. The charcoal with the bound cyclic nucleotide was removed by a brief centrifugation step. 300 μ l of the supernatant was mixed with Ecospint and the cAMP content was determined (see 2.2.9.5.).

2.2.9.2. Preparation of cyclic AMP binding protein

A crude preparation of cAMP binding protein was made according to the procedure of (Brown et al., 1972) using bovine adrenal glands which are a rich source of this enzyme. Adrenal glands (20-30), obtained from the abattoir were transported to the laboratory on ice and all procedures were carried out at 4 °C. The fat was removed from the outside of glands, and they were then hemisected revealing the pale coloured inner medulla and the darker outer cortex. The medulla was removed and discarded while the cortex was retained. One volume of tissue was homogenised in one and a half volumes of buffer (250 mM sucrose, 25 mM KCl, 5 mM MgSO₄, 50 mM Tris/HCl, pH7.4) in a Waring blender. The homogenate was filtered through muslin and then centrifuged at 15 000 rpm using an MSE 18 centrifuge for 15 min at 4 °C. The supernatant was decanted through filter paper and the eluate was aliquoted into 1 ml fractions and stored at -20 °C for up to 3 months. Separate samples were thawed and diluted for each assay.

2.2.9.3. Assessing intracellular cAMP concentrations

Jurkat T-cells were prepared as described previously (section 2.2.1.2.) and resuspended at a density of 1×10^7 cells/ml in RPMI-1640 medium. The agonist was added to the culture and incubated at 37 °C. After the appropriate incubation period, 100 μ l (1×10^6 cells/assay) of ligand treated sample was placed into a microfuge tube containing 100 μ l of 4 % perchloric acid to terminate the reaction

(samples were assayed in triplicate for each condition). The cells were incubated at 4 °C for 3 min to allow the lysing of the membrane and the extraction of the cyclic nucleotides. After this time the cell debris was removed by centrifuging at 16 000 g_{av} for 2 min. Universal indicator was added to the supernatant which made the solution turn pink. The solution was then neutralised by addition of 2 M KOH/0.5 M triethanolamine (TEA) dropwise until the solution turned green. Any precipitate that formed was pelleted in a microfuge for 3 min and 50 μ l of the supernatant was removed for determination of intracellular cAMP concentration using a cAMP binding protein prepared as described previously (section 2.2.9.2.).

2.2.9.4. Preparation of reagents for assay

(i) [5, 8-³H]-cyclic AMP: 65 μ l (~50 000 cpm) radioactive cAMP was added to 100 ml of cAMP assay binding buffer (50 mM Tris/HCl pH 7.4, 4 mM EDTA) and stored at 4 °C until required for use.

(ii) Binding protein: the binding protein was prepared (section 2.2.9.2) and then the aliquoted sample diluted in cAMP assay binding buffer to the desired concentration.

(iii) Charcoal solution: The charcoal solution was made up of 2 % (w/v) activated charcoal and 1 % (w/v) bovine serum albumin in cAMP binding buffer. This was stirred on ice for at least 45 min before it was required.

2.2.9.5. Assay procedure

As mentioned previously, a standard curve was carried out with each assay, for cAMP concentrations between 0.0625 and 16 pmols. This part of the assay was

carried out in duplicate, whilst the unknown samples were assayed in triplicate and was set up as follows:

Tube	Samples	Buffer (μ l)	[3 H]-cAMP (μ l)	Binding Protein (μ l)
1-2	-	200	100	-
3-4	-	100	100	100
5-22	Standards (0.0625-16)	50	100	100
23-25	Unknowns	50	100	100

Tube 1 and 2 were blanks, calculating the amount of cAMP not bound by charcoal, tubes 3 and 4 represented the total binding of cAMP and tubes 5-22 represent the standard curve, giving counts for fixed concentrations of cAMP, allowing unknown cAMP values to be calculated. The tubes were set up at 4 °C, with binding protein added last which allows a fair competition for binding sites between the labelled and unlabelled cAMP. They were vortexed and incubated at 4 °C for 2-3 h. After this 250 μ l charcoal solution was added and the tubes were immediately vortexed and spun in a microfuge for 5 min. This step was crucial because if the charcoal solution was not centrifuged promptly, cyclic nucleotides would be stripped from the binding protein. An aliquot of 300 μ l was removed from the resulting supernatant and added to 4ml Ecoscint and counted using scintillation counter fitted with a curve fitting programme. The results are determined as an average of the triplicates assayed and expressed as pmols cAMP produced/ 10^6 cells.

2.2.10. Protein determination

Protein was routinely measured by the method of (Bradford, 1976) with BSA as a standard. A standard curve was constructed using 0-20 μ g range of bovine serum albumin. The standard and unknown protein solutions were made up to a volume of 800 μ l with distilled water before the addition of 200 μ l of Bradford reagent and

the tubes were vortexed. Absorbance was determined at 595 nm using a Shimadzu UV-1201 spectrophotometer. Unknown concentrations were determined by plotting the standard curve (x axis = mg/ml of protein concentration, y axis = A_{595}) (Figure 2.2).

2.2.11. Immunoprecipitation

Homogenates (0.5-1 mg of protein) were resuspended in immunoprecipitation buffer (1 % Triton X-100, 10 mM EDTA, 100 mM $\text{NaH}_2\text{PO}_4 \cdot 2\text{H}_2\text{O}$, 50 mM HEPES, pH 7.2) containing protease inhibitors. For the solubilisation of the proteins this mixture was left at 4 °C for 10 min and centrifuged at 16 000 g_{av} for 4 min in a microfuge. Antiserum (1:50 final dilution) was added and the sample was mixed for 2 h at 4 °C. An aliquot (100 μl) of 10 % Pansorbin was washed twice in ice-cold PBS (140 mM NaCl, 2.7 mM KCl, 8 mM NaH_2PO_4 , 1.5 mM KH_2PO_4 , pH 7.4) then added to the homogenate. This mixture was then incubated as before. Following this, the sample was centrifuged in a microfuge for 2 min, the pellet was washed twice in PBS buffer and resuspended in Tris/MgCl₂ buffer (2.2.5.1.) for determination of PDE activity.

2.2.12. Expression of the PDE cDNAs in COS7 cells

2.2.12.1. DEAE dextran method of transient transfection

For the characterisation of various phosphodiesterases the SV-40 transformed monkey kidney cell line (COS7) was used. The cells were split at approximately 1/3 confluence by plating in 80 cm² flask or 10 cm diameter plates, 18 h before the transfection. For transfection, the culture medium was replaced with 5 ml of DMEM [10 % (v/v) Nuserum together with 0.1 mM chloroquine]. DNA for transfection (5-10 μg) was diluted in 250 μl of TE buffer (10 mM Tris/HCl, 0.1 mM EDTA, pH 7.6) and 200 μl of a 10 mg/ml DEAE-dextran solution. This

DNA/dextran mixture was incubated at room temperature for 15 min before being added dropwise to the cell culture. The cells were incubated at 37 °C for 4 h. The transfection medium was aspirated and the cells 'shocked' for 2 min with a 5 ml of 10 % DMSO in PBS at room temperature. The culture was then rinsed with PBS before DMEM, containing 10 % (v/v) foetal bovine serum, was added and the plates were incubated at 37 °C for 72 h. Mock-transfected cells were treated as above without addition of DNA.

2.2.12.2. Disruption of transfected COS7 cells

After cells were transfected as described above, they were prepared for homogenisation as follows: the growth medium was aspirated and the cells incubated in 5 ml (for 80 cm² flask) complete KHEM (50 mM KCl, 50 mM Hepes/pH 7.4, 10 mM EGTA, 1.92 mM MgCl₂, 1 mM DTT and a mixture of protease inhibitor cocktail (see section 2.2.1.2.) for 45 min at 4 °C. The cells were then washed with 5 ml of TEA/KCl (10 mM Triethanolamine/pH 7.2, 150 mM KCl) at 4 °C for 10 min, the buffer was aspirated and cells washed with 5 ml of KHEM incomplete buffer (as KHEM complete buffer but without protease inhibitors). Finally cells were washed with 1 ml of complete KHEM for 2 min and then the buffer drained. The cells were scraped into a final volume of about 100 µl per 80 cm² plate and this cell suspension was disrupted by 20 strokes of the pestle in a Dounce homogeniser.

2.2.12.3. Subcellular fractionation

A post-nuclear (P1) fraction was generated by centrifuging the cell homogenate for 10 min at 1 000 g_{av} in a refrigerated centrifuge at 4 °C. High-speed centrifugation for 1 h at 100 000 g_{av} at 4 °C of remaining supernatant yielded a membrane fraction (P2) pellet and a high speed supernatant (S) termed the cytosolic fraction.

The P2 pellet was then washed in KHEM and recentrifuged as before. Finally, the P2 pellet was resuspended in KHEM buffer to the same volume as the S fraction.

2.2.12.4. Treatment of membrane with high salt concentration

Membranes (200 μ g of protein) from COS7 cells previously transfected with various plasmid DNAs were treated with KHEM (100 μ l) buffer containing the indicated NaCl concentrations (final pH 7.2). The extracts were left on ice for 30 min before centrifugation at 100 000 g_{av} for 1 h at 4 $^{\circ}$ C. The resulting pellet was resuspended in KHEM buffer containing the appropriate NaCl concentration and the pellet and supernatant fractions analysed by Western blotting.

2.2.12.5. Solubilisation of membranes with Triton X-100

Detergent solubilisation involved the membranes (200 μ g of protein) from COS7 cells previously transfected with various plasmid DNAs. The extracts were treated with KHEM (100 μ l) buffer containing the indicated Triton X-100 concentrations. The membranes were left on ice for 30 min before centrifugation at 100 000 g_{av} for 1 h at 4 $^{\circ}$ C. The resulting pellet was resuspended in KHEM buffer containing the appropriate Triton X-100 concentration and the pellet and supernatant fractions analysed by Western blotting.

2.2.13. Lactate dehydrogenase assay

Lactate dehydrogenase activity was measured by the rate of oxidation of NADH which absorbs at a wavelength 340 nm therefore, the rate of decrease of optical density at 340 nm is a measure of enzyme activity. Briefly, 1.35 ml of 0.15 M Tris/HCl pH 7.4 and 50 μ l each of 10 mM sodium pyruvate and tissue sample were added to a 1.5 ml cuvette and used to zero a spectrophotometer set at 340 nm

and linked to a pen recorder. Free lactate dehydrogenase activity was measured by the addition of 50 μ l of 2 mM β -NADH and the trace followed for several minutes. Finally 10 % Triton/Tris was then added to the cuvette to release entrapped activity and the total activity was calculated from this trace. Lactate dehydrogenase activity was then calculated using the following:

$$\% \text{ cells broken} = \frac{(\text{Free LDH}) \times 100}{(\text{Total LDH})}$$

2.2.14. Precipitation of oligonucleotides

Synthesised oligonucleotides were supplied as NH_4OH solutions and had to be purified before use. 300 μ l of oligonucleotide solution, 30 μ l of 3 M sodium acetate (pH 4.6) and 1 ml of absolute ethanol were mixed together and incubated at -70°C for at least 30 min or overnight at -20°C . Oligonucleotides were then spun in a microcentrifuge at 16 000 g_{av} for 15 min. The supernatant was removed and discarded, leaving the pellet visible in the bottom of the tube. The pellet was then washed with 1 ml of 75 % ethanol and spun as above, after which it was either vacuum dried for 15 min or dried on air for about 30 min and then resuspended in 40 μ l of sterile dH_2O .

2.2.14.1. Quantitation of oligonucleotides

The principles of oligonucleotide concentration measurements are the same as for RNA (section 2.2.15.1.) except that here a solution of oligonucleotides with an $\text{OD}_{260} = 1$ contains approximately 33 μg of RNA per ml, therefore the reading was multiplied by the dilution factor and then by 33 to give the concentration per ml.

2.2.15. RNA extraction by Tri-Reagent

Total RNA was extracted from the cultured cells using a modification of the protocol originally described by (Chomczynski & Sacchi, 1987). Cells were lysed by the addition with 1ml of Tri-Reagent™ to either pre-washed 10×10^6 cells or confluent 80 cm² flask. Then the cell suspension was transferred into an Eppendorf tube and homogenised by 5-10 passages through a Gilson pipette tip. The homogenate was stored at room temperature for 5 min. Cell membranes/high molecular weight DNA and polysaccharides were pelleted by centrifugation (11 000 g_{av} for 10 min at 4 °C) and the supernatant transferred to a fresh microfuge tube. RNA was then separated from DNA and protein by the following phase separation: to each tube 0.2 ml RNase-free chloroform/ml of Tri-Reagent™ originally used was added and vortexed for 15 s and then stored at room temperature for 3 min. Following centrifugation at 11 000 g_{av} for 15 min at 4 °C most of the upper aqueous phase was transferred to new tube.

The RNA was then precipitated from this phase by adding 0.5 ml of propan-2-ol per 1 ml of Tri-Reagent used initially. Samples were left at room temperature for 5-10 min and centrifuged at 11 000 g_{av} for 10 min at 4 °C. RNA pelleted on the side and bottom of tubes.

The supernatant was discarded and 1 ml of 75 % ethanol was added to wash the RNA. Ethanol was removed by spinning at 7 000 g_{av} for 5 min at 4 °C and the RNA pellet either air-dried or dried under vacuum for 5-10 min. The RNA was resolubilised in (1 %) DEPC treated water by pipetting a few times and incubated for 10-15 min at 55-60 °C if necessary to help dissolve it.

2.2.15.1. Determination of RNA concentration

The concentration of the RNA was determined by measuring the absorbance, or optical density (OD), of a 10 μ l of sample at wavelengths of 260 nm and 280 nm in quartz cuvettes using a Shimadzu UV-1201 spectrophotometer. A 1/100 dilution of the resuspended RNA was used to read the absorbance against a dH₂O blank. The OD₂₆₀/A₂₈₀ ratio was determined, ideally yielding, a result of 1.8 to 2.0. The concentration of RNA as μ g/ml was calculated by the multiplication of the OD₂₆₀ by the dilution factor (100) and by a constant (40) where 40 = 1 OD gives 40 μ g RNA at 260 nm. Isolated total RNA (5 μ g/lane) was then checked by electrophoresis on 1.5 % agarose gel. Extracted RNA was either used fresh or stored at -80 °C until use.

2.2.16. First-strand cDNA synthesis

Preparation of first-strand cDNA was achieved using the 'First-strand cDNA synthesis kit' with a total reaction volume of 33 μ l. 5 μ g of total RNA was diluted with DEPC treated water to a total volume of 20 μ l. This was then denatured by heating to 65 °C for 10 min. Denatured RNA was then incubated with murine reverse transcriptase, 6 mM dithiothreitol, 0.6 mM of each dNTPs and 0.2 μ g of the supplied poly(dT) primer [*Not*I-d(T)₁₈] for 1 h at 37 °C. The resultant first strand cDNA synthesised using the RNA as a template was then stored at -20°C.

2.2.17. The Polymerase Chain Reaction (PCR)

The polymerase chain reaction is a technique for the *in vitro* amplification of specific DNA sequences by the simultaneous primer extension of complementary strands of DNA. Standard PCR amplification reactions were performed in 1 x PCR buffer (50 mM KCl, 20 mM Tris/HCl) with a total reaction volume of 50 μ l.

This contained final concentrations of 0.2 mM of each dNTP (adenine, guanine, thymidine and cytosine bases), 1.5 mM MgCl₂ together with 25 pmoles of 5'-end and 3'-end primers, 5 units of *Taq* DNA polymerase and 3 µl of template DNA. The PCR machine was programmed for denaturation/annealing and extension of the selected region by the primers. These were performed using various times, temperatures and repeated cycles. See individual experiments for relevant cycling conditions.

2.2.18. Agarose gel electrophoresis

The required amount of high melting temperature agarose (1.5 to 2 %) was dissolved in 18 ml of 0.5 x TBE buffer (45 mM Tris/HCl, 45 mM boric acid, 1 mM EDTA, pH 8.0) and melted in a microwave for 1 min. After cooling, the agarose was poured into an electrophoresis tank and allowed to settle. 5 to 10 µl of RT-PCR reaction mixture was loaded. In order to determine the size of the RNA/DNA fragments, Phix174 DNA/Hae III Markers were loaded also. Samples were analysed by electrophoresis in TBE buffer containing ethidium bromide (50 µg/150 ml buffer) at 75 mA for 90 min. After electrophoresis, the gel was visualised under UV light and photographed.

2.2.19. Purification of DNA from PCR products

RT-PCR products were separated by electrophoresis through 1.5 % low melting agarose gel. DNA bands (~ 300 mg) were excised using a sterile scalpel and transferred to Eppendorf tubes. DNA purification was performed according to 'Promega DNA purification systems'. The DNA slice was incubated in a waterbath until the agarose completely melted (~3 min). Then 1 ml of the purification resin was added and the solution mixed through for 20 s. The resin/DNA mix was then transferred into syringe barrels and a vacuum applied to

draw the solution through the syringe. Columns were washed by running 2 ml of 80 % isopropyl alcohol through the syringe and the vacuum re-applied. The resin was dried by continuing to draw a vacuum for an additional 1-2 min. After discarding the syringe, the minicolumn was transferred to a 1.5 ml microfuge tube and spun for 20 s in a microfuge to elute the bound DNA fragment. The minicolumn was placed in a fresh microcentrifuge tube and 30-50 μ l of dH₂O (preheated to 70 °C) was added to the minicolumn. After incubation at room temperature for 1 min the DNA was collected by centrifuging the tube in a microfuge at 16 000 g_{av} for 5 s. 50 μ l of purified DNA fragment was then blunt-ended by incubating with 1 μ l of *Pfu* DNA polymerase (Stragene) in the presence of 5 μ l of 10 x polymerase buffer and 5 μ l of 10 mM dNTPs. The tubes were covered with 20 μ l of mineral oil and incubated for 30 min at 72 °C. Blunt-ended fragments were subsequently cloned into pCRscript using the pCRscript AMP SK cloning kit. *E. coli* strain JM109 was used for routine plasmid transformation and propagation (Nishimura et al., 1990). Plasmid DNA was purified using the Wizard™ Miniprep kit and inserts sequenced using the PRISM Ready Reaction DyeDeoxy Terminator Cycle Sequencing kit (Perkin-Elmer). Sequence analyses was performed on model 373 automated sequencer (Applied Biosystems).

2.2.20. Competent cell preparation

JM109 *E. Coli* cells was first grown in 10 ml of Luria-Bertani (LB) medium (5 g NaCl, 2.5 g yeast extract, 5 g tryptone in 500 ml water, sterilised by autoclaving at 121 °C for 15 min) overnight at 37 °C with shaking. 2 ml of the culture was transferred into 100 ml of fresh prewarmed medium and was grown at 37 °C until OD₆₀₀ = 0.6-1. The culture was then harvested by centrifugation at 950 g_{av} for 5 min at room temperature and the pellet was resuspended in 20 ml of 0.1M MgCl₂. This suspension was recentrifuged as before and the final pellet was resuspended

in 2 ml of ice cold 0.1 M CaCl₂ and left on ice for 30 min then immediately used or stored at -80 °C.

2.2.21. Transformation of plasmid vector into competent cells

1 µg of the plasmid DNA was added to 50 µl of competent *E. coli* cells and incubated on ice for 15 min. Bacteria were then heat shocked for 90 s at 42 °C and again incubated on ice for 1min. All of these transformed bugs were then transferred to 1 ml of LB medium and incubated for 45 min at 37 °C with shaking. 100 µl of the culture was smeared onto LB bacto-agar (as LB medium plus the addition of 1.5 % of agar and 50 µg/ml Ampicillin) with negative control. The plates were incubated at 37 °C overnight. A single colony was used to inoculate 10 ml of LB medium containing Ampicillin and grown overnight at 37 °C with shaking. 4 ml of this starter culture was then transferred to 500 ml of LB medium and grown as above.

2.2.22. Storage of *E. coli* cells

E. coli cells were maintained on LB bacto agar at 4 °C for short term storage. For long term storage, 1 ml of culture was taken from 10 ml of overnight culture and then mixed with glycerol to a final concentration of 15 % (v/v) and stored at -70°C.

2.2.23. Plasmid DNA purification

500 ml of plasmid DNA containing culture was harvested at 5300 g_{av} for 10 min at room temperature and the DNA purified using the Promega Maxiprep kit. Here the pellet was resuspended in 15 ml of cell lysis solution and mixed gently. Lysis was determined to be complete when the solution became clear and viscous. The mixture was neutralised with neutralisation solution and immediately mixed by

gently inverting the centrifuge bottle several times. This suspension was centrifuged at 14 000 g_{av} for 15 min at room temperature. The cleared supernatant was transferred by filtering it through muslin. 0.5 volume of isopropanol was added to the filtered supernatant and mixed by inversion and recentrifuged as above. The supernatant was discarded and the DNA pellet resuspended in 2 ml of TE buffer. 10 ml of resin was added to the DNA solution and mixed.

The Maxicolumn tip was inserted into the vacuum source and the resin/DNA mix transferred into the column. Vacuum was applied to pull the mixture through the column. 13 ml of Column wash solution was added to rinse the centrifuge bottle and then poured into the column. The vacuum was applied and 12 ml of same solution was added to wash the column. 5 ml of 80 % of ethanol was added to the column to rinse the resin. The vacuum was allowed to draw the ethanol through and then continued for a further 1 min. The column was centrifuged in a 50 ml tube at 500 g_{av} for 5 min and the resin was dried by applying an additional 5 min of vacuum. Finally 1.5 ml of 65 °C preheated distilled water was applied to the column and left for 1 min to elute the DNA, again the column was centrifuged as above and plasmid DNA was taken.

2.2.24. Estimation of DNA concentration

The concentration of probe DNA was estimated by measuring the optical density (OD) at 260 nm in Shimadzu UV-1201 spectrophotometer. The optical density of 1 ml distilled water was measured at 260 nm and then the spectrophotometer settled to zero. 10 μ l of aliquot probe DNA was added to 990 μ l distilled water, vortexed and then estimated at 260 nm and 280 nm in quartz cuvettes. The purity of the DNA was determined by division of the OD_{260} by the OD_{280} , yielding, ideally, a result of 1.8-2.0. The concentration of DNA in the suspension as μ g/ml

was calculated by the multiplication of the OD₂₆₀ by the dilution factor (100) and by a constant (50), where 50 = 1 OD gives 50 µg DNA at 260 nm.

2.2.25. Storage of plasmid DNA

DNA was routinely stored in TE buffer at -20 °C. DNA stored in this way remains stable for several years. Long-term storage of DNA was under 100 % ethanol at -70 °C.

2.2.26. Analysis of data and statistics

The data given in this study represent the mean \pm SD of *n* independent determinations. The significance of differences was calculated with the Student's t-test.

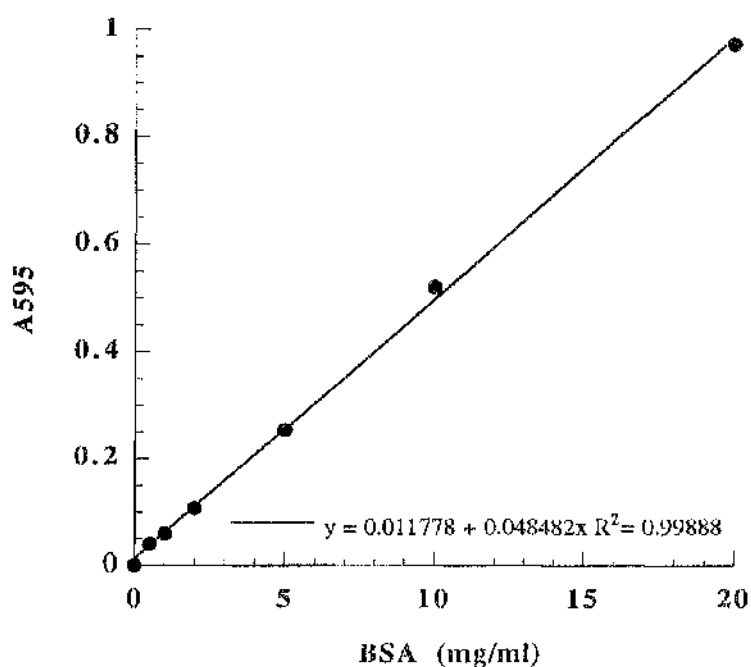


Figure 2.2. Standard curve for a Bradford protein assay

The samples for the standard curve were prepared as described in section 2.2.10. Bovine serum albumin concentrations of 0-20 μg were used as indicated and the absorbance was read at 595 nm. The blank without protein was used to zero the spectrophotometer. The assays were carried out in duplicate. This is a representative experiment which has been carried out at least twenty times.

CHAPTER 3

***INVESTIGATION OF THE EFFECT OF cAMP
ELEVATING AGENTS ON PHOSPHODIESTERASE
ACTIVITIES IN HUMAN JURKAT T-CELLS***

3.1. Introduction

Cyclic adenosine monophosphate (cAMP) is an important second messenger that mediates biological responses generated by a variety of extracellular signals, including hormones, neurotransmitters and pathogenic bacterial toxins (Alava et al., 1992, Kammer, 1988, Manganiello et al., 1995a). Control of intracellular cAMP concentration is critical to the regulation of many cellular responses to extracellular stimuli. Generation of cAMP is initiated via cell surface transmembrane receptors which, through a G-protein-transduced process, leads to changes in the activity of the enzyme adenylate cyclase (Figure 1.1). Adenylate cyclase produces cAMP within the cell which serves to activate cAMP dependent protein kinase A (PKA) activity. PKA then exerts its action through the phosphorylation of specific target proteins, leading to altered cell function (Houslay et al., 1995, Kammer, 1988).

Many hormones exert their actions on target cells by elevating the intracellular concentration of cAMP, through coupling of their specific cell surface receptor to the stimulatory G-protein, G_s . However, enhanced cAMP concentration return towards basal levels in spite of the continuous presence of hormone. This phenomenon involves the expression of active intracellular mechanisms terminating the hormonal stimulation, since extracellular dissociation of the hormone from the receptor might not be the primary cause of cessation of a stimulus (Collins et al., 1992, Dohlman et al., 1991). It is also thought to be the result of mechanisms that protect the cell from excessive stimulation (desensitisation) or adjust the cell sensitivity to circulating hormone levels (cell adaptation). The regulation of cAMP hydrolysis has been shown to play an important role in terminating the hormonal stimulus and inducing desensitisation in the target cell. The only known mechanism for the degradation of cAMP is by the

action of PDEs; these enzymes therefore provide important sites for hormonal regulation (Giembycz, 1996).

Degradation of intracellular cAMP levels can be regulated by a complex family of cyclic nucleotide phosphodiesterases (PDEs). PDEs catalyse the hydrolysis of the 3'-phosphoester bond on adenosine cyclic 3',5'-monophosphate (cAMP) and guanosine cyclic 3',5'-monophosphate (cGMP) to form the 5'-monophosphate products AMP and GMP, respectively (Figure 2.1). In turn, 5'-AMP and 5'-GMP cannot activate cyclic nucleotide dependent PKA and PKG, respectively. Seven distinct mammalian PDE families (Beavo, 1995, Beavo et al., 1994, Rybalkin & Beavo, 1996) have been identified on the basis of molecular cloning and enzymatic characterisation (Table 1.1). These are encoded by distinct genes. The PDE classes are: PDE1, Ca²⁺/calmodulin-stimulated; PDE2, cGMP-stimulated; PDE3, cGMP-inhibited; PDE4, cAMP-specific and rolipram-inhibited; PDE5, cGMP-specific; PDE6, cGMP-specific photoreceptor and PDE7, cAMP-specific but insensitive to inhibition by the non-selective PDE inhibitor IBMX (Beavo et al., 1994, Manganiello et al., 1995a). In the seven gene families at least 14 different PDE genes generate more than 34 different PDE isoforms (Beavo et al., 1994). PDEs are encoded by different genes but with additional multiplicity representing splice variants and possibly different transcriptional start products of the same gene (Beavo & Reifsnyder, 1990). Mammalian PDEs possess a central conserved region of approximately ~ 300 amino acids which is thought to contain the catalytic domain. However, they vary widely in their extreme N- and C-terminal amino acid sequences, kinetic characteristics, substrate affinities, biochemical and pharmacologic properties, cellular distribution and subcellular localisation (Beavo, 1988, Manganiello et al., 1990a, McLaughlin et al., 1993, Swinnen et al., 1989b).

Two regulatory processes may provide a highly coordinate mechanism for short- and long-term control of cAMP levels through PDE action. One of these is the short term regulation by phosphorylation of PDEs by cAMP-dependent protein kinase (Beltman et al., 1993, Gettys et al., 1987). This can play an important role in terminating the hormonal stimulus and in inducing desensitisation in the target cells. Rapid regulatory changes can be elicited by the phosphorylation of PDE3 enzymes (Houslay & Kilgour, 1990, Manganiello et al., 1995b) and isoforms of PDE4 enzymes (Marchmont & Houslay, 1980a, Sette et al., 1994a). Long-term regulation requires hours to develop, may be mediated again via a cAMP-dependent protein kinase mechanism, but which involves inducing PDE isoform expression (Conti et al., 1991). This has been defined as an adaptive response to chronic increases in intracellular cAMP levels (Conti et al., 1995b, Thompson, 1991) and described in particular detail for splice variants arising from the PDE4D gene (Conti et al., 1995a, Conti et al., 1995b, Sette et al., 1994b).

Current studies have been focussed on the cAMP-specific PDE4 isoenzymes where compounds able to exert selective inhibition of such enzymes can exert anti-depressant and anti-inflammatory actions (DiSanto & Heaslip, 1995). Presently, such PDE4 selective inhibitors are being considered for the treatment of asthma, multiple sclerosis, septic and toxic shock and atopy (Barnes, 1991). PDE4 isoforms can be selectively inhibited by certain drugs such as rolipram and Ro 20-1724 (Beavo et al., 1994, Bolger, 1994, Manganiello et al., 1995a). Both inhibitors exhibit considerably higher affinity for the binding site rather than the catalytic domain of the enzyme (Kelly et al., 1996).

Molecular cloning approaches have recently demonstrated that PDE4 is a family of enzymes comprising four distinct genes, designated PDE4A, 4B, 4C and 4D which produce a variety of splice variants in both humans (Baecker et al., 1994, Bolger, 1994, Livi et al., 1990) and rats (Davis et al., 1989) (Figure 1.3 and

3.20). These subtypes share much greater catalytic domain sequence homology with each other (> 90 %) than with other PDEs and they also share two highly conserved regions (UCR1 and UCR2) in the putative regulatory domain upstream of the catalytic region (Bolger, 1994). Mapping studies have been shown that human PDE4 forms are localised to three chromosomes with PDE4A (Horton et al., 1995) and PDE4C being located on chromosome 19 (Milatovich et al., 1994), PDE4B on chromosome 1 and PDE4D on chromosome 5 (Szpirer et al., 1995). Over 16 isoforms of the PDE4 family (Bolger, 1994) are produced by these genes as a result of alternative splicing. This predominantly takes the form of 5'-domain swops, leading to the production of enzymes with distinct N-terminal regions. The amino termini of these proteins has been postulated to have regulatory functions which include stabilisation of the enzymes (Shakur et al., 1993), intracellular targeting (Scotland & Houslay, 1995) and protein-protein interactions (O'Connell et al., 1996).

The cyclic AMP-specific PDE (PDE4) is the predominant cAMP hydrolysing isoenzyme class found in most, if not all, immune and inflammatory cells (Alvarez et al., 1995, Manning et al., 1996, Torphy & Udem, 1991). The precise role(s) of cAMP in the immune response remains unclear. However, it is well defined that cAMP has a role as a second messenger mediating a generalised suppression of immune and inflammatory cell activity (Kammer, 1988). Recent investigations have led to the recognition that PDE4 plays a critical role in regulating the function of these cells (Torphy et al., 1995, Verghese et al., 1995). Most interest to date has focused on the development of inhibitors of PDE4 isoenzymes for the treatment of inflammatory diseases including arthritis, atopic dermatitis and, in particular, asthma (Asthon et al., 1994, Kelly et al., 1996). Although, the therapeutic potential of PDE4 inhibitors in chronic inflammatory disorders seems considerable, the utility of isoenzyme non-selective PDE4 compounds induces

side-effects. Development of isozyme-selective therapeutic agents may avoid unwanted effects.

T lymphocytes play key role in regulating immune responses. There is general agreement that cAMP is a negative modulator on mitogenesis and activation of mature T lymphocytes (Alexander & Cantrell, 1989, Goodwin & Ceuppens, 1983, Kammer, 1988). The rise in cAMP also inhibits interleukin-2 (IL-2) production (Anastassiou et al., 1992, Wacholtz et al., 1991) and stimulation of thymic apoptosis (Kaye & Ellenberger, 1992), although the precise molecular mechanisms that underlie such effects are not understood in detail. However, consistent with such a notion, leukemic lymphocytes appear to have lowered cAMP levels by 3 - 25 fold than normal T cells in murine and in human systems (Epstein & Hachisu, 1984). This may be attributable to the elevated PDE activity that has been observed in such instances (Thompson, 1991). One possible route through which cAMP might exerts an inhibitory effect on cell growth is that, in many cells, protein kinase A can seemingly inhibit the activation of MAP kinase by eliciting the phosphorylation and inactivation of B-raf (Cook & McCormick, 1993). However, there is evidence which suggests that this does not occur in T-cells, but that elevated cAMP levels serve to inhibit c-Jun N-terminal kinase (JNK) (Hsueh & Lai, 1995). As T-cell activation, including IL-2 gene activation, requires the integration of Raf-1 and JNK pathways, then a block in either will lead to an inhibitory effect (Hsueh & Lai, 1995).

3.1.1. Aim of the study

The purpose of this study was to investigate whether chronic elevation of intracellular cAMP concentrations can adaptively alter the expression of specific PDE isoforms in T lymphocytes and, in particular, the control of expression of PDE4 splice variants. Here the human leukemic T-cell line, Jurkat J6, has been studied as a model of T lymphocytes activation with either the adenylate cyclase activator forskolin or G-protein activator cholera toxin used to elevate cAMP levels.

3.2. Results

3.2.1. Characterisation of the phosphodiesterase isoforms of Jurkat T-cells

To determine which forms of PDE activity are present in human Jurkat leukemic T-cells, a pharmacological approach was employed using selective inhibitors and activators. Compounds selective for effects on specific PDE isoforms (Beavo et al., 1994, Beavo & Rcifsnyder, 1990, Houslay & Kilgour, 1990, Spence et al., 1995) were used to identify and gauge the magnitude of various PDE isoforms in this cell line.

Homogenates of Jurkat T-cells exhibited cAMP phosphodiesterase activity of 18.0-20.5 pmol of cAMP hydrolysed/min per mg of protein when assayed with 1 μ M cAMP as substrate (mean \pm SD; $n = 8$). Jurkat cells appeared to express PDE1, PDE2, PDE3, PDE4 and PDE7 activities (Table 3.1). Ca^{2+} /CaM-stimulated PDE1 activity was assayed by performing PDE assays in the presence of EGTA, to chelate any endogenous Ca^{2+} and then adding excess Ca^{2+} /calmodulin (50 μ M and 20 ng/ml respectively) in order to determine the degree of stimulation of this isoform (Manganiello et al., 1995a). There is a possibility that sufficient endogenous Ca^{2+} might elicit the full activation of any

PDE1 activity without added exogenous Ca^{2+} (Spence et al., 1995). PDE assays were also carried out in the presence of EGTA (2 mM) to determine whether the subsequent addition of Ca^{2+} (5 mM) then caused stimulation. However, in no instance was any difference observed between analyses done in this fashion and those where Ca^{2+} was added without EGTA. Here, Ca^{2+} / CaM (50 μM ; 20 ng/ml) elicited an increase in PDE1 activity of some 3.5 ± 1.0 pmol/min/mg protein, indicating that low levels of PDE1 were present (Table 3.1).

PDE1 family is one of the key enzymes involved in the complex interactions which occur between the cyclic-nucleotide and Ca^{2+} second-messenger systems (Yan et al., 1996). PDE1 isoenzymes are expressed in distinct cell types in various tissues and have different substrate affinities and molecular and/or catalytic properties and tissue-specificities (Rybalkin & Beavo, 1996, Wang et al., 1990). Stimulation of this group of enzymes require the simultaneous presence of both Ca^{2+} and calmodulin (Wang et al., 1990). At least three different genes (*PDE1A*, *PDE1B* and *PDE1C*) have been identified in the CaM-PDE family (Loughney et al., 1996). Here RT-PCR analyses are used to detect PDE1 forms employing degenerate primers based upon on all known PDE1 sequences from rat, mouse, human and bovine sources. One set could be designed to detect both PDE1A and PDE1B but not PDE1C isoforms (Spence et al., 1995). A second set of degenerate primers were used to detect PDE1C. The PDE1C specific primers did not amplify any fragment using RNA from either this Jurkat cell line or from Chinese hamster ovary cells (CHO), although they did from the human thyroid carcinoma FTC133 cell line. Thus the PDE1C isoform was not expressed in Jurkat cells. Using the PDE1A/B degenerate primer pair a 601 bp fragment of the predicted size was successfully amplified (Figure 3.1) from RNA preparations from human Jurkat T-cells. In addition, using the same primers with RNA extracts from PMA- and ATP-treated CHO cells a similar sized fragment was amplified (Spence et al., 1997). Sequencing of both the CHO and Jurkat T-cell PCR products yielded 602

bp and 554 bp of novel sequence, respectively, which have been deposited in the GenBank data base (accession numbers, U40585 and U40584, respectively) (Spence et al., 1997) (Figure 3.2). These both show strong identity with sequence reported for bovine (M94867) and mouse (M94538) PDE1B forms. Indeed, pairwise alignments found that the two existing PDE1B sequences shared 91-95 % and 90-92 % nucleotide identity with the chinese hamster sequence and the human Jurkat T-cell sequence, respectively, whereas the PDE1A (U40371) and PDE1C (U40370) sequences show 68-69 % identity to chinese hamster and 67-71 % identity to human sequence (Figure 3.2). Moreover, alignment of the amino acid sequences found that the conservation between the CHO sequence was 99 % and Jurkat T-cell sequence 96-97 % identity when compared pairwise with the other *PDE1B* sequences. In contrast the CHO sequence has 65-69 % and Jurkat T-cell sequence 66-70 % amino acid identity when compared pairwise with the non-homologous *PDE1A* and *PDE1C* sequences. Analysis of Jurkat T-cell PDE1 sequence and recently published (Jiang et al., 1996) full length human *PDE1B* sequence (GenBank; U56976), from human RPMI-8392 B-cells, showed that the two share 99 % nucleotide identity. This suggests that the cDNA fragment amplified from human Jurkat T-cells by RT-PCR clearly belongs to the *PDE1B* gene family.

Low concentrations of cGMP serve as a competitive inhibitor of PDE3 activity (Beavo et al., 1994, Manganiello et al., 1995a) and stimulator of PDE2 activity (Manganiello et al., 1990a, Manganiello et al., 1995b, Michie et al., 1996, Tenor et al., 1995). The PDE3 isoform can also be selectively inhibited, with high specificity, by the compound cilostimide (Beavo & Reifsnyder, 1990, Manganiello et al., 1995b). In order to gauge PDE3 activity, PDE assays were performed with 1 μ M cAMP as substrate and in the presence and absence of 10 μ M cilostimide, which can be expected to inhibit all of the PDE3 activity. Using this it appears that PDE3 forms ~ 55 % of total Jurkat T-cell cAMP homogenate PDE activity (Table

3.1). Low concentrations of cGMP caused a profound, dose-dependent, inhibition of Jurkat cell PDE activity (Figure 3.3), with an IC_{50} of $0.9 \pm 0.2 \mu\text{M}$. A similar degree of profound, dose-dependent, inhibition was also elicited (Figure 3.4) using the PDE3 selective inhibitor cilostimide with an IC_{50} of $178 \pm 38 \text{ nM}$.

cGMP can also affect cAMP PDE activity by causing the stimulation of any PDE2 activity. However, the similarity in the magnitude of inhibition caused by both cGMP and by cilostimide would appear to suggest that any PDE2 activity in Jurkat T-cells was relatively small in comparison to that of PDE3 activity. PDE2 activity can be gauged by the selective inhibitor EHNA (previously known as MEP-1) (Beavo et al., 1994, Mery et al., 1995, Michie et al., 1996) which appears to exert its most profound effect on the cGMP-stimulated state of PDE2 (Michie et al., 1996). EHNA achieved but a very small inhibitory ($\sim 5\%$) effect on the cGMP-stimulated PDE activity of Jurkat T-cells (Table 3.1), consistent with this PDE form providing a minor component of the total cellular PDE activity. The IC_{50} of $3.2 \pm 0.5 \mu\text{M}$ (Figure 3.5) noted was of a similar magnitude for that reported for the inhibition of PDE2 activity in both hepatocytes and thymocytes (Michie et al., 1996).

Rolipram is a highly selective inhibitor for cAMP-specific PDE4 family enzymes (Beavo & Reifsnnyder, 1990, Bolger, 1994, Manganiello et al., 1995a, Marcoz et al., 1993b, Nicholson et al., 1991, Shakur et al., 1993). These enzymes typically exhibit IC_{50} values of $0.1 \mu\text{M}$ to $1 \mu\text{M}$ range for rolipram when assayed at $1 \mu\text{M}$ cAMP (Lobban et al., 1994, Michie et al., 1996, Nicholson et al., 1991), whereas other PDE species are either insensitive to rolipram or show IC_{50} values at least 100-1000 fold higher (Nicholson et al., 1991, Torphy & Cieslinski, 1989). Thus the inhibition of PDE4 monitored in the presence of $10 \mu\text{M}$ rolipram, with $1 \mu\text{M}$ cAMP as substrate, can be expected to lead to maximal inhibition of this isoform group with either little or no effects on other species. Rolipram caused a marked,

dose-dependent, inhibition of Jurkat T-cell cAMP PDE activity with an IC_{50} of 13 ± 7 nM (Figure 3.6). At concentrations between 1 and 20 μ M, where it can be expected to have selectively inhibited all of the PDE4 activity, the magnitude of the inhibition seen suggested that PDE4 activity provided ~ 22 % of the total PDE.

PDE7 family enzymes specifically hydrolyse cAMP and are resistant to inhibition by the non-selective reversible PDE inhibitor, IBMX (Lavan et al., 1989, Michaeli et al., 1993). There is no satisfactory way to measure PDE7 activity, but one can reasonably calculate, on the basis of K_m (cAMP) and K_i (IBMX) values for various PDE species (Houslay & Kilgour, 1990, Jin et al., 1992) that 100 μ M concentration of IBMX could be expected to achieve ~ 82 % inhibition of PDE activity. Here I found that IBMX caused ~ 85 % inhibition of PDE activity with 1 μ M cAMP as substrate. This suggests that there might be a small amount of PDE7 activity in Jurkat T-cells (Table 3.1). Indeed, transcripts for PDE7 have recently been identified in human T-cells (Giembyez et al., 1996).

These data suggest that PDE3 and PDE4 isoforms provide the major PDE activities in Jurkat T-cells, accounting for ~ 77 % of the total under the assay conditions used here.

3.2.2. Effect of cyclic AMP-elevating agents on phosphodiesterases of Jurkat T-cells

Forskolin binds to and directly activates the catalytic subunit of adenylate cyclase both in the absence and presence of the stimulatory G-protein (G_s) (Seamon et al., 1981). Prolonged treatment of Jurkat T-cells with this diterpene produced a dramatic but transient increase in intracellular cAMP content (Figure 3.7). In order to appreciate if changes in PDE activity contributed to the mechanism responsible for the transience of this accumulation of cAMP, the effect of forskolin on PDE

activity in human Jurkat T-cells was investigated. Jurkat T-cells were treated for different times up to 24 h with 100 μ M forskolin and the total PDE activity was measured. This time course study showed that forskolin produced a profound elevation of total homogenate PDE activity (Figure 3.7). Treatment with 1 μ g/ml cholera toxin, which elicits the NAD⁺-dependent ADP-ribosylation of G_s causing adenylate cyclase to become constitutively activated (Nel & Daniels, 1988, Sommermeyer et al., 1990), produced an even larger stimulation of the PDE activity (Table 3.2; Figure 3.9). Using isoenzyme-selective activators and inhibitors to make an estimation of the relative contribution of different PDE classes to the total homogenate PDE activity of Jurkat T-cells, it was assessed whether chronic elevation of intracellular cAMP levels could alter cellular PDE activities.

Elevation of cAMP levels by chronic exposure to forskolin did not cause any significant change in either PDE1 (Figure 3.10), PDE2 (Figure 3.11) or IBMX-insensitive PDE activity over a period of up to 24 h. In contrast, PDE3 activity was increased profoundly (Figures 3.12-13). An initial transient increase in PDE3 activity occurred over the first 45 min (Figure 3.12) and was followed by a sustained increase, which began after about 3-4 h of exposure and continued through to 24 h (Figure 3.13). While no immediate increase in PDE4 activity occurred upon challenge of cells with forskolin, after an initial lag period of 3-4 h a profound increase in PDE4 activity occurred which remained elevated over the 24 h period (Figure 3.14). The long term activation of PDE3 and PDE4 activities, which began after about 3 h forskolin challenge, were completely prevented by inhibiting transcription using actinomycin D (Table 3.2). This indicates that the up-regulation of PDE3 and PDE4 activity depended upon the synthesis of protein. Actinomycin D treatment, however, did not block the rapid, transient increase in PDE3 activity (<5 % change; $n = 3$; 45 min exposure to 100 μ M forskolin in the

presence compared with the absence of actinomycin D), suggesting that this increase not involving enzyme induction.

In a similar way using cholera toxin instead of forskolin to stimulate adenylate cyclase activity, a profound increase in the homogenate PDE activity also occurred (Figure 3.9). For treatment of the cells with cholera toxin PDE3 activity was maximal in the first 45 min and then gradually decreased (Figure 3.15). PDE3 activity was also measured after 6 h challenge and shown to be increased by about 1-fold (Table 3.2). At this time of exposure PDE4 activity was also increased by ~2.5-fold (Table 3.2; Figure 3.16). As found with forskolin activation of PDE activity the long-term up-regulation of PDE3 and PDE4 activities by cholera toxin was also inhibited by actinomycin D (Table 3.2).

Incubation of Jurkat cells with the cell-permeable cAMP analogue 8-bromo-cAMP, also induced both PDE3 and PDE4 activities (Table 3.2). However, this occurred to a lesser extent than seen with the other agents, which may reflect the metabolism of this compound.

Intracellular cAMP content was measured at various times over a 24 h period. In forskolin treated cells, basal cAMP content was rapidly increased by ~ 18-fold within ~ 3 min. This reached a maximum value after about 6 h and was followed by a gradual decline to a new steady-state which was still elevated above that seen in cells which had not been treated with forskolin (Table 3.3; Figure 3.7). When the forskolin-elevated intracellular cAMP levels began to decline then total PDE activity began to be elevated (Figure 3.8). At the point where the increase in PDE activity reached maximum levels, 6-9 h after forskolin challenge, selective PDE inhibitors were used to determine the effect of blockade of this PDE activity on the regulation of intracellular cAMP levels. The non-selective PDE inhibitor IBMX is known to inhibit PDE activity and to increase cAMP levels synergistically when

adenylate cyclase is stimulated. Therefore, the presence of IBMX led to forskolin-stimulated cAMP levels being increased by ~ 5-fold (Table 3.3). Interestingly, the PDE4-selective inhibitor rolipram was able to elicit a similar amplification to that seen with IBMX, whereas the PDE3-selective inhibitor cilostimide appear to be far less potent in increasing intracellular cAMP levels in these cases by only ~ 50 % (Table 3.3). Such effects appear to be a little surprising in that homogenate PDE assays showed PDE3 activity to be considerably greater than PDE4 activity (Table 3.1). One possibility is that cilostimide did not achieve equilibrium concentrations inside the T-cells over the 9 h period. However, this seems somewhat unlikely, especially as cilostimide did cause an increase in cAMP levels and achieves inhibition of PDE3 at very low concentrations (Manganiello et al., 1995a) (Figures 3.3-4). It has also been shown that effect of the PDE4 activity on cAMP regulation is more important than PDE3 activity in human monocytes (Verghese et al., 1995). The data indicate that Jurkat T-cell PDE4 species may play a major role in controlling the bulk or major pool of cAMP produced by the forskolin-stimulated activation of adenylate cyclase and that the action of PDE3 may be more limited. This might explain why PDE4 inhibitors are potent anti-inflammatory agents (Barnes, 1991), inhibiting T-cell functions, whilst PDE3 inhibitors have little effect (Marcoz et al., 1993b).

The effect of the transcriptional inhibitor actinomycin D on cAMP content was also examined in cells which had been challenged with forskolin. Incubation of cells with actinomycin D considerably enhanced, by ~ 2.4-fold, the ability of forskolin to increase intracellular cAMP concentrations in Jurkat T-cells (Table 3.3). Such a treatment will have stopped PDE4 induction by forskolin. The forskolin-mediated induction of PDE enzyme was clearly able to exert a considerable influence on intracellular cAMP levels. That addition of actinomycin D did not affect the forskolin-stimulated rise in cAMP, assessed in the presence of the PDE inhibitor

rolipram (Table 3.3), showing that inhibition of transcription did not affect the forskolin-stimulated adenylate cyclase activity itself.

Multiple biochemical and biological events are triggered by the interaction of the T-cell antigen receptor/CD3 complex (TCR) with processed antigens in the context of the major histocompatibility complex (MHC) molecules found on the surface of antigen-presenting cells (Weiss et al., 1986). Ligand-mediated perturbation of the TCR complex provokes an increase in protein-tyrosine kinase, phospholipase C and protein kinase C activities as well as changes in phosphatidylinositol breakdown, lymphokine secretion, calcium accumulation and a transient increase in cAMP concentrations (Cooke et al., 1991, Kvanta et al., 1990). It has also been shown that lectins [phytohemagglutinine (PHA)] bind specific glycoproteins on the cell surface of the cells which leads to the polyclonal stimulation of lymphoid cells. Initial events in lectin-induced activation include tyrosine phosphorylation (Hirata et al., 1984), calcium influx (Coffey et al., 1981) and inositol phosphate production (Taylor et al., 1984). Observations concerning fluctuations in the intracellular concentrations of cyclic nucleotide levels are, however, confused (Derubertis et al., 1974, Hurwitz et al., 1990). This may be due to complex changes in both adenylate cyclase and PDE activities and to various ligands having been used. In order to see whether ligation of the T-cell receptor can alter Jurkat T cell PDE activity I used the monoclonal antibody OKT3 which is directed against the CD3 complex (Phillips et al., 1991) and also the mitogenic lectin PHA. However, incubation of the cells for various times with either OKT3 or the PHA antibody (Figures 3.18-19) did not lead to any clear change in total PDE activity. These results suggest that the signalling pathways emanating from the TCR/CD3 complex are not coupled to the regulation of PDE activities in Jurkat T-cells.

TCR ligation can however be bypassed as a requirement for T-cell activation through the synergistic action of the PKC activator phorbol 12-myristate 13-acetate (PMA), implying that the activation of PKC is one of the 'on' signals for T-cell activation (Albert et al., 1985). Recently, Spence et al. (1995) have demonstrated that PMA can rapidly induce PDE1 activity and this activity was related to activation of specific protein kinase C isoforms. This suggests that there might be 'cross-talk' between the cAMP- and lipid-signalling pathways in CHO cells. Here, however, incubation of Jurkat T-cell with 1 μ M PMA for various times showed that neither total PDE nor PDE1 activity were changed (Figure 3.19). This suggest that the 'cross-talk' between the cAMP- and lipid-signalling pathways occurs in a cell-specific manner.

3.2.3. Determination of PDE4 subtype gene expressions and the effect of elevated cyclic AMP

PDE4 activity is encoded for by four genes which produce a variety of protein products due to multiple splicing (Bolger, 1994). Such multiple splicing takes the form of 5' domain swops with resultant considerable heterogeneity among the mRNAs of PDE4 family members at their 5' regions. In contrast, the 3' region of each active member of particular PDE4 gene families is unique and is thus common to all active isoforms produced from a particular PDE4 gene. Thus, in order to identify PDE4 isoforms occurring in Jurkat T-cells, I first designed generic PCR primers which would be able to identify all active members of each of the four isoform families. This approach was taken in order to maximize the chances of detecting changes due to any unknown active PDE4 isoforms. The design of these generic, PDE4-class specific primers was based on the fact that, within each PDE4 class, all active splice variants have identical sequences 3' to the splice junction. I also, however, employed primers able to detect specific, known, splice variants. This is shown schematically in figure 3.20 and the primers used are given in the

individual legends. Finally, immunological methods were employed to identify protein products.

Using sets of generic primers, I was able to identify transcripts for both PDE4A and PDE4D (Table 3.4; Figures 3.21-22) in control Jurkat T-cells but none for PDE4B and PDE4C (Table 3.4; Figures 3.23-24). I also confirmed the absence of the two known forms of human PDE4B isoforms PDE4B1 (PDE72) and PDE4B2 (PDE32) (Bolger, 1994, Bolger et al., 1993, McLaughlin et al., 1993) and PDE4B3 (Huston et al., 1997) in both control and forskolin-treated cells by using isoform-specific primers (Figure 3.25) and by Western blotting procedures. Forskolin treatment did not cause the induction of PDE4C isoforms on the basis of analyses done using generic primers (Figure 3.24).

The rat *PDE4A* gene produces multiple splice variants which all arise from 5' domain swops. There have been three rat PDE4A gene products cloned from various specialised cells which are called RD1 (Davis et al., 1989), rPDE-6 (Bolger et al., 1994, McPhee et al., 1995) and rPDE-39 (Bolger et al., 1996). On the other hand, products of its counterpart, the human PDE4A gene, are poorly understood. A full length human PDE4 species has been characterised as PDE46 (HSPDE4A4B) (Bolger et al., 1993), together with a splice variant, called 2EL (HSPDE4A8), which unlike PDE46 exhibits no apparent PDE activity (Horton et al., 1995). PDE46 provides a distinct PDE4A splice variant which is expressed natively in cells (Torphy et al., 1995). In this study PDE4A transcripts were detected in untreated Jurkat T-cells using generic primers. However, probing RNA preparations from 9 h forskolin-treated cell for PDE4A transcripts (Figure 3.21) consistently yielded signals of considerably lower intensity than those obtained using preparations from untreated cells. Equivalent intensities of the β -actin-specific bands were seen in control *versus* treated cell, confirming successful normalisation of the mRNA (Figures 3.21 and 3.33). This suggests that levels of PDE4A were actually decreased upon elevation of intracellular cAMP. To

characterise this further, I assessed the ability of a PDE4A-specific antiserum to immunoprecipitate PDE activity from solubilised Jurkat T-cells (section 2.2.11). In such experiments, cell extracts from control and from 9 h forskolin-treated cells were incubated with an anti-PDE4A polyclonal antibody and absorbed to Pansorbin. PDE4 activity was indeed immunoprecipitated from control cells, yielding a specific activity of 5.1 ± 0.2 pmol/min per mg of protein (mean \pm SD; $n = 3$ experiments; units expressed relative to T-cell homogenate PDE activity). This fraction of activity was very similar to the rolipram-inhibited PDE component determined using Jurkat T-cell homogenates (4.9 ± 0.5 pmol/min per mg of protein; $n = 3$) suggesting that, in control cells, PDE4 activity provides the major, if not the sole, PDE4 activity. However, in cells treated with forskolin, the immunoprecipitated PDE4A activity recorded was some 3.1 ± 0.3 pmol/min per mg of protein (mean \pm SD; $n = 3$ separate experiments using different cell preparations; units expressed relative to T-cell homogenate PDE activity), implying a decrease in PDE4A expression of $\sim 40\%$. In each instance $>96\%$ of the immuno-absorbed activity was inhibited upon addition of $10 \mu\text{M}$ rolipram, indicating that this was indeed exclusively PDE4 activity. Such a reduction in the amount of presumed PDE4A activity seen in forskolin-treated cells was consistent with the decreased signal seen by RT-PCR transcript analysis (Figure 3.21). Western blot analyses of PDE4A immunoreactivity was carried out using a specific monoclonal antibody. Using this technique, a single band (118 ± 2 kDa) of immunoreactivity was detected (Figure 3.26). However, after 9 h of treatment with forskolin a band of considerably diminished intensity was seen ($45 \pm 6\%$; $n = 3$ experiments) (Figure 3.26). This immunoreactive species migrated considerably faster on SDS/PAGE than did the PDE46 (Huston et al., 1996, Verghese et al., 1995) product of the human *PDE4A* gene which migrated as an 125 kDa species (Figure 3.27). It could be thought that such a difference was due to proteolysis. However, a single species of reproducible size was obtained in all our PDE4A immunoblot studies done with Jurkat T-cells. This was also apparent when cells

were boiled directly in SDS/PAGE sample buffer so I believe it unlikely that this is a proteolysed species and suggest that it may be a novel splice variant. To try and test this I used PCR primers designed to detect specifically the extreme 5' region of PDE46 which should be unique to this species. However, I failed to obtain a signal in extracts from Jurkat T-cells (Figure 3.27) but did for control using PDE46 expressed in COS7 cells. A further indication that this species may be a novel splice variant is that the IC₅₀ value for inhibition of this species by rolipram is about 50-fold lower than that seen h6.1 (HSPDE4A4C) (Sullivan et al., 1994, Wilson et al., 1994) and PDE46 (Huston et al., 1996), indicating a particularly potent action of this selective inhibitor on the T-cell PDE4A isoform.

The pattern of expression of multiple variants from the rat (Monaco et al., 1994, Sette et al., 1994b) and human (Bolger et al., 1997) *PDE4D* gene has shown that the heterogeneity of the different mRNA lies in the 5' region. At least five different, active splice variants have been identified to date. In rats, three different transcripts from this gene (Bolger et al., 1994, Swinnen et al., 1989b): PDE4D1, PDE4D2 and PDE4D3, and in human five splice variants have been reported: PDE4D1 to PDE4D5 (see chapter 4 for more details) (Bolger et al., 1993, Bolger et al., 1997, Nemoz et al., 1996). Analysis of the products of this gene by RT-PCR, using a set of generic primer pairs, allowed me to detect a weak signal in RNA preparations from untreated Jurkat cells (Table 3.4 and Figure 3.22). However, using 9 h forskolin-treated cells I consistently obtained a very much stronger signal (Figure 3.22). This implied an increase in the level of PDE4D transcripts upon chronic elevation of intracellular cAMP concentrations. Using sets of primers able to detect each of these reported variants I failed to detect any signal for PDE4D3 (Figure 3.28), PDE4D4 (Figure 3.29) and PDE4D5 (Figure 3.30) species in either untreated or forskolin-treated cells. However, I was able to obtain a signal for PDE4D1 in RNA extracts from control cells, although this was rather weak (Table 3.4; Figure 3.31). I also detected transcripts for PDE4D2 in

forskolin treated cells but not in untreated cells (Table 3.4; Figure 3.32). In all these experiments similar signals were obtained using primers designed to amplify up a region of the cytoskeletal protein actin (Figure 3.32), showing that similar levels of mRNA were present in all experiments. These experiments were all done using at least three different RNA preparations.

To determine whether the increase in PDE4D mRNA resulted in an increase in PDE4D protein content, Jurkat T-cell extracts were subjected to Western blot analysis. Using monoclonal antisera able to recognise PDE4D species, I failed to identify any signal in extracts from untreated cells (Figure 3.33). This suggests that the expression of PDE4D species in untreated cells is minimal and is consistent with the notion obtained from immunoprecipitation of PDE4 activity using anti PDE4A antisera that the predominant component of PDE4 activity in resting cell is due to a PDE4A isoform. However, in forskolin-treated cells I obtained a very clear, strong signal for a 67 ± 2 kDa species (Figure 3.33) which co-migrated with PDE4D1 expressed in transfected COS7 cells. This is consistent with my RT-PCR analyses which implied that cAMP mediated the induction of the PDE4D1 splice variant. Immunoblot studies, however, also identified a species, with an apparent size 65 ± 2 kDa, which consistently migrated just below that identified as PDE4D1 (Figure 3.33). This species seems most likely to be PDE4D2, as it is highly related to PDE4D1 but has a small internal deletion of 86 bp in its 5' alternatively spliced region which would make the encoded protein product slightly smaller than PDE4D1. Consistent with this I was able to identify transcripts for PDE4D2 in extracts from forskolin-treated cells (Figure 3.33). I also routinely detected a weakly staining species at 75 ± 3 kDa in PDE4D immunoblot studies done on forskolin-treated Jurkat T-cells (Figure 3.33). Whether this reflects an as yet unreported PDE4D splice variants has yet to be seen.

3.3. Conclusions and Discussion

The pharmacological examination of human Jurkat T-cells indicated that cGMP-inhibited PDE3 and cAMP-specific PDE4 families provide the majority of PDE activity (Table 3.1). Chronic elevation of cAMP levels in this cell line caused a profound, time-dependent, increase in overall cellular PDE activity (Figure 3.8). This effect was predominantly achieved through regulation of the expression of PDE3 and PDE4 isoforms (Figures 3.13-14), although a transient activation of PDE3 was also noted (Figure 3.12). Moreover, increasing intracellular cAMP levels by other mechanisms using cholera toxin or 8-bromo-cAMP also mimicked this induction (Table 3.2). The delayed "up-regulation" of PDE3 and PDE4 activities were blocked by actinomycin D, therefore indicating that RNA synthesis is necessary for the rise in these PDE activities (Table 3.3). The immediate increase in PDE3 activity was not blocked by actinomycin D, indicating that this fast "up-regulation" may involve the protein kinase A-mediated phosphorylation of the enzyme. Indeed, the rapid phosphorylation of PDE3 in response to PKA activation has been shown in adipocytes and hepatocytes (Degerman et al., 1990, Manganiello et al., 1995b). The PDE4 isoforms appear to be of major importance in regulating bulk Jurkat T-cell intracellular cAMP levels. This is demonstrated by the findings that the PDE4 selective inhibitor rolipram is consistently more effective than the PDE3 inhibitor cilostimide at increasing cAMP levels in response to forskolin in Jurkat T-cells (Table 3.3). This may have relevance to the design of therapeutic agents aimed at inhibiting T-cell functions. Certainly PDE4, but not PDE3 inhibitors appears to be most effective (Marcoz et al., 1993b).

RT-PCR analyses with generic primers (Figure 3.20) specific for distinct human PDE4 subtypes demonstrated that mRNA for PDE4A and PDE4D subtypes (Table 3.4; Figures 3.21-22) were present but neither PDE4B nor PDE4C transcripts were detectable in control Jurkat T-cells (Table 3.4; Figures 3.23-24). The

absence of the three known forms (PDE4B1, PDE4B2 and PDE4B3) (Bolger et al., 1993, McLaughlin et al., 1993, Huston et al., 1997) in both control and forskolin-treated cells was also confirmed using isotype specific primers (Figure 3.25). These observations contrast with studies done on various monocyte cell lines (Manning et al., 1996, Torphy et al., 1995, Verghese et al., 1995) and in Sertoli cells (Swinnen et al., 1991b), where elevation of cAMP levels induced PDE4B expression. Time-course studies done with Mono Mac 6 monocytes showed that the induction of PDE4B was transient, with maximal induction occurring ~ 5 h after elevated of cAMP levels (Verghese et al., 1995). However, even when I studied cell extracts for transcripts and immunoreactive species at 1h intervals over 9 h, I failed to observe any expression of PDE4B isoforms.

Performing Western blotting analyses for PDE4A forms identified a single ~118 kDa protein band which migrated considerably faster than the PDE46 (125 kDa) species (Figure 3.26). Moreover, when carrying out RT-PCR with primers specific for the N-terminal end of PDE46, 2EL and h6.1 the lack of signal showed that this was not any known form of PDE4A (Figure 3.27). Indeed, the IC₅₀ value for inhibition of this species by rolipram was ~ 50-fold lower than that seen for h6.1 and PDE46. This suggests that the active PDE4A isoform in Jurkat T-cells may be a novel *PDE4A* gene product.

The effect of chronic elevation of cAMP levels with forskolin exposure, on PDE4 expression were apparently exclusively targeted to actions on genes encoding PDE4A and PDE4D. Intriguingly, despite a profound increase in PDE4 activity, I observed a marked reduction in the expression of the single PDE4A isoform which appeared to supply the majority, if not all, of the PDE4 activity in untreated Jurkat T-cells. This decrease in the expression of PDE4A in Jurkat T-cells contrasts with the effect of chronically elevated cAMP levels on monocyte cell lines (Manning et al., 1996, Torphy et al., 1995, Verghese et al., 1995) where increased expression

of a PDE4A species was seen. However, in those cell lines the PDE4A splice variant expressed appeared to reflect PDE46 (Manning et al., 1996, Verghese et al., 1995). Interestingly, Engels et al. (1994) observed that treating another Jurkat T-cell line (JKE6-1) with dibutyryl-cAMP led to 2-fold increase in PDE4A species. This may reflect differences between various Jurkat cell lines. The decrease of PDE4A protein and mRNA in forskolin-treated Jurkat T-cells seen here leads to speculation that this subtype could be down-regulated by cAMP. Indeed, in a study (Zeng, L. & Houslay, MD. unpublished work) done on rat hepatocyte P9 cells, challenging with forskolin for 6h demonstrated decreased PDE4A mRNA and protein levels. Such data may thus signal differences in the control of expression of splice variants in various cell types in response to elevation of intracellular cAMP concentrations. The down-regulation of the expression of the novel PDE4A isoform was more than compensated for, however, by the profound induction of the PDE4D forms over long term challenge with forskolin. Western blotting showed that increased [cAMP] led to PDE4D protein levels being increased following such a treatment (Figure 3.33). This change in PDE4D protein synthesis was confirmed by their expression at mRNA levels (Figure 3.22). Five distinct protein variants (Bolger et al., 1993, Bolger et al., 1997, Nemoz et al., 1996) are derived from the *PDE4D* gene. PDE4D1 is a short protein with an amino terminus different from the long forms (PDE4D3, D4 and D5) and the PDE4D2 is derived from an internal deletion of the unique N-terminal region of PDE4D1 which, again, results from alternative mRNA splicing (Bolger et al., 1997, Sette et al., 1994b). Whilst profound induction of the PDE4D1 (67 ± 2 kDa) and a much smaller level of induction of the PDE4D2 (65 ± 2 kDa) isoforms were detectable in forskolin-challenged Jurkat T-cell extracts, neither PDE4D1 nor PDE4D2 proteins were detectable in the control cells extracts (Figure 3.33). This induction of PDE4D isoforms is similar to that reported in Sertoli cells (Sette et al., 1994b), where elevation of cAMP levels caused a profound induction of both PDE4D1 and PDE4D2 isoforms. Increased PDE4D1 levels were also noted in

Mono Mac 6 monocytes in response to chronic elevation of cAMP concentrations (Verghese et al., 1995). A weakly staining protein at 75 ± 3 kDa was also routinely detected in PDE4D immunoblot studies done on forskolin-treated Jurkat T-cells (Figure 3.33). Further work is needed to characterise whether this species reflects an as yet unreported PDE4D splice variants of 4D. Induction of PDE4D1 and PDE4D2 gives additional support to the notion (Conti et al., 1995b) that cAMP-response elements (CREB) determine the expression of specific PDE4D splice variants, as well as demonstrating that inhibitory effects can be exerted on *PDE4A* gene expression.

The functional significance of changes in the expression of specific PDE4 splice variants remains to be ascertained. However, the observations that PDE4 isoforms appear to exhibit marked differences in their activity, intracellular targeting (Bolger et al., 1996, McPhee et al., 1995, Shakur et al., 1995), protein-protein interaction (O'Connell et al., 1996) and regulation by covalent modification (Conti et al., 1995b) might mean that there are specific functional consequences resulting from these changes. This might explain why the pattern of changes in PDE4 isoform expression in response to elevated intracellular cAMP levels appears to have cell-specific attributes. Thus, such induction of PDE isoforms is likely to reflect a cell-specific adaptive mechanism. This may have implications for the use of therapeutic regimens which lead to elevated intracellular cAMP levels, and also for disease states which involve adenylate cyclase activation.

In conclusion, this study demonstrate that the cAMP-specific PDE can be activated by the long-term incubation with cAMP elevating agents through a cAMP-dependent protein kinase cascade. In Jurkat T-cells where the PDE4D1 and PDE4D2 are induced at the same time as activated PDE3, both enzymes are activated upon the increase in cAMP levels. Phosphorylation of PDE3 may contribute to the short-term activation seen with cAMP elevating agents.

Table 3.1. Assessment of cAMP phosphodiesterase activities in Jurkat T-cells

Phosphodiesterase	Effectors	pmol/min/mg protein
Total PDE	none	19.2±1.5
PDE1	Ca ²⁺ /CaM (50µM/20ng/ml)	3.5±1.0
PDE2	EHNA (10µM)	1.0±0.2
PDE2	EHNA + cGMP (10µM/10µM)	3.5±0.5
PDE3	cGMP (10µM)	10.8±0.4
PDE3	Cilostimide (10µM)	11.3±0.6
PDE4	Rolipram (10µM)	4.8±0.4
PDE7	IBMX (100µM)	3.2±0.3

PDE isoforms were assayed in the presence of 1 µM cAMP as substrate to yield the respective control activity with Jurkat T-cell homogenates. PDE1 activity was determined in the presence of Ca²⁺ / CaM. Inhibition by EHNA indicates the presence of PDE2 activity. PDE2 activity was also determined in the presence of a stimulatory concentration of 10 µM cyclic GMP, which will maximally activate this enzyme if present and so allow amplification of any action of EHNA. Cilostimide and high level of cGMP inhibition indicates PDE3 activity. Inhibition by rolipram indicates PDE4 activity and IBMX indicates PDE7 activity. Data are mean ± SD for at least 3 to 8 separate experiments employing different cell preparations. In each experiment triplicate PDE assays were performed and an average value taken.

Table 3.2. The effect of actinomycin D on the increase in Jurkat T-cell PDE3 and PDE4 activities induced upon activation of adenylate cyclase by forskolin and cholera toxin

	PDE3 increase (%)	PDE4 increase (%)
forskolin	131±11	215±19
forskolin + Act-D	-38±12	11±16
Act-D	-12±8	-18±14
cholera toxin	104±14	218±49
cholera toxin + Act-D	18±12	23±15
8-Bromo-cAMP	69±7	58±7

Jurkat T-cells were treated for 9 h with 100 μ M forskolin, 6 h with 1 μ g/ml cholera toxin and 9 h with 100 μ M 8-Bromo-cAMP. In some experiments actinomycin D (100 ng/ml) was added to incubations. After indicated times, the cells were harvested and homogenate prepared for assay of PDE activity using 1 μ M cAMP as substrate. PDE3 activity was gauged as that fraction of the total PDE activity which was inhibited by 10 μ M cilostimide. PDE4 activity was gauged as that fraction of the total PDE activity which was inhibited by 10 μ M rolipram. The data represent mean \pm SD of three to five separate assays, performed in triplicate, using different cell preparations. The change in PDE activities is given as a percentage of the activity. Act-D is actinomycin D.

Table 3.3. The enhancement of forskolin-stimulated cAMP accumulation in Jurkat T-cells by PDE inhibitors

ligands	[cAMP] (pmol/10 ⁶ cells)	fold change
none (control)	1.6±0.4	-
forskolin	29±3	(1)
forskolin + rolipram	154±8	5.3
forskolin + Act-D	70±5	2.4
forskolin + Act-D + rolipram	158±9	5.4
forskolin + cilostimide	44.2±4	1.5
forskolin + IBMX	148±12	5.1

Jurkat T-cells were cultured for 9 h in the presence of indicated ligands. These were either no added ligand (control) or the indicated combinations of 100 µM forskolin, 10 µM rolipram, 10 µM cilostimide, 100 µM IBMX and 100 ng/ml actinomycin D. After this time cells were harvested and the intracellular concentration of cyclic AMP was determined as described in section 2.2.9. These are shown as pmol/10⁶ cells. Data are mean ± SD for *n* = 3 separate experiments using different cell preparations and each carried out in triplicate. The fold change indicated the fold potentiation of the forskolin-induced elevation of intracellular cAMP levels. Act-D is actinomycin D.

Table 3.4. Summary of forskolin mediated induction of PDE4 splice variants

	untreated	forskolin-treated
PDE4A (generic)	++++	++
PDE4B (generic)	-	-
PDE4B1	-	-
PDE4B2	-	-
PDE4C (generic)	-	-
PDE4D (generic)	++	++++
PDE4D1	+	++++
PDE4D2	-	++
PDE4D3	-	-
PDE4D4	-	-
PDE4D5	-	-

This summarises the occurrence of PDE4 splicing RNA transcripts after treating Jurkat T- cells with 100 μ M forskolin for 9 h.

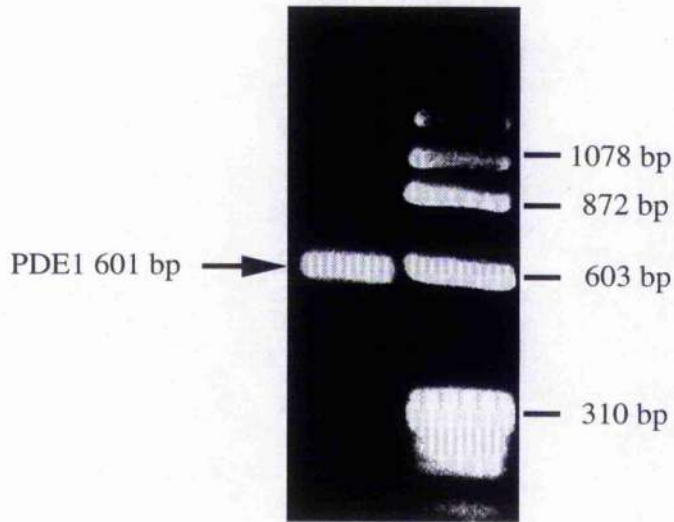


Figure 3.1. RT-PCR analysis of PDE1 'generic' transcripts in Jurkat T-cells

Total RNA was isolated from cultured Jurkat T-cells and reverse transcribed into cDNA (section 2.2.15-16). PCR was then performed (section 2.2.17) using a set of primers designed to detect 601 bp fragment found in all PDE1A and PDE1B transcripts. The primers were: GR18 sense 5'-RYCTYATCARCCGYTTYAAG-ATTCC-3' and GR19 antisense 5'-RAAYTCYTCCATKAGGGGCCWTGG, as described previously (Spence et al., 1995). (In these primers, R=A/G, Y=C/T, K=G/T and W=A/T). PCR reaction employed 1 min at 95 °C, 80 s at 50 °C and 70 s at 72 °C for 40 cycles. The products were electrophoresed on 2 % agarose gel and visualised with ethidium bromide under UV light. The results are representative of three experiments using RNA from different extractions.

Figure 3.2. Alignment of PDE1 transcript RT-PCR products from human Jurkat T-cells

The sequence of Jurkat T-cell PDE1B (GenBank accession number U40584) from PCR products was aligned together with sequences for the equivalent region of published data for *C. hamster* (U40585), human PDE1A (U40371) and human PDE1C1 (U40370) sequences for comparison. Alignment was carried out with a PDE1 consensus sequence [a degenerate consensus of the three full-length PDE1B sequences; mouse PDE1B form (M94538), rat PDE1B form (M94537), bovine PDE1B form (M94867), where M = A/C, R = A/G, W = A/T, S = C/G, Y = T/C, K = G/T]. Matches to the consensus are printed within the boxed area.

consensus.
C. Hamster I B (1-802)
Human I B (1-854)
Human I A (047-1248)
Human I C1 (769-1870)

```
A C C T C A T D A G C C G T T V A A G A Y T C C C A C M C T C T T Y Y G A I 40  
A F T C T C A T C A G C C G T T T Y A A G A Y T C C C A C T C T T T T C T G A I 40  
A T G T T A T C A A C C G T T Y C A A G A Y T C C C A C T C T T T T C T G A I 15  
A T C T T A T C A G C C G T T Y C A A G A Y T C C C A C T T C T G C A C T T G T 40
```

consensus.
C. Hamster I B (1-802)
Human I B (1-854)
Human I A (047-1248)
Human I C1 (769-1870)

```
G A T T T T Y C T G G A G C C G T T N G A E A H A G C T A Y G G A A A T A Y 80  
G A C T T T T C T G G A G C C G T T G S S W A B A B C T A T C C G A A A T A Y 80  
E A G T T T T C T G G A G C C G T T T G S A G A C A C C T T A T E G G A A G F A C 85  
C A C C T T T C C A G A A C C T T T G S A A G T T C E T T A A E C A A K F A C 85  
C T C A T T T Y T S E A P R C C G T T G S A A G T C E T T A A E C A A C G A C 85
```

consensus.
C. Hamster I B (1-802)
Human I B (1-854)
Human I A (047-1248)
Human I C1 (769-1870)

```
A A G A A Y C C T A C C A E A A C C A C A Y T C C A Y E K M C Y E A A C T S A 120  
A A G A A C C C T T A C C A C A A T C A C A T C C A T C C A S C T B A T C T G A 120  
A A G A A C C C T T A C C A C A A C C A S A T C C A C C A S C C G A T C T A 85  
A A A A A T C C A T T A C C A A A T T T A T T C A T G C A A C T C A T G T G A 120  
A A A A T C C T A C C A C A C T T A A T T A T T G A C C C T C C S A T G T G T 120
```

consensus.
C. Hamster I B (1-802)
Human I B (1-854)
Human I A (047-1248)
Human I C1 (769-1870)

```
C C C A C A C K E T S C A Y I G T Y G Y T T C C G C R C A G S A T G T G T 180  
C C C A G A C A G T G C A T T E C T T T C T C C T C C C C B A G G C A T G C E T 180  
C C C A C A C A G T G C A T T E C T T T C T C C T C C C C B A G G C A T G C E T 185  
C T C A A A C T H T A T T A G A T A A Y C S T T A T A C A G S T A T C R T 185  
C A C A S A G A R E T G S A T A G G T C C T A T A S A C A G S A R T E G C 185
```

consensus.
C. Hamster I B (1-802)
Human I B (1-854)
Human I A (047-1248)
Human I C1 (769-1870)

```
G C A C T G C C T T C R G A R A Y T G A S E T E Y T G C C A T G A I C T Y T 200  
G C A C T G C C T T C A C A C A T T G A S E T C T Y T G C C A T G A I C T Y T 200  
G C A C T G C C T T C A C C A A T T C C A A A T T T T H C C A T G A I C T Y T 176  
G C A C T G C C T T C A C C A A T T C C A A A T T T T H C C A T G A I C T Y T 200  
G A A C T Y G C T E A C G R A G C C C G A A T T C C T A T A T A T S T T C 200
```

consensus.
C. Hamster I B (1-802)
Human I B (1-854)
Human I A (047-1248)
Human I C1 (769-1870)

```
G C T G C A S C C A T C E A Y G A C T A T E A G G A D A G W E C C A W A C C A 240  
G C T G C A S C C A T C E A Y G A C T A T E A G G A D A G W E C C A W A C C A 240  
G C T G C A S C C A T C E A Y G A C T A T E A G G A D A G W E C C A W A C C A 216  
G C T G C T G C C A T T C A T G A T T A T A C A S C A C C G C R A C T A C C A 240  
T C A R G Y T G C E A Y G C A T G A G T A E S A S E A T A C C E S A A C C A C C A 240
```

consensus.
C. Hamster I B (1-802)
Human I B (1-854)
Human I A (047-1248)
Human I C1 (769-1870)

```
A C A C C T T C C A C A Y Y C A C A C C A A R T C R G A A T Y G C C A T C C T 280  
A C A R C T T C C A C A T C C A G A C C A A R T C R G A A T Y G C C A T C C C 290  
A C A C T T T C C A C A Y C C A C C A C C A S T C A G A A T Y G C C A T C C T 286  
A C A A C T T C C A C A T T C A G A C R A C C G T C A T T S C C A T T T Y T 230  
A C A A T T T C C A T T C A G A C C C T C C T C A T T C C A S C A T T F I T 280
```

consensus.
C. Hamster I B (1-802)
Human I B (1-854)
Human I A (047-1248)
Human I C1 (769-1870)

```
G T A G A A Y G A Y C E M T C R G T C C T G B A G A A T C A C C A C A T C A E C 300  
G T A G A A C G A T C C G C C T C C T G B A G A A T C A C C A C A T C A E C 320  
G E A C A A T G T C C G T T C C C C T C C A G A A T C A C C A C A T C A E C 296  
G T A T A T R A T C C C T C F S Y C C T G B A A A T C A C C A C A T T C A G T 320  
G T A T A T R A S A W A R T C T E T A C T G R A R A A T C A C C A T T T A A S T 320
```

consensus.
C. Hamster I B (1-802)
Human I B (1-854)
Human I A (047-1248)
Human I C1 (769-1870)

```
T C K C T T T Y C G A T T G A T T C A G G A Y G A Y C A G . . . A T G A C A C A 357  
T C T G T T T Y C G A T T G A T T C A G G A Y G A Y C A G . . . A T G A C A C A 357  
T C T G T T T Y C G A T T G A T T C A G G A Y G A Y C A G . . . A T G A C A C A 332  
G C A S C T T A T C C A A T T T A T G C A A C A C A C A C A . . . A T G A C A T A 357  
G C A S C T T A T C G C C T T C T C C A A R A T G A C C A B F A A R T G A R T A 360
```

consensus.
C. Hamster I B (1-802)
Human I B (1-854)
Human I A (047-1248)
Human I C1 (769-1870)

```
T Y T T A T C A A Y C T C A C C A R C C A T G A R T T Y G A B S C T E C G 387  
T T T T A T C A A Y C C C A C C C A A G G A T G A S T T T C T A C C A C T T C G 397  
T T T T A T C A A Y C C C A C C C A A G G A T G A R T T T T C A C A C T T C G 372  
T Y T T G A T A A T T T A T G A A A G A T G A C C G G A G A C A T C T C T 387  
T C T T R A T T A A C C T E T C A A A S S A T R A C T G G A A G R A A T T T T C 408
```

consensus.
C. Hamster I B (1-802)
Human I B (1-854)
Human I A (047-1248)
Human I C1 (769-1870)

```
G C C Y C T G G T A T Y A S A T C G T G T H G C C A C A C A C A T E Y C C 437  
G C C C T T C C T A T T G A A T C G T G T T G C C C A C A C A C A T E Y C C 437  
A G C C T T C C T A T T G A A T C G T G T T G C C C A C A C A C A T E Y C C 432  
G A A C S T A C T G A T T C A A A T C G T T T A T C C A G A G A A T C T C A 437  
A A C S T E C G T A A T T R A A T C G T S A T C C A G A G R T A T C T C A 440
```

consensus.
C. Hamster I B (1-802)
Human I B (1-854)
Human I A (047-1248)
Human I C1 (769-1870)

```
T C C A T T T C C A G C A A S T G A E M C Y A T G A A G A C A C C H Y T G 477  
T C C C A T T T C C A G C A A S T G A A T C T A T G A A G A C A C C C T T G C 477  
T C C C A T T T C C A G C A A S T G A A T C T A T G A A G A C A C C C T T G C 482  
G T T C A C T T C C A G C A A A T T A A A A R A T A A G A A A C A C T T T G S 477  
T C T E A C T T C C A A E A A A T C A A A S G A A T A A A G A C T E R T G T G S 480
```

consensus.
C. Hamster I B (1-802)
Human I B (1-854)
Human I A (047-1248)
Human I C1 (769-1870)

```
A G C A G Y T K G A A A R S A Y T C A C A A H T C C A A G C C C T Y T C T C T 517  
A G C A G Y T C G A A A R S A Y T C A C A A C T C C A A G C C C T A T G C T 517  
A A C A C C T T C G A A C S A Y T G A C A A G T C C A A G C C C T G T C T C T 482  
A G C A G C C T G A A G S A T T G A C A E A G C C A A A C C A T G T C C C T 517  
A G C A G C C A E A R A M C A T T G A A A R C G A A A A E C C T T B T C C C T 520
```

consensus.
C. Hamster I B (1-802)
Human I B (1-854)
Human I A (047-1248)
Human I C1 (769-1870)

```
K C T C G T T C A T E C Y G T E R C A T D A G S C A L C C M A C Y A A C C A G 557  
K C T C G T T C A T E C T G T E R C A T D A G S C A L C C M A C C E R A C C A G 557  
K C T C G T T C A T E C T G T E R C A T D A G S C A L C C M A C C E R A C C A G 532  
K A Y T C T C G C A C C A G A G A G A S A T E A S C C A A G C C A A T A T C C 557  
A A T S C T G A T A C A G S A G A T T A S C C A T C C A E C A A A G C A 580
```

consensus.
C. Hamster I B (1-802)
Human I B (1-854)
Human I A (047-1248)
Human I C1 (769-1870)

```
T C C T C A E T Y C A C A C C C S E T E A C C A A S C C C T M A T G E A R G 597  
T C C T C A G T C C A C A C C C A T T E R A C C A A Y S C C E T C A T G S A S 597  
T C C T C A G T C C A C A C C C A T T E R A C C A A Y S C C E T C A T G S A S 554  
T C C A A A C T C C A T A T C C G T G G A C C A T T C C C E C T A T T G G A G 597  
T C C A C C T C C A T C A T E S C T E R C A A T S T T C A E T C C T G G A G 600
```

consensus.
C. Hamster I B (1-802)
Human I B (1-854)
Human I A (047-1248)
Human I C1 (769-1870)

```
A A T T A 802  
A S T T T 802  
A A T T Y 554  
A C T T C 802  
805
```

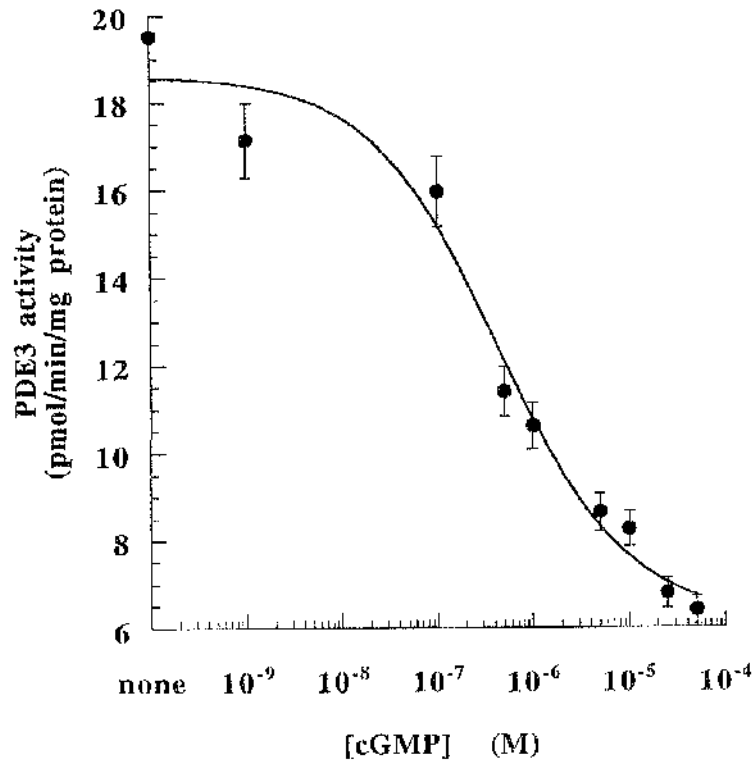


Figure 3.3. Identification of PDE3 activity in Jurkat T cells: Inhibition by cGMP

Homogenates of Jurkat T-cells were assayed for PDE activity using 1 μ M cAMP as substrate as described in section 2.2.7. The dose-dependent changes in Jurkat T-cell PDE activity elicited by cGMP are shown. The data reflect mean \pm SD for triplicate assays done in a single experiment. These data are typical of experiments done three times for which IC_{50} values were calculated and are given in the text. PDE activity is expressed in pmol cAMP hydrolysed/min/mg protein.

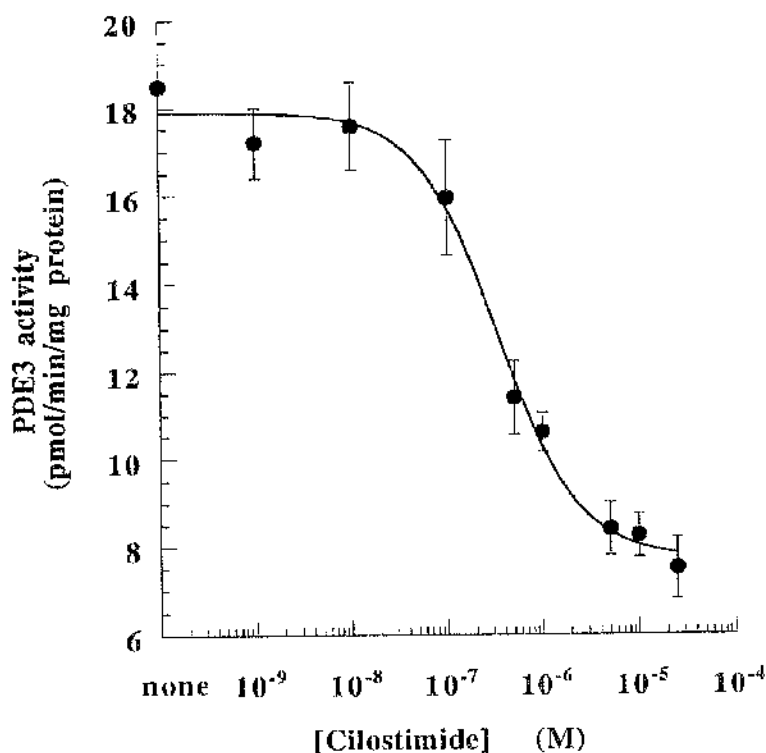


Figure 3.4. Identification of PDE3 activity in Jurkat T cells: Inhibition by cilostimide

Homogenates of Jurkat T-cells were assayed for PDE activity using 1 μ M cAMP as substrate as described in section 2.2.7. The dose-dependent changes in Jurkat T-cell PDE activity elicited by the PDE3 selective inhibitor cilostimide are shown. The data reflect mean \pm SD for triplicate assays done in a single experiment. These data are typical of experiments done three times for which IC_{50} values were calculated and are given in the text. PDE activity is expressed in pmol cAMP hydrolysed/min/mg protein.

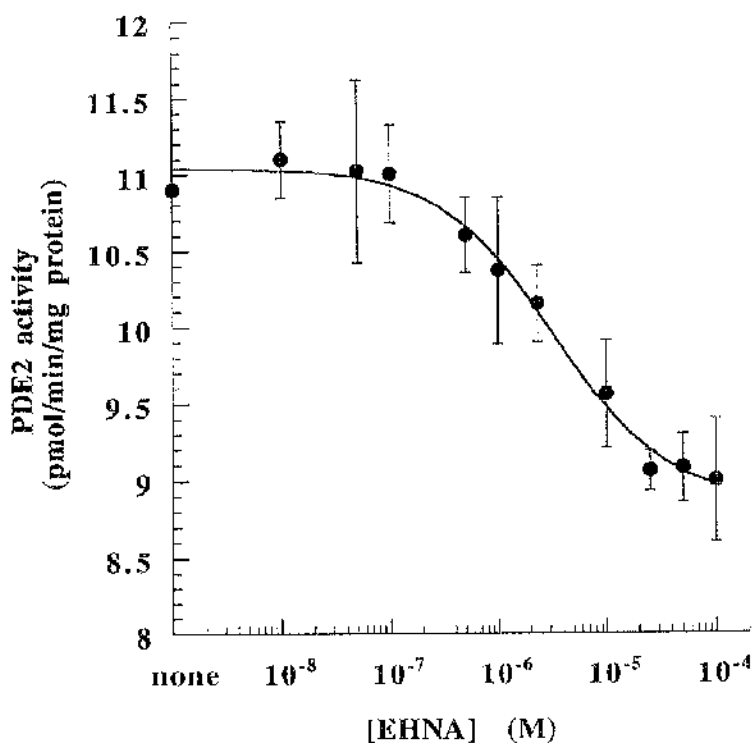


Figure 3.5. Identification of PDE2 activity in Jurkat T cells: Inhibition by EHNA

Homogenates of Jurkat T-cells were assayed for PDE activity using 1 μ M cAMP as substrate as described in section 2.2.7. The dose dependent inhibition of PDE activity by EHNA is shown for assays done in the presence of stimulatory concentrations (10 μ M) of cyclic GMP. The data reflect mean \pm SD for triplicate assays done in a single experiment. These data are typical of experiments done three times for which IC_{50} values were calculated and are given in the text. PDE activity is expressed in pmol cAMP hydrolysed/min/mg protein.

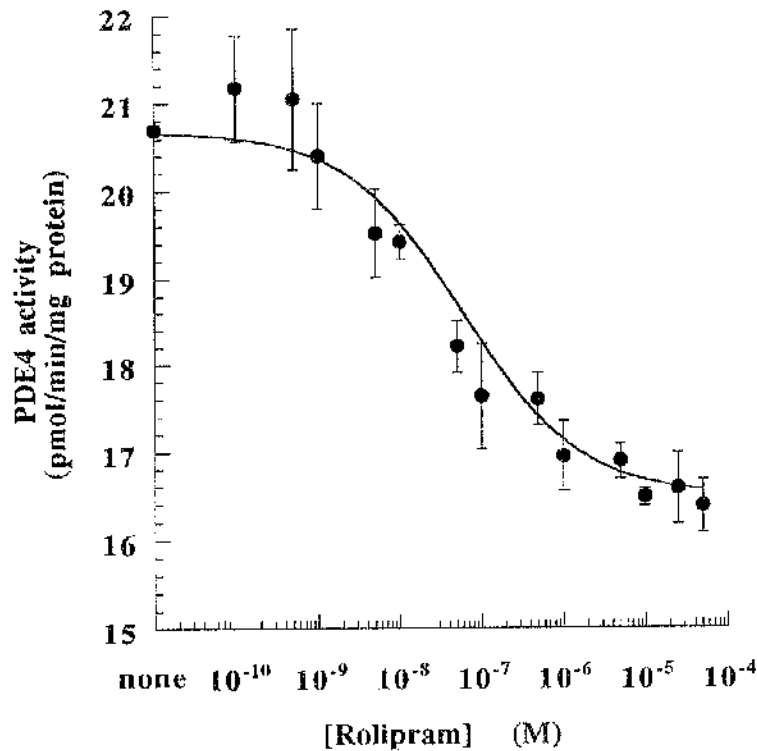


Figure 3.6. Identification of PDE4 activity in Jurkat T cells: Inhibition by rolipram

Homogenates of Jurkat T-cells were assayed for PDE activity using 1 μ M cAMP as substrate as described in section 2.2.7. The dose-dependent changes in Jurkat T-cell PDE activity elicited by the PDE4 selective inhibitor rolipram are shown. The data reflect mean \pm SD for triplicate assays done in a single experiment. These data are typical of experiments done three times for which IC_{50} values were calculated and are given in the text. PDE activity is expressed in pmol cAMP hydrolysed/min/mg protein.

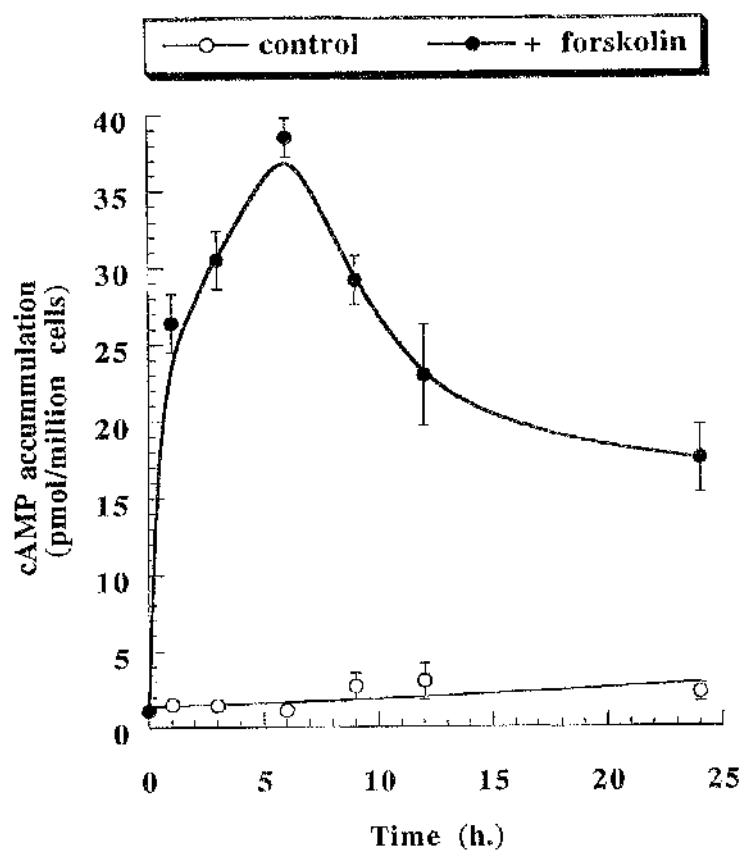


Figure 3.7. The effect of forskolin on the accumulation of intracellular cAMP concentrations in Jurkat T-cells

Jurkat T-cells were incubated at 37 °C for the indicated times with and without 100 μ M forskolin. The reaction was terminated at the indicated times by the addition of cold 4 % perchloric acid (PCA). cAMP was measured as indicated in section 2.2.9. Values represent the mean \pm SD of triplicate determinations. Data presented are from a representative experiment that was repeated three times with similar results.

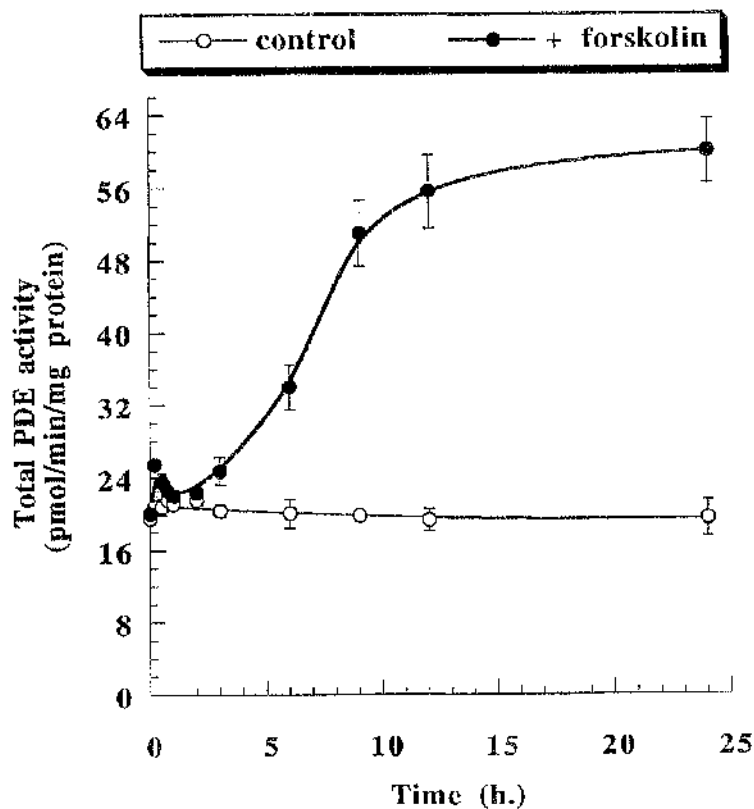


Figure 3.8. Time course of total PDE activity in the presence of forskolin

Jurkat T-cells were grown in suspension in medium with 5 % serum . They were then incubated for the indicated times up to 24 h in the absence (regarded as controls) or presence of 100 μ M forskolin. At the end of the incubations, cells were washed twice with serum free medium, harvested and homogenised (section 2.2.1.2). The total PDE activity was determined using the cell homogenates with 1 μ M cAMP as substrate. Each point represents the mean \pm SD for triplicate assays done in a single experiment. These data are typical of experiments done three times.

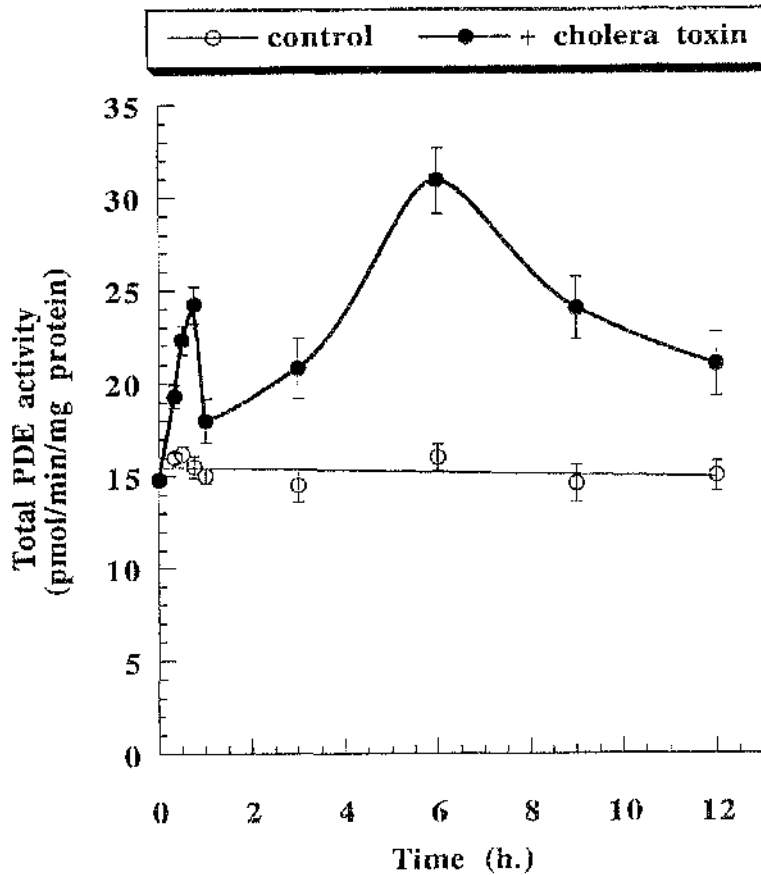


Figure 3.9. Time course of cholera toxin activated total PDE activity

Jurkat T-cells were incubated for different times up to 12 h in the absence (control) or presence of 1 $\mu\text{g/ml}$ cholera toxin. At the end of the incubation, cells were rinsed twice, harvested and homogenised as described in section 2.2.1.2. Total PDE activity was observed in the presence of 1 μM cAMP as substrate. Each point represents the mean \pm SD of at least three different experiments, each carried out in triplicate.

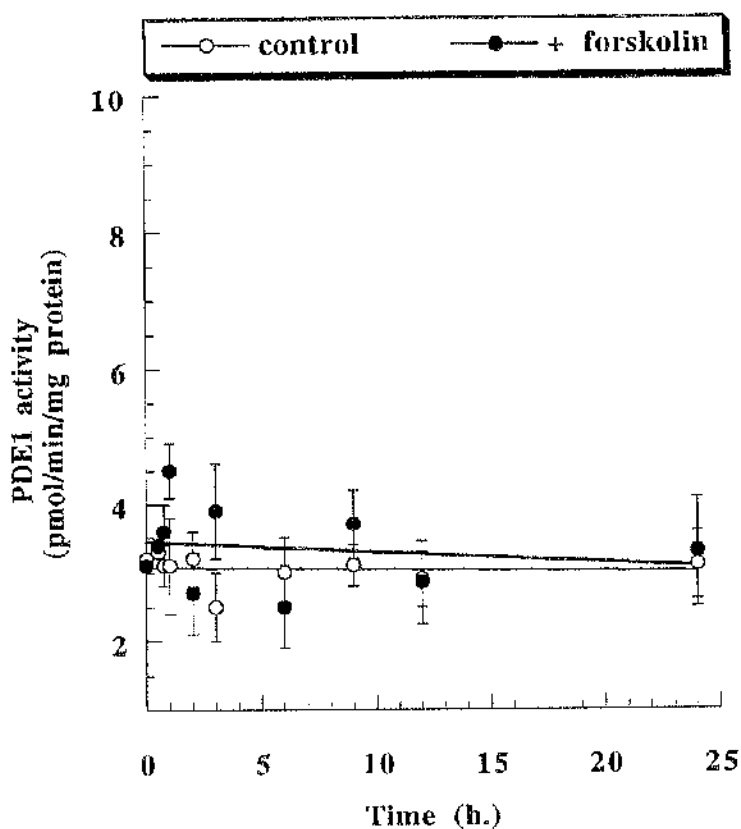


Figure 3.10. Time course of forskolin activated PDE1 activity

Jurkat T-cells were incubated for the indicated times either in the absence (0.1 % DMSO, control) or presence of 100 μM forskolin. At the end of the incubation, cells were washed twice with serum free RPMI-1640 medium, harvested and counted then homogenised as described in section 2.2.1.2. Changes in PDE1 activity were assessed by determining the incremental increase in PDE activity achieved by the addition of Ca^{2+} / CaM (50 μM ; 20 ng/ml) to assays. Activity in the absence of Ca^{2+} / CaM indicates basal PDE activities. Assays employed with 1 μM cAMP as substrate. Each point represents the mean \pm SD of three different experiments, each carried out in triplicate.

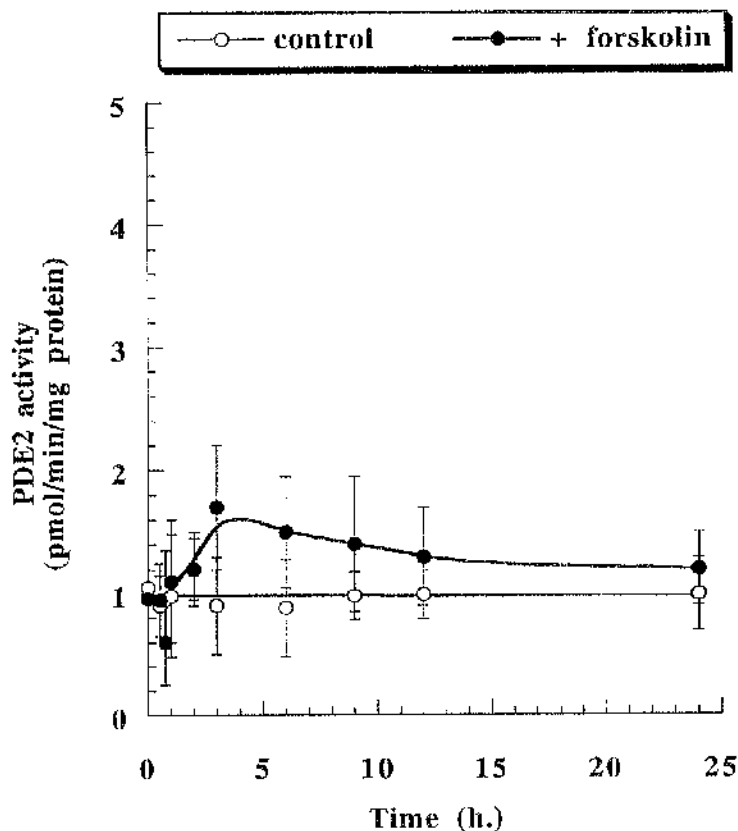


Figure 3.11. Time course of forskolin activated PDE2 activity

Jurkat T-cells were incubated for the indicated times either in the absence (0.1 % DMSO) or presence of 100 μ M forskolin. At the end of the incubation, cells were washed twice with serum free RPMI-1640 medium, harvested and counted then homogenised as described in section 2.2.1.2. Changes in PDE2 activity were calculated by determining the incremental inhibition of cAMP-PDE activity achieved by the selective inhibitor EHNA for assays done in the presence of 10 μ M cGMP, which would be expected to activate maximally any PDE2. Assays employed with 1 μ M cAMP as substrate. Each point represents the mean \pm SD of three different experiments, each carried out in triplicate.

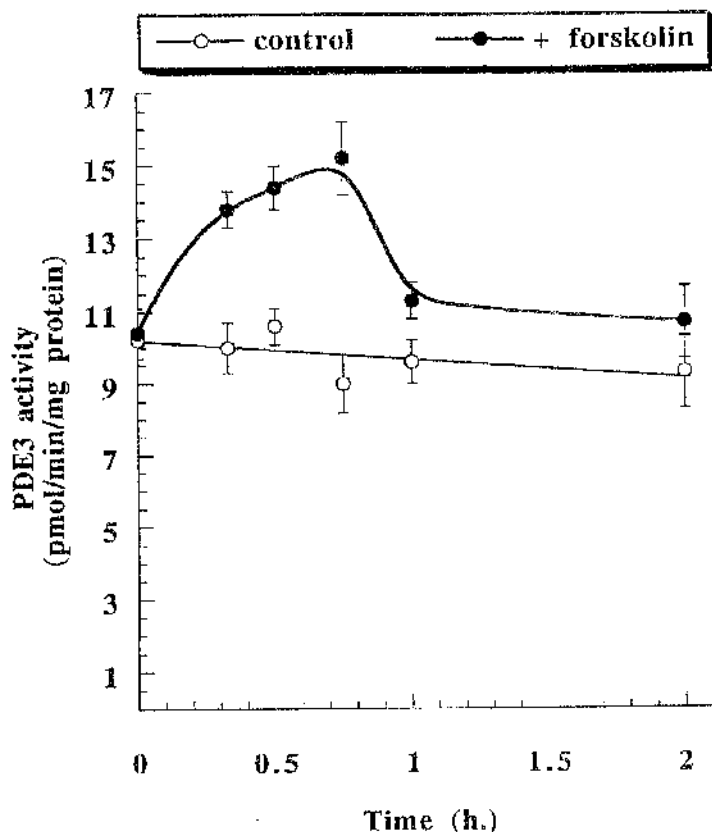


Figure 3.12. Time course of forskolin activated PDE3 activity over first two hours

Jurkat T-cells were incubated for the indicated times up to 2 h either in the absence (0.1% DMSO control) or presence of 100 μ M forskolin. At the end of the incubations, cells were washed twice with serum free RPMI-1640 medium, harvested and homogenised as described in section 2.2.1.2. The PDE activity was determined at the time indicated, in the presence of 10 μ M final concentration of cilostimide (regarded as PDE3 activity) using the cell homogenates. Assays employed with 1 μ M cAMP as substrate. Each point represents the mean \pm SD of at least three different experiments, each carried out in triplicate.

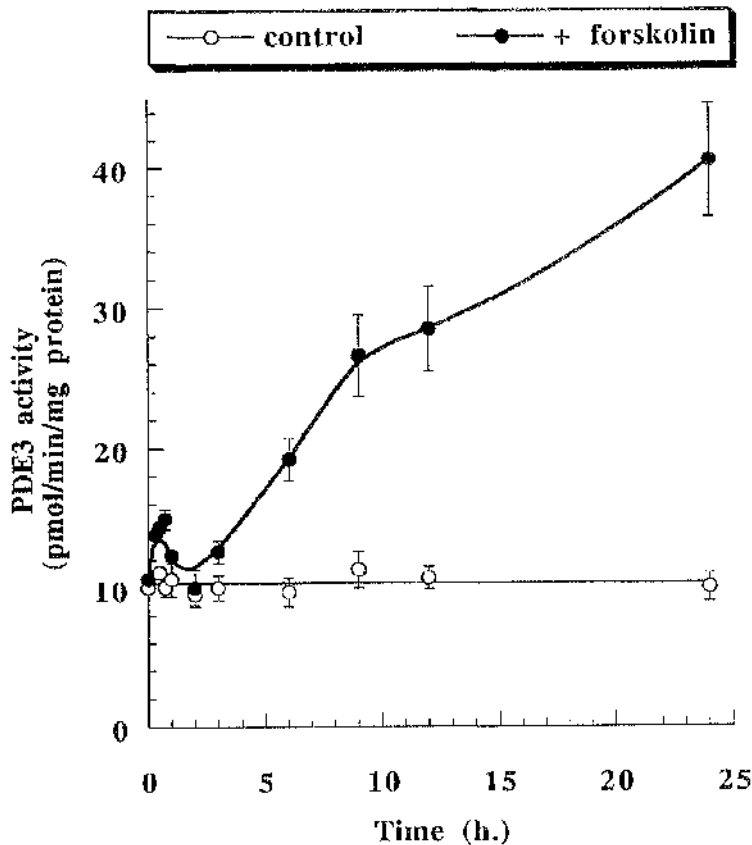


Figure 3.13. Time course of forskolin activated PDE3 activity

Jurkat T-cells were incubated for the indicated times either in the absence (0.1 % DMSO control) or presence of 100 μ M forskolin. At the end of the incubations, cells were washed twice with serum free RPMI-1640 medium, harvested and homogenised as described in section 2.2.1.2. The PDE activity was determined at the time indicated, in the presence of 10 μ M final concentration of cilostimide (regarded as PDE3 activity) using the cell homogenates. Assays employed with 1 μ M cAMP as substrate. Each point represents the mean \pm SD of at least three different experiments, each carried out in triplicate.

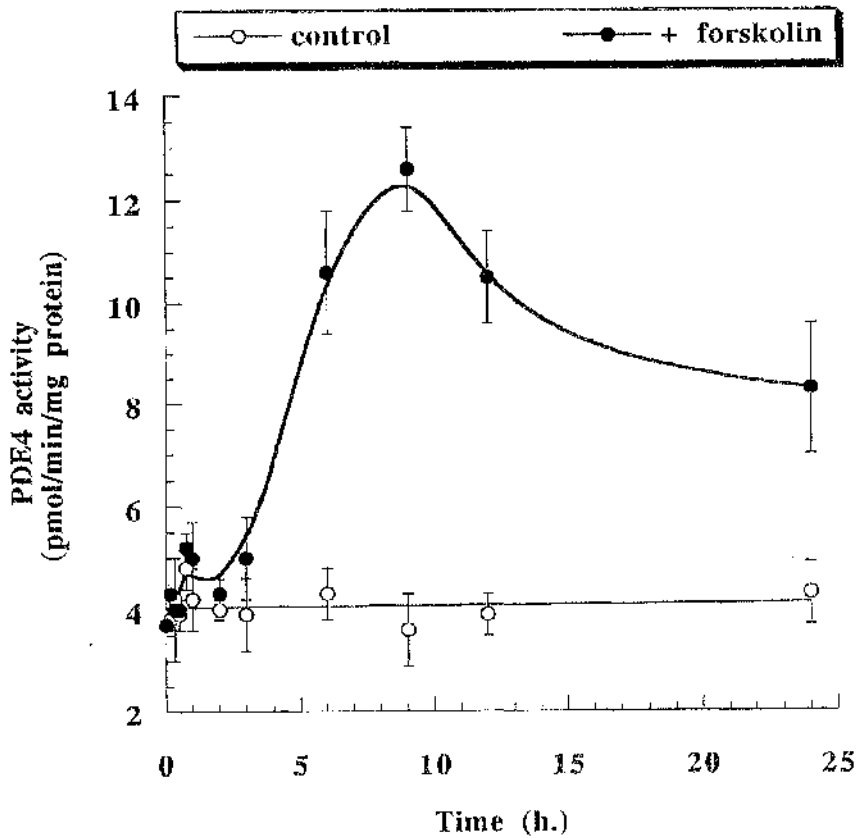


Figure 3.14. Time course of forskolin activated PDE4 activity.

Jurkat T-cells were incubated for the indicated times either in the absence (0.1 % DMSO control) or presence of 100 μM forskolin. At the end of the incubations, cells were washed twice with serum free RPMI-1640 medium, harvested and homogenised as described in section 2.2.1.2. The PDE activity was determined at the time indicated, in the presence of 10 μM final concentration of rolipram (regarded as PDE4 activity) using the cell homogenates. Assays employed with 1 μM cAMP as substrate. Each point represents the mean \pm SD of at least four different experiments, each carried out in triplicate.

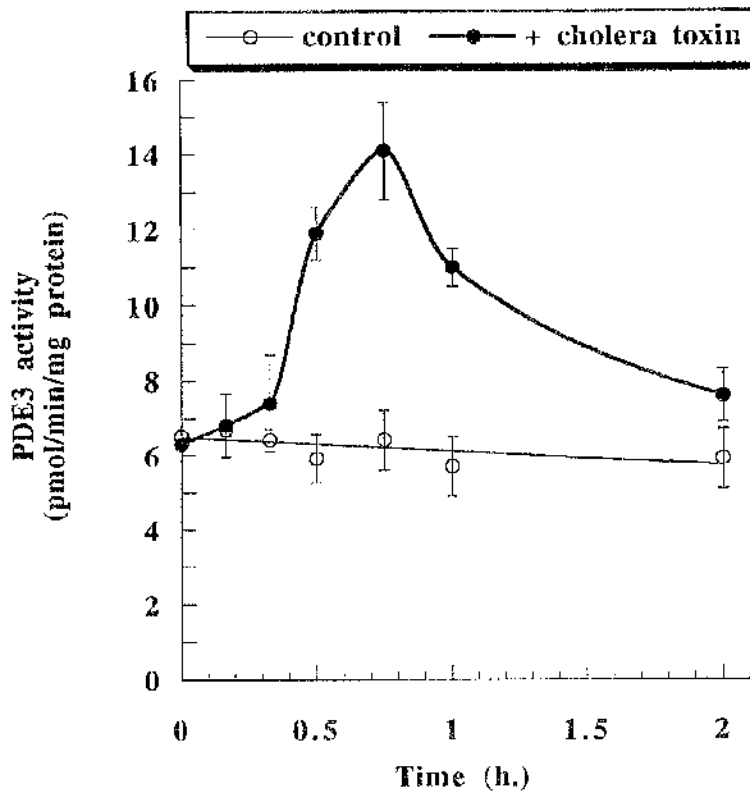


Figure 3.15. Time course of cholera toxin activated PDE3 activity

Jurkat T-cells were incubated for different times up to 2 h in the absence (control) or presence of 1 $\mu\text{g/ml}$ cholera toxin. At the end of the incubation, cells were rinsed twice, harvested and homogenised (see section 2.2.1.2). The PDE3 activity was determined at the time indicated, in the presence of 10 μM final concentration of cilostimide using the cell homogenates. Assays employed with 1 μM cAMP as substrate. Each point represents the mean \pm SD of at least three different experiments, each carried out in triplicate.

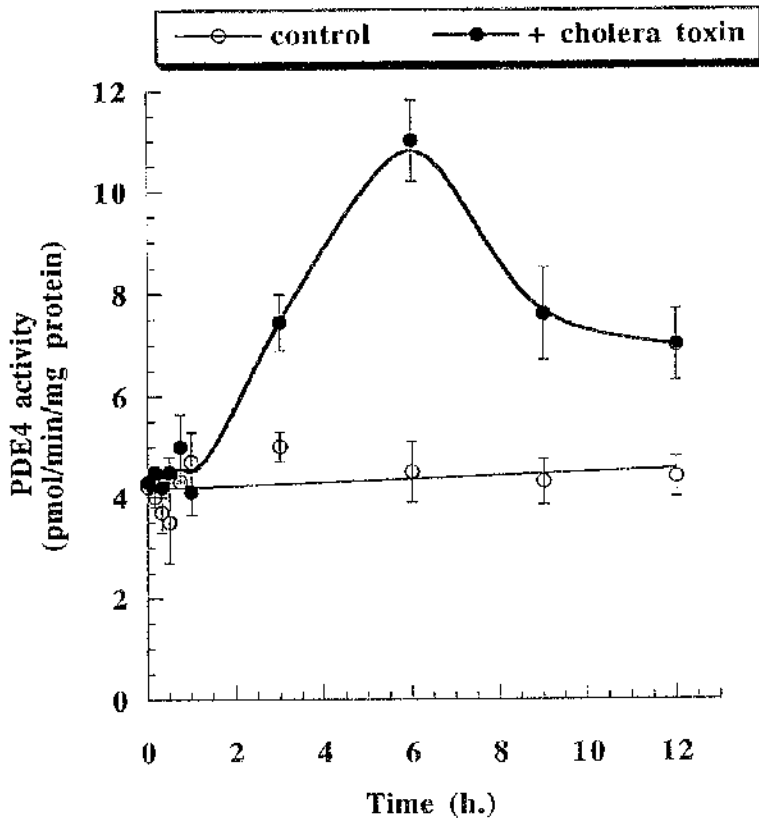


Figure 3.16. Time course of cholera toxin activated PDE4 activity

Jurkat T-cells were incubated for different times up to 12 h in the absence (control) or presence of 1 $\mu\text{g/ml}$ cholera toxin. At the end of the incubation, cells were rinsed twice, harvested and homogenised as described in section 2.2.1.2. The PDE4 activity was determined at the time indicated, in the presence of 10 μM final concentration of rolipram using the cell homogenates. Assays employed 1 μM cAMP as substrate. Each point represents the mean \pm SD of at least three different experiments, each carried out in triplicate.

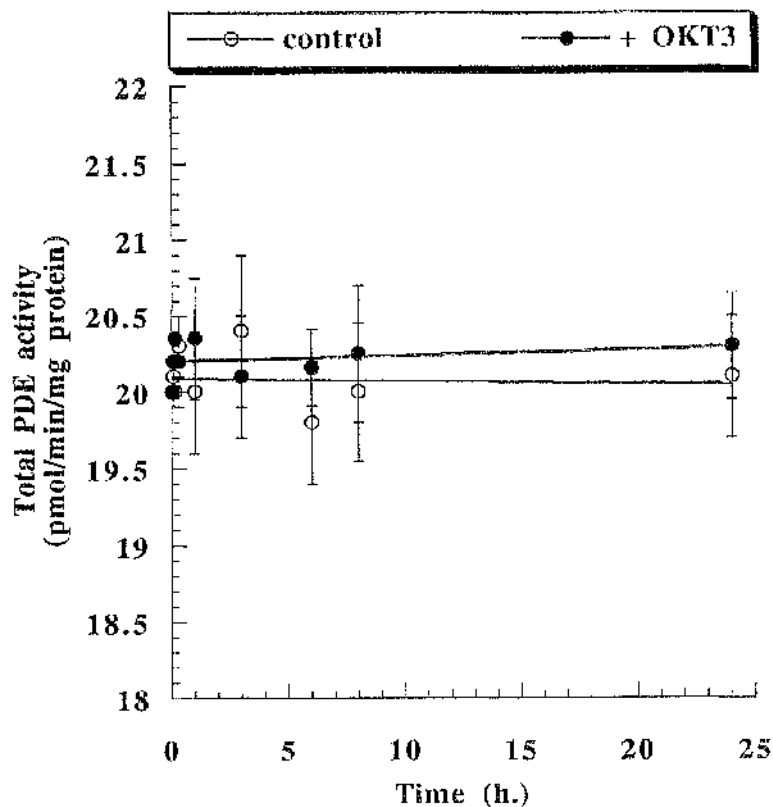


Figure 3.17. Total PDE activity in the Jurkat T-cell line upon stimulation with anti-CD3 antibodies

Jurkat T-cells were stimulated with anti-CD3 monoclonal antibodies (1 $\mu\text{g/ml}$) for different times up to 24 h. Then cells were extensively washed with serum-free medium, harvested and homogenised (section 2.2.1.2). Changes in the total PDE activity were assessed with 1 μM cAMP as substrate. The data reflect mean \pm SD for triplicate assays and are representative values of three experiments.

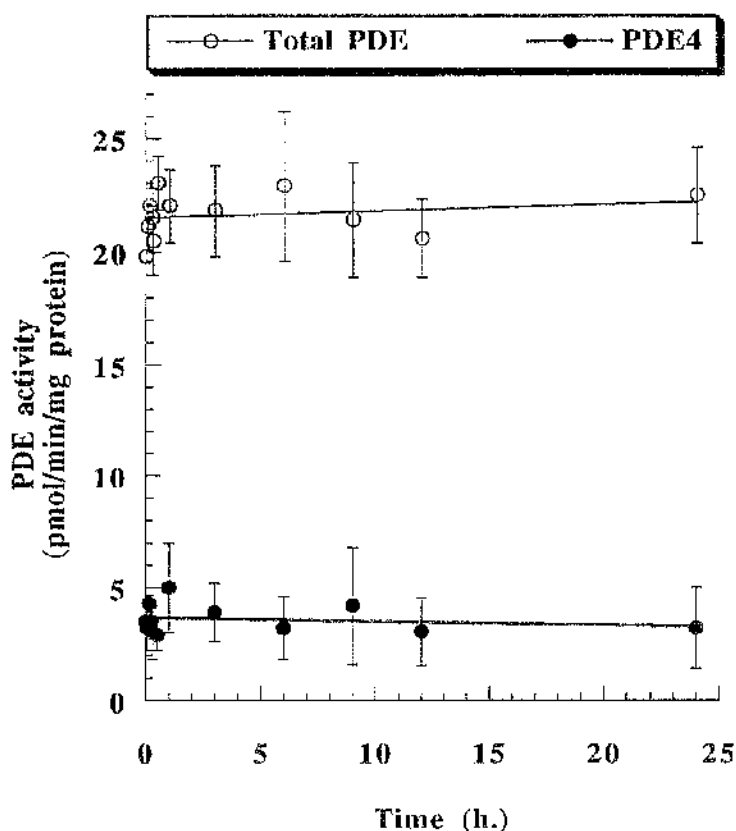


Figure 3.18. Time course of total PDE and PDE4 activities in the presence of PHA

Jurkat T-cells were challenged with PHA (1 $\mu\text{g}/\text{ml}$) for different times up to 24 h. Then cells were washed with serum-free medium, harvested and homogenised (section 2.2.1.2). Changes in the total PDE activity were assessed with 1 μM cAMP as substrate. The PDE4 activity was measured at the time indicated in the presence of rolipram (10 μM) using the cell homogenates. The data reflect mean \pm SD for triplicate assays and are representative values of three experiments.

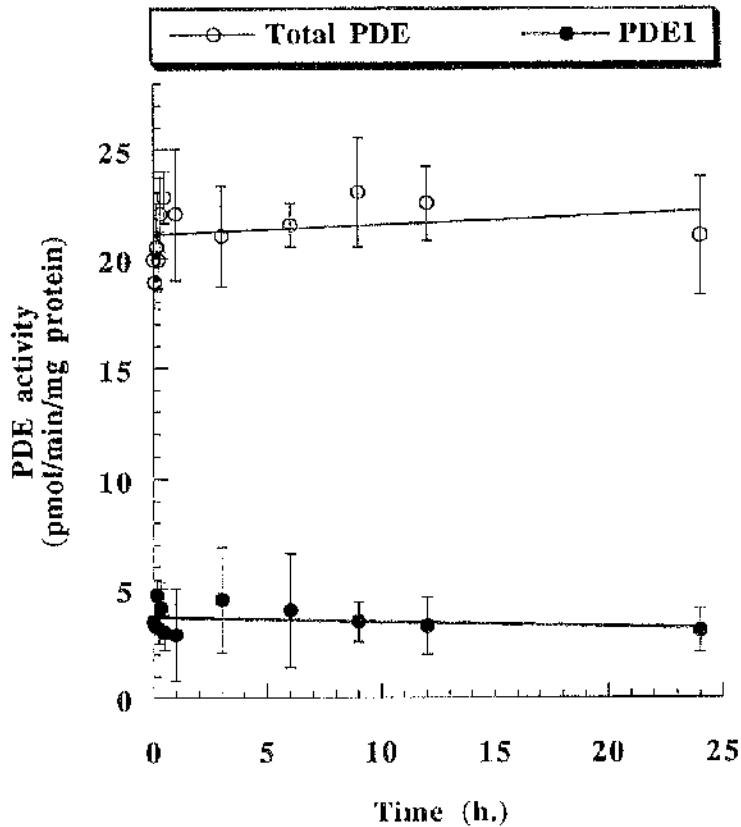


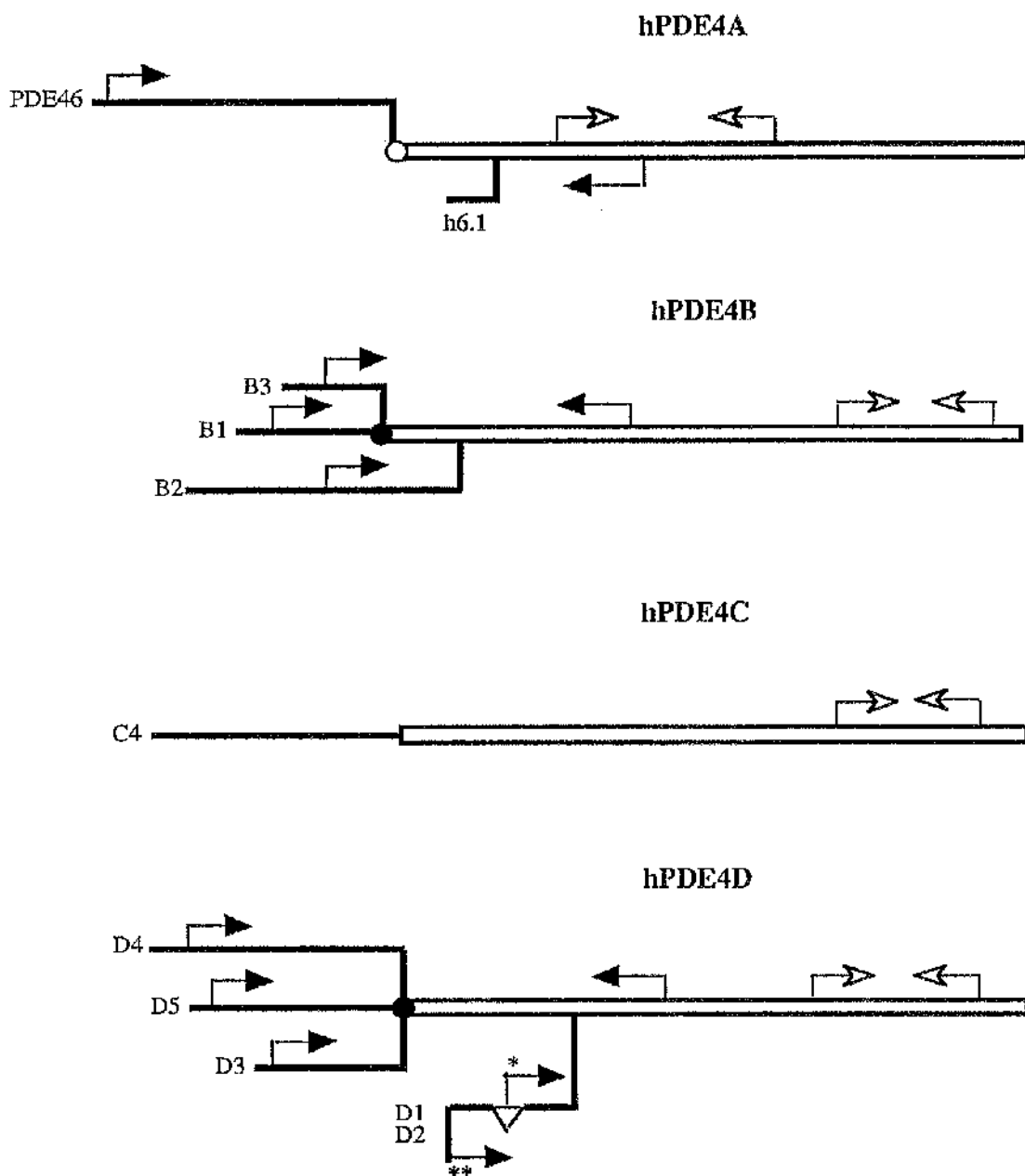
Figure 3.19. Time course of total PDE and PDE1 activities in the presence of PMA

Jurkat T-cells were challenged with PMA (1 μ M) for different times up to 24 h. Then cells were washed with serum-free medium, harvested and homogenised (section 2.2.1.2). Changes in PDE1 activity were assessed by determining the incremental increase in PDE activity achieved by the addition of Ca^{2+} / CaM (50 μ M; 20 ng/ml) to assays; activity in the absence of Ca^{2+} / CaM indicates basal PDE activities. Assays employed 1 μ M cAMP as substrate. The data reflect mean \pm SD for triplicate assays and are representative values of three experiments.

Figure 3.20. Schematic representation of primers used to analyse human PDE4 transcripts by RT-PCR

The primers used in this study for RT-PCR analyses of human cAMP-specific PDE4 transcripts are shown schematically. The PDE4 products of the four genes are shown with (•) splice junctions indicated and the names of the established active splice variants are given. Open arrows indicate the relative positions of the generic primer pairs used to identify the presence of transcripts encoding active members of a PDE4 isoforms. Filled arrows indicate the relative positions of primer pairs used to identify the presence of specific splice variants. These are given for the sense (left to right) and antisense (right to left) directions. The PDE4A schematic shows the two identified active species. These are PDE46 (Bolger et al., 1993), which is analogous to the rat PDE4 isoform RPDE6 and truncated species h6.1 which is closely related to hPDE-1 (Livi et al., 1990). The fragment amplified using the generic primers represents nucleotides 857-1362 in PDE46 and 407-912 in h6.1. The fragment amplified with the PDE46-specific primers represents nucleotides 101-917. The PDE4B schematic shows the three splice variants PDE4B1 (Bolger et al., 1993), PDE4B2 (McLaughlin et al., 1993) and PDE4B3 (Huston et al., 1997). Specific primers amplified a product which reflected bases 505-1373 in PDE4B1, bases 322-1190 in PDE4B3 and bases 805-1484 in PDE4B2. Generic primers amplified an identical sequence found in transcripts of both products which reflected nucleotides 2311-2478 and 2422-2589 in PDE4B1 and PDE4B2 respectively. The PDE4C schematic shows the single reported full length PDE4C4 form identified to date (Oberholte et al., 1997). The generic primers used were designed to amplify a fragment which represents nucleotides 2279-2373 in PDE4C4. The PDE4D schematic shows the human splice variants identified to date (Bolger et al., 1993, Bolger et al., 1997, Conti et al., 1995b, Nemoz et al., 1996), which show analogy with the rat forms (Conti et al., 1995b). Generic primers were designed to amplify a 3' fragment found in all human PDE4D species reported so far which encode an enzymically active protein: PDE4D1 (nucleotides 586-847), PDE4D2 (nucleotides 500-761), PDE4D3 (nucleotides 978-1239), PDE4D4 (nucleotides 1674-1935) and PDE4D5 (nucleotides 1180-1441). Specific primers amplified fragments for PDE4D1 (nucleotides 64-432), PDE4D1+PDE4D2 (nucleotides 7-432 and nucleotides 7-346 respectively), PDE4D3 (nucleotides 25-824), PDE4D4 (nucleotides 757-1520) and PDE4D5 (nucleotides 226-1026). The single asterisk indicates the position of the sense primer used to detect PDE4D1 specifically. This is placed with the 86 bp sequence which is deleted from PDE4D2 (Nemoz et al., 1996). The double asterisk indicates the position of the sense primer used to detect PDE4D1 and PDE4D2.

Figure 3.20. Schematic representation of primers used to analyse human PDE4 transcripts by RT-PCR



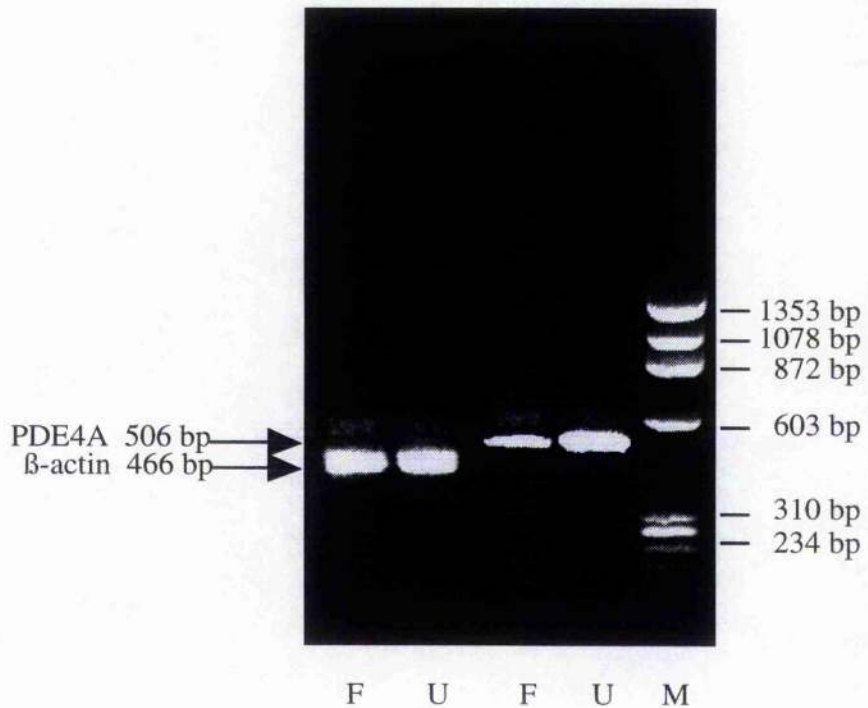


Figure 3.21. RT-PCR analysis of hormone effects on PDE4A 'generic' transcripts in Jurkat T-cells

Jurkat T-cells were untreated or exposed to 100 μ M forskolin for 9 h. After the treatment period, RNA was extracted and reverse transcribed into cDNA (sections 2.2.15-16). PCR was then performed (section 2.2.17) using the degenerate primers designed to detect transcripts selectively for PDE4A isoforms. These primers were: sense-2067, ATGCAGACCTATCGCTCTGTTCAGC and antisense-2071, ACCATCGTGTCCACAGGGATGC, defining a 506 bp fragment. Oligonucleotides were designed to amplify a 3' fragment found in all PDE4A species reported so far that encode an enzymically active protein. PCR reaction employed 1 min at 95 $^{\circ}$ C, 2 min at 57 $^{\circ}$ C and 3 min at 72 $^{\circ}$ C for 35 cycles. The products were electrophoresed on 1.5 % agarose gel and visualised with ethidium bromide under UV light. The results are representative of three experiments using RNA from different extractions. F: forskolin treated, U: untreated, M: marker.

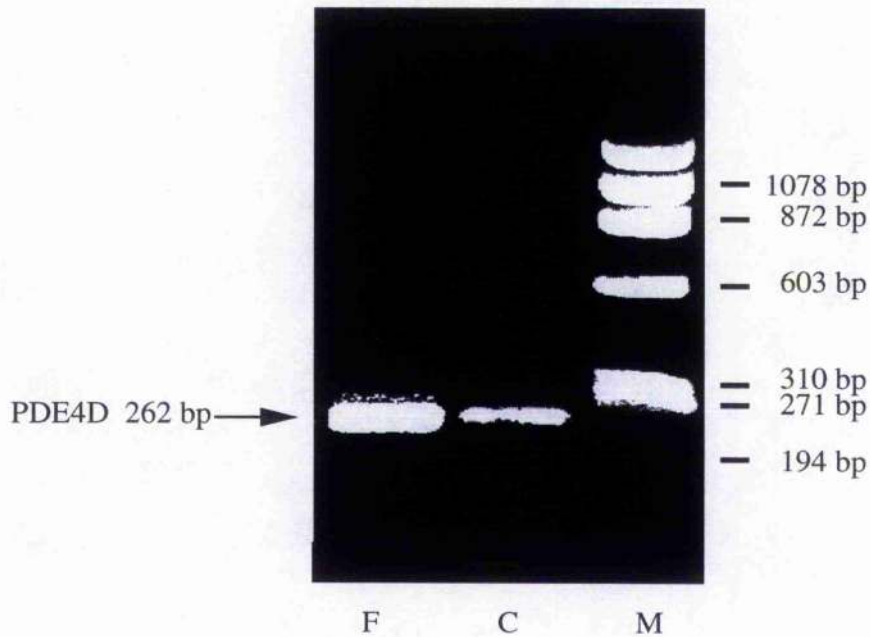


Figure 3.22. RT-PCR analysis of hormone effects on PDE4D 'generic' transcripts in Jurkat T-cells

Jurkat T-cells were untreated or exposed to 100 μ M forskolin for 9 h. After the treatment period, RNA was extracted and reverse transcribed into cDNA (sections 2.2.15-16). PCR was then performed (section 2.2.17) using the degenerate primers designed to detect transcripts selectively for PDE4D isoforms. These oligonucleotide primers were: sense-GR34, CCCTTGACTGTTATCATGCACA-CC and antisense-GR35, GATCTACATCATGTATTGCACTGGC defining a 262 bp PCR product. PCR reaction employed 1 min at 95 $^{\circ}$ C, 2 min at 55.3 $^{\circ}$ C and 3 min at 72 $^{\circ}$ C for 40 cycles. The products were electrophoresed on 1.5 % agarose gel and visualised with ethidium bromide under UV light. The results are representative of three experiments using RNA from different extractions. F: forskolin treated, U: untreated, M: marker.

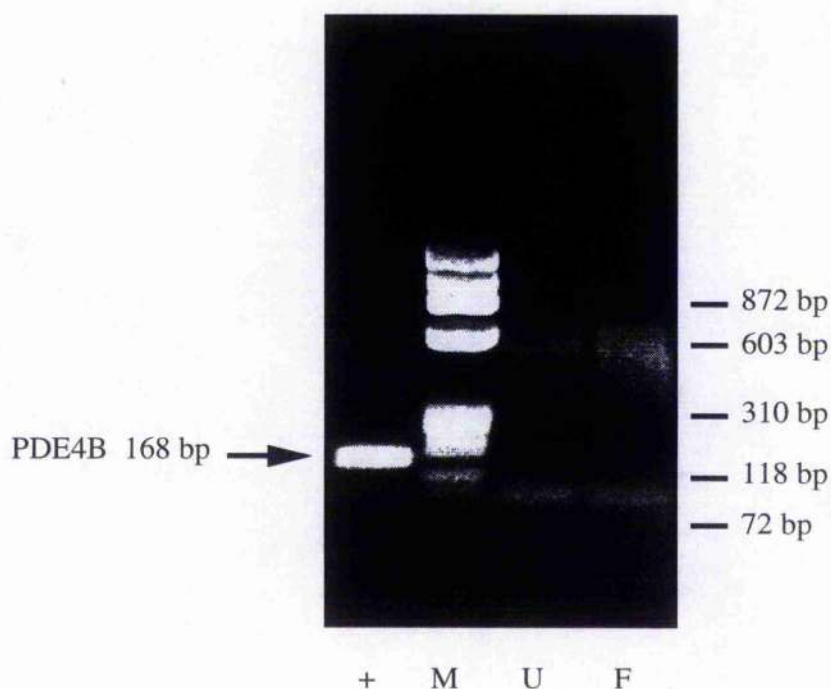


Figure 3.23. RT-PCR analysis of hormone effects on PDE4B 'generic' transcripts in Jurkat T-cells

Jurkat T-cells were untreated or exposed to 100 μ M forskolin for 9 h. After the treatment period, RNA was extracted and reverse transcribed into cDNA (sections 2.2.15-6). PCR was then performed (section 2.2.17) using the degenerate primers designed to amplify a fragment characteristic of the two reported human PDE4B species (PDE4B1, PDE4B2 and PDE4B3). These oligonucleotides were: sense-SE5, GACATTGCAACAGAAGACAAGTCCCC and antisense-SE6 ACTCAAGTAACTGAAAGGCCAGGTGG, defining a 168 bp product. PCR reaction employed 1 min at 95 $^{\circ}$ C, 90 s at 57 $^{\circ}$ C and 2 min at 72 $^{\circ}$ C for 35 cycles. The products were electrophoresed on 1.8 % agarose gel and visualised with ethidium bromide under UV light. The results are representative of three experiments using RNA from different extractions. (+): positive control, M: marker, U: untreated, F: forskolin treated.

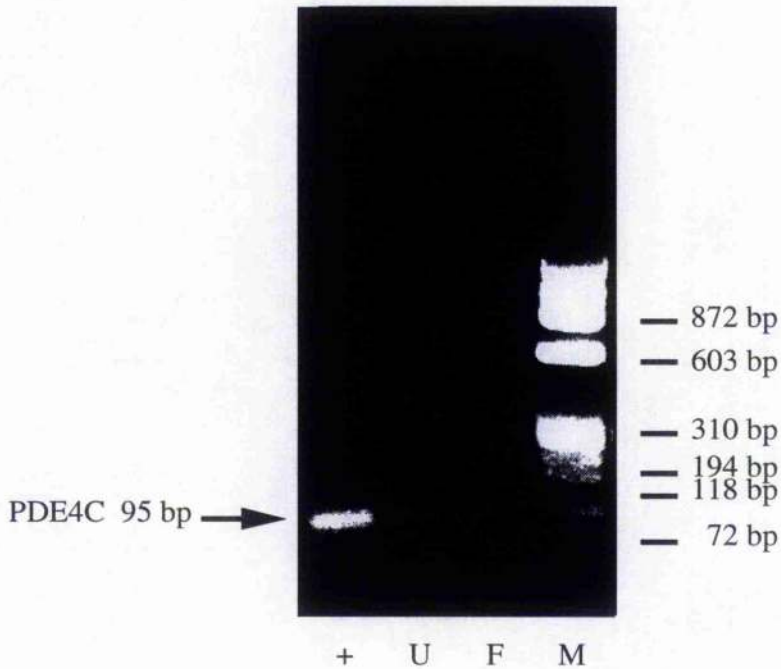


Figure 3.24. RT-PCR analysis of hormone effects on PDE4C 'generic' transcripts in Jurkat T-cells

Jurkat T-cells were untreated or exposed to 100 μ M forskolin for 9 h. After the treatment period, RNA was extracted and reverse transcribed into cDNA (sections 2.2.15-16). PCR was then performed (section 2.2.17) using the degenerate primers designed to detect transcripts selectively for PDE4C isoforms. These oligonucleotides were: sense-SE7, ATGGATGGTAAAGCCCTTTGGCTCTTGG and antisense-SE8, GTCTCCCTAAATGGGTGGGAAAGTGAAG, defining a 95 bp product. PCR reaction employed 1 min at 95 $^{\circ}$ C, 2 min at 58 $^{\circ}$ C and 3 min at 72 $^{\circ}$ C for 35 cycles. The products were electrophoresed on 2 % agarose gel and visualised with ethidium bromide under UV light. The results are representative of three experiments using RNA from different extractions. (+): positive control, U: untreated, F: forskolin treated, M: marker.

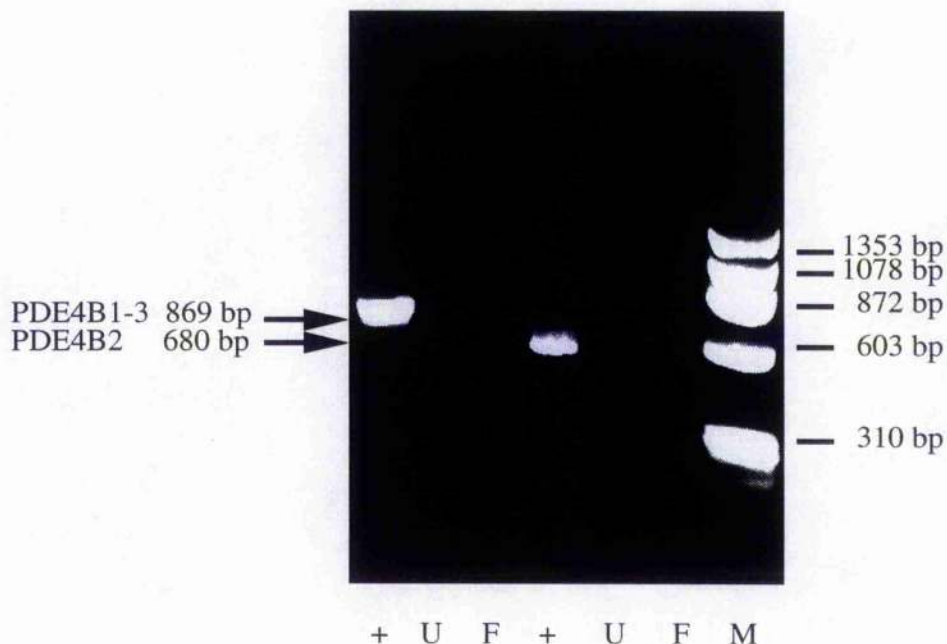


Figure 3.25. RT-PCR analysis of Jurkat T-cells using PDE4B1, PDE4B2 and PDE4B3 specific primers

Jurkat T-cells were untreated or exposed to 100 μ M forskolin for 9 h. After the treatment period, RNA was extracted and reverse transcribed into cDNA (sections 2.2.15-16). PCR was then performed (section 2.2.17) using primers specific for PDE4B2. These primers were: sense-hB1, AGCGGTGGTAGCGGTGACTC and antisense-hB2-601, GCTGCGTGCAGGCTGTTGTG, defining a 680 bp fragment. PCR reaction employed here was: 1 min at 95 $^{\circ}$ C, 2 min at 59 $^{\circ}$ C and 3 min at 72 $^{\circ}$ C for 35 cycles. RT-PCR was also employed for PDE4B1 and PDE4B3 using sense-SE14, ACCTTTCCTGGGCACAGCCAG and antisense-hB2-601. The reaction conditions used were as described above. The products were electrophoresed on 1.5 % agarose gel and visualised with ethidium bromide under UV light. The results are representative of three experiments using RNA from different extractions. (+): positive control, U: untreated, F: forskolin treated, M: marker.

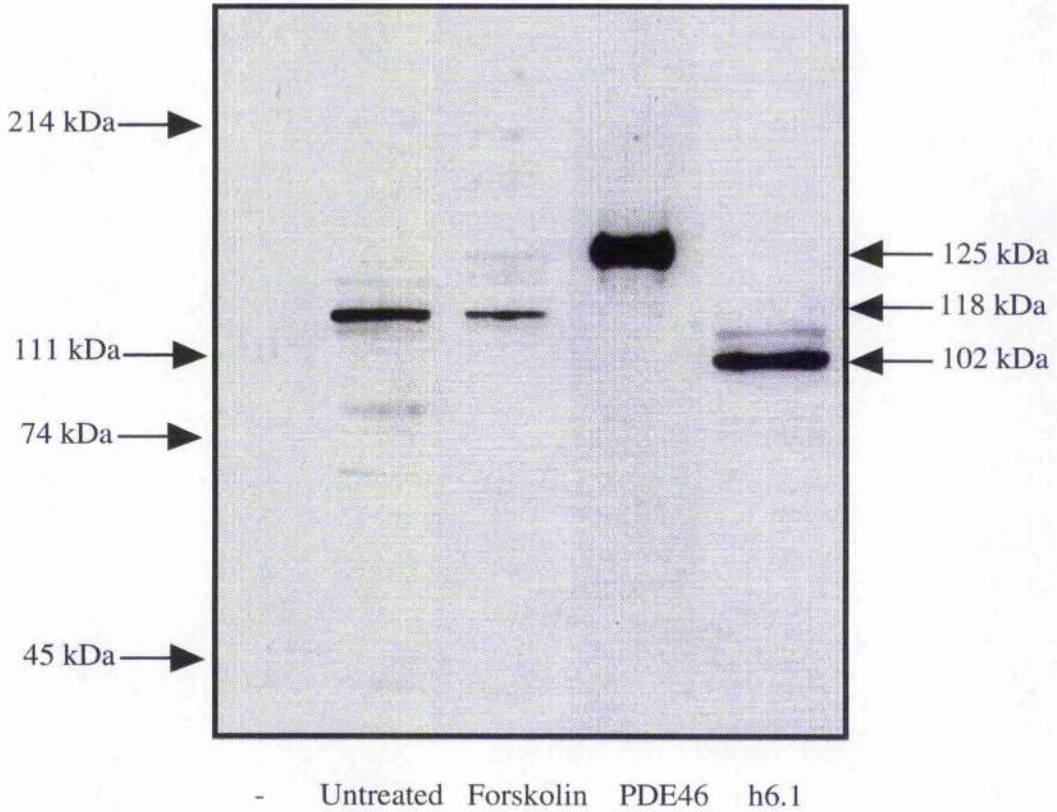


Figure 3.26. Immunoblot analysis of PDE4A immunoreactivity in Jurkat T-cells

Jurkat T-cells were either untreated or exposed to 100 μ M forskolin for 9 h. After the treatment period cells were washed and homogenised. Identical amounts of protein (100 μ g of protein) and COS7 cells transfected with PDE46, h6.1 or no proteins (as positive and negative controls) respectively were run on SDS-polyacrylamide gel electrophoresis (section 2.2.3) and then transferred to nitrocellulose membranes (section 2.2.4). The blot was probed with antiserum specific for C-terminus of PDE4A. The figure shown is typical of experiments performed at least three times using proteins from different homogenates.

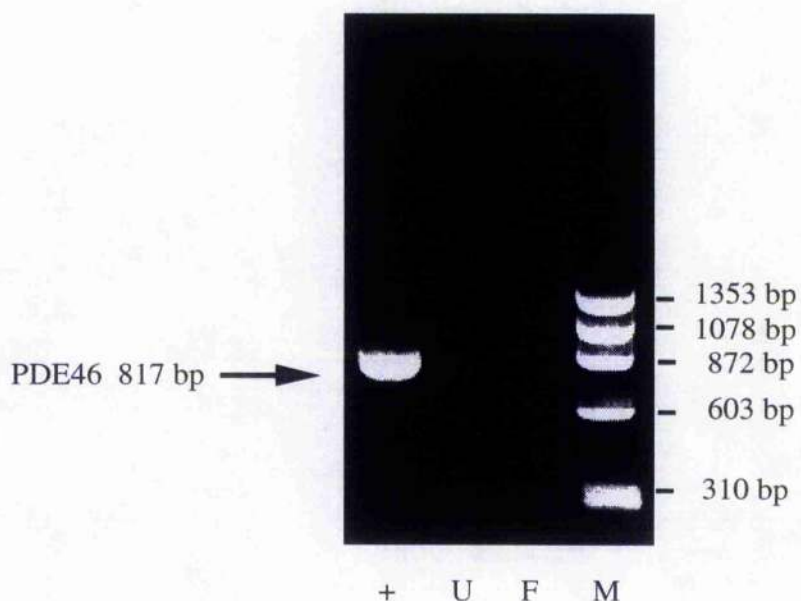


Figure 3.27. RT-PCR analysis of Jurkat T-cells using PDE46 specific primers

Jurkat T-cells were untreated or exposed to 100 μ M forskolin for 9 h. After the treatment period, RNA was extracted and reverse transcribed into cDNA (sections 2.2.15-16). PCR was then performed (section 2.2.17) using primers specific for the established human PDE4A splice variant PDE46. These primers were: Sense-2260, GTGGGGGCCGATCCATGGAACCCCGACC and antisense-2261, GGTTC AACAGATATCTGAACTTGTGCGAGG, defining a 817 bp fragment. PCR reaction employed here was: 1 min at 95 $^{\circ}$ C, 1 min at 59 $^{\circ}$ C and 90 s at 72 $^{\circ}$ C for 35 cycles. The products were electrophoresed on 1.5 % agarose gel and visualised with ethidium bromide under UV light. The results are representative of three experiments using RNA from different extractions. (+): positive control, U: untreated, F: forskolin treated, M: marker.

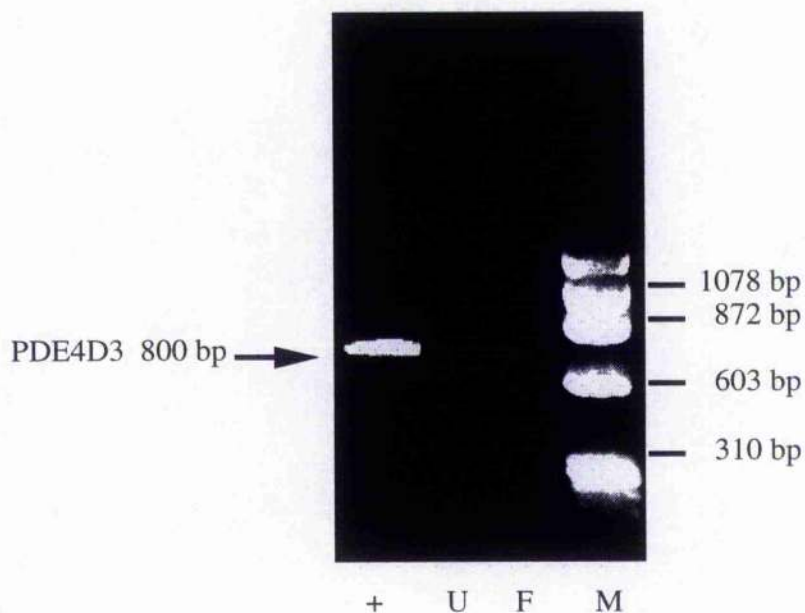


Figure 3.28. RT-PCR analysis of Jurkat T-cells using PDE4D3 specific primers

Jurkat T-cells were untreated or exposed to 100 μ M forskolin for 9 h. After the treatment period, RNA was extracted and reverse transcribed into cDNA (sections 2.2.15-16). PCR was then performed (section 2.2.17) using primers specific for PDE4D3. These oligonucleotides were: Sense PDE43-SE11, ATTGCCACGATAGCTGCTC and antisense COM-D SE13, GACTCCA CTGATCTGAGACATTG. PCR reaction employed: 1 min at 95 $^{\circ}$ C, 70 s at 55 $^{\circ}$ C and 100 s at 72 $^{\circ}$ C for 35 cycles. This allowed the detection of a 800 bp fragment found specifically in PDE4D3. The products were electrophoresed on 1.5 % agarose gel and visualised with ethidium bromide under UV light. The results are representative of three experiments using RNA from different extractions. (+) positive control, U: untreated, F: forskolin treated, M: marker.

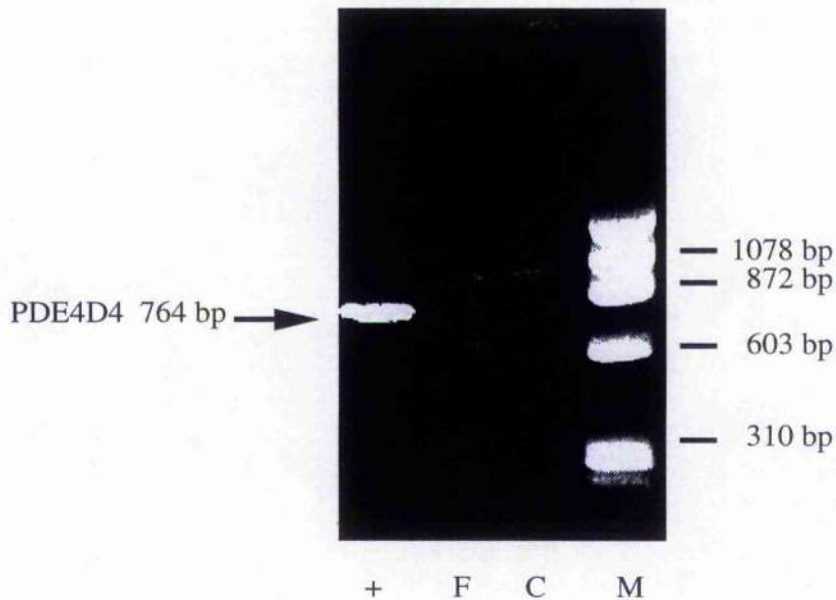


Figure 3.29. RT-PCR analysis of Jurkat T-cells using PDE4D4 specific primers

Jurkat T-cells were untreated or exposed to 100 μ M forskolin for 9 h. After the treatment period, RNA was extracted and reverse transcribed into cDNA (sections 2.2.15-16). APCR was then performed (section 2.2.17) using primers specific for PDE4D4. These oligonucleotides were: sense PDE39-SE10, AGCGCTACCTGTACTGTCG and antisense COM-D SE13, GACTCCACTGAT CTGAGACATTG. PCR reaction employed: 1 min at 95 $^{\circ}$ C, 70 s at 55 $^{\circ}$ C and 100 s at 72 $^{\circ}$ C for 35 cycles. This allowed the detection of a 764 bp fragment found specifically in PDE4D4 representing nucleotides 757-1520. The products were electrophoresed on 1.5 % agarose gel and visualised with ethidium bromide under UV light. The results are representative of three experiments using RNA from different extractions. (+) positive control, F: forskolin treated, U: untreated, M: marker.

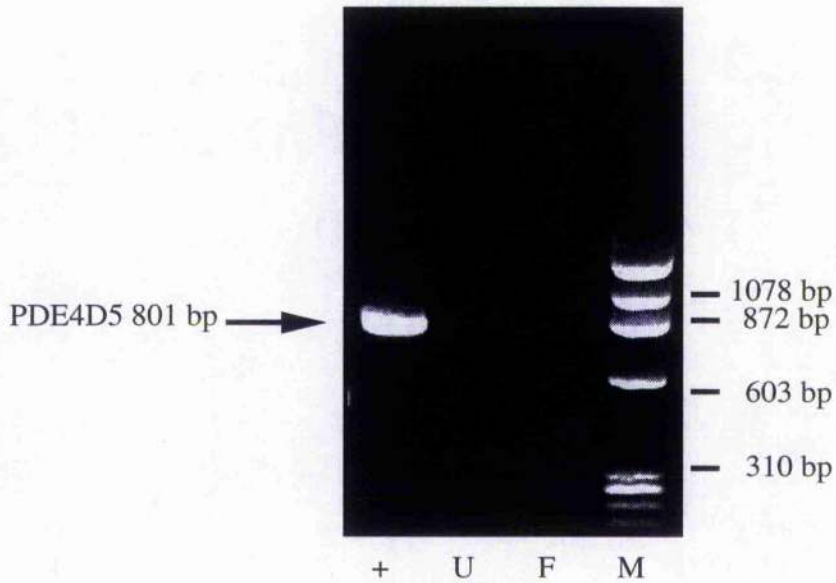


Figure 3.30. RT-PCR analysis of Jurkat T cells using PDE4D5 specific primers

Jurkat T-cells were untreated or exposed to 100 μ M forskolin for 9 h. After the treatment period, RNA was extracted and reverse transcribed into cDNA (sections 2.2.15-16). PCR was then performed (section 2.2.17) section using primers specific for PDE4D5. These oligonucleotides were: Sense PDE79-SE10, CTGTTGCAGCATGAGAAGTCC, antisense COM-D SE13, GACTCCACTGATCTGAGACATTG. PCR reaction employed: 1 min at 95 $^{\circ}$ C, 70 s at 55 $^{\circ}$ C and 100 s at 72 $^{\circ}$ C for 35 cycles. This allowed the detection of a 801 bp fragment found specifically in PDE4D5 representing nucleotides 226-1026. The products were electrophoresed on 1.5 % agarose gel and visualised with ethidium bromide under UV light. The results are representative of three experiments using RNA from different extractions. (+): positive control, U: untreated, F: forskolin treated, M: marker.

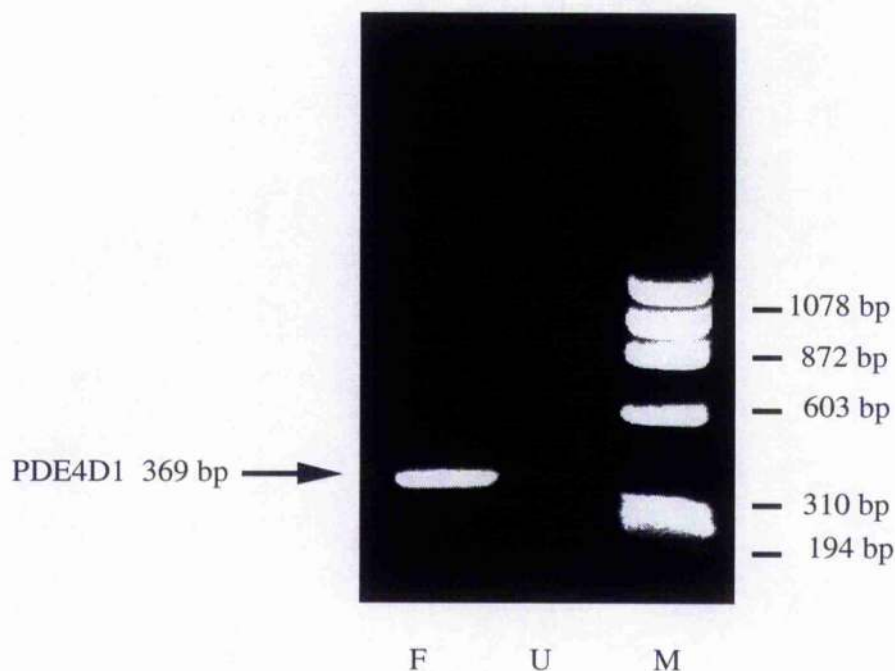


Figure 3.31. RT-PCR analysis of Jurkat T-cells using PDE4D1 specific primers

Jurkat T-cells were untreated or exposed to 100 μ M forskolin for 9 h. After the treatment period, RNA was extracted and reverse transcribed into cDNA (sections 2.2.15-16). PCR was then performed (section 2.2.17) using primers specific for the established human PDE4D splice variant PDE4D1. These oligonucleotide primers were: sense PDE4D1-SE9, ATGGCCCCCTTTGAACTCGC and antisense-COM-D SE13, GACTCCACTGATCTGAGACATTG, defining a 369 bp product. PCR reaction employed: 1 min at 95 $^{\circ}$ C, 70 s at 55 $^{\circ}$ C and 100 s at 72 $^{\circ}$ C for 35 cycles of each condition utilised. The products were electrophoresed on 1.8 % agarose gel and visualised with ethidium bromide under UV light. The results are representative of three experiments using RNA from different extractions. F: forskolin treated, U: untreated, M: marker.

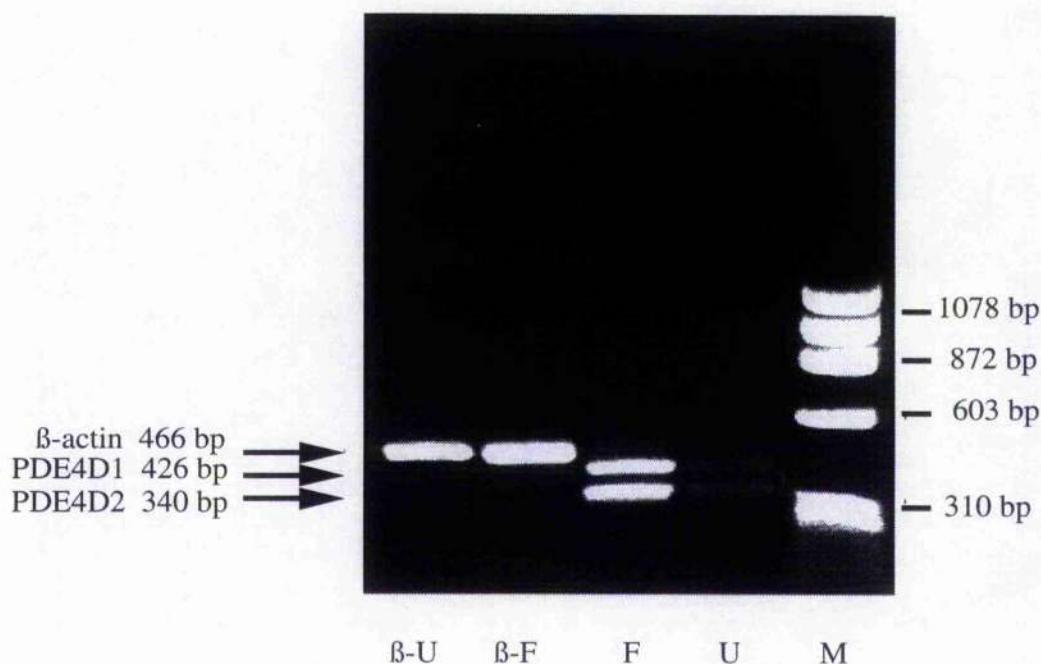


Figure 3.32. RT-PCR analysis of Jurkat T-cells using PDE4D1/2 specific primers

Jurkat T-cells were untreated or exposed to 100 μ M forskolin for 9 h. After the treatment period, RNA was extracted and reverse transcribed into cDNA (sections 2.2.15-16). PCR was then performed (section 2.2.17) using primers specific for the established human PDE4D splice variants PDE4D1/2. These oligonucleotide primers were: sense PDE4D1/2-SE16, AAGGAGCAGCCATCATGTGC and antisense-COM-D SE13, GACTCCACTGATCTGAGACATTG. This allowed the detection of a 426 bp fragment found in hPDE4D1 and was also capable of detecting a 340 bp fragment in hPDE4D2. PCR reaction was 1 min at 95 $^{\circ}$ C, 70 s at 55 $^{\circ}$ C and 72 $^{\circ}$ C at 100 s for 35 cycles. The products were electrophoresed on 1.5% agarose gel and visualised with ethidium bromide under UV light. The results are representative of three experiments using RNA from different extractions. β -U: beta actin untreated, β -F: beta actin forskolin treated, F: forskolin treated, U: untreated, M: marker.

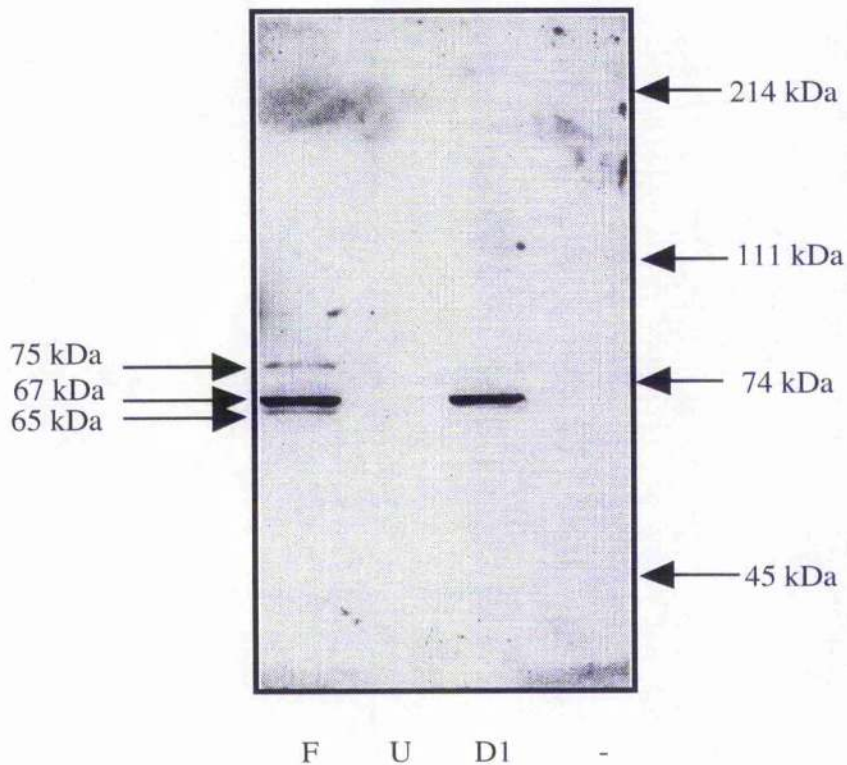


Figure 3.33. Immunoblot analysis of PDE4D immunoreactivity in Jurkat T-cells

Jurkat T-cells were either untreated or exposed to 100 μ M forskolin for 9 h. After the treatment period cells were washed and homogenised. Identical amounts of protein (100 μ g of protein) and COS7 cells transfected with PDE4D1 (D1) or no proteins (as positive and negative controls, respectively) were run on SDS-polyacrylamide gel electrophoresis (section 2.2.3) and then transferred to nitrocellulose membranes (section 2.2.4). The blot was probed with antiserum specific for the C-terminus of PDE4Ds. Figure shown is typical of experiments performed four times using proteins from different homogenates. F: forskolin treated, U: untreated control, D1: positive control.

CHAPTER 4

*CHARACTERISATION OF FIVE HUMAN PDE4D
ISOFORMS*

4.1. Introduction

The PDE4 cAMP-specific phosphodiesterases are a large family of enzymes that are characterised by a high specificity and affinity for cAMP, their inhibition by the antidepressant rolipram (Beavo et al., 1994, DiSanto & Heaslip, 1995) and insensitivity to both cyclic GMP and Ca^{2+} /CaM (Livi et al., 1990, Shakur et al., 1995, Wilson et al., 1994) (Table 1.1). The human PDE4s are highly homologous to the *Drosophila melanogaster* 'dunce' gene (Chen et al., 1986) in terms of DNA and protein sequences, similar kinetics and genomic structure (Monaco et al., 1994) (Figure 1.4). The first PDE4 cDNA to be isolated was for the *Drosophila dunce* enzyme (Chen et al., 1986). This cDNA was used to probe mammalian cDNA libraries so as to isolate cDNAs encoding PDE4 isoforms from rat (Conti & Swinnen, 1990, Davis, 1990, Swinnen et al., 1989a) and human (Baecker et al., 1994, Bolger et al., 1993, Livi et al., 1990, Mchala et al., 1990).

Analysis of cDNA clones derived from human (Baecker et al., 1994, Beavo et al., 1994, Conti et al., 1995b) and rat (Davis et al., 1989, Swinnen et al., 1989a) have indicated that four gene families (PDE4A, 4B, 4C and 4D) encoding closely related proteins are present. Three of these genes (PDE4A, 4B and 4D) encode multiple PDE isoforms, due to different alternatively spliced mRNA transcripts. These PDE isoforms have identified two conserved splice junctions (Bolger, 1994, Conti et al., 1995b). The first splice point occurs where the PDE4D3, 4D4 and 4D5 mRNAs converge. A second splice junction occurs where the PDE4D1 and 4D2 mRNAs diverge from the consensus sequence (Figure 4.1). In the PDE4D sequences there are three distinct homologous regions. One of these regions was shown to encode the putative catalytic region (Jin et al., 1992). The other two blocks of strong sequence homology which were located in the N-terminal regions of the proteins were called UCR1 and UCR2, Upstream Conserved Region 1 and 2 (Figure 4.1), (Bolger, 1994). PDE4D1 and PDE4D2 lack the UCR1 region and

they represent the so-called 'short' form PDE isoforms. PDE4D3, PDE4D4 and PDE4D5 have both conserved regions and are so-called 'long' form PDE isoforms. UCR1 and UCR2 regions appears to be distinct and they lack homology to each other. Additionally, these regions of human and *Drosophila melanogaster*, respectively show more homology to each other than to any other sequences in the GenBank or EMBL data bases (Bolger, 1994), although the functional significance of these regions is not known. However, that they are conserved in long form products of the various PDE4 isoforms suggests that they may have an essential function (Bolger, 1994).

The *PDE4D* gene (Bolger, 1994, Sette et al., 1994b) encodes a number of mRNA variants that differ in the 5'-domain. In rats, four different transcripts from this gene have been demonstrated (Bolger et al., 1994, Sette & Conti, 1996, Swinnen et al., 1989b), these are: rat PDE4D1, rat PDE4D2, rat PDE4D3 (formerly known as ratPDE3.1, ratPDE3.2 and ratPDE3.3, respectively) and PDE4D4 (Vicini and Conti, unpublished data). The human counterparts of PDE4D1 and PDE4D2 (the 4D2 transcript is missing one or more exon(s) (86 bp) (Figure 4.1) that are present within the 5' region of 4D1 (Nemoz et al., 1996), PDE4D3 and PDE4D4 (Bolger et al., 1993) isoforms) have been reported. The novel human PDE4D splice variant PDE4D5 has recently been cloned by Bolger et al. (1997) (Figures 4.1). Alignment of the rat and human PDE4D1, PDE4D2 and PDE4D3 amino acid sequences shows highly conservative features. Each of the human proteins is nearly identical in length to its rat counterpart and has greater than 90 % amino acid identity. However, recent data suggest that each of the various isoforms has a distinct function. For example, they differ in their ability to be induced by changes in cAMP levels (Erdogan & Houslay, 1997, Sette et al., 1994a, Verghese et al., 1995) and protein-protein interaction (O'Connell & Houslay, unpublished data). The rat PDE4D1, PDE4D2 and PDE4D3 proteins vary in their enzymologic

properties and in their regulation by phosphorylation (Sette & Conti, 1996, Sette et al., 1994a).

4.1.1. Aim of the study

In this chapter, different cDNA clones (isolated by Dr. Bolger, Utah/USA) derived from different mRNA transcripts of the human *PDE4D* gene were transiently expressed in COS7 cells and their ability to hydrolyse cAMP, subcellular localisation of their encoded proteins, biochemical and pharmacologic properties were analysed.

4.2. Results

4.2.1. Expression and subcellular distribution of human PDE4D1, PDE4D2, PDE4D3, PDE4D4 and PDE4D5 cDNAs in COS7 cells

In order to characterise the five different PDE enzymes encoded by the pPDE39, pPDE43, pPDE79, pPDE82 and pDun411 cDNAs (PDE4D4, PDE4D3, PDE4D5, PDE4D2 and PDE4D1 respectively) these were engineered into expression plasmids (pcDNA3) under the control of the cytomegalovirus (CMV) intermediate early gene promoter which allowed transcript expression in COS7 cells (section 2.2.12.1). The clones have been identified with their isoforms and their GenBank accession numbers are given in the table 4.1.

Homogenates of transfected COS7 cells were subjected to centrifugation in order to isolate a low-speed pellet (P1), a high-speed pellet (P2: particulate fraction) and a high-speed supernatant (S: cytosol) (see section 2.2.12.3). The PDE activities were measured in these fractions using 1 μ M cAMP as substrate (2.2.5). The average PDE activity in the mock transfection with the parent plasmid was 10 ± 4 pmol/min/mg of protein ($n = 4$ separate experiments). Transfection with the parent

plasmid had no effect (<3 %) on either the total endogenous COS7 cell PDE activity or rolipram inhibited fractions.

Typically, cytosolic fractions (S) of the 'short' form of the PDE4D1 and PDE4D2 exhibited PDE activities of 298 ± 21 and 160 ± 13 pmol/min/mg of protein, respectively ($n = 4$ experiments using different transfections). This increased homogenate PDE activity was completely inhibited (>96 %) by the addition of rolipram (10 μ M). However, no observable increase in the PDE activities of the P1 and P2 fractions (<2 - 3 % change; $n = 4$) were detected. This demonstrates that PDE4D1 and PDE4D2 proteins were located exclusively in the cytosol fraction (Table 4.2).

The three 'long' forms of human PDE4D isoforms were distributed between both particulate and cytosol compartments (Table 4.2). The cytosolic fractions of PDE4D3, PDE4D4 and PDE4D5 activities were considerably greater, with specific activities of 351 ± 21 , 410 ± 25 and 379 ± 18 pmol/min/mg of protein, respectively ($n = 4$ experiments using different transfections). All of this increased PDE activity (>95 %) was inhibited by rolipram (10 μ M). The majority of PDE4D4 activity was in the particulate fraction (60 %), whereas, about 30 % of PDE4D3 and PDE4D5 activities were associated with the membrane fraction with the major fraction occurring in the cytosol (Table 4.2). In addition, the three species differed in their distribution between P1 and P2, with PDE4D5 present in a higher relative amount in P1, compared to PDE4D3 and PDE4D4 (Table 4.2).

4.2.2. Immunological detection of human PDE4D1, PDE4D2, PDE4D3, PDE4D4 and PDE4D5 cDNAs expressed in COS7 cells

The human *PDE4D* gene products share sequence homology in their carboxyl-terminal regions (Figure 4.1). A monoclonal antibody generated against the C-

terminal region found in common with all of the known human PDE4D proteins was used for the detection of PDE protein. To characterise whether the different mRNA variants were translated into different protein products, the five cDNAs were expressed in COS7 cells. The signals generated with the antibody in Western blots were linear over a wide range of amounts of protein loaded on the immunoblot (Figures 4.2 and 4.3). Each of the five recombinant proteins migrated as single, distinct species with the exception of the PDE4D4 and PDE4D5 isoforms (see below for figure numbers), where an additional band of much weaker intensity (~5 %) was present. These additional bands migrated near PDE4D3 in both cases and may represent initiation of translation at a second downstream start codon. The PDE4D1 and PDE4D2 variants were found as soluble immunoreactive species of about 68 kDa with no immunoreactivity associated with the pellet fractions (Figures 4.4 and 4.5 respectively). Thus both the immunoblot data and activity data were consistent and showed that PDE4D1 and PDE4D2 isoforms were evident solely in the cytosol fraction. In contrast PDE4D3, PDE4D4 and PDE4D5 isoforms (molecular mass of 95 ± 2 kDa, 119 ± 2 kDa and 105 ± 2 kDa respectively) were found in both particulate-associated and soluble forms (Figures 4.6, 7 and 8 respectively). This indicated that the 'long' forms contain information in their N-terminal extension regions that allows anchoring to particulate/membrane fraction.

All five PDE4D variants migrated on SDS-PAGE gel slower (*i.e.* larger apparent size) than their predicted amino acid sequence (Table 4.3). This may reflect particular conformational properties, or the anomalous binding to SDS of these proteins in SDS-PAGE. Similar anomalous results on SDS-PAGE has been observed for recombinant rat and human PDE4A proteins (Bolger et al., 1996, Huston et al., 1996).

4.2.3. Solubilisation of particulate fractions of the human PDE4D3, PDE4D4 and PDE4D5 by Triton X-100 and NaCl

The rat PDE4A1 protein RD1 has been shown to be released from the particulate fraction by the detergent Triton X-100 (Shakur et al., 1995), whereas the human PDE4A4B (Huston et al., 1996), rat PDE4A5 (McPhee et al., 1995) and rat PDE4A8 (Bolger et al., 1996) proteins were not able to be eluted from the particulate fraction by either detergent or high salt concentrations. Therefore, I set out to see whether the human PDE4D particulate-associated proteins could be released from the particulate fraction by detergent and high salt treatments. COS7 cell high-speed pellets expressing either PDE4D3, PDE4D4 or PDE4D5 were either solubilised with the non-ionic detergent Triton X-100 (5 %) or high salt (NaCl) concentration (1 M) or both. The resulting high-speed pellet and supernatant were then analysed by immunoblotting (Table 4.4). The PDE4D5 protein could be released, at least in part, from the particulate fraction by either of these treatments and was completely released by a combination of the two (Figure 4.9). PDE4D3 could be partly solubilised by Triton X-100 alone and was completely released by a combination of the two (Figure 4.10). PDE4D4 was resistant to either treatment alone, but could be solubilised by a combination of both (Figure 4.11). Detergent treatment was used to solubilise integral proteins and high salt to release peripheral proteins. Of course release of these PDEs might reflect the liberation of the PDE4D species together with anchoring protein.

4.2.4. Kinetics of cAMP hydrolysis by five human PDE4D isoforms

To examine the biochemical properties of these enzymes PDE4D1, PDE4D2, PDE4D3, PDE4D4 and PDE4D5 were transiently expressed in COS7 cells. Soluble (S; cytosol) and particulate (P2; membrane) fractions were isolated from

COS7 cells expressing the indicated isoforms. K_m values were determined (section 2.2.6) over a cAMP range of 0.25 μ M - 25 μ M at seven different concentrations. The K_m values were obtained for both soluble PDE4D1, 4D2, 4D3, 4D4 and 4D5 (Figures 4.12, 13, 14, 15 and 16 respectively) and particulate-associated fractions of PDE4D3, 4D4 and 4D5 (Figures 4.17, 18 and 19 respectively) by non-linear fitting of data to the Michaelis equation. The soluble and particulate fractions exhibited similar (0.7 μ M - 1.3 μ M cAMP) low K_m values for cAMP hydrolysis (Table 4.5). These values reflect those reported for other PDE4 enzymes (Bolger, 1994, Conti et al., 1995b, Conti et al., 1992, Engels et al., 1995, Huston et al., 1996, Michaeli et al., 1993).

The relative amounts of PDE4D protein in the isolated cytosolic and particulate fractions was obtained by immunoblotting. V_{max} values were then obtained from double-reciprocal (Lineweaver-Burk) plots (Figures 4.2 and 4.3). From these data the relative V_{max} values of these isoforms were determined so as to see if the five different PDE4Ds had different maximal activities. The relative V_{max} values for the cytosolic forms were compared relative to that of the PDE4D1 enzyme, which was determined as 1.0 (Table 4.6). The cytosolic forms of PDE4D2, PDE4D3 and PDE4D5 showed relatively similar V_{max} values, whereas PDE4D4 had a relative V_{max} 2- to 3-fold higher than that of the other four cytosolic enzymes ($p < 0.001$). The ratios of particulate to cytosolic relative V_{max} of both PDE4D4 and PDE4D5 were 2.5- to 3.3-fold higher ($p < 0.001$), respectively, implying that the activity of the particulate forms were higher. The V_{max} of the particulate form of PDE4D3 was the same of that of the cytosolic form and 2- to 3-fold lower than that of both PDE4D4 and PDE4D5.

4.2.5. Inhibition of particulate and cytosolic forms of the five human PDE4D enzymes by rolipram

Rolipram caused the dose-dependent inhibition of both cytosolic and particulate PDE4D isoforms. The values were typical for members of the PDE4 family (Bolger et al., 1996, Huston et al., 1996, McPhee et al., 1995). High concentrations of rolipram almost completely abolished detectable PDE activity in the extracts of D1, D2, D3, D4 and D5 (Figures 4.20, 21, 22, 23 and 24 respectively) and of particulate fractions (Figures 4.25, 26 and 27 respectively). The concentration of rolipram needed for 50 % inhibition of enzyme activity (IC_{50}) of the various cytosolic forms was similar (Table 4.7). However, particulate fractions of PDE4D3 and PDE4D5 were 2- to 7-fold less sensitive to rolipram inhibition than those of their respective cytosolic forms ($p < 0.01$ and $p < 0.001$, respectively).

All the PDE4D isoforms, with the exception of PDE4D3, deviated from the simple Michaelian kinetics. The inhibitor curves for the cytosolic forms of the five proteins were quite similar, except PDE4D3, which had a much steeper slope (for figures see above, Table 4.8). Similarly, the dose-effect curves for the particulate forms of PDE4D3 and PDE4D5 had a steeper slope than that of the particulate form of PDE4D4. The association of PDE4D3, PDE4D4 and PDE4D5 with membranes produced a modest (less than 2-fold) difference in slope (Table 4.8), despite the changes in IC_{50} for PDE4D3 and PDE4D5. The data demonstrate that only the cytosolic and particulate forms of PDE4D3 showed simple Michaelian kinetics, with a Hill coefficient approaching unity and that the other forms demonstrated apparent negative co-operativity.

4.3. Conclusion and Discussion

It has been shown that multiple PDE isoforms can be derived by different transcription initiation sites, alternative mRNA splicing and RNA editing. The five human PDE4D cDNA clones described in this chapter were generated by alternative mRNA splicing. Comparison of the nucleotide sequences of PDE4D4 and PDE4D5 cDNAs to those encoding three other human PDE4D proteins (PDE4D1, PDE4D2 and PDE4D3), demonstrated that each corresponding mRNA transcript has a unique region of sequence at or near its 5' end (Figure 4.1). Three of the five cDNAs encoded proteins (PDE4D3, PDE4D4 and PDE4D5) which contained UCR1 and UCR2 as well as the catalytic region, whereas the two other cDNAs encoded proteins (PDE4D1 and PDE4D2) which lack UCR1, but contain at least a portion UCR2 and the complete catalytic region. For these five different cAMP-PDE isoforms, all encoded by the human *PDE4D* gene, their enzymatic properties and subcellular localisation were compared subsequent to transient expression in COS7 cells. It is believed that the five human cDNA clones do not represent artefacts of cloning for two reasons. First, each of the five cDNAs generated a protein very similar in size to PDE4D species occurring naturally. Secondly, all of the proteins appear to have homologs in the rat. cDNAs encoding rat homologs of PDE4D1, PDE4D2 and PDE4D3 have been reported previously (Bolger et al., 1993, Monaco et al., 1994, Sette & Conti, 1996, Swinnen et al., 1989b). Bolger et al. (1997) has shown that homologs of the all human PDE4D proteins exist in rat brain.

The 'short' forms, PDE4D1 and PDE4D2, were present only in cytosol whereas 'long' forms (PDE4D3, PDE4D4 and PDE4D5) also exist in the particulate fraction (Figures 4.4, 5, 6, 7 and 8 respectively) expressed in COS7 cells. Treatment with either Triton X-100 or high concentrations of NaCl or both were shown to solubilise the PDE4D3, PDE4D4 and PDE4D5 membrane forms

(Figures 4.10, 11 and 9 respectively). This complexity may reflect the binding of these PDE4D species to anchor proteins. Thus release of the PDE4D forms may occur due to disruption of their interaction with the anchor protein(s) or the solubilisation of the anchor proteins. Solubilisation data (Table 4.4) suggest that considerable differences occur between the 'long' forms in their ability to be dissociated from the particulate fraction. This may reflect differences in the anchor proteins for the various species and suggests that the variant N-terminal regions are important for the specificity of subcellular localisation of these isoforms. Indeed, Huston et al. (1996) showed that the 'long' form of human hPDE46 (HSPDE4A4B) was associated with the particulate fraction, whereas h6.1 (HSPDE4A4C) which lacks the N-terminal extension seen in PDE46, was completely cytosolic. Three rat PDE4A species were demonstrated to have identical catalytic regions but contained unique N-terminal regions. However, amino-terminal domains of these species apparently regulate activity and the propensity to interact with other specific proteins (McPhee et al., 1995, Scotland & Houslay, 1995, Shakur et al., 1993, Shakur et al., 1995). This data suggests that the UCR1 region may be involved or, alternatively, that other parts of the amino-terminal regions of PDE4 proteins have either a prime role for membrane-binding or interaction with specific proteins or regulation of the enzyme.

Comparison of the K_m values of five different PDE4Ds showed that each form hydrolysed cAMP with high affinity (Figures 4.12, 13, 14, 15, 16, 17, 18 and 19). The analysis of the K_m values calculated for each enzyme form, demonstrated that the values were not significantly different between either 'long' and 'short' forms or cytosolic and particulate fractions (Table 4.5). The five PDE4Ds all share an identical core catalytic region which would explain the observed similarity in the K_m values. To determine if there were any differences in the V_{max} values for each of the reported enzymes in this present study an antibody against the C-terminus of PDE4D isoforms was used. The PDE4D

antiserum was used to immunoblot equal amounts of PDE protein from each of the COS7 cell extracts. This enabled the use of equal amounts of protein in activity assays by determination of the density on the immunoblot. I was able to define the relative V_{\max} values of these isoforms and determine any differences between isoforms. The cytosolic form of PDE4D4 protein was shown to have a V_{\max} that was 2- to 3-fold higher than that of the other four cytosolic isoforms (Table 4.6), which were very similar. This suggests that the amino-terminal regions of these proteins affect the conformation of the protein in a highly specific way, by attenuating the V_{\max} , but not K_m . The V_{\max} of the particulate forms of both PDE4D4 and PDE4D5 were 2.5- to 3.3-fold higher than that of the cytosolic fractions (Table 4.6). The V_{\max} of the particulate form of PDE4D3 was the same of that of the cytosolic form and 2- to 3-fold lower than that of both PDE4D4 and PDE4D5. This suggests that the extreme amino-terminal regions of PDE4D4 and PDE4D5 may contain specific information for regulation of the catalytic activity of particulate enzymes.

IC₅₀ values were calculated from the dose-response curves to rolipram for each of the enzyme forms (Figures 4.20, -21, 22, 23, 24, 25, 26 and 27). Rolipram caused the dose-dependent inhibition of both particulate and soluble forms of the five different human PDE4D isoforms expressed in COS7 cells. The inhibitor sensitivity of the five cytosolic forms were found to be quite similar (Table 4.7). However, particulate forms of PDE4D3 and PDE4D5 were approximately 2- to 7-fold less sensitive to inhibition by rolipram than that of cytosolic forms. On the other hand, cytosolic and particulate forms of PDE4D4 were equally sensitive to rolipram inhibition (Table 4.7).

Five different human PDE4D isoforms were analysed by expression in COS7 cells. It is possible that the recombinant proteins may be processed differently in COS7 cells or tissues or that overexpression of the proteins in COS7 cells may

affect their intracellular distribution. However, it is considered that data obtained by expressing PDE4 cDNAs in COS7 cells is likely to provide a good representation of the native enzyme. This is based on previous studies (Bolger et al., 1996, McPhee et al., 1995, Shakur et al., 1995) which yielded similar subcellular localisation data for the rat PDE4A1 and PDE4A5 proteins, as expressed in COS7 cells, compared to the corresponding native proteins in the brain.

There may be other ways in which the 'long' PDE4D variants differ from the 'short' ones. Whilst the human and rat PDE4D1 and PDE4D2 isoforms are differentially regulated by cAMP at the level of transcription and/or *de novo* synthesis in various cells (Erdogan & Houslay, 1997, Sette et al., 1994a, Sette et al., 1994b, Swinnen et al., 1989b, Swinnen et al., 1991b). Whereas the rat PDE4D3 is phosphorylated by a cAMP-dependent protein kinase (Sette & Conti, 1996). The serine residue shown to be required for the phosphorylation of the rat PDE4D3 protein, which corresponds to serine⁵⁴ in human PDE4D3, is shared by all the human PDE4D3, PDE4D4 and PDE4D5 isoforms. The proline rich amino-terminal regions of the rat PDE4A5 (O'Connell et al., 1996) and the human PDE4D4 but not PDE4D1 or PDE4D2 (O'Connell & Houslay, unpublished data) isoforms interact with SH3 domains on other proteins. This suggests that the regulation of 'long' forms differ from 'short' forms due to their amino-terminal regions.

Table 4.1. cDNA clones corresponding to transcripts from the human PDE4D isoforms

Plasmid name	Isoform name	Accession number
pDun411	PDE4D1	U50157*, U79571
pPDE82	PDE4D2	U50158*, S:1059275
pPDE43	PDE4D3	L20970
pPDE39	PDE4D4	L20969
pPDE79	PDE4D5	S:1059276

The clones are identified with their isoform names and GenBank accession numbers. Accession numbers with an asterisk (*) correspond to the clones of Nemoz, et al. (1996). All other accession numbers are from Bolger, et al. (1993) or Bolger, et al. (1997).

Table 4.2. Subcellular distribution of human PDE4D activities, as expressed in COS7 cells

	P1	P2	Supernatant	P1/P2 ratio	Particulate
	(%)	(%)	(%)	(%)	(%)
PDE4D1	4±2	3±1	93±3	n/a	7
PDE4D2	2±2	4±2	94±6	n/a	6
PDE4D3	11±3	20±2	69±6	0.55	31
PDE4D4	20±4	40±7	40±3	0.5	60
PDE4D5	18±3	15±1	67±9	1.2	33

Homogenates from COS7 cells expressing plasmids encoding various isoforms were fractionated into a low speed pellet (P1), a high speed pellet (P2) and high speed supernatant, as described in section 2.2.12.3. PDE activity assays were performed in the presence of a final concentration of 10 μ M rolipram using 1 μ M cAMP as substrate (section 2.2.5) in the assay. Each value represents the mean \pm SD of at least three different experiments, each using separate transfections and were carried out in triplicate. n/a: not applicable

Table 4.3. Properties of human PDE4D proteins expressed in COS7 cells

Isoform	Amino acids	Predicted size (kDa)	Observed size (kDa)
PDE4D1	586	66.5	68±1
PDE4D2	508	57.8	68±1
PDE4D3	673	76.5	95±2
PDE4D4	810	91.1	119±2
PDE4D5	746	84.4	105±2

The predicted and experimentally determined sizes of the five human PDE4D proteins are shown in the table. In order to determine the size of the proteins, homogenates from COS7 cells expressing (section 2.2.12.3) the five plasmids were immunoblotted and the relative sizes of the recombinant proteins were determined.

Table 4.4. Solubilisation of membrane-associated human PDE4D proteins by detergents or high salt concentrations

	Amount solubilised (%)			
	Buffer only	1M NaCl	5% Triton X-100	[1M NaCl + 5% Triton X-100]
PDE4D3	5±3	13±6	39±8	93±6
PDE4D4	6±4	9±7	12±9	86±11
PDE4D5	2±3	42±7	47±8	94±5

The high speed membranes (P2 pellets) were isolated from COS7 cells expressing the indicated isoforms and treated with high concentrations of the salt NaCl, non-ionic detergent Triton X-100 or both. After the incubation and centrifugation, as described in section 2.2.12.4, the residual pellet and supernatant fractions were subjected to SDS/PAGE and Western blotting (sections 2.2.3 - 4) with anti-PDE4D antibody. The resultant ECL/autoradiographs were scanned and absorbance changes quantified. Wash buffer (KHEM) was used as a negative control. Values are expressed as mean ± SD for 3 separate experiments.

Table 4.5. K_m values for cAMP for human PDE4D isoforms transfected in COS7 cells

	cytosol	membranes
PDE4D1	1.2±0.3	n/d
PDE4D2	1.3±0.2	n/d
PDE4D3	1.2±0.3	0.7±0.2
PDE4D4	1.1±0.1	0.8±0.1
PDE4D5	1.0±0.2	0.8±0.2

The human PDE4D cDNAs were transfected into COS7 cells and then cytosolic (S; supernatant) and membrane (P2; high speed pellet) fractions were isolated as described in section 2.2.12.3. K_m values (in μM) were determined over a substrate range of 0.25 to 25 μM cAMP (7 different concentrations) and were obtained by non-linear fitting of data to the Michaelis equation. Values are given as mean \pm SD for three independent experiments, each using separate transfections. n/d = not determined.

Table 4.6. V_{\max} values for cAMP for human PDE4D isoforms transfected in COS7 cells

	cytosol relative to PDE4D1	V_{\max} particulate/cytosol activity ratio
PDE4D1	(1)	n/a
PDE4D2	1.1±0.2	n/a
PDE4D3	1.2±0.3	0.91±0.2
PDE4D4	2.9±0.3	2.5±0.1
PDE4D5	1.5±0.2	3.3±0.1

The relative V_{\max} values were determined from Lineweaver-Burk plots, with enzyme amounts quantitated by immunoblotting. V_{\max} values for the cytosolic activities are given relative to those of the PDE4D1 protein, which is set as 1.0. Values are given as mean ± SD, for three independent experiments, each using separate transfections. n/a: not applicable

Table 4.7. Inhibition of human PDE4D isoforms from COS7 transfected cells by rolipram

	cytosol	membranes	membrane/cytosolic ratio
PDE4D1	0.05±0.01	n/a	n/a
PDE4D2	0.05±0.01	n/a	n/a
PDE4D3	0.14±0.01	0.32±0.05	2.3±0.3
PDE4D4	0.06±0.05	0.05±0.02	0.8±1.1
PDE4D5	0.08±0.01	0.59±0.05	7.4±0.5

The human PDE4D cDNAs were transfected into COS7 cells and then cytosolic (S; supernatant) and membrane (P2; high speed pellet) fractions were isolated as described in section 2.2.12.3. PDE assays were performed in the presence of 1µM cyclic AMP as substrate with 7 different concentrations of the inhibitor rolipram. The values are given (in µM) as mean ± SD for three independent experiments, each using different transfections. IC₅₀ was the concentration which resulted in 50 % inhibition. n/a = not applicable.

Table 4.8. Hill coefficients for the inhibition of human PDE4D isoforms by rolipram

Isoform	cytosol	particulate
PDE4D1	0.47±0.12	n/a
PDE4D2	0.61±0.05	n/a
PDE4D3	0.93±0.08	0.94±0.03
PDE4D4	0.50±0.05	0.35±0.08
PDE4D5	0.54±0.05	0.75±0.09

The data is calculated using by the KaleidaGraph computer programme.

Figure 4.1. Alignment of the amino acid sequences of the human PDE4D isoforms

The five human PDE4D amino acid sequences have been aligned. * denoted an identical amino acid residue. Horizontal lines indicate the positions of UCR1, UCR2 and the catalytic region of the proteins.

300

```

.....
PDE4D1 QTRHSVSEMASNKFKRMLNRELTHLSEMSRSGNOVSEFI SNTFLDKQHE
PDE4D2 -----ASNKFKRMLNRELTHLSEMSRSGNOVSEFI SNTFLDKQHE
PDE4D3 QTRHSVSEMASNKFKRMLNRELTHLSEMSRSGNOVSEFI SNTFLDKQHE
PDE4D4 QTRHSVSEMASNKFKRMLNRELTHLSEMSRSGNOVSEFI SNTFLDKQHE
PDE4D5 QTRHSVSEMASNKFKRMLNRELTHLSEMSRSGNOVSEFI SNTFLDKQHE

```

UCR2 ends..

350

```

.....
PDE4D1 VEIPSP TQKEKEKKRPM SQISGVK KLMHSSSLTNSSIPRFGVKTEQED
PDE4D2 VEIPSP TQKEKEKKRPM SQISGVK KLMHSSSLTNSSIPRFGVKTEQED
PDE4D3 VEIPSP TQKEKEKKRPM SQISGVK KLMHSSSLTNSSIPRFGVKTEQED
PDE4D4 VEIPSP TQKEKEKKRPM SQISGVK KLMHSSSLTNSSIPRFGVKTEQED
PDE4D5 VEIPSP TQKEKEKKRPM SQISGVK KLMHSSSLTNSSIPRFGVKTEOED

```

...Catalytic begins

400

```

.....
PDE4D1 VLAK ELEDV NKWGLHVFRIAELSGNRPLTVIMHTIFQERDLLKTFKIPV
PDE4D2 VLAK ELEDV NKWGLHVFRIAELSGNRPLTVIMHTIFQERDLLKTFKIPV
PDE4D3 VLAK ELEDV NKWGLHVFRIAELSGNRPLTVIMHTIFQERDLLKTFKIPV
PDE4D4 VLAK ELEDV NKWGLHVFRIAELSGNRPLTVIMHTIFQERDLLKTFKIPV
PDE4D5 VLAK ELEDV NKWGLHVFRIAELSGNRPLTVIMHTIFQERDLLKTFKIPV

```

450

```

.....
PDE4D1 DTLIT YLMTLEDHYHADVAYHNNIHAADV VQSTHVLLSTPALEAVFTDL
PDE4D2 DTLIT YLMTLEDHYHADVAYHNNIHAADV VQSTHVLLSTPALEAVFTDL
PDE4D3 DTLIT YLMTLEDHYHADVAYHNNIHAADV VQSTHVLLSTPALEAVFTDL
PDE4D4 DTLIT YLMTLEDHYHADVAYHNNIHAADV VQSTHVLLSTPALEAVFTDL
PDE4D5 DTLIT YLMTLEDHYHADVAYHNNIHAADV VQSTHVLLSTPALEAVFTDL

```

500

```

.....
PDE4D1 EILAAIFASAIHDVDHPGVSNOFLINTNSELALMYNDSSVLENHHLAVG
PDE4D2 EILAAIFASAIHDVDHPGVSNOFLINTNSELALMYNDSSVLENHHLAVG
PDE4D3 EILAAIFASAIHDVDHPGVSNOFLINTNSELALMYNDSSVLENHHLAVG
PDE4D4 EILAAIFASAIHDVDHPGVSNOFLINTNSELALMYNDSSVLENHHLAVG
PDE4D5 EILAAIFASAIHDVDHPGVSNOFLINTNSELALMYNDSSVLENHHLAVG

```

550

800

```

.....
PDE4D1 FKLLQEENCDIFQNL T-----EEAVGEEEEESQPEACVIDDRSPDT
PDE4D2 FKLLQEENCDIFQNL T-----EEAVGEEEEESQPEACVIDDRSPDT
PDE4D3 FKLLQEENCDIFQNL T-----EEAVGEEEEESQPEACVIDDRSPDT
PDE4D4 FKLLQEENCDIFQNL T-----EEAVGEEEEESQPEACVIDDRSPDT
PDE4D5 FKLLQEENCDIFQNL T-----EEAVGEEEEESQPEACVIDDRSPDT

```

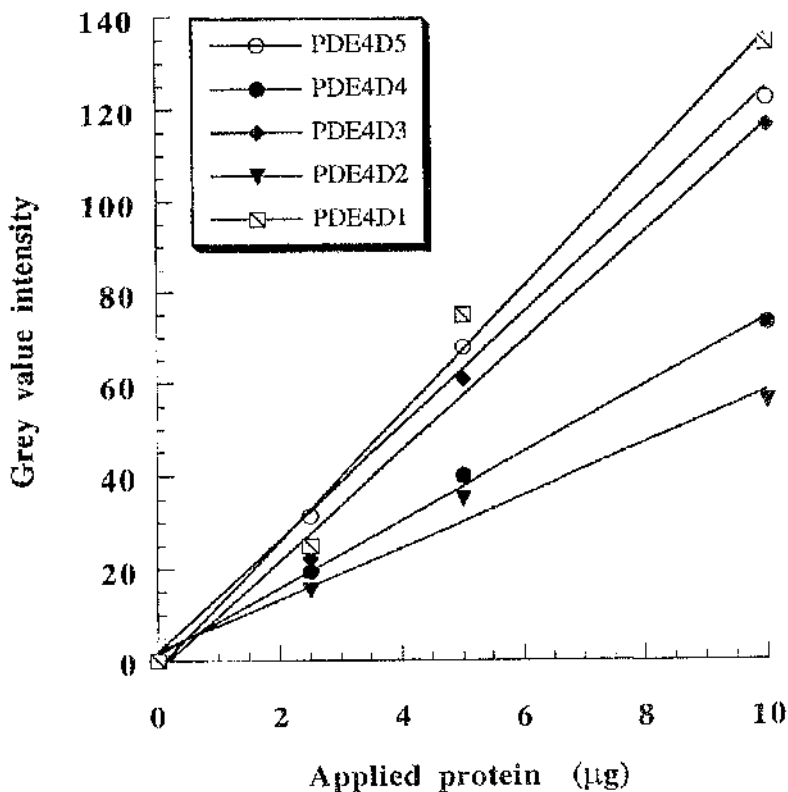


Figure 4.2. Linearity of detection of various cytosolic PDE4D proteins

This data shows that with increasing concentrations of cytosolic (supernatant) protein (2.5 µg to 10 µg) from COS7 cells (transfected with indicated PDE4D isoforms), a linear relationship between intensity and applied protein was observed. The proteins were immunoblotted by monoclonal antibody and the blots were scanned. The intensity of the signal is plotted for each plasmid. Such analyses were used to determine the relative amounts of PDE4Ds for the determination of relative V_{\max} values in table 4.6.

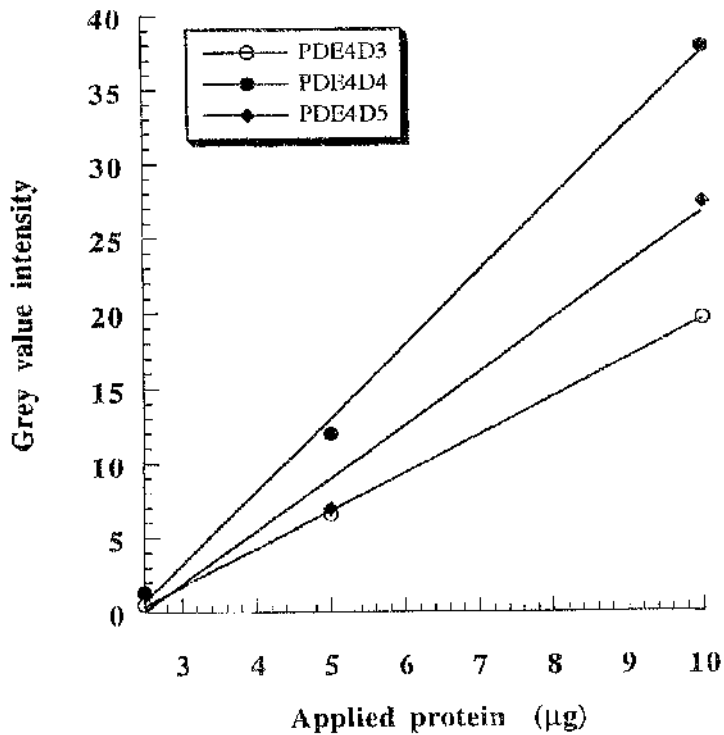


Figure 4.3. Linearity of detection of various membrane PDE4D proteins

This data shows that with increasing concentrations of membrane (P2 pellet) protein (2.5 µg to 10 µg) from COS7 cells (transfected with indicated PDE4D isoforms), a linear relationship between intensity and applied protein was observed. The proteins were immunoblotted by monoclonal antibody and the blots were scanned. The intensity of the signal is plotted for each plasmid. Such analyses were used to determine the relative amounts of PDE4Ds for the determination of relative V_{max} values in table 4.6.

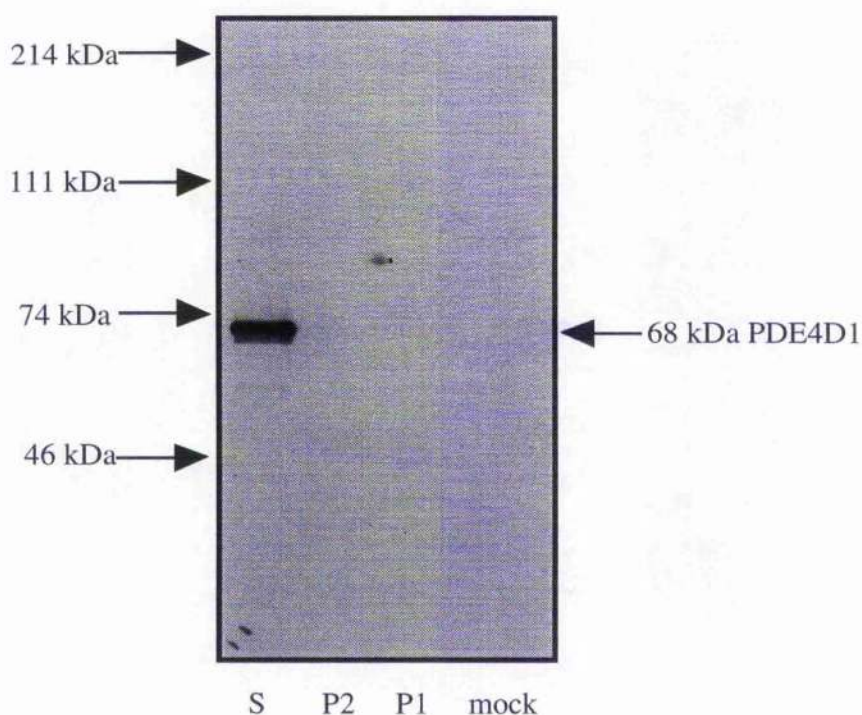


Figure 4.4. Immunoblotting of COS7 cells transfected with the cDNA for human PDE4D1

PDE4D1 plasmid was transfected into COS7 cells. After 72 h the cells were harvested, disrupted, and extracts were then subjected to differential centrifugation in order to give low-speed pellet (P1), high-speed pellet (P2) and cytosol/supernatant (S) fractions (section 2.2.12.3). Samples were then subjected to SDS/PAGE followed by Western blotting with the C-terminus monoclonal antiserum. Results are from a typical experiment which was performed at least three times with different transfections.

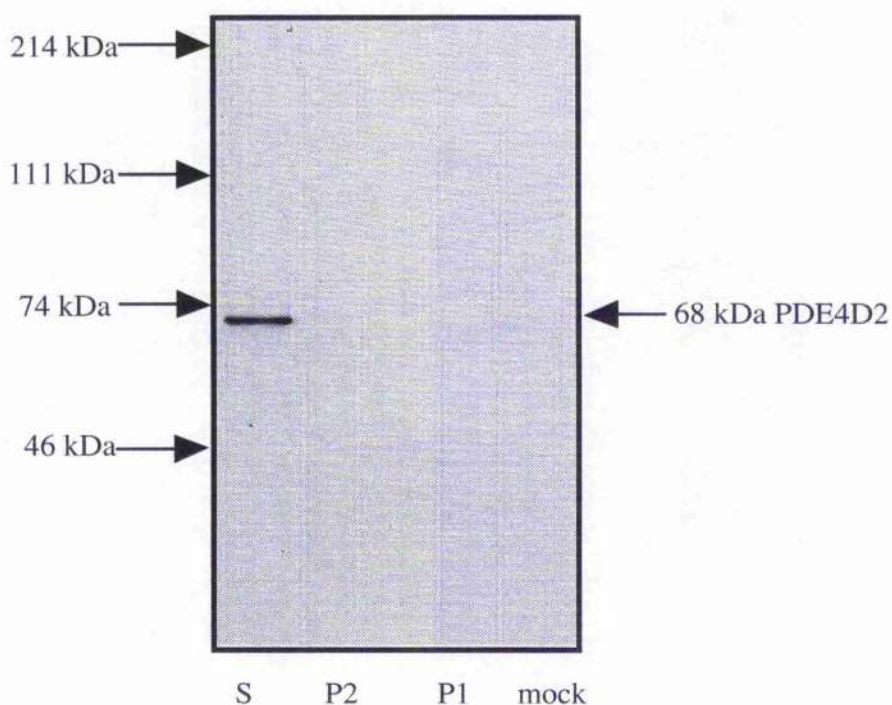


Figure 4.5. Immunoblotting of COS7 cells transfected with the cDNA for human PDE4D2

PDE4D2 plasmid was transfected into COS7 cells. After 72 h the cells were harvested, disrupted, and extracts were then subjected to differential centrifugation in order to give low-speed pellet (P1), high-speed pellet (P2) and cytosol/supernatant (S) fractions (section 2.2.12.3). Samples were then subjected to SDS/PAGE followed by Western blotting with the C-terminus monoclonal antiserum. Results are from a typical experiment which was performed at least three times with different transfections.

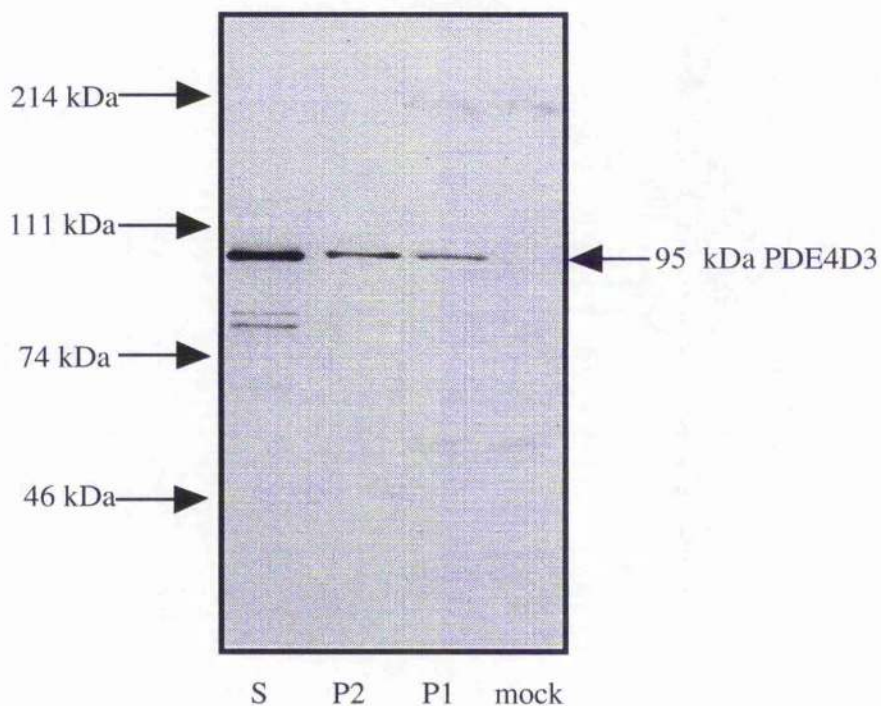


Figure 4.6. Immunoblotting of COS7 cells transfected with the cDNA for human PDE4D3

PDE4D3 plasmid was transfected into COS7 cells. After 72 h the cells were harvested, disrupted, and extracts were then subjected to differential centrifugation in order to give low-speed pellet (P1), high-speed pellet (P2) and cytosol/supernatant (S) fractions (section 2.2.12.3). Samples were then subjected to SDS/PAGE followed by Western blotting with the C-terminus monoclonal antiserum. Results are from a typical experiment which was performed at least three times with different transfections.

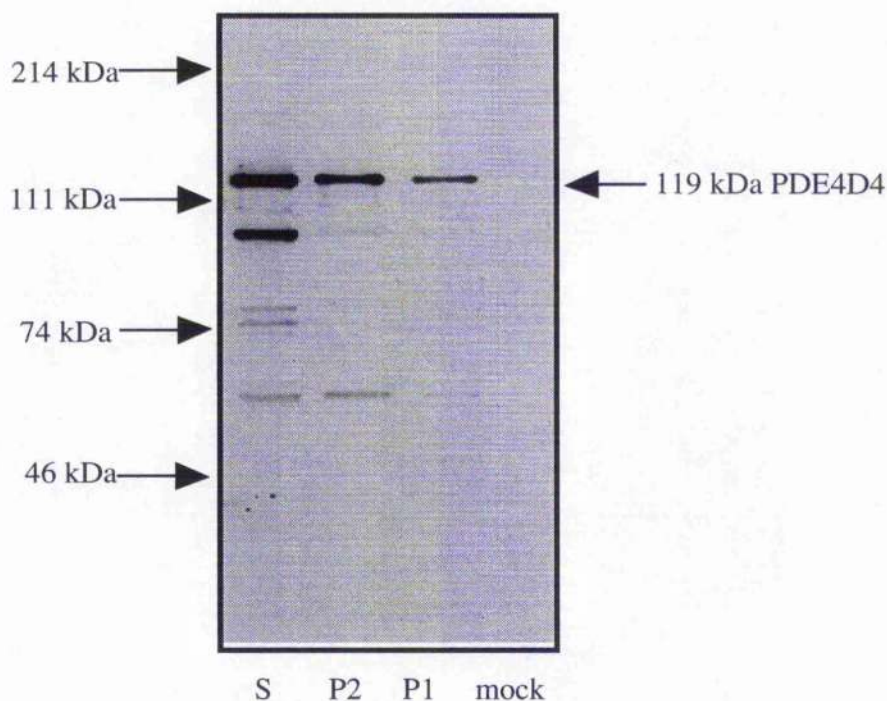


Figure 4.7. Immunoblotting of COS7 cells transfected with the cDNA for human PDE4D4

PDE4D4 plasmid was transfected into COS7 cells. After 72 h the cells were harvested, disrupted, and extracts were then subjected to differential centrifugation in order to give low-speed pellet (P1), high-speed pellet (P2) and cytosol/supernatant (S) fractions (section 2.2.12.3). Samples were then subjected to SDS/PAGE followed by Western blotting with the C-terminus monoclonal antiserum. Results are from a typical experiment which was performed at least three times with different transfections.

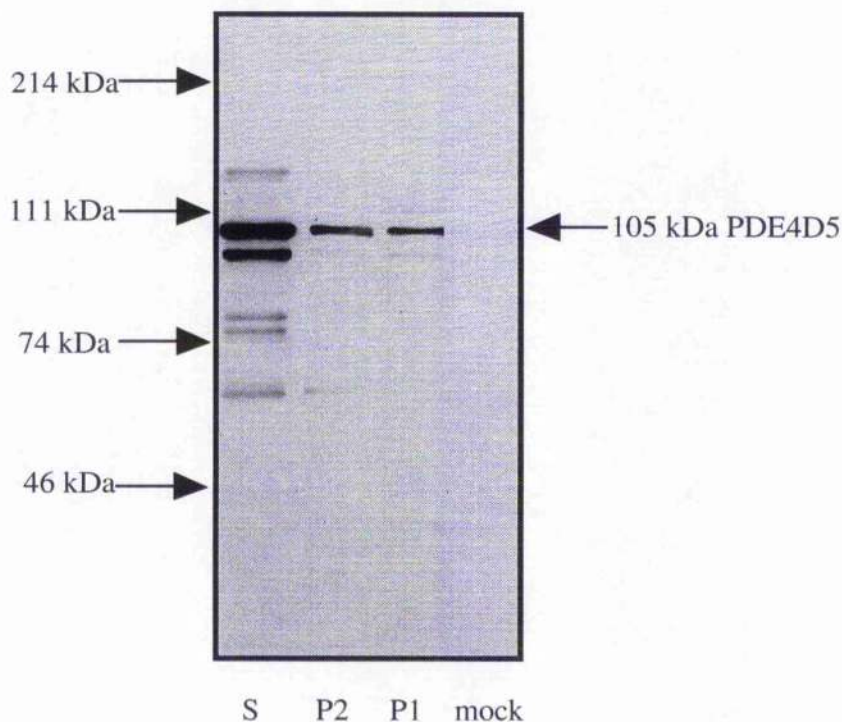


Figure 4.8. Immunoblotting of COS7 cells transfected with the cDNA for human PDE4D5

PDE4D5 plasmid was transfected into COS7 cells. After 72 h the cells were harvested, disrupted, and extracts were then subjected to differential centrifugation in order to give low-speed pellet (P1), high-speed pellet (P2) and cytosol/supernatant (S) fractions (section 2.2.12.3). Samples were then subjected to SDS/PAGE followed by Western blotting with the C-terminus monoclonal antiserum. Results are from a typical experiment which was performed at least three times with different transfections.

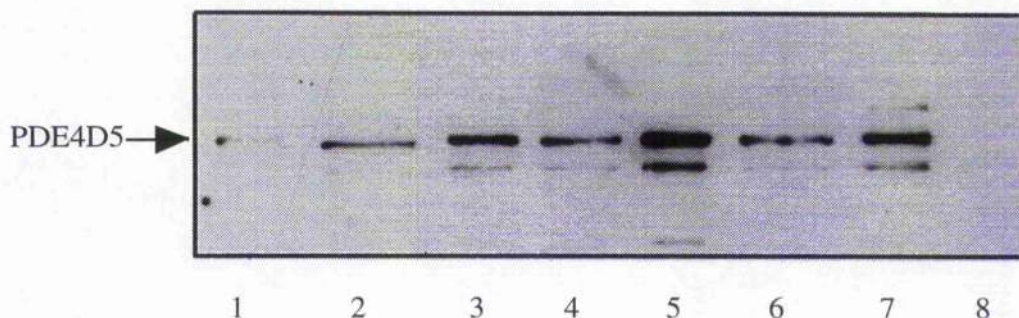


Figure 4.9. Solubilisation of human PDE4D5 protein from membranes using high salt and non-ionic detergent treatments

The high speed membranes (P2 pellets) were isolated from COS7 cells expressing the indicated PDE isoforms and treated with 1M NaCl, 5% Triton X-100 or both. After incubation and centrifugation, as described section 2.2.12.4 - 5, the residual pellet and supernatant fractions were subjected to SDS/PAGE and Western blotting with anti-PDE4D antibody. The resultant ECL/autoradiographs were scanned and absorbance changes quantified (Table 4.4). These data are from a typical experiment which was performed at least three times with different membranes. Residual supernatants; 1: buffer only, 2: 1 M NaCl, 3: 5 % Triton X-100, 4: 1 M NaCl + 5 % Triton X-100. Residual pellets; 5: buffer only, 6: 1 M NaCl, 7: 5 % Triton X-100, 8: 1 M NaCl + 5 % Triton X-100.

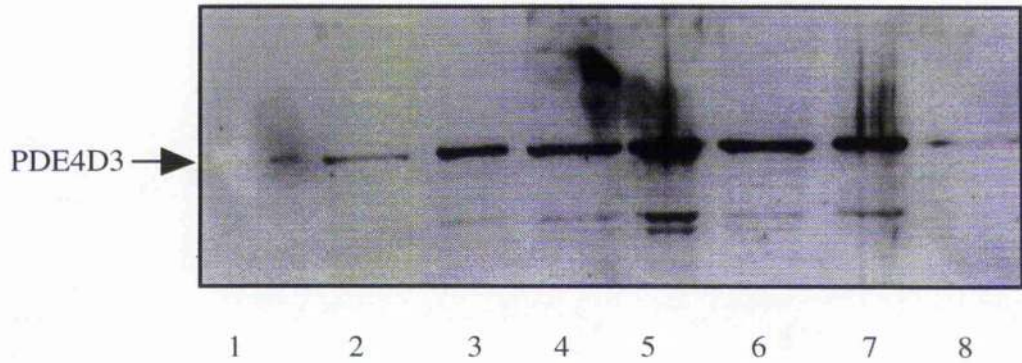


Figure 4.10. Solubilisation of human PDE4D3 protein from membranes using high salt and non-ionic detergent treatments

The high speed membranes (P2 pellets) were isolated from COS7 cells expressing the indicated PDE isoforms and treated with 1M NaCl, 5% Triton X-100 or both. After incubation and centrifugation, as described sections 2.2.12.4-5, the residual pellet and supernatant fractions were subjected to SDS/PAGE and Western blotting with anti-PDE4D antibody. The resultant ECL/autoradiographs were scanned and absorbance changes quantified (Table 4.4). These data are from a typical experiment which was performed at least three times with different membranes. Residual supernatants; 1: buffer only, 2: 1 M NaCl, 3: 5 % Triton X-100, 4: 1 M NaCl + 5 % Triton X-100. Residual pellets; 5: buffer only, 6: 1 M NaCl, 7: 5 % Triton X-100, 8: 1 M NaCl + 5 % Triton X-100.

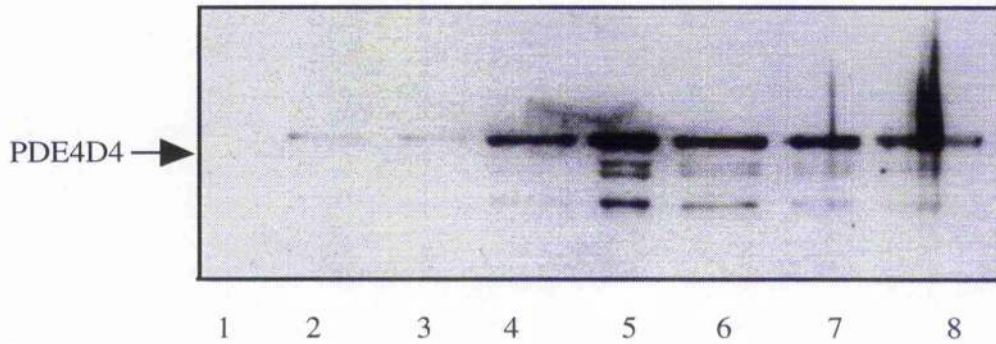


Figure 4.11. Solubilisation of human PDE4D4 protein from membranes using high salt and non-ionic detergent treatments

The high speed membranes (P2 pellets) were isolated from COS7 cells expressing the indicated PDE isoforms and treated with 1M NaCl, 5% Triton X-100 or both. After incubation and centrifugation, as described section 2.2.12.4-5, the residual pellet and supernatant fractions were subjected to SDS/PAGE and Western blotting with anti-PDE4D antibody. The resultant ECL/autoradiographs were scanned and absorbance changes quantified (Table 4.4). These data are from a typical experiment which was performed at least three times with different membranes. Residual supernatants; 1: buffer only, 2: 1 M NaCl, 3: 5 % Triton X-100, 4: 1 M NaCl + 5 % Triton X-100. Residual pellets; 5: buffer only, 6: 1 M NaCl, 7: 5 % Triton X-100, 8: 1 M NaCl + 5 % Triton X-100.

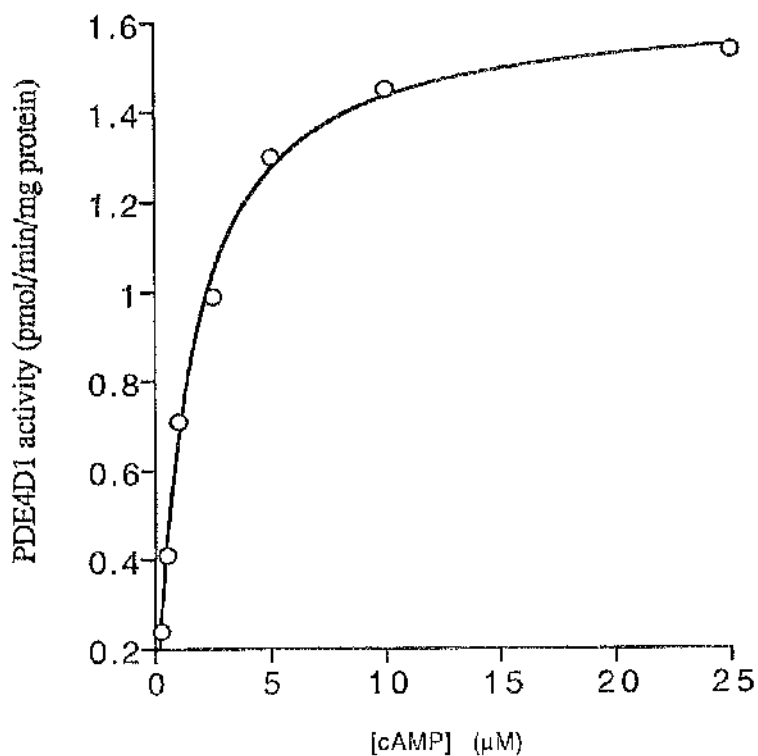


Figure 4.12. Effect of cAMP concentration on the velocity of soluble hPDE4D1 activity

Cytosolic extracts were isolated from COS7 cells expressing hPDE4D1. K_m values were determined over a substrate range of 0.25 to 25 μM cAMP (7 different concentrations). Activity is given in pmoles of cAMP hydrolysed/min/mg of protein. The data shown is typical of three independent experiments with details of values given in table 4.5.

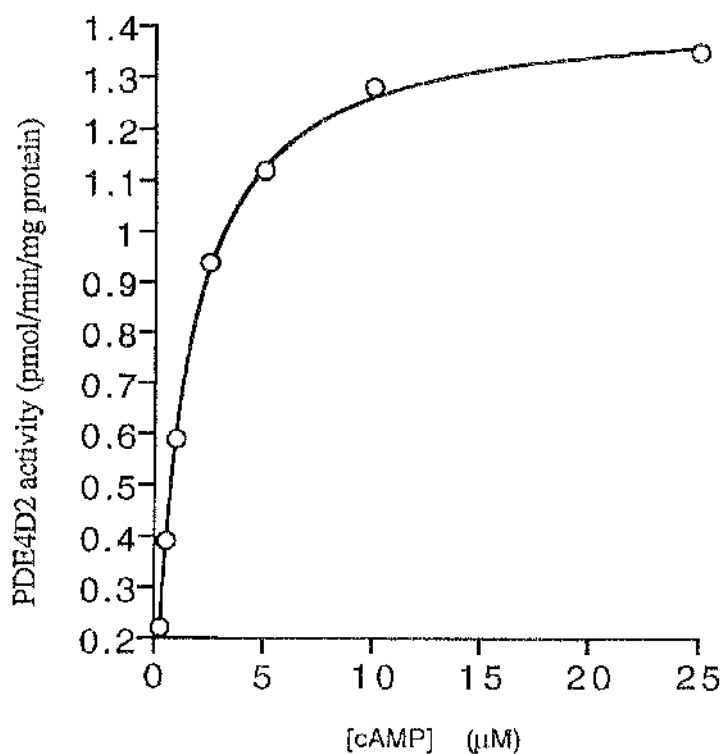


Figure 4.13. Effect of cAMP concentration on the velocity of soluble hPDE4D2 activity

Cytosolic extracts were isolated from COS7 cells expressing hPDE4D2. K_m values were determined over a substrate range of 0.25 to 25 μM cAMP (7 different concentrations). Activity is given in pmoles of cAMP hydrolysed/min/mg of protein. The data shown is typical of three independent experiments with details of values given in table 4.5.

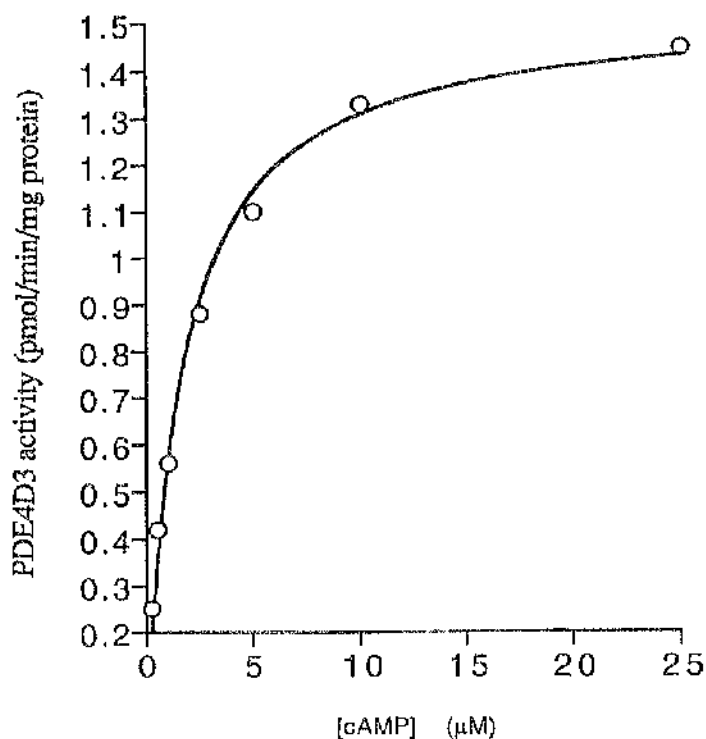


Figure 4.14. Effect of cAMP concentration on the velocity of soluble hPDE4D3 activity

Cytosolic extracts were isolated from COS7 cells expressing hPDE4D3. K_m values were determined over a substrate range of 0.25 to 25 μM cAMP (7 different concentrations). Activity is given in pmoles of cAMP hydrolysed/min/mg of protein. The data shown is typical of three independent experiments with details of values given in table 4.5.

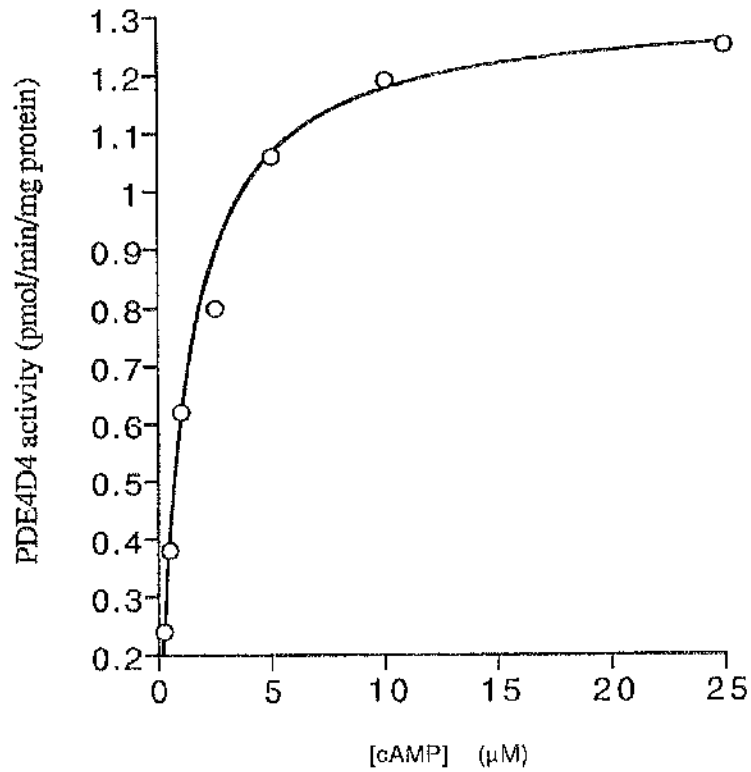


Figure 4.15. Effect of cAMP concentration on the velocity of soluble hPDE4D4 activity

Cytosolic extracts were isolated from COS7 cells expressing hPDE4D4. K_m values were determined over a substrate range of 0.25 to 25 μM cAMP (7 different concentrations). Activity is given in pmoles of cAMP hydrolysed/min/mg of protein. The data shown is typical of three independent experiments with details of values given in table 4.5.

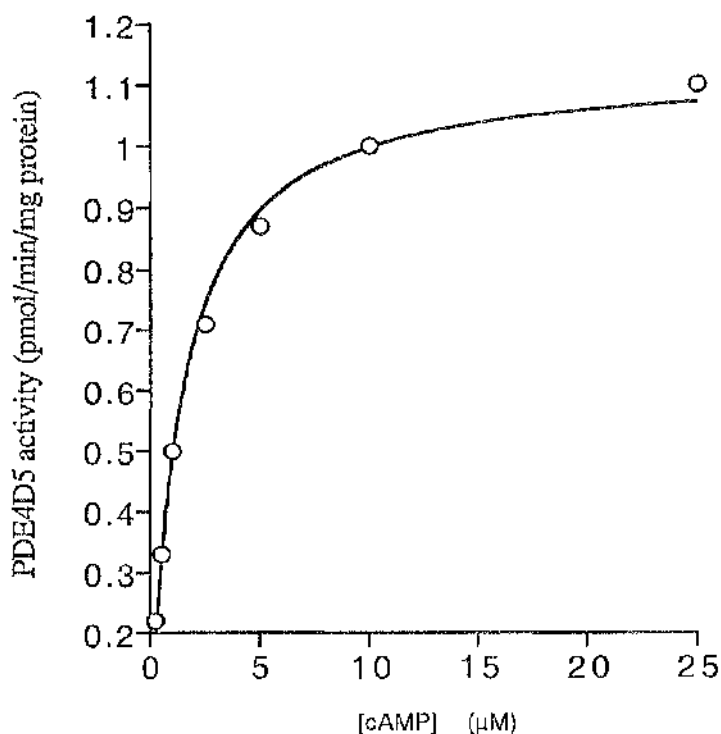


Figure 4.16. Effect of cAMP concentration on the velocity of soluble hPDE4D5 activity

Cytosolic extracts were isolated from COS7 cells expressing hPDE4D5. K_m values were determined over a substrate range of 0.25 to 25 μM cAMP (7 different concentrations). Activity is given in pmoles of cAMP hydrolysed/min/mg of protein. The data shown is typical of three independent experiments with details of values given in table 4.5.

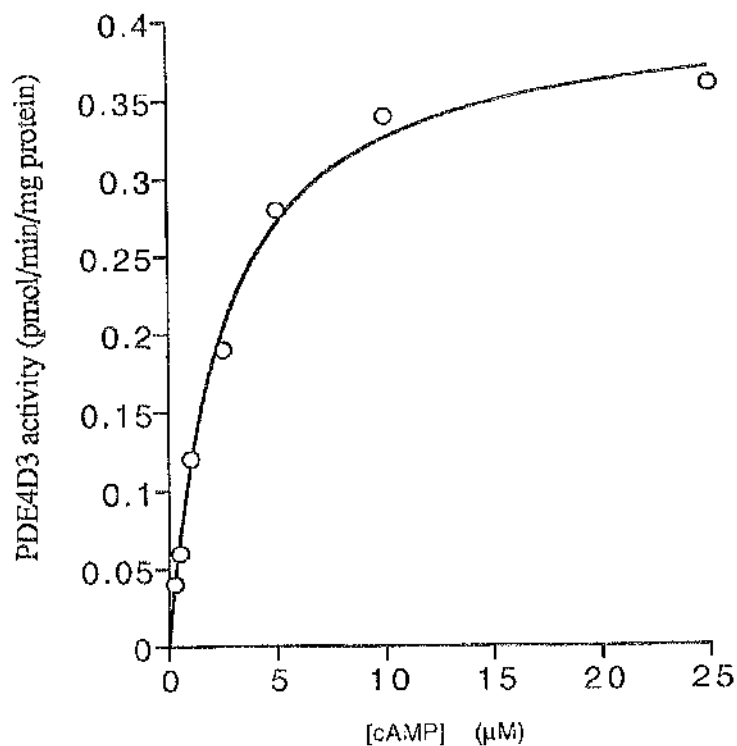


Figure 4.17. Effect of cAMP concentration on the velocity of particulate hPDE4D3 activity

Particulate (P2) extracts were isolated from COS7 cells expressing hPDE4D3. K_m values were determined over a substrate range of 0.25 to 25 μM cAMP (7 different concentrations). Activity is given in pmoles of cAMP hydrolysed/min/mg of protein. The data shown is typical of three independent experiments with details of values given in table 4.5.

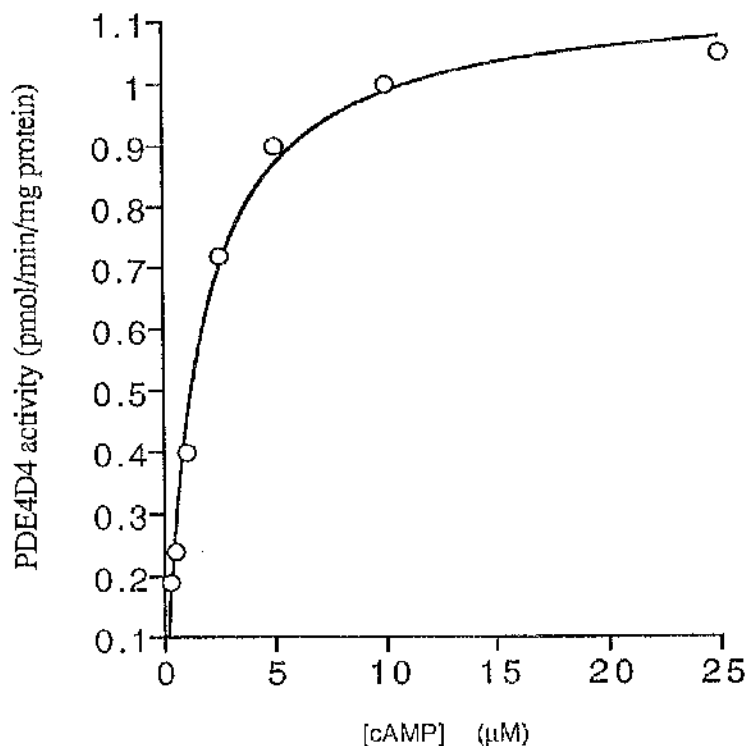


Figure 4.18. Effect of cAMP concentration on the velocity of particulate hPDE4D4 activity

Particulate (P2) extracts were isolated from COS7 cells expressing hPDE4D4. K_m values were determined over a substrate range of 0.25 to 25 μM cAMP (7 different concentrations). Activity is given in pmoles of cAMP hydrolysed/min/mg of protein. The data shown is typical of three independent experiments with details of values given in table 4.5.

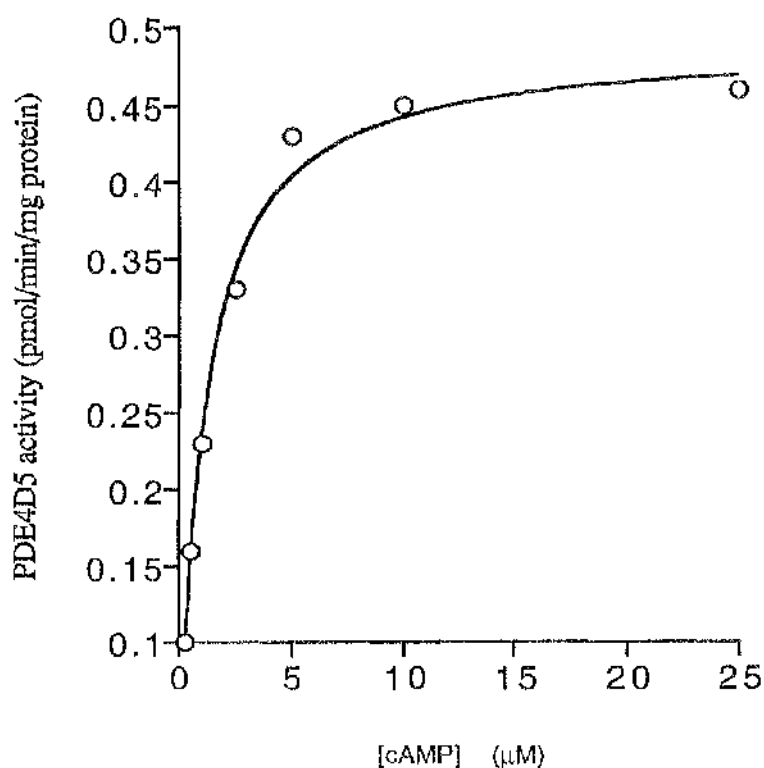


Figure 4.19. Effect of cAMP concentration on the velocity of particulate hPDE4D5 activity

Particulate (P2) extracts were isolated from COS7 cells expressing hPDE4D5. K_m values were determined over a substrate range of 0.25 to 25 μM cAMP (7 different concentrations). Activity is given in pmoles of cAMP hydrolysed/min/mg of protein. The data shown is typical of three independent experiments with details of values given in table 4.5.

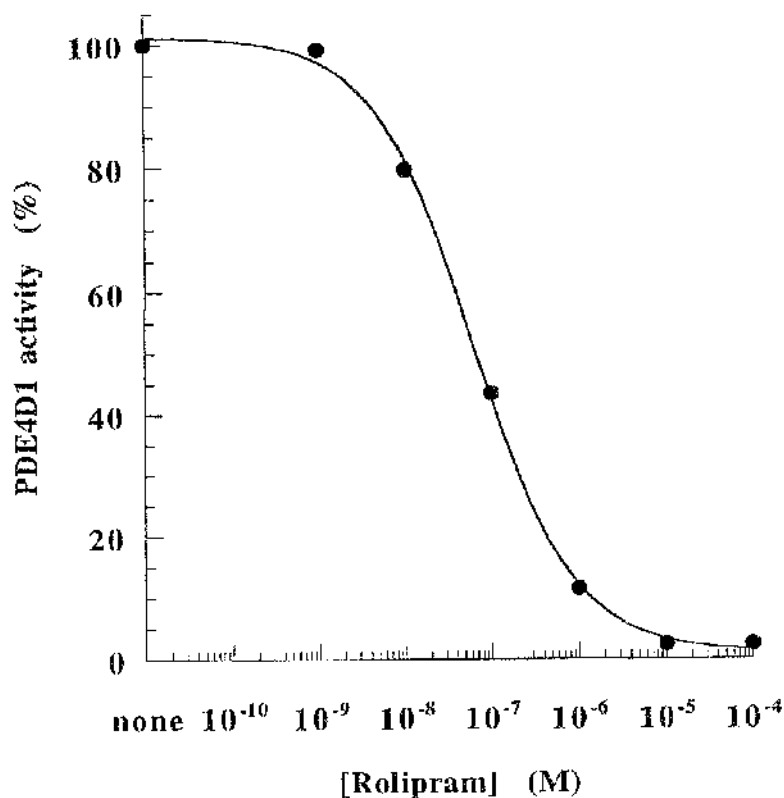


Figure 4.20. Dose-dependent inhibition of soluble hPDE4D1 activity by rolipram

The activity of the soluble forms of hPDE4D1 was determined in the presence of 1 μ M cAMP as substrate with the indicated increasing concentrations of rolipram. 100 % activity is denoted as that observed in the absence of inhibitor. The data shown is typical of an experiment done three times in triplicate, each using separate transfections. Resultant IC_{50} values are given in table 4.7.

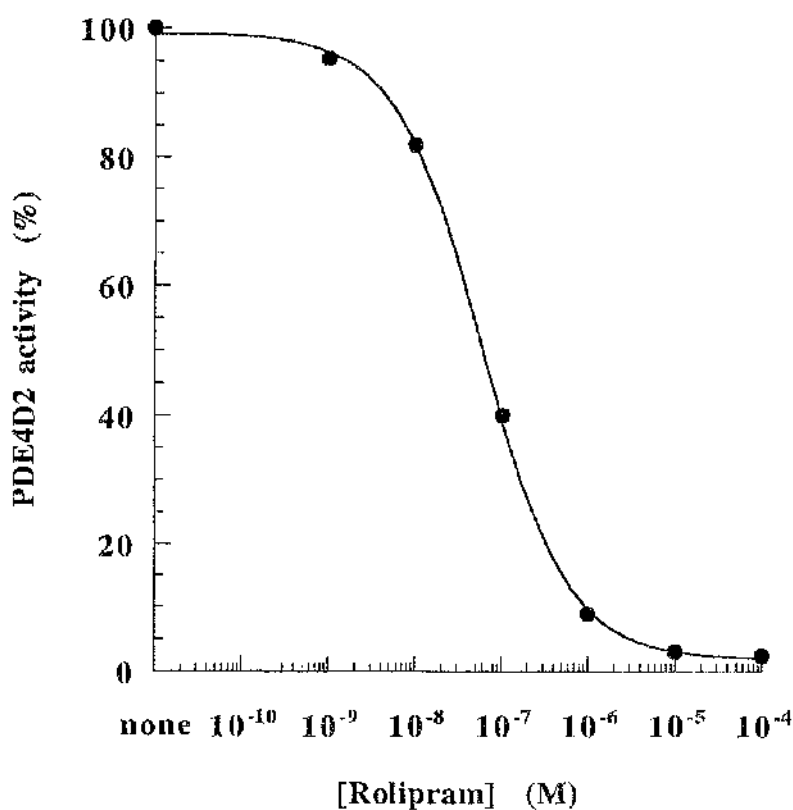


Figure 4.21. Dose-dependent inhibition of soluble hPDE4D2 activity by rolipram

The activity of the soluble forms of hPDE4D2 was determined in the presence of 1 μ M cAMP as substrate with the indicated increasing concentrations of rolipram. 100 % activity is denoted as that observed in the absence of inhibitor. The data shown is typical of an experiment done three times in triplicate, each using separate transfections. Resultant IC_{50} values are given in table 4.7.

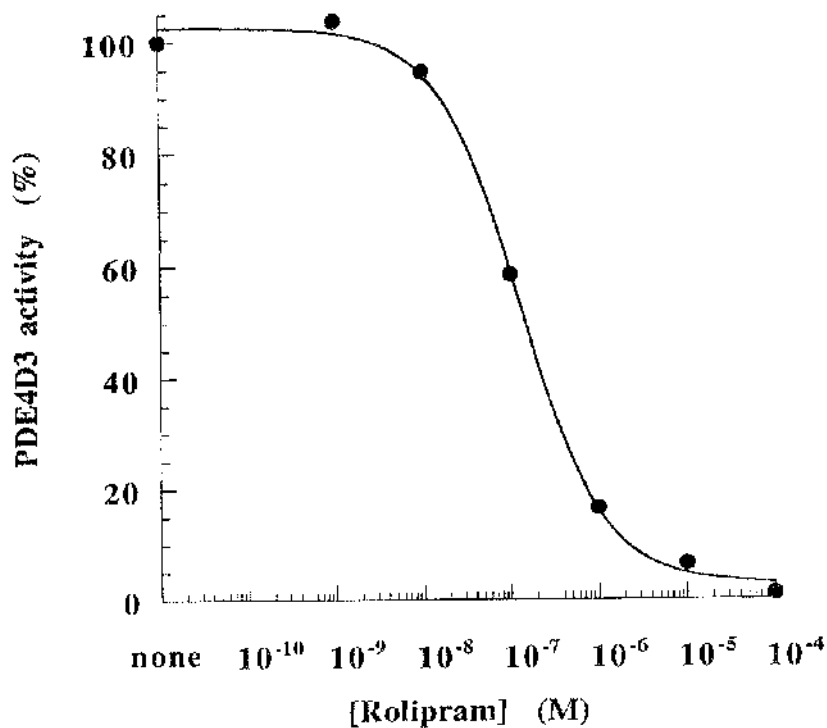


Figure 4.22. Dose-response curve for the inhibition of soluble hPDE4D3 activity by rolipram

The activity of the soluble forms of hPDE4D3 was determined in the presence of 1 μ M cAMP as substrate with the indicated increasing concentrations of rolipram. 100 % activity is denoted as that observed in the absence of inhibitor. The data shown is typical of an experiment done three times in triplicate, each using separate transfections. Resultant IC₅₀ values are given in table 4.7.

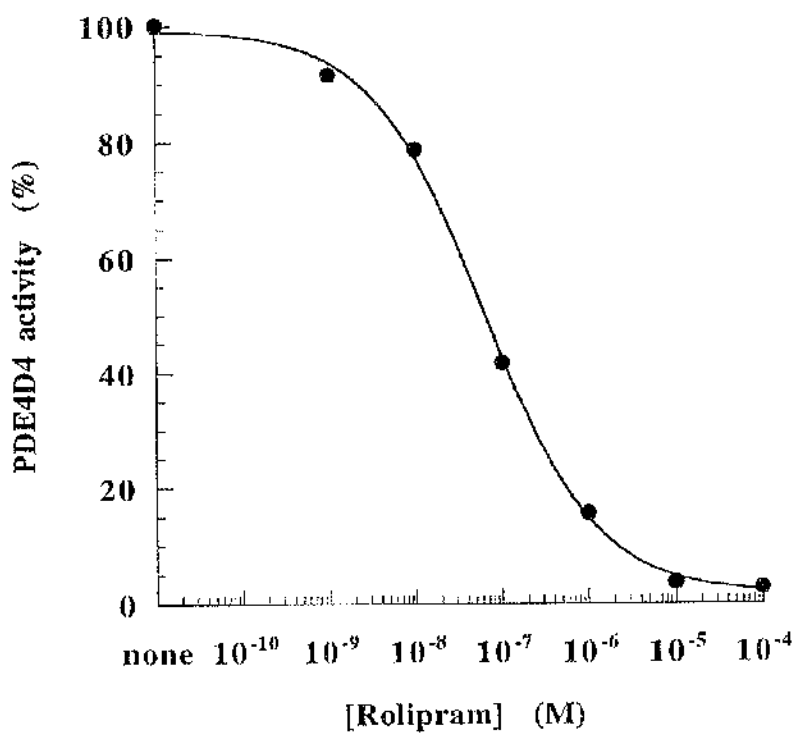


Figure 4.23. Dose-response curve for the inhibition of soluble hPDE4D4 activity by rolipram

The activity of the soluble forms of hPDE4D4 was determined in the presence of 1 μ M cAMP as substrate with the indicated increasing concentrations of rolipram. 100 % activity is denoted as that observed in the absence of inhibitor. The data shown is typical of an experiment done three times in triplicate, each using separate transfections. Resultant IC_{50} values are given in table 4.7.

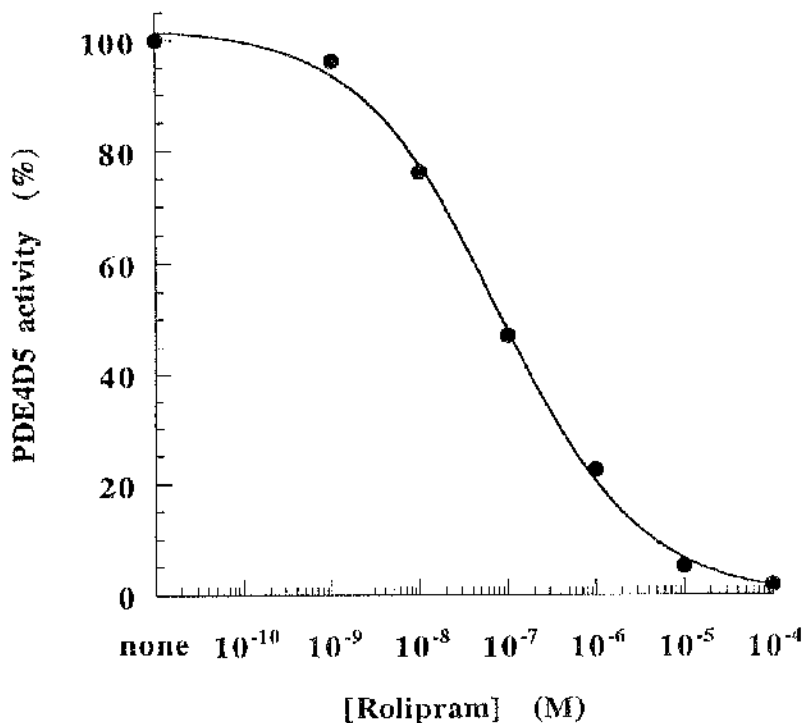


Figure 4.24. Dose-response curve for the inhibition of soluble hPDE4D5 activity by rolipram

The activity of the soluble forms of hPDE4D5 was determined in the presence of 1 μ M cAMP as substrate with the indicated increasing concentrations of rolipram. 100 % activity is denoted as that observed in the absence of inhibitor. The data shown is typical of an experiment done three times in triplicate, each using separate transfections. Resultant IC_{50} values are given in table 4.7.

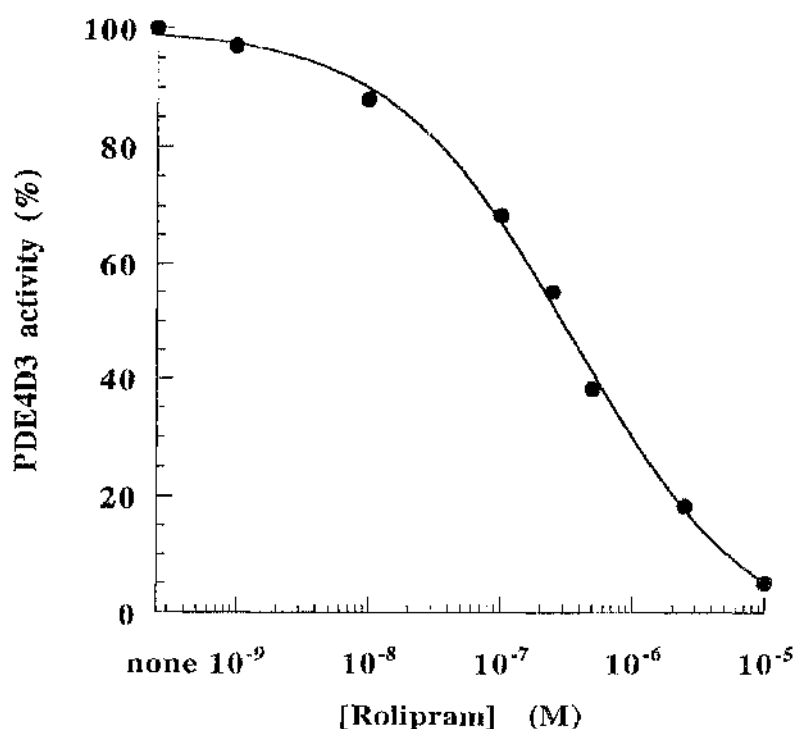


Figure 4.25. Dose-response curve for the inhibition of particulate hPDE4D3 activity by rolipram

The activity of the particulate (P2) forms of hPDE4D3 was determined in the presence of 1 μ M cAMP as substrate with the indicated increasing concentrations of rolipram. 100 % activity is denoted as that observed in the absence of inhibitor. The data shown is typical of an experiment done three times in triplicate, each using separate transfections. Resultant IC_{50} values are given in table 4.7.

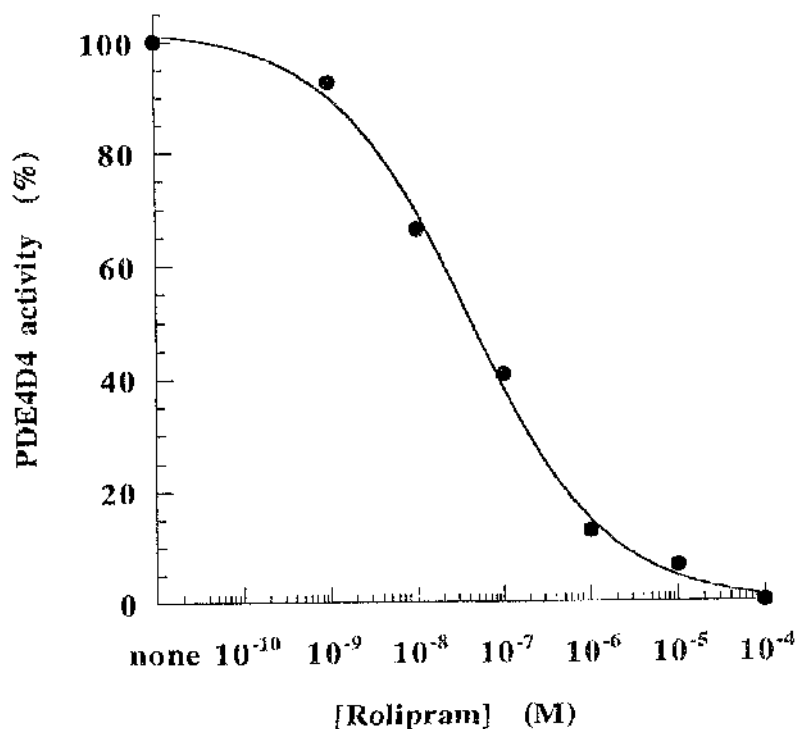


Figure 4.26. Dose-response curve for the inhibition of particulate hPDE4D4 activity by rolipram

The activity of the particulate (P2) forms of hPDE4D4 was determined in the presence of 1 μ M cAMP as substrate with the indicated increasing concentrations of rolipram. 100 % activity is denoted as that observed in the absence of inhibitor. The data shown is typical of an experiment done three times in triplicate, each using separate transfections. Resultant IC_{50} values are given in table 4.7.

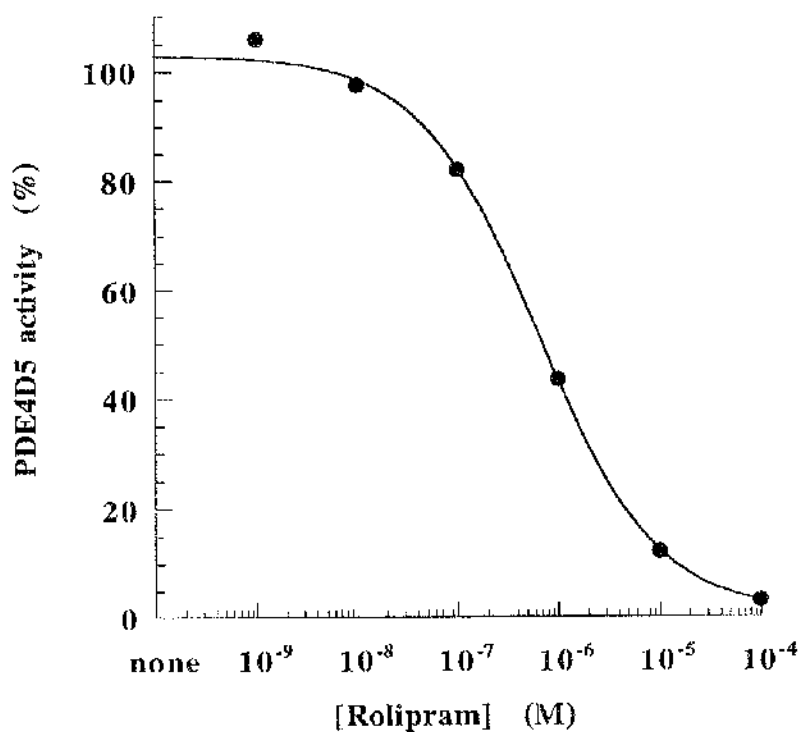


Figure 4.27. Dose-response curve for the inhibition of particulate hPDE4D5 activity by rolipram

The activity of the particulate (P2) forms of hPDE4D5 was determined in the presence of 1 μ M cAMP as substrate with the indicated increasing concentrations of rolipram. 100 % activity is denoted as that observed in the absence of inhibitor. The data shown is typical of an experiment done three times in triplicate, each using separate transfections. Resultant IC_{50} values are given in table 4.7.

CHAPTER 5

***ANALYSIS OF CHIMERIC SPECIES FORMED
BETWEEN N- AND C-TERMINAL REGION OF
INACTIVE HUMAN PDE4A SPLICE VARIANT 2EL***

5.1. Introduction

The human cAMP-specific PDE4 family comprises a series of enzymes encoded by four distinct genes located on three different chromosomes. The gene for human PDE4A and PDE4C isoforms is localised on chromosome 19, but evidence suggest that they might be located on different regions (Horton et al., 1995, Milatovich et al., 1994, Sullivan et al., unpublished data). They are both distinct from PDE4B and PDE4D, which are found on chromosomes 1 and 5 respectively (Milatovich et al., 1994, Szpirer et al., 1995). Analysis of the catalytic 'core' domain shows that, whilst members of any one PDE class show 60 - 90 % homology in the catalytic region, those belonging to different classes are much less homologous (~30 %) (Bolger, 1994). The 'core' region of PDE4 can be identified by homology with other PDE species and is conserved throughout the PDE4 class (Jin et al., 1992). However, the N- and C-terminal region of PDE4A-D isoforms differ widely (Bolger et al., 1993). The complex family of isoforms produced by PDE genes results from alternative splicing, which predominantly takes the form of 5' domain swaps, leading to isoforms having distinct N-terminal regions (Figures 5.1 - 5.2). In contrast the C-terminal region of each particular PDE4 gene family is unique and is thus common to all active isoforms produced from a particular PDE4 gene (Bolger, 1994, Conti et al., 1995b).

It has been identified that the human *PDE4A* gene family consists of at least three catalytically active and two catalytically inactive isoforms. Catalytically active forms are; PDE46 (Bolger et al., 1993), hPDE-IV_{A-h6.1} (h6.1) (Sullivan et al., 1994) and hPDE-IV_{A-Livi} (hPDE-1) (Livi et al., 1990). Catalytically inactive products are; 2EL (Horton et al., 1995) and TM73 (Bolger et al., 1993) (Table 5.1 and Figure 5.2). GeneBank accession numbers are given in table 5.1. It is possible that more PDE4A isoforms will be isolated in the future. Indeed, this study has shown that an active human PDE4A species exists in human Jurkat T-

cells (see chapter 3) which is distinct from PDE46 with differences in molecular weight, sensitivity to rolipram and in its extreme N-terminal region. The characteristics of PDE4A family enzymes, like other members of the PDE4 family is that they are potently inhibited by low-concentrations of rolipram and Ro 17-2074, that they have a high specificity for cAMP and that they are insensitive to cGMP and Ca^{2+} / CaM (Beavo et al., 1994, Conti et al., 1995b, Huston et al., 1996).

The PDE46 and h6.1 isoforms have been biochemically and pharmacologically characterised. When transiently expressed in transfected COS7 cells human PDE46 was localised to both particulate and cytosol compartments, whereas h6.1 was found only in the soluble fraction (Huston et al., 1996). The amino acid alignment shows that h6.1 and hPDE-1 are highly related proteins but differ with respect to five amino acids contained within, or adjacent to, the putative catalytic domain (Sullivan et al., 1994). They both are N-terminally truncated forms of PDE46. It is possible that hPDE-1, the first human PDE4A to be cloned may reflect an artefact of cloning and, based upon h6.1 analyses may suffer from errors in sequencing (Bolger, 1994). Wilson et al. (1994) have shown that rolipram served as a simple competitive inhibitor of h6.1, whereas Livi et al. (1990) showed that rolipram inhibited hPDE-1 in a more complex fashion. The different inhibitory kinetic mechanisms for the action of rolipram on these two isoforms suggests that they may be conformationally and functionally distinct forms.

A catalytically inactive PDE4A splice variant, called 2EL, was cloned from resting human Jurkat T-cell library (Horton et al., 1995), which was screened with a PDE specific probe (Sullivan et al., 1994). Neither the functional significance of producing such a protein, nor the molecular basis for lack of catalytic function is known. 2EL is a 323 residue protein which differs markedly from PDE46 or h6.1 in two regions. In 2EL, the catalytic 'core' region is truncated at both its N- and

C-terminal ends (Horton et al., 1995), leaving a portion of the 'core' region which reflects residues 365 and 643 in PDE46 (Bolger et al., 1993). It is believed that 2EL represents the catalytic domain of PDE46 located within the region encompassed by residues 335 - 658 on the basis of homology between other PDE species and the cAMP binding subunit of protein kinase A (Bolger, 1994, Bolger et al., 1993). Therefore 2EL does contain the 'core' catalytic region common in other PDE4 species albeit somewhat truncated at both its C- and N-termini. Sequence analysis of the putative catalytic proteins by 2EL, h6.1 or PDE46 shows that 2EL has a sequence of 30 novel amino acids at the N-terminal sequence (Figure 5.1). After this region, their identity extends over a further 278 amino acids. At the end of the identical region, there is 34 bp insertion, within the catalytic region, where premature termination of 2EL occurs as a result of the frameshift of the 2EL open reading frame (ORF). Thus 2EL has a unique sequence of 15 amino acids which forms its novel C-terminal region (Horton et al., 1995). It is possible that loss of either or both the N- and C-terminal regions found in active PDE46 and h6.1 might account for 2EL being catalytically inactive. To investigate the function of the unique N- and C-terminal regions of 2EL, HYB1, HYB2 and Delta-1 isoforms were constructed (Dr. Sullivan, Astra Charnwood/U.K). HYB1 was generated by replacing the unique C-terminal regions of the putative catalytic domain of 2EL with one reflecting that seen in the active PDE4A forms PDE46, h6.1 and hPDE-1. However, the chimera still has the unique N-terminal splice region found in 2EL together with a foreshortened N-terminal end of the putative 'core' catalytic region (Figure 5.2). Delta-1 was constructed by truncation of the N-terminal region of PDE46 which lacks the corresponding unique 30 amino acids region of 2EL. Therefore, Delta-1 does not contain unique the C-terminal 15 amino acids found in 2EL (Figure 5.2). The HYB2 chimeric species was created by exchanging the N-terminal region of 2EL with the corresponding region of h6.1 to assess the effect of the N-terminal region of 2EL on catalytic activity (Figure 5.2). To examine the effect of the structural

modification of the truncated enzymes, HYB1, HYB2 and Delta-1, were studied assaying the kinetics of cAMP hydrolysis, the effect of rolipram inhibition and the relative V_{\max} values (if the constructs were catalytically active).

5.1.2. Aim of the study

The purpose of this study was to investigate the role of N- and C-terminal regions of the inactive 2EL enzyme. For this reason, Dr. M. Sullivan generated three chimeras, called HYB1, HYB2 and Delta-1, by replacing the unique N- or C-terminal regions of 2EL with the corresponding region of the active form of h6.1. These constructs were transiently transfected into COS7 cells to investigate the effects on catalysis, rolipram sensitivity and substrate specificity. In addition, transcription analyses were done on these transfected cells using RT-PCR techniques.

5.2. Results

5.2.1. Sequence alignments of 2EL, HYB1, HYB2, Delta-1, PDE46 and h6.1

The human PDE4A species, truncated form and hybrids are shown schematically in Figure 5.2. The amino acid sequences of the chimeric species, 2EL and h6.1 are all aligned to the sequence of PDE46 (Figure 5.1). HYB1 was generated by replacing the unique C-terminal regions of 2EL with that of PDE46, h6.1. HYB2 was constructed by exchanging the unique N-terminal region of 2EL with that of h6.1. Delta-1 was truncated in the N-terminal region of h6.1, which lacks the corresponding unique region of 2EL. Therefore Delta-1 is similar with 2EL i.e. HYB1 without the unique N-terminal region of 2EL.

5.2.2. Expression and subcellular distribution of HYB1, HYB2, Delta-1 cDNAs in COS7 cells

HYB1, HYB2, Delta-1, h6.1 and PDE46 plasmids (pSV.SPORT-hyb1, -hyb2, -delta1, -h6.1 and -pde46 respectively), as well as native vector (pSV.SPORT) alone were transfected (section 2.2.12.1) into COS7 cells to express the indicated PDEs. HYB1 was also stably expressed in a strain of *Saccharomyces cerevisiae* (Wilson, 1996). Cell homogenates were subjected to centrifugation for 1 h at 100 000 g_{av} at 4 °C in order to gain a high-speed pellet (P2; particulate) and supernatant (S; cytosolic) fraction (Section 2.2.12.3). Then, fractions were either immunoblotted or assayed for PDE activity at a substrate concentration of 1 μ M cAMP. Transfection of COS7 cells with HYB1 cDNA led to an increase in the PDE activity of these cells of 230 ± 11 pmol/min/mg of protein in the cytosol fraction (mean \pm SD; $n = 4$ different transfections). In a parallel set of experiments, activities of 1.1 ± 0.1 nmol/min/mg of protein ($n = 3$) were seen after transfection to express h6.1 protein and 1.05 ± 0.2 nmol/min/mg of protein ($n = 3$) after transfection to express PDE46 cytosolic proteins. The novel PDE4 activity seen in pSV.SPORT-hyb1 transfected COS7 cells was, as with h6.1 (Sullivan et al., 1994), found exclusively in the cytosol fraction of these cells with <5 % of the total activity seen in the pellet fraction. Mock transfection with the parent plasmid had no effect (<3 %) on either the total endogenous COS7 cell PDE activity or the rolipram inhibited cytosol fraction.

S. cerevisiae was transfected so as to express the HYB1 and YMS6 (h6.1) isoforms with the activity of soluble extracts being some 1.4 ± 0.3 and 5-9 pmol/min/mg of protein, respectively (Wilson, 1995, Wilson et al., 1994). This evidence suggests that HYB1 is an active, chimeric novel PDE enzyme. Indeed, the increase in PDE activity seen in pSV.SPORT-hyb1 transfected COS7 cells was unaffected (<5 % change; $n = 3$) by the addition of either Ca^{2+} / CaM (50 μ M/20

ng/ml); which would stimulate any PDE1 activity, or by 1 μ M cGMP (<5 % change; $n = 3$); which would alter either PDE2 or PDE3 activities (Kilgour et al., 1989, Wilson et al., 1994). However, the increased PDE activity seen in these HYB1 expressing transfected cells was inhibited by >95 % upon addition of 10 μ M rolipram (1 μ M cAMP as substrate). Such observations are consistent with HYB1 behaving as a PDE of the PDE4 isoform class.

However, neither pSV.SPORT-hyb2 nor pSV.SPORT-delta1 transfected COS7 cells extracts expressed measurable PDE activity (<1 % change; $n = 3$, different proteins preparations). Delta-1 was generated by the truncation of the N-terminal region of h6.1 which lacks the corresponding unique 30 amino acid region of 2EL. HYB2 chimera was constructed by exchanging the unique N-terminal region of 2EL with the corresponding region of h6.1 (Figure 5.2). This suggests that deletions of unique N-terminal region amino acids prevents the production of catalytically activity enzyme by expression of chimeric HYB1. Premature truncation at the C-terminal end of 2EL may prevent the correct assembly of a functional catalytic centre for the hydrolysis of cAMP by 2EL.

5.2.3. Immunological detection of HYB1 and Delta-1

The alignment of PDE46 and h6.1 sequences shows that C-terminal amino acids are identical (Figure 5.2). Using the polyclonal antibody, raised against the C-terminal end of human PDE4A-GST fusion protein (section 2.2.2), allowed the detection of a single 82 ± 2 kDa immunoreactive species in the cytosolic fraction of HYB1 expressing COS7 cells (Figure 5.3). However this was not observed in those cells which had been transfected with a control vector. From such immunoblot and activity studies (see section 5.2.2) it was evident that HYB1 PDE was localised in cytosol but not in the membrane. This species was, as might be predicted (Figure 5.1) smaller than that of h6.1, which migrated as a 102 ± 2 kDa

species and PDE46 which migrated as a 127 ± 1 kDa species (means \pm SD; $n = 3$) (Figure 5.3). The catalytically inactive form, truncated PDE46 specie Delta-1 was also expressed in COS7 cells to allow immunoblot analysis. It was found that this species was expressed solely in the cytosolic fraction with molecular mass of 80 ± 2 kDa (Figure 5.3).

5.2.4. Transcriptional analysis of HYB1 and HYB2 chimeras

HYB1, HBY2, 2EL and h6.1 plasmids were transfected into COS7 cells as detailed in section 2.2.12. Then, after ~ 72 h, RNAs were isolated (section 2.2.15) from each of the transfected COS7 cell lines, transcribed into cDNA and PCR was performed. The sense-2069 and antisense-Pharmacia primers were designed to amplify a fragment unique to the 5'-end of 2EL and HYB1 chimera which represent nucleotides 333 - 726 in 2EL. This allowed the detection of a 393 bp fragment (Figure 5.4). In order to examine h6.1 and HYB2 transcripts, sense-2726 and antisense-2728 primers were used to amplify a 576 bp fragment. The fragment amplified represents nucleotides 64 - 639 in h6.1 (Figure 5.5). The primer pairs and PCR conditions are given in the appropriate figure legends. 2EL and HYB1 specific primers yielded signals with similar intensity (changes $< 5\%$) (Figure 5.4). h6.1 and HYB2 specific primers amplified to produce a higher intensity signal for HYB2 than h6.1.

5.2.5. Kinetics of cyclic AMP hydrolysis by HYB1

The K_m value for the hydrolysis of cAMP by the cytosol fraction of COS7 cell expressing HYB1 was determined. The data was obtained from the PDE activity assay using 8 different cAMP concentrations ($0.5 \mu\text{M}$ to $30 \mu\text{M}$ cAMP) as substrate. This was then analysed by computer fitting to the hyperbolic form of the Michaelis-Menten equation using the Ultrafit graphical package (section 2.2.6).

The 'robust weighting' facility was used and the 'goodness of fit' index was no less than 0.99 with the estimation, 1 being a perfect fit (Figure 5.6). This analysis yielded a K_m value of $2.7 \pm 0.3 \mu\text{M}$ ($n = 4$) for HYB1 which is similar to that found for this enzyme expressed in *S. cerevisiae* (Table 5.2). These values were, however, about half those seen for h6.1 but were similar to those seen for PDE46 (Table 5.2)

In order to determine relative V_{max} values, increasing concentrations of proteins (10 μM to 30 μM) from the cytosolic fraction of transfected COS7 cells were immunoblotted. The anti-human PDE4A antisera (section 2.2.2) was used to detect the specific PDE proteins and then the labelled bands were visualised using the ECL procedure according to the manufacturers instructions (section 2.2.4). The appropriate signal absorbance (A) versus amount of protein (μg) were plotted (Figure 5.7). Relative concentrations of PDE protein were calculated from this plot. For the V_{max} determination, equal amounts of COS7 cell extracts (PDE protein) were taken for PDE assay. Then, the relative V_{max} values were calculated using the Michaelis-Menten equation and the experimentally derived K_m values. It was demonstrated that HYB1 was ~70 % more active than the full length species PDE46 but much less active than h6.1 (Table 5.2).

5.2.6. Dose-dependent inhibition of HYB1 by rolipram

HYB1 activity was potently inhibited in a dose-dependent fashion by the selective inhibitor rolipram, yielding IC_{50} values of $\sim 2.1 \mu\text{M}$ ($n = 3$) (Figure 5.8 and Table 5.2). In the inhibition studies, 3 μM cAMP concentration was used as substrate which reflects that of the K_m value. Rolipram was used in the concentration range of 0.001 μM - 100 μM . IC_{50} values (concentration of inhibitor which produced 50 % reduction in substrate hydrolysis) were then calculated from the dose-response curve using the KaleidaGraph computer programme.

5.3. Conclusion and Discussion

Both human and rat PDE4 genes appear to produce multiple transcripts involving 5'-domain swopping (Beavo, 1995, Conti et al., 1995b) to yield alternative splice forms with different N-terminal domains. Catalytically active human PDE4A forms PDE46 (Bolger et al., 1993), h6.1 (Sullivan et al., 1994) and hPDE-1 (Livi et al., 1990) yield protein products that have identical catalytic sites and C-terminal regions but show highly different N-terminal domains. However, two catalytically inactive isoforms, 2EL (Horton et al., 1995) and TM3 (Bolger et al., 1993), also exhibit unique C-terminal regions as well as unique N-terminal regions. This suggests that these unique N- and C-terminal regions may perform specific functions, such as, affecting catalytic activity and interaction with other proteins. 2EL is an enzymatically inactive PDE4A isoform by virtue of the premature truncation within the putative catalytic region of the enzyme (Horton et al., 1995). This property of 2EL could not be examined by expression in a cell system. Therefore the molecular basis and their functional significance are unknown. However, it is a possibility that 2EL and TM3 perhaps represent the products of a mechanism to control the level of mRNAs for functional PDEs (Horton et al., 1995). In this study, PDE4A isoform 2EL was shown to be inactive, however, it was unknown as to whether this was due to the presence of 30 novel amino acids in the N-terminal end or an inhibitory 34 bp insert in the C-terminal end. In order to investigate the unique 5'- end and 3'-end roles, two constructs and one truncated PDE46 form (made by Dr. Sullivan) were analysed in this study. HYB1 chimeric species was generated by replacing the C-terminal region of the inactive 2EL with one equivalent to that seen in active splice variants PDE46 and h6.1. HYB2 chimera was constructed by swopping the N-terminal unique 30 amino acid region of 2EL with the corresponding region of h6.1. The truncated form Delta-1 was generated by deletion of the N-terminus of PDE46 at residues 1 - 365. These

hybrids and truncated form are shown diagrammatically in Figure 5.2 and their amino acid sequences are given in the alignment in Figure 5.1.

Transient transfection with HYB2 and Delta-1 cDNAs showed that they lack PDE activity. However, the HYB1 chimera expressed cAMP-specific PDE4 activity indicating that it is the foreshortened C-terminal region which renders ZEL catalytically inactive. Deletion of the unique 30 amino acid region on HYB2 and Delta-1 constructs showed that this region plays an important role in rendering HYB1 chimera catalytically active. The inhibition by low-concentrations of rolipram, insensitivity to Ca^{2+} / CaM and cGMP and specificity to cAMP suggest that the pSV.SPORT-hyb1 cDNA encodes a PDE4. HYB1 PDE activity was only seen in the cytosol fraction when expressed in COS7 cells. This was similar to h6.1 expressed in COS1 and COS7 cells (Huston et al., 1996, Sullivan et al., 1994). Immunoblotting studies also showed that HYB1 was solely localised to the soluble fraction, where a novel ~82 kDa immunoreactive species was seen (Figure 5.3). This species was smaller than that of h6.1 and PDE46 (Figure 5.1). Similar study also demonstrated that inactive construct, Delta-1, was 80 kDa protein (Figure 5.3).

Comparison of the K_m values calculated for HYB1 expressed in COS7 cells and *S. cerevisiae* (Wilson, 1995) were similar (Table 5.2). These values were, however, about half those exhibited by h6.1 (Sullivan et al., 1994) but were similar to those seen for PDE46 (Huston et al., 1996) (Table 5.2). This may imply that a role exists for the unique N-terminal 30 amino acid region of HYB1 in catalysis. The relative V_{max} values were determined from equalised PDE protein by immunoblotting (section 2.2.8). From this study, HYB1 chimera was demonstrated to be ~70 % more active than the full length species PDE46 but much less active than h6.1 (Table 5.2). This was as shown by (Huston et al., 1996), that h6.1, which lacks the N-terminal extension of PDE46, was about 11-fold more

active than PDE46. It has also been shown that the extended N-terminal region of rat PDE4A enzyme RD1 was less active than the N-terminally truncated species met²⁶RD1 (Shakur et al., 1995). From these studies HYB1 would be expected to be much more active than PDE46. This would be explained by either, the unique 30 amino acids at the N-terminal end of HYB1 having an inhibitory effect on the catalytic activity compared to that seen in h6.1, or this could be due to the 131 amino acid extension of the N-terminus of h6.1 enhancing the catalytic activity.

The PDE4 specific inhibitor rolipram caused dose-dependent inhibition of soluble HYB1 activity (Figure 5.8). The calculated IC₅₀ value for HYB1 was ~2.4 μM when expressed in COS7 cells and this was similar when expressed in *S. cerevisiae* (Wilson, 1995) (Table 5.2). Again these values were distinct from h6.1 but similar to that seen for PDE46 (Huston et al., 1996) (Table 5.2). This observation indicates that the N-terminus of h6.1 must contain specific information for inhibitor interaction. Indeed, Wilson (1995) has demonstrated that deletion of either C-terminus only (608 - 692 in yeast) or the N- and C-terminus (1 - 172 and 608 - 692 in yeast) of h6.1 PDE together, have similarly less sensitivity to rolipram inhibition. These findings supports that the N-terminal region of h6.1 has a role for interaction with inhibitor and for catalytic activity.

The enzymatically active HYB1 chimeric PDE demonstrated that premature truncation of the putative catalytic domain prevents the correct assembly of a functional catalytic centre for the hydrolysis of cAMP by 2EL. In addition, the inactive Delta-1 truncated form showed that the unique N-terminal region of 2EL has a functional role in rendering HYB1 PDE catalytically active. Thus the splice variant 2EL is catalytically inactive because of the premature truncation occurring at the C-terminus. This region provides the basis for lack of PDE activity in 2EL.

Table 5.1. The human PDE4A splice variants

Isoform name	Short name	Accession No	Active (A) / Inactive (I)
HSPDE4A4B	PDE46	L20965	A
HSPDE4A4C	h6.1	U18087	A
HSPDE4A4A	hPDE-1	M37744	A
HSPDE4A5?	TM73	L20967	I
HSPDE4A8	2EL	U18088	I

The table shows the isoforms of human PDE4A family with their catalytic activity (A) and inactivity (I). The isoforms are identified with their GenBank accession numbers from the references PDE46 and TM73 (Bolger et al., 1993), h6.1 (Sullivan et al., 1994), hPDE-1 (Livi et al., 1990) and 2EL (Horton et al., 1995).

Table 5.2. Properties of the chimeric PDE4A species HYB1

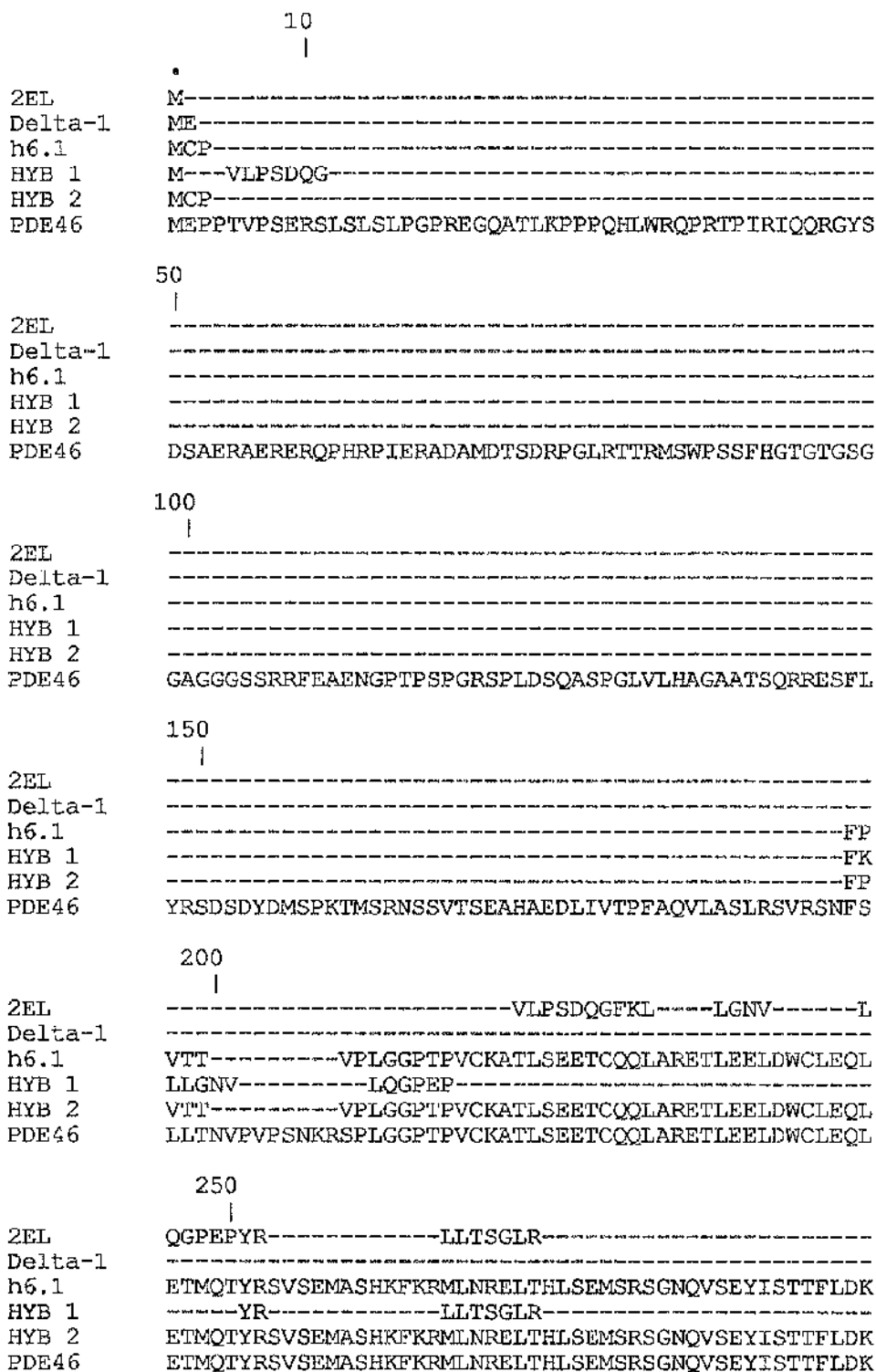
PDE species	Cell system	K_m	IC ₅₀ rolipram	Relative V_{max}
HYB1	<i>S. cerevisiae</i>	2.4±0.2 #	2.0±0.2 #	-
HYB1	COS7	2.9±0.4	2.1±0.5	1.7±0.3
h6.1	<i>S. cerevisiae</i>	6±2 #	0.6±0.1 #	-
h6.1	COS7	6±2 †	0.6±0.2 †	9.6±0.9
PDE46	COS7	2.3±0.4 †	3.5±0.5 †	(1)

Data is give for the enzymes expressed in the indicated transfected cells. Values of the apparent K_m (in μM) and V_{max} were determined over a wide range of cAMP substrate concentrations (0.5 - 30 μM , 8 different concentrations) by fitting data to the Michaelis-Menten equation (section 2.2.6). Relative V_{max} values were derived from such data upon assessment of the relative levels of expression of these PDE4A forms in transfected COS7 cells (2.2.8). IC₅₀ values (in μM) for rolipram were derived in assays done at 3 μM cAMP as substrate. Each value is the mean \pm SD of three independent experiments each using seperate transfections (triplicate determinations of each experiment). #Data were taken from Wilson et al., 1994, †Huston et al., 1996.

Figure 5.1. Alignment of the amino acid sequences of the PDE46, h6.1, 2EL, HYB1, HYB2 and Delta-1

Amino acid alignments were made using the Gene Jockey programme and were aligned to the sequence of PDE46. * denoted an identical amino acid residue in both sequences.

Figure 5.1. Alignment of the amino acid sequences of the PDE46, h6.1, 2EL, HYB1, HYB2 and Delta-1



300

2EL -----
 Delta-1 -----
 h6.1 QNEVEIIPSPIMKEREKQOAPRPRPSQPPPPFVPHLQPM SQITGLK KLMH
 HYB 1 -----
 HYB 2 QNEVEIIPSPIMKEREKQOAPRPRPSQPPPPFVPHLQPM SQITGLK KLMH
 PDE46 QNEVEIIPSPIMKEREKQOAPRPRPSQPPPPFVPHLQPM SQITGLK KLMH

350

2EL -----LHQELENLNKWGLNIFCVSDYAGGRSLT
 Delta-1 -----LENLNKWGLNIFCVSDYAGGRSLT
 h6.1 SNSLNNSNIPRF'GVKTDQEELLAQELENLNKWGLNIFCVSDYAGGRSLT
 HYB 1 -----LHQELENLNKWGLNIFCVSDYAGGRSLT
 HYB 2 SNSLNNSNIPRF'GVKTDQEELLAQELENLNKWGLNIFCVSDYAGGRSLT
 PDE46 SNSLNNSNIPRF'GVKTDQEELLAQELENLNKWGLNIFCVSDYAGGRSLT

400

2EL C1MYMIFQERDLLKKFRIPVDTMV'TYMLTLEDHYHADVAYHNSLHAADV
 Delta-1 C1MYMIFQERDLLKKFRIPVDTMV'TYMLTLEDHYHADVAYHNSLHAADV
 h6.1 C1MYMIFQERDLLKKFRIPVDTMV'TYMLTLEDHYHADVAYHNSLHAADV
 HYB 1 C1MYMIFQERDLLKKFRIPVDTMV'TYMLTLEDHYHADVAYHNSLHAADV
 HYB 2 C1MYMIFQERDLLKKFRIPVDTMV'TYMLTLEDHYHADVAYHNSLHAADV
 PDE46 C1MYMIFQERDLLKKFRIPVDTMV'TYMLTLEDHYHADVAYHNSLHAADV

450

2EL LQSTHVLLATPALDAVF'TDLEILAALFAAAIHDVDHPGVSNOFLINTNS
 Delta-1 LQSTHVLLATPALDAVF'TDLEILAALFAAAIHDVDHPGVSNOFLINTNS
 h6.1 LQSTHVLLATPALDAVF'TDLEILAALFAAAIHDVDHPGVSNOFLINTNS
 HYB 1 LQSTHVLLATPALDAVF'TDLEILAALFAAAIHDVDHPGVSNOFLINTNS
 HYB 2 LQSTHVLLATPALDAVF'TDLEILAALFAAAIHDVDHPGVSNOFLINTNS
 PDE46 LQSTHVLLATPALDAVF'TDLEILAALFAAAIHDVDHPGVSNOFLINTNS

500

2EL ELALMYNDESVLENHHLAVGFKLLQEDNCDIFQNL SKRQRQSLRKMVID
 Delta-1 ELALMYNDESVLENHHLAVGFKLLQEDNCDIFQNL SKRQRQSLRKMVID
 h6.1 ELALMYNDESVLENHHLAVGFKLLQEDNCDIFQNL SKRQRQSLRKMVID
 HYB 1 ELALMYNDESVLENHHLAVGFKLLQEDNCDIFQNL SKRQRQSLRKMVID
 HYB 2 ELALMYNDESVLENHHLAVGFKLLQEDNCDIFQNL SKRQRQSLRKMVID
 PDE46 ELALMYNDESVLENHHLAVGFKLLQEDNCDIFQNL SKRQRQSLRKMVID

550

2EL MVLATDMSKHM'TLLADLKT MVET'KKVTSSGVLLLDNYSDRIQVLRNMVH
 Delta-1 MVLATDMSKHM'TLLADLKT MVET'KKVTSSGVLLLDNYSDRIQVLRNMVH
 h6.1 MVLATDMSKHM'TLLADLKT MVET'KKVTSSGVLLLDNYSDRIQVLRNMVH
 HYB 1 MVLATDMSKHM'TLLADLKT MVET'KKVTSSGVLLLDNYSDRIQVLRNMVH
 HYB 2 MVLATDMSKHM'TLLADLKT MVET'KKVTSSGVLLLDNYSDRIQVLRNMVH
 PDE46 MVLATDMSKHM'TLLADLKT MVET'KKVTSSGVLLLDNYSDRIQVLRNMVH

600

```

|
.....
2EL CADLSNPTKPLELYRQWTD RIMAEFFQ QGDRERERGM EISPMCDKHTAS
Delta-1 CADLSNPTKPLELYRQWTD RIMAEFFQ QGDRERERGM EISPMCDKHTAS
h6.1 CADLSNPTKPLELYRQWTD RIMAEFFQ QGDRERERGM EISPMCDKHTAS
HYB 1 CADLSNPTKPLELYRQWTD RIMAEFFQ QGDRERERGM EISPMCDKHTAS
HYB 2 CADLSNPTKPLELYRQWTD RIMAEFFQ QGDRERERGM EISPMCDKHTAS
PDE46 CADLSNPTKPLELYRQWTD RIMAEFFQ QGDRERERGM EISPMCDKHTAS

```

650

```

|
..... | • | •
2EL VEKSQV-----QARGI-----
Delta-1 VEKSQVGFIDYIVHPLWETWADLVHPDAQEILD TLEDNRDWYYS AIROS
h6.1 VEKSQVGFIDYIVHPLWETWADLVHPDAQEILD TLEDNRDWYYS AIROS
HYB 1 VEKSQVGFIDYIVHPLWETWADLVHPDAQEILD TLEDNRDWYYS AIROS
HYB 2 VEKSQV-----QARGI-----
PDE46 VEKSQVGFIDYIVHPLWETWADLVHPDAQEILD TLEDNRDWYYS AIROS

```

700

```

|
|| • | •
2EL -----DGRAQG-----
Delta-1 PSPPPPEEESRGP GHPPLPDKFQFELTLEEEEEEE EISMAQIPCTAQEALT
h6.1 PSPPPPEEESRGP GHPPLPDKFQFELTLEEEEEEE EISMAQIPCTAQEALT
HYB 1 PSPPPPEEESRGP GHPPLPDKFQFELTLEEEEEEE EISMAQIPCTAQEALT
HYB 2 -----DGRAQG-----
PDE46 PSPPPPEEESRGP GHPPLPDKFQFELTLEEEEEEE EISMAQIPCTAQEALT

```

750

```

|
| .....
2EL -----GFY
Delta-1 AQGLSGVEEALDATI AWEASPAQESLEVMAQEAS LEAELEAVYLTQQAQ
h6.1 EQGLSGVEEALDATI AWEASPAQESLEVMAQEAS LEAELEAVYLTQQAQ
HYB 1 EQGLSGVEEALDATI AWEASPAQESLEVMAQEAS LEAELEAVYLTQQAQ
HYB 2 -----GFY
PDE46 AQGLSGVEEALDATI AWEASPAQESLEVMAQEAS LEAELEAVYLTQQAQ

```

800

```

|
.....
Delta-1 STGSAPVAPDEFSSR EEFVAVSHSSPSALALQSP LLLPAWRTLSVSEHA
h6.1 STGSAPVAPDEFSSR EEFVAVSHSSPSALALQSP LLLPAWRTLSVSEHA
HYB 1 STGSAPVAPDEFSSR EEFVAVSHSSPSALALQSP LLLPAWRTLSVSEHA
PDE46 STGSAPVAPDEFSSR EEFVAVSHSSPSALALQSP LLLPAWRTLSVSEHA

```

850

```

|
.....
Delta-1 PGLPGLPSTAAEVEAQ REHQAAKRAC SACAGTFG EDTSALPAPGGGGSG
h6.1 PGLPGLPSTAAEVEAQ REHQAAKRAC SACAGTFG EDTSALPAPGGGGSG
HYB 1 PGLPGLPSTAAEVEAQ REHQAAKRAC SACAGTFG EDTSALPAPGGGGSG
PDE46 PGLPGLPSTAAEVEAQ REHQAAKRAC SACAGTFG EDTSALPAPGGGGSG

```

```

.....
Delta-1 GDPT
h6.1 GDPT
HYB 1 GDPT
PDE46 GDPT

```

600

	
2EL		CADLSNPTKPLELYRQWTD RIMAEFFQ QGDRERERGM EISPMCDKHTAS
Delta-1		CADLSNPTKPLELYRQWTD RIMAEFFQ QGDRERERGM EISPMCDKHTAS
h6.1		CADLSNPTKPLELYRQWTD RIMAEFFQ QGDRERERGM EISPMCDKHTAS
HYB 1		CADLSNPTKPLELYRQWTD RIMAEFFQ QGDRERERGM EISPMCDKHTAS
HYB 2		CADLSNPTKPLELYRQWTD RIMAEFFQ QGDRERERGM EISPMCDKHTAS
PDE46		CADLSNPTKPLELYRQWTD RIMAEFFQ QGDRERERGM EISPMCDKHTAS

650

		• •
2EL		VEKSQV-----	QARGI-----
Delta-1		VEKSQVGFIDYIVHPLWETWADLVHPDAQEILD TLEDNRDWYYSAIRQS	
h6.1		VEKSQVGFIDYIVHPLWETWADLVHPDAQEILD TLEDNRDWYYSAIRQS	
HYB 1		VEKSQVGFIDYIVHPLWETWADLVHPDAQEILD TLEDNRDWYYSAIRQS	
HYB 2		VEKSQV-----	QARGI-----
PDE46		VEKSQVGFIDYIVHPLWETWADLVHPDAQEILD TLEDNRDWYYSAIRQS	

700

		• •
2EL		-----DGRAQG-----
Delta-1		PSPPPPEEESRGP GHPPLPDKFQFELTLEEEEEEEI SMAQIPCTAQEALT
h6.1		PSPPPPEEESRGP GHPPLPDKFQFELTLEEEEEEEI SMAQIPCTAQEALT
HYB 1		PSPPPPEEESRGP GHPPLPDKFQFELTLEEEEEEEI SMAQIPCTAQEALT
HYB 2		-----DGRAQG-----
PDE46		PSPPPPEEESRGP GHPPLPDKFQFELTLEEEEEEEI SMAQIPCTAQEALT

750

		
2EL		-----	GFY
Delta-1		AQGLSGVEEALDATI AWEASPAQESLEVMAQEASLEAELEAVYLTQQAQ	
h6.1		EQGLSGVEEALDATI AWEASPAQESLEVMAQEASLEAELEAVYLTQQAQ	
HYB 1		EQGLSGVEEALDATI AWEASPAQESLEVMAQEASLEAELEAVYLTQQAQ	
HYB 2		-----	GFY
PDE46		AQGLSGVEEALDATI AWEASPAQESLEVMAQEASLEAELEAVYLTQQAQ	

800

	
Delta-1		STGSAPVAPDEFSSREEFV VAVSHSSPSALALQSPLLPAWRTL SVSEHA
h6.1		STGSAPVAPDEFSSREEFV VAVSHSSPSALALQSPLLPAWRTL SVSEHA
HYB 1		STGSAPVAPDEFSSREEFV VAVSHSSPSALALQSPLLPAWRTL SVSEHA
PDE46		STGSAPVAPDEFSSREEFV VAVSHSSPSALALQSPLLPAWRTL SVSEHA

850

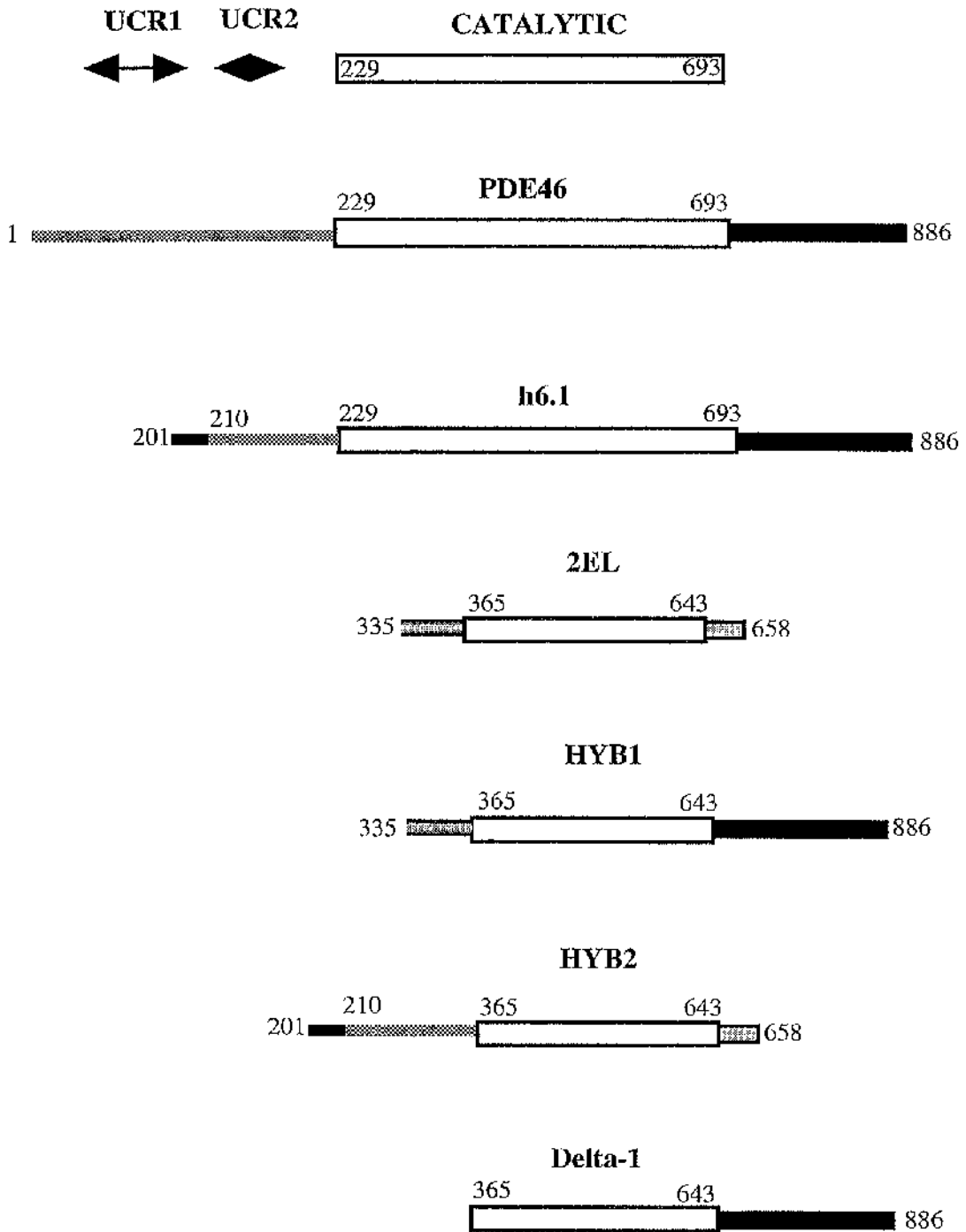
	
Delta-1		PGLPGLPSTAAEVEAQREHQAAKRAC SACAGTFGEDTSALPAPGGGGSG
h6.1		PGLPGLPSTAAEVEAQREHQAAKRAC SACAGTFGEDTSALPAPGGGGSG
HYB 1		PGLPGLPSTAAEVEAQREHQAAKRAC SACAGTFGEDTSALPAPGGGGSG
PDE46		PGLPGLPSTAAEVEAQREHQAAKRAC SACAGTFGEDTSALPAPGGGGSG

Delta-1	GDPT
h6.1	GDPT
HYB 1	GDPT
PDE46	GDPT

Figure 5.2. Schematic representation of human PDE4A forms, HYB1 and HYB2 chimeras and Delta-1 truncated forms

This figure diagrammatically shows the structural features of human PDE4A forms discussed in this study.

Figure 5.2. Schematic representation of human PDE4A forms, HYB1 and HYB2 chimeras and Delta-1 truncated forms



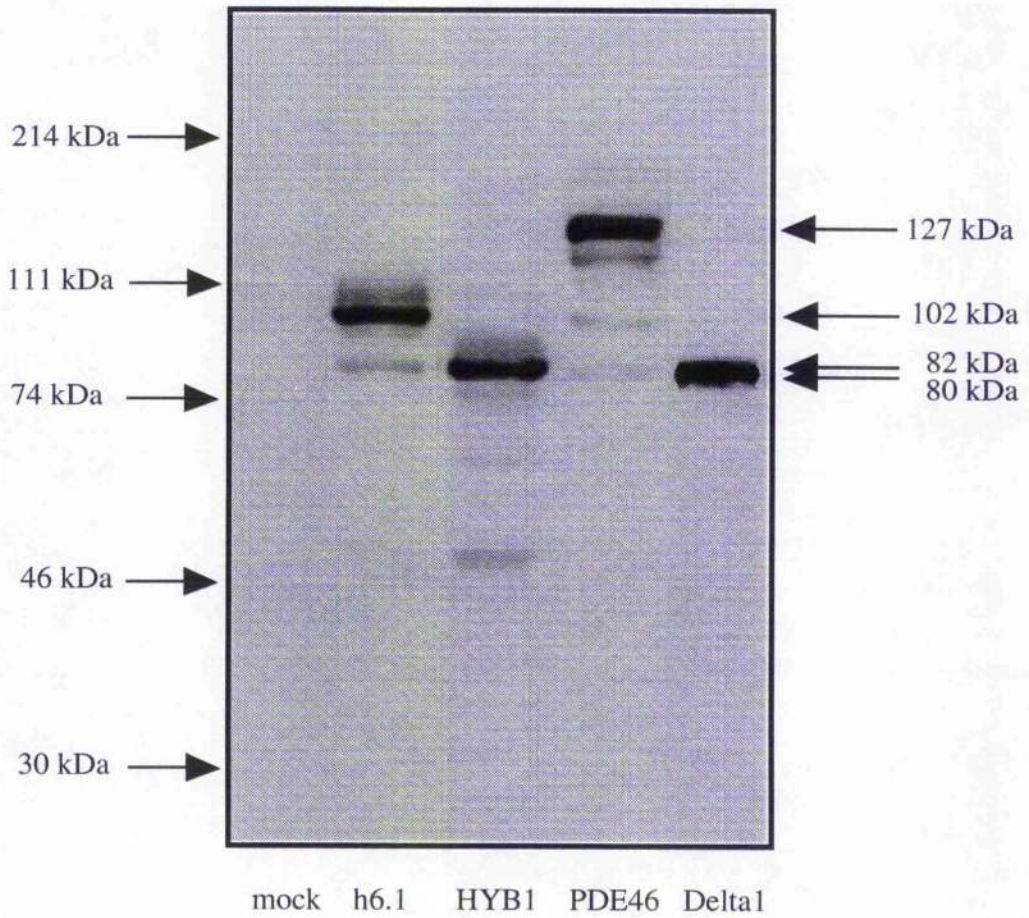


Figure 5.3. Immunoblot of HYB1 and Delta-1 expressed in COS7 cells

The plasmids encoding h6.1, HYB1, PDE46 and Delta-1 were transfected into COS7 cells and the cytosol (S) fractions were yielded by high-speed centrifugation (2.2.12.3). Samples were then subjected to SDS/PAGE followed by Western blotting using the C-terminus human PDE4A specific antiserum. Data is typical of experiments done three times using separate transfections.

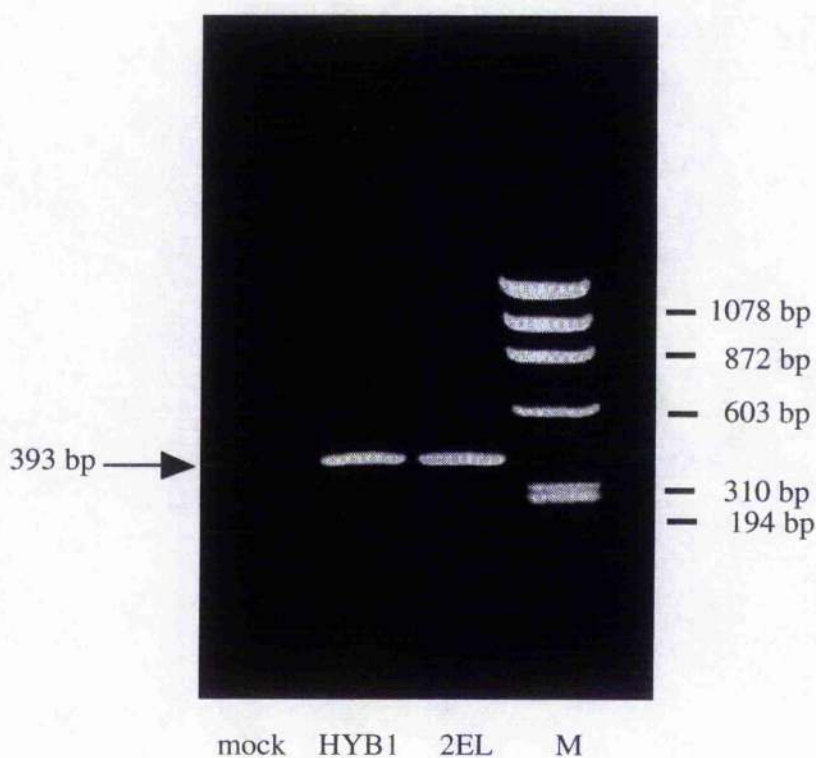


Figure 5.4. Transcriptional analysis of HYB1 chimera by RT-PCR

Total RNA was extracted from COS7 cells transfected with HYB1 and 2EL plasmids. RT-PCR was performed as described in sections 2.2.16-17. Primers were used to amplify a 393 bp fragment. These primers were: sense-2069 ATGGTGCTTCCTTCAGACCAAGG and antisense-Pharmacia CGGCGAGAA-TCTCCAGGTCC. PCR reaction employed 1 min at 95 °C, 70 s at 58 °C and 100 s at 72 °C for 35 cycles. The products were then electrophoresed on 1.5 % agarose gel and visualised with ethidium bromide under UV light. These results are representative of three experiments using RNA from different isolations.

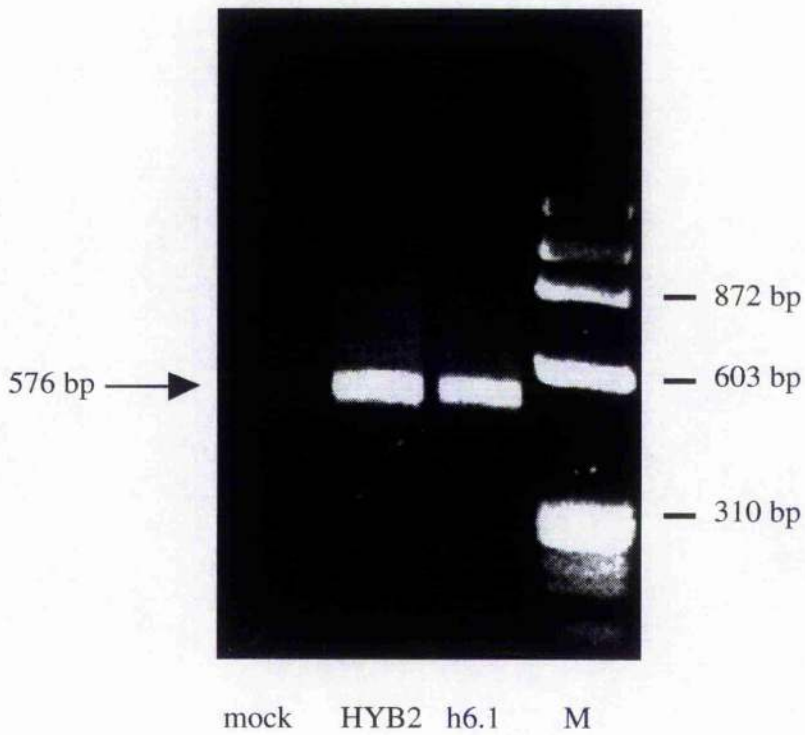


Figure 5.5. Transcriptional analysis of HYB2 chimera by RT-PCR

Total RNA was extracted from COS7 cells transfected with HYB2 and h6.1 plasmids. RT-PCR performed as described in sections 2.2.16-17. Primers were used to amplify a 576 bp fragment. These primers were: sense-2726 AAGGC CACGCTGTCA and antisense-2728 GATGCGGAATTTCTTCA. PCR reaction employed 1 min at 95 °C, 70 s at 57 °C and 100 s at 72 °C for 35 cycles. The products were then electrophoresed on 1.5 % agarose gel and visualised with ethidium bromide under UV light. These results are representative of three experiments using RNA from different isolations.

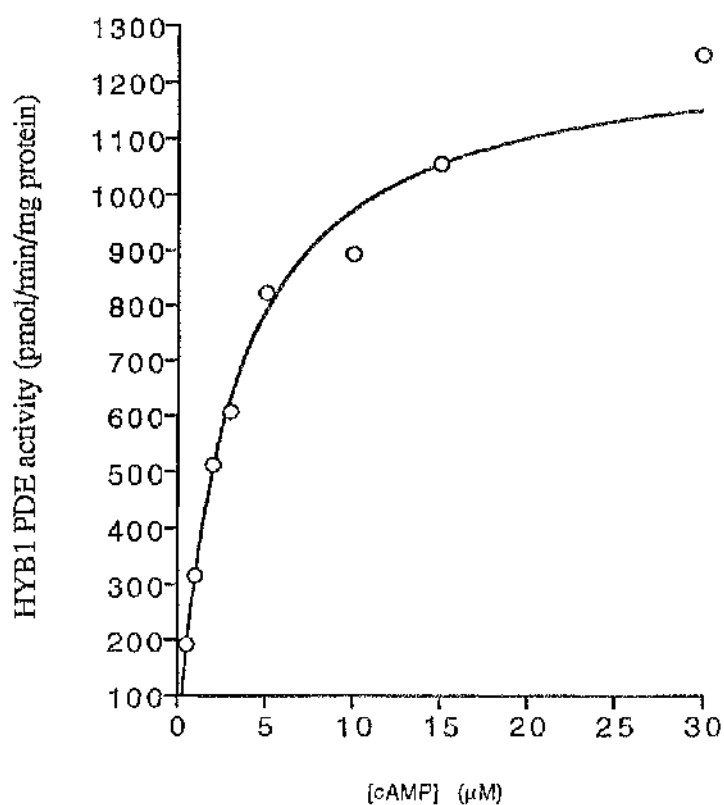


Figure 5.6. Determination of K_m for the cytosolic HYB1 fraction

Cytosolic HYB1 extracts were isolated from COS7 cells transfected with the HYB1 plasmid. K_m values were determined over a substrate range 0.5 to 30 μM cAMP. K_m values were calculated using the Ultrafit programme as described in section 2.2.6 and the data is shown in table 5.2. This experiment is representative of one carried out three times.

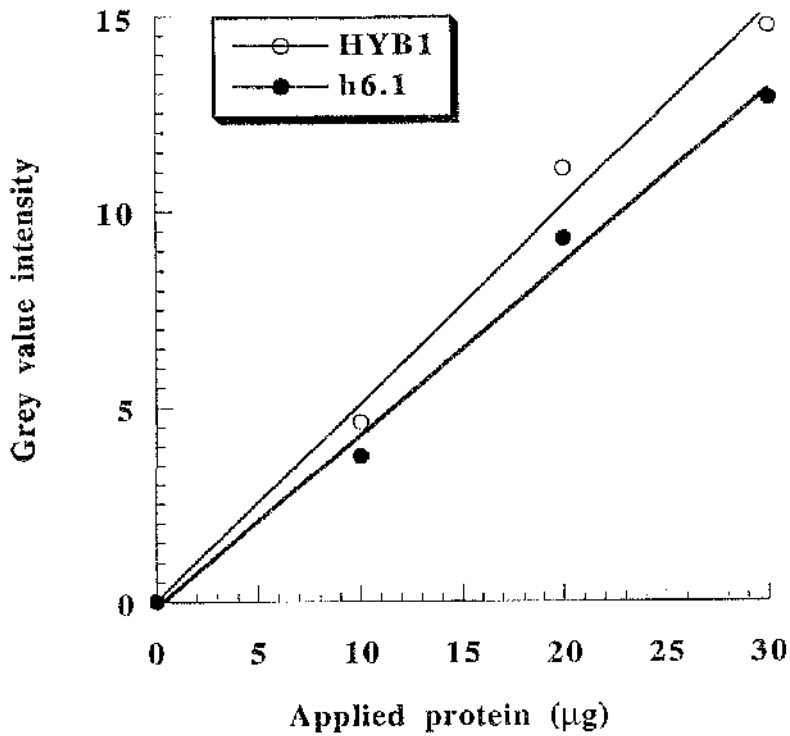


Figure 5.7. Linearity of detection of various concentrations of cytosolic h6.1 and HYB1

This data shows that using increasing concentrations of cytosolic protein (5 - 10 µg) from COS7 cells transfected with indicated cDNAs, a linear relationship between intensity and applied protein was observed. The proteins were immunoblotted with human PDE4A antibody and the blots were scanned. The intensity of the resultant signal is plotted for each plasmid. Such analyses were used to determine the relative amounts of indicated PDEs for the determination of relative V_{max} values in table 5.2.

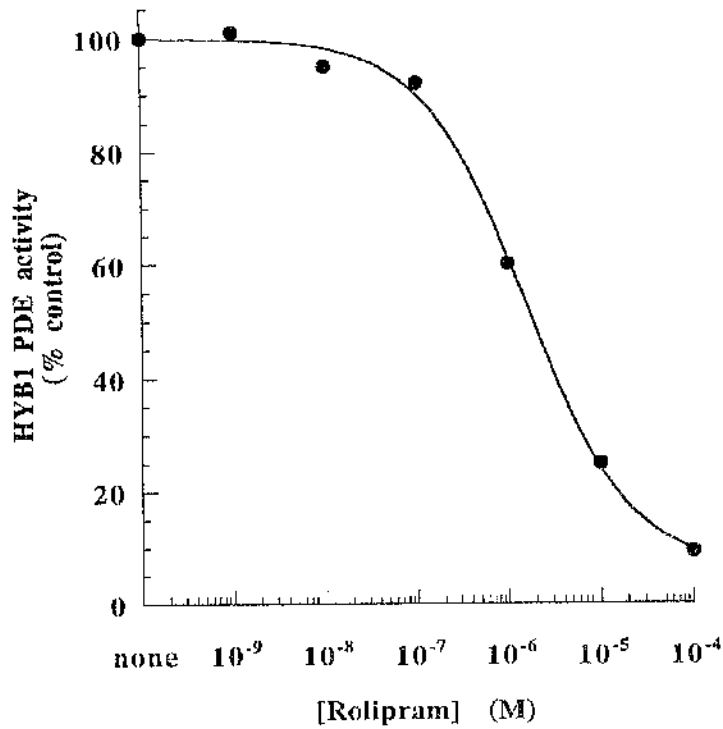


Figure 5.8. Dose-response curve for the inhibition of cytosolic HYB1 activity by rolipram

The activity of the soluble forms of HYB1 was determined in the presence of 3 μ M cAMP as substrate with the indicated concentrations of rolipram. 100 % activity is denoted as that observed in the absence of inhibitor. The data shown is typical of an experiment done three times in triplicate, each using separate transfections. Resultant IC_{50} values are given in table 5.2.

CHAPTER 6

FINAL DISCUSSION

6.1. FINAL DISCUSSION

Homeostasis of intracellular cAMP levels is critical to the regulation of many cellular responses to extracellular stimuli such as hormones and neurotransmitters. This is achieved through the regulation of both cAMP synthesis by adenylate cyclases and its degradation by cyclic nucleotide phosphodiesterases (PDEs). This system is also dependent upon protein kinase A which after activation subsequent to increase cAMP levels phosphorylates serine/threonine residues of target proteins either in the nucleus or in the cytoplasm. Thus the cAMP signalling system provides on part of the core machinery needed for the integration of signalling within the cell.

PDE isoform expression is tissue specific and can be differentially regulated by hormones. That individual PDE enzymes are regulated in both positive and negative manners has highlighted their pivotal role in mediating cross-talk between second messenger pathways. It has also provided a conceptual basis for understanding many of the distinctive, cell type-specific differences in the amplitude and duration of cAMP signals produced in response to stimulation of adenylate cyclase.

Increased cAMP has been associated with inhibition of the function of various types of cells including immune and inflammatory cells. The mechanisms by which cAMP modulates cell function are not completely understood. However, it appears to depend on the activation of PKA and subsequent phosphorylation of its target proteins which are expressed in a cell-specific fashion. A study in T-cells has been shown that activated PKA down-regulates c-Jun N-terminal kinase (JNK) activity (Hsueh & Lai, 1995, Tamir et al., 1996) which then blocks T-cell activation including IL-2 secretion (Su et al., 1994).

It has been demonstrated that PDE4 enzymes play a predominant role for cAMP hydrolysing activity in lymphocytes, monocytes, eosinophils, leukocytes, basophils and mast cells (Erdogan & Houslay, 1997, Manning et al., 1996, Teixeira et al., 1996, Torphy & Udem, 1991, Torphy et al., 1995). These cells have been implicated in various diseases such as arthritis, asthma and multiple sclerosis, for instance where elevated cAMP levels attenuate their functioning and thus inflammatory responses. Currently, therefore, members of the PDE4 family provide molecular targets for the design of novel therapeutic agents carried at treating these diseases.

In this study I have shown that the up-regulation of PDE4 activity can occur in response to either chronic stimulation of adenylate cyclase or a cAMP elevating agent. This led to the production of novel PDE4D transcripts and increased expression of specific PDE4D isoforms in Jurkat T-cells. In addition to this, the PDE3 activity was also increased in two distinct phases. Namely, rapid transient one followed by a delayed phase in response to cAMP elevating agents. The profound 'up-regulation' of both PDE3 and PDE4 activities were blocked by the transcriptional inhibitor factor actinomycin D, suggesting that RNA synthesis was necessary for the rise in these PDE activities. To define the roles of individual PDEs on the hydrolysis of cAMP, selective PDE inhibitors were added to Jurkat T-cells together with the adenylate cyclase activator, forskolin. The PDE4 selective inhibitor rolipram enhanced the forskolin-induced elevation of intracellular cAMP concentrations to levels which were similar to those seen with IBMX which is non-selective PDE inhibitor. This suggests that bulk cAMP levels are determined almost exclusively by PDE4 enzymes. Indeed, whilst PDE3 activity predominated in unstimulated Jurkat T-cells, the PDE3 selective inhibitor cilostimide was only weakly capable of enhancing forskolin stimulated cAMP accumulation. Indeed, a similar situation has been seen for thymocytes (Marcoz et

al., 1993b). Thus PDE4 activity appears to play a major role in controlling intracellular cAMP levels in Jurkat T-cells.

Using transcript analysis, immunoprecipitation and immunoblotting I demonstrated that unstimulated Jurkat T-cell PDE4 activity was solely due to a 118 kDa PDE4A isoform. The size of this species does not correlate with any known PDE4A form and RT-PCR analysis suggested that this was a novel long PDE4A form. Intriguingly, PDE4A activity appeared to decrease ~50 % after forskolin exposure. The down-regulation of PDE4A protein and mRNA levels in Jurkat T-cells contrasts with the effect of chronically elevated cAMP levels in monocytic cell lines (Manning et al., 1996, Torphy et al., 1995, Verghese et al., 1995) where increased PDE4A expression was seen. However, the PDE4A splice variant expressed in those cells appears to reflect the 125 kDa PDE46 species (Manning et al., 1996, Verghese et al., 1995). Similar to these results, Engels et al. (1994) have reported that elevated intracellular cAMP levels led to an increase in PDE4A species in another Jurkat T-cell line (JKE6-1). This may indicate differences between various Jurkat T-cell lines. However, in a similar fashion to the Jurkat T-cell studied here, elevation of cAMP levels down-regulated PDE4A mRNA and protein levels in rat hepatocyte P9 cells chronically exposed to forskolin (Zeng, L. & Houslay, MD., unpublished data). Thus cell-type-specific changes in PDE4 splice variants expression can occur in response to elevation of cAMP levels.

Neither PDE4B nor PDE4C transcripts were detected in either untreated or prolonged forskolin treated Jurkat T-cells. However, unlike Jurkat T-cells, long-term elevation of cAMP has been shown to increase PDE4B transcripts in human monocytes and a human monocytic cell line (U937) (Manning et al., 1996, Torphy et al., 1995) and rat Sertoli cells (Swinnen et al., 1991b). This suggests that the expression of various PDE4 splice variants may be very different and this may relate to their cell-specific functions.

It has been shown that challenge of various cells with either hormones or cAMP elevating agents induces the 'short' forms (PDE4D1 and PDE4D2) of the PDE4D enzyme family. Studies with follicle-stimulating (FSH), thyroid-stimulating hormones (TSH) and dibutyryl cAMP indicated that the 'short' forms, PDE4D1 and PDE4D2, were induced by the elevation of intracellular cAMP levels in rat Sertoli cells (Sette et al., 1994b, Swinnen et al., 1991b). Similar results have demonstrated using human monocytes and human monocytic cell lines (Mono Mac 6), namely that chronic elevation of intracellular cAMP levels cause the up-regulation of PDE4D1 and PDE4D2 (Verghese et al., 1995). In this study I showed that chronic exposure of Jurkat T-cells to the adenylate cyclase activator forskolin led to induction of the 'short' forms of PDE4D enzymes (Erdogan & Houslay, 1997). Whilst RT-PCR analysis implied a large increase in transcripts for PDE4D1 and PDE4D2, the induction of PDE4D protein expression appeared to be completely dominated by PDE4D1. None of the 'long' forms of PDE4D (PDE4D3, PDE4D4 and PDE4D5) enzymes were present in quiescent Jurkat T-cells, nor was their expression detectable after chronic exposure to forskolin.

The situation described above differs from that described by (Sette et al., 1994a) where PKA has been demonstrated to mediate the expression of 'short' forms of PDE4D1 and PDE4D2, whilst increasing activity of PDE4D3 by phosphorylation in response to TSH in FRTL-5 thyroid cells. TSH causes a transient elevation of intracellular cAMP levels and this led to rapid increase in PDE4D3 activity which can be seen within 3 min of TSH application and which returns to basal levels after 15 min. Unlike the 'short' forms the PDE4D3 isoform can be phosphorylated through the action of protein kinase A. This has also been shown for the recombinant enzyme expressed in MA-10 cells and insect Sf9 cells (Sette & Conti, 1996, Sette et al., 1994a, Sette et al., 1994b). The target phosphorylation site has been shown to be serine⁵⁴ residue, which is located in the UCR1 region of PDE4D3. This variety in the regulation of the various 'short' and 'long' PDE4D

forms suggests that splice variants from the same locus may have specific functional roles.

It appears currently that the *PDE4D* gene produces more isoforms than any other cAMP-specific PDE4s. Four cloned active human PDE4D isoforms, namely PDE4D1, 4D2, 4D3 and 4D4 (Bolger et al., 1993, Bolger et al., 1997, Nemoz et al., 1996) and three rat PDE4D isoforms (PDE4D1, 4D2 and 4D3) (Bolger et al., 1994, Jin et al., 1992, Sette et al., 1994b, Swinnen et al., 1989a) have been reported. In addition to human splice variants a novel PDE4D5 has recently been cloned from HeLa cells (Bolger et al., 1997). Although five members of the human PDE4D isoforms have been cloned, no study has been done to compare their characteristics.

The PDE4D1 species and PDE4D2 form which lack UCR1 are the so called 'short' PDE4D forms. These were first isolated from rat by (Swinnen et al., 1989a) who suggested that PDE4D1 was found in both cytosolic and low-speed particulate (P1) fraction of COS7 cell transfected cells. However, whilst <20 % of the PDE activity was found in P1 fraction it was unclear as to how much of this was due to either the presence of unbroken cells or to residual cytosol as the pellet fraction had not been subjected to any washing procedures. Five human PDE4D isoforms were characterised and expressed in COS7 cells in this study (chapter 4) (Bolger et al., 1997). Fractionation studies demonstrated that the two 'short' form activities were found exclusively in the cytosol (≥ 94 %) whereas, the three 'long' forms were found in the both cytosol and the pellet fractions. PDE4D3 and PDE4D5 were located ~ 35 % in the combined particulate fractions (P1 and P2) and this value rose to ~ 60 % for PDE4D4. Whilst the molecular basis of such differences has yet to be ascertained it is very clear that its basis must lie in the very different nature of the N-terminal alternatively spliced regions. Indeed, the 'short' rat PDE4A species RD1 was found exclusively associated with the membrane (P2)

fraction (Scotland & Houslay, 1995, Shakur et al., 1993). However, the mutant met²⁶-RD1, which was engineered by the deletion of unique N-terminus first 25 amino acids of RD1, proved to be a solely cytosolic PDE (Shakur et al., 1993). It is thus suggested that a membrane targeting domain is found within the extreme N-terminal domain of RD1.

Solubilisation of various PDE proteins from membrane/particulate fractions has indicated that attachment could also be effected in rather different ways. In contrast to the PDE4A forms (rPDE6, PDE39, PDE46) (Bolger et al., 1996, Huston et al., 1996, McPhee et al., 1995) and PDE4B form (PDE4B3) (Huston et al., 1997) which were not solubilised by detergent added together with high [NaCl], PDE4B1/2 (Huston et al., 1997), all three 'long' forms of PDE4D (in chapter 4) proteins were completely released by such a treatment. In contrast, detergent alone served only to partially release PDE4D3 and PDE4D5 and did not release PDE4D4 at all. High [NaCl] alone partially solubilised PDE4D5 but had little effect on PDE4D3 and PDE4D4. This suggests that the differences in the mode of anchorage of these PDE isoforms is likely to be attributable to distinct properties of their extreme N-terminal domains and distinct interacting species.

Selective PDE4 inhibitor rolipram caused dose-dependent inhibition of both cytosolic and particulate forms of the five PDE4D enzymes expressed in COS7 cells. These inhibitions were similar to other known human PDE4 isoforms (0.05-6 μ M) (McPhee et al., 1995, Huston et al., 1997, Owens et al., 1997). However, the IC₅₀ values of the particulate forms of PDE4D3 and PDE4D5 were 2- to 7-fold higher than those of their respective cytosolic forms. This suggest that the membrane-association of these enzymes can influence the sensitivity of components to inhibition by rolipram (Wilson et al., 1994, Bolger et al., 1996, McPhee et al., 1995).

The K_m values for cAMP utilisation of all PDE4D isoforms were in the range of 0.7 - 1.3 μ M. These values were similar to the other PDE4 enzymes, with values within the range of 1 - 5 μ M (Huston et al., 1997, Huston et al., 1996, McPhee et al., 1995, Wang et al., 1997). The V_{max} value of cytosolic PDE4D4 was 2-3-fold higher than that of the other four cytosolic enzymes indicating an isoform specific difference. Analysis of the particulate forms shown that the catalytic activity of PDE4D4 and PDE4D5 was ~3-fold higher than that of their respective cytosolic PDE forms. In contrast to this the cytosolic and particulate forms of PDE4D3 were very similar. Although all members of the PDE4D family share identical core catalytic domains, the properties of these enzymes were rather different. This provides evidence that the N-terminal regions of the PDE4D proteins can regulate their biochemical properties.

The human PDE4A splice variant 2EL was cloned from resting Jurkat T-cells (Horton et al., 1995). 2EL exhibits both a 5' domain swap together with an insertion toward the 3' end which results in a frameshift inducing premature truncation within the putative catalytic region of the enzyme. Transfection into the either COS1 or COS7 cells or *S. cerevisiae* demonstrated that 2EL exhibits no detectable catalytic PDE activity (Horton et al., 1995, Sullivan et al., 1997, Wilson, 1995). This species consists of a segment of 278 residues found within the catalytic core together with small and unique N- and C-terminal regions of 30 and 15 residues, respectively. The lack of activity of 2EL suggests that sequences outwith this central segment are essential to maintain functional integrity of the catalytic unit.

To investigate the functional role of N- and C-terminal regions the chimeras and truncated form were studied. Replacing the unique C-terminal domain (HYB1 chimera) reconstituted activity whilst replacing the N-terminal domain did not (HYB2 chimera) (Figure 5.2). The catalytically active HYB1 chimera showed

similar rolipram sensitivity, insensitivity to cGMP and Ca^{2+} / calmodulin and subcellular distribution with an active PDE4A form called h6.1. However, HYB1 exhibited a K_m value for cAMP which was about half of exhibited by h6.1, but was similar to that seen for a full length PDE4A species PDE46. The HYB1 chimera was enzymatically as active as PDE46 but was less active than h6.1. These variations may suggest that unique N-terminal 30 amino acid region of HYB1 can influence the functioning of catalytic unit. Indeed, in support of this, the truncation of the N-terminal region of 1 - 365 residues of the active PDE46 (Delta-1 mutant), which lacks the corresponding unique 30 amino acids region of 2EL, was catalytically inactive. This not only demonstrates that 2EL is catalytically inactive by virtue of C-terminal truncation alone but also suggests that, again, the unique 30 amino acid residues found in N-terminal region of 2EL can affect the structure (folding ?) (Houslay, 1996) of the catalytic unit and will in fact maintain its activity.

The physiological function of both inactive human PDE4A splice variants 2EL (Horton et al., 1995) and TM3 (Bolger et al., 1993) is not understood at present. One suggestion is that the mRNAs of these non-functional splice variants may control the level of mRNA for functional PDEs. Alternatively they may be expressed as proteins which form complexes with the functional species and serve to modulate their activity.

The control of cAMP PDEs appears to play as an important role in regulating the metabolism of cAMP as adenylate cyclase. In this regard it will be critical to determine which PDE isoforms are expressed and regulated by the immune and inflammatory cells as well as other cell systems concerning with different pathogenetic states. A consistent finding of many laboratories has been shown that inhibition of PDE4 enzymes causes suppression of inflammation. Thus, individual PDE4s are likely to be good targets for therapeutic intervention of

diseases which are related to changes in cAMP levels. However, despite development of many PDE4 inhibitors, they appear to have some side effects such as emesis. Sub-family specific therapeutic agents may avoid such an unwanted effect and provide a specific cure for diseases involving inflammation.

REFERENCES

REFERENCES

- Adestein, R. S., Conti, M. A., Hathaway, D. R., & Klee, C. B. (1978) *J. Biol. Chem.* 253, 8347-8350.
- Alava, M. A., Debell, K. E., Conti, A., Hoffman, T., & Bonvini, E. (1992) *Biochem. J.* 284, 189-199.
- Albert, F., Hua, C., Truneh, A., Pierres, M., & Schmitt-Verhulst, A.-M. (1985) *J. Immunology* 134, 3649-3655.
- Alexander, D. R., & Cantrell, D. A. (1989) *Immunol. Today* 10, 200-205.
- Alvarez, R., Sette, C., Yang, D., Eglen, R. M., Wilhelm, R., Shelton, E. R., & Conti, M. (1995) *Mol. Pharmacol.* 48, 616-622.
- Alvarez, R., Taylor, A., Fazzari, J. J., & Jacobs, J. R. (1981) *Mol. Pharmacol.* 20, 302-309.
- Anastassiou, E. D., Paliogianni, F., Balow, J. P., Yamada, H., & Boumpas, D. T. (1992) *J. Immunology* 148, 2845-2852.
- Anderson, N. G., Kilgour, E., & Houslay, M. D. (1989) *Biochem. J.* 262, 867-872.
- Ashman, D. F., Lipton, R. L., Melicow, M. M., & Price, T. D. (1963) *Biochem. Biophys. Res. Commun.* 11, 330-334.
- Asthan, M. J., Cook, D. C., Fenton, G., Karlsson, J. A., Palfreyman, M. N., Raeburn, D., Ratcliffe, A. J., Souness, J. E., Thurairatnam, S., & Vicker, N. (1994) *Journal of Medical Chemistry* 37, 1696-1703.
- Averill, L. E., Stein, R. L., & Kammer, G. M. (1988) *Cell. Immunol.* 115, 88-99.
- Baecker, P. A., Obernolte, R., Bach, C., Yee, C., & Shelton, E. A. (1994) *Gene* 138, 253-256.
- Baehr, W., Devlin, M. J., & Applebury, M. L. (1979) *J. Biol. Chem.* 254, 11669-11677.
- Barnes, P. J. (1991) *TIBS* 16, 365-369.
- Bastin, B., Payet, M. D., & Dupuis, G. (1990) *Cell. Immunol.* 128, 385-399.
- Beavo, J. A. (1988) in *Advances in second messenger and phosphoprotein research.* (Robison, P. G. and Greengard, P. Ed.) pp 1-38, Raven Press, New York & Chichester.
- Beavo, J. A. (1995) *Physiological Reviews* 75, 725-748.
- Beavo, J. A., Conti, M., & Heaslip, R. J. (1994) *Mol. Pharmacol.* 46, 399-405.
- Beavo, J. A., Hardman, J. G., & Sutherland, E. W. (1970) *J. Biol. Chem.* 245, 5649-5655.
- Beavo, J. A., Hardman, J. G., & Sutherland, E. W. (1971) *J. Biol. Chem.* 246, 3841-3846.

- Beavo, J. A., & Reifsnyder, D. H. (1990) *TIPS 11*, 150-155.
- Beebe, S. J., Redmon, J. B., Blackmore, P. F., & Corbin, J. D. (1985) *J. Biol. Chem.* 260, 2226-2233.
- Beltman, J., Sonnenberg, W. K., & Beavo, J. A. (1993) *Mol. Cell. Biol.* 127/128, 239-253.
- Bentley, J. K., Kadlecsek, A., Sherbert, C. H., Seger, D., Sonnenberg, W. K., Charbonneau, H., Novack, J. P., & Beavo, J. A. (1992) *J. Biol. Chem.* 267, 18676-18682.
- Bloom, T., & Beavo, J. A. (1994) *FASEB J.* 8, A372.
- Bolger, G. (1994) *Cellular Signalling* 6, 851-859.
- Bolger, G., Michaeli, T., Martins, T., John, T. S., Steiner, B., Lodgers, L., Riggs, M., Wigler, M., & Ferguson, K. (1993) *Molecular and Cellular Biology* 13, 6558-6571.
- Bolger, G. B., Erdogan, S., Jones, R. E., Loughney, K., Wilkinson, I., Farrel, C., & Houslay, M. D. (1997) *Biochem. J. in press.*
- Bolger, G. B., McPhee, I., & Houslay, M. D. (1996) *J. Biol. Chem.* 271, 1065-1071.
- Bolger, G. B., Rodgers, L., & Riggs, M. (1994) *Gene* 149, 237-244.
- Bourne, H. R., Lichtenstein, L. M., Melmon, K. L., Henney, C. S., Weinstein, Y., & Shearer, G. M. (1974) *Science* 184, 19-28.
- Bradford, M. M. (1976) *Analytical Biochemistry* 72, 248-254.
- Brown, B. L., Ekins, R. P., & Albano, J. D. M. (1972) *Advances in Cyclic Nucleotide Research* 2, 25-40.
- Burns, F., & Pyne, N. J. (1992) *Biochem. Biophys. Res. Commun.* 189, 1389-1396.
- Burns, F., Rodger, I. W., & Pyne, N. J. (1992) *Biochem. J.* 283, 487-491.
- Byers, D., Davis, R. L., & Kiger Jr, J. A. (1981) *Nature* 289, 79-81.
- Cali, J. J., Parekh, R. S., & Krupinski, J. (1996) *J. Biol. Chem.* 271, 1089-1095.
- Carr, D. W., Stofko-Hahn, R. E., Fraser, I. D. C., Bishop, S. M., Acott, T. S., Brennan, R. G., & Scott, J. D. (1991) *J. Biol. Chem.* 266, 14188-14192.
- Carr, D. W., DeManno, D. A., Atwood, A., Hunzicker-Dunn, M., & Scott, J. D. (1993) *J. Biol. Chem.* 268, 20729-20732.
- Carr, D. W., Hausken, Z. E., Fraser, I. D. C., Stofko-Hahn, R. E., & Scott, J. D. (1992) *J. Biol. Chem.* 267, 13376-13382.
- Casey, P. J., & Gilman, A. G. (1988) *J. Biol. Chem.* 263, 2577-2580.
- Chan, S. C., Reifsnyder, D., Beavo, J. A., & Hanifin, J. M. (1993) *J. Allergy and Clin. Immunol.* 91, 1179-1188.

- Charbonneau, H. (1990) in *Molecular Pharmacology of Cell Regulation* (Beavo, J. A., & Houslay, M. D., Eds.) pp 267-296, John Wiley & Sons Ltd, Chichester.
- Charbonneau, H., Beier, N., Walsh, K. A., & Beavo, J. A. (1986) *Proc. Natl. Acad. Sci. USA* 83, 9308-9312.
- Charbonneau, H., Kumar, S., Novack, J. P., Blumenthal, D. K., Griffin, P., Shabanowitz, J., D.F., H., Beavo, J. A., & Walsh, K. A. (1991) *Biochemistry* 30, 7931-7940.
- Charbonneau, H., Prusti, R. K., LeTrong, H., Sonnenburg, W. K., Stith-Coleman, I. E., Vaughan, M., Mullaney, P. J., Walsh, K. A., & Beavo, J. A. (1989) *Proc. Natl. Acad. Sci. USA* 87, 288-292.
- Chen, C.-N., Denome, S., & Davis, R. L. (1986) *Proc. Natl. Acad. Sci. USA* 83, 9313-9317.
- Chen, J., & Iyengar, R. (1993) *J. Biol. Chem* 268, 12253-12256.
- Cheung, W. Y. (1967) *Biochem. Biophys. Res. Commun.* 29, 478-482.
- Cheung, W. Y. (1971) *J. Biol. Chem.* 246, 2859-2869.
- Cheung, W. Y. (1978) *Adv. Cyclic Nucleotide Res.* 9, 233-251.
- Chomczynski, P., & Sacchi, N. (1987) *Anal. Biochem.* 162, 156-159.
- Chouaib, S., Robb, R. J., Welte, K., & Dupont, B. (1987) *J. Clin. Invest.* 80, 339-346.
- Clegg, C. H., Cadd, C. G., & McKnight, G. S. (1988) *Proc. Natl. Acad. Sci. U.S.A.* 85, 3703-3707.
- Coffey, R. G., Hadden, E. M., & Hadden, J. W. (1981) *J. Biol. Chem.* 256, 4418-4424.
- Coghlan, V. M., Jangeberg, L. K., Fernandez, A., Lamb, N. J. C., & Scott, J. D. (1994) *J. Biol. Chem.* 269, 7658-7665.
- Coghlan, V. M., Perrino, B. A., Howard, M., Langeberg, L. K., Hicks, J. B., Gallatin, W. M., & Scott, J. D. (1995) *Science* 267, 108-111.
- Colicelli, J., Birchmeier, C., Micheali, T., O'Neill, K., Riggs, M., & Wigler, M. (1989) *Proc. Natl. Acad. Sci. USA* 86, 3599-3603.
- Collins, S., Caron, M. G., & Lefkowitz, R. J. (1992) *Trends Biol. Sci.* 17, 37-39.
- Comb, M., Birnberg, N. C., Seasholtz, A., Herbert, E., & Goodman, H. M. (1986) *Nature* 323, 353-356.
- Conti, M., Iona, S., Cuoma, M., Swinnen, J. V., Odeh, J., & Svoboda, M. E. (1995a) *Biochemistry* 34, 7979-7987.
- Conti, M., Jin, S.-L. C., Monaco, L., Repaske, D. R., & Swinnen, J. V. (1991) *Endocrine. Rev.* 12, 218-234.
- Conti, M., Nemoz, G., Sette, C., & Vicini, E. (1995b) *Endocr. Rev.* 16, 370-389.

- Conti, M., & Swinnen, J. V. (1990) *Molecular Pharmacology of Cell Regulation* 2, 243-266.
- Conti, M., Swinnen, J. V., Tsikalas, K. E., & Jin, S.-L. C. (1992) in *Adv. in Second Mess. and Phosphoprotein Res.* (Strada, S. J., & Kidaka, H., Eds.) pp 87-99, Raven Press, New York.
- Cook, S. J., & McCormick, F. (1993) *Science* 262, 1069-1072.
- Cooke, M. P., Abraham, K. M., Forbush, K. A., & Perlmutter, R. M. (1991) *Cell* 65, 281-291.
- Coquil, J. F. (1983) *Biochim. Biophys. Acta* 743, 359-369.
- Dauwalder, B., & Davis, R. L. (1995) *Journal of Neuroscience* 15, 3490-3499.
- Davis, C. W., & Kuo, J. F. (1977) *J. Biol. Chem.* 252, 4078-4084.
- Davis, R., & Kauvar, L. (1984) *Adv. Cyclic Nucl. Protein Phos. Res.* 16, 393-402.
- Davis, R. L. (1990) *Molecular Genetics of the Cyclic Nucleotide Phosphodiesterases*, Vol. 2, John Wiley & Sons Ltd., Chichester.
- Davis, R. L., & Davidson, N. (1986) *Molecular and Cellular Biology* 6, 1464-1470.
- Davis, R. L., & Kiger, J. A. (1981) *J. Cell. Biol.* 90, 101-107.
- Davis, R. L., Takayasu, H., Eberwine, M., & Myres, J. (1989) *Proc. Natl. Acad. Sci. USA* 86, 3604-3608.
- de Groot, R. P., & Sassone-Corsi, P. (1992) *Oncogene* 7, 2281-2286.
- Degerman, E., Belfrage, P., & Manganiello, V. C. (1996) *Biochemical Society Transactions* 24, 1010-1014.
- Degerman, E., Belfrage, P., Newman, A. H., Rice, K. C., & Manganiello, V. C. (1987) *J. Biol. Chem.* 262, 5797-5807.
- Degerman, E., Moos, J. R., Rascon, A., Vasta, V., Meacci, E., Smith, E. J., Lindgren, S., Andersson, K. E., Belfrage, P., & Manganiello, V. C. (1994) *Biochem. Biophys. Acta* 1205, 189-198.
- Degerman, E., Smith, C. J., Tornqvist, H., Vasta, V., Belfrage, P., & Manganiello, V. C. (1990) *Proc. Natl. Acad. Sci. USA* 87, 533-537.
- Derubertis, F. R., Zenser, T. V., Adler, W. H., & Hudson, T. (1974) *The J. Immunology* 113, 151-161.
- DiSanto, M. E., & Heaslip, R. J. (1995) *European Journal of Pharmacology* 290, 169-172.
- Dohlman, H. G., Thorner, J., Caron, M. G., & Lefkowitz, R. J. (1991) *Annu. Rev. Biochem.* 60, 653-688.
- Dudai, Y. (1988) *Annu. Rev. Neurosci.* 11, 537-563.
- Engels, P., Fichtel, K., & Lubbert, H. (1994) *Febs Letters* 350, 291-295.

- Engels, P., Sullivan, M., Muller, T., & Lubbert, H. (1995) *Febs Letters* 358, 305-310.
- Epstein, P., Yang, Q., Paskind, M., Salfeld, J., Kamen, R., Bolger, G., Thompson, W. J., & Cutler, L. (1994) *FASEB J.* 8, A82.
- Epstein, P. M., & Hachisu, R. (1984) in *Advances in Cyclic Nucleotide and Protein Phosphorylation Research* (Thompson, S. J. S. a. W. J., Ed.) pp 303-323, Raven Press, New York.
- Erdogan, S., & Houslay, M. D. (1997) *Biochem. J.* 321, 165-175.
- Erneux, C., Moit, F., Van Haastert, P. J. M., & Jastorff, B. (1985) *J. Cyclic nucleotide Prot. Phosphor. Res.* 10, 463-470.
- Fauci, A. S., Schnittman, S. M., Poli, G., Koenig, S., & Pantaleo, G. (1991) *Ann. Intern. Med.* 114, 678-693.
- Faux, M. C., & Scott, J. D. (1996) *Cell* 85, 9-12.
- Feinstein, M. D., Rodan, G. A., & Cutler, L. S. (1981) in *Platelets in Biology and Pathology 2* (Gordon, J. L., Ed.) pp 437-472, North-Holland, Amsterdam.
- Francis, S. H., Colbran, J. L., McAllister-Lucas, M. L., & Corbin, J. D. (1994) *J. Biol. Chem.* 269, 77-80.
- Francis, S. H., & Corbin, J. D. (1988) *Methods Enzymol.* 159, 722-729.
- Francis, S. H., Noblett, B. D., Todd, B. W., Wells, J. N., & Corbin, J. D. (1988) *Molecular Pharmacology* 34, 506-517.
- Francis, S. H., Thomas, M. K., & Corbin, J. D. (1990) in *Molecular Pharmacology of Cell Regulation* (Beavo, J. A., & Houslay, M. D., Eds.) pp 117-140, John Wiley & Sons Ltd, Chichester.
- Gao, B., & Gilman, A. G. (1991) *Proc. Natl. Acad. Sci. USA* 88, 10178-10182.
- Gettys, T. W., Blackmore, P. F., Redman, J. E., Beebe, S. I., & Corbin, J. D. (1987) *J. Biol. Chem.* 262, 333-339.
- Giembycz, M. A. (1996) *TIPS* 17, 331-336.
- Giembycz, M. A., Corrigan, C. J., Seybold, J., Newton, R., & Barnes, P. J. (1996) *British Journal of Pharmacology* 118, 1945-1958.
- Gillespie, P. G. (1990) in *Molecular Pharmacology of Cell Regulation* (Beavo, J. A., & Houslay, M. D., Eds.) pp 163-184, John Wiley & Sons Ltd., Chichester.
- Gillespie, P. G., & Beavo, J. A. (1989) *Mol. Pharmacol.* 36, 773-781.
- Gilman, A. G. (1984) *Cell* 36, 577-579.
- Gilman, A. G. (1987) *Ann. Rev. Biochem* 56, 615-649.
- Glantz, S. B., Li, Y., & Rubin, C. S. (1993) *J. Biol. Chem.* 268, 12796-12804.
- Gonzalez, G. A., Menzel, P., Leonard, J., Fischer, W. H., & Montminy, M. R. (1991) *Mol. Cell. Biol.* 11, 1306-1312.

- Gonzalez, G. A., Yamamoto, K. K., Fischer, W. H., Karr, D., Menzel, P., Biggs III, W., Vale, W. W., & Montminy, M. R. (1989) *Nature (London)* 337, 749-752.
- Goodwin, J., & Ceuppens, J. (1983) *J. Clin. Immuno.* 129, 295.
- Grance, M., Picq, M., Prigent, A.-F., Lagarde, M., & Nemoz, G. (1997) *in press*.
- Grant, P. G., & Coleman, R. W. (1984) *Biochemistry* 23, 1801-1807.
- Greten, T. F., Eigler, A., Sinha, B., Moeller, J., & Endres, S. (1995) *International Journal of Immunopharmacology* 17, 605-610.
- Gunts, S. J., & Stropp, J. Q. (1988) *J. Appl. Physiol.* 64, 635-641.
- Hagawara, M., Alberts, A., Brindle, P., Meinkoth, J., Feramisco, J., Deng, T., Karin, M., Shenolikar, S., & Montminy, M. R. (1992) *Cell* 70, 105-113.
- Hait, W. N., & Weiss, B. (1977) *Biochimica et Biophysica Acta* 497, 86 - 100.
- Hamet, P., & Coquil, J. F. (1978) *J. Cyclic Nucleotide Res.* 4, 281-290.
- Harnett, M. M., Holman, M. J., & Klaus, G. G. B. (1991) *J. Immunol.* 147, 3831-3836.
- Harrison, S. A., Reifsnnyder, D. H., Gallis, B., Cadd, G. G., & Beavo, J. A. (1986) *Mol. Pharmacol.* 29, 506-514.
- Hashimoto, Y., Sharma, R. K., & Soderling, T. R. (1989) *J. Biol. Chem.* 264, 10884-10887.
- Hausken, Z. E., Coghlan, V. M., Schafer-Hastings, C. A., Reimann, E. M., & Scott, J. D. (1994) *J. Biol. Chem.* 269, 24245-24251.
- Heyworth, C. M., Wallace, A. V., & Houslay, M. D. (1983) *Biochem. J.* 214, 99-110.
- Hidaka, H., & Endo, T. (1984) *Adv. Cyclic Nucleotide Protein Phosphor. Res.* 16, 245-259.
- Hirata, F., Matsuda, K., Notsu, Y., Hattori, T., & Carmine, R. D. (1984) *Proc. Natl. Acad. Sci. USA* 81, 4717-4721.
- Hoeffler, J. P., Meyer, T. E., Yun, Y., Jameson, J. L., & Habener, J. F. (1988) *Science* 242, 1430-1433.
- Horton, Y. M., Sullivan, M., & Houslay, M. D. (1995) *Biochem. J.* 308, 683-691.
- Houslay, M. D. (1992) *Clinical Endocrinology* 36, 525-534.
- Houslay, M. D., & Kilgour, E. (1990) in *Molecular Pharmacology of Cell Regulation* (Beavo, J. A., & Houslay, M. D., Eds.) pp 185-226, John Wiley & Sons Ltd., Chichester.
- Houslay, M. D., & Milligan, G. (1997) *TIBS* 22, 217-224.
- Houslay, M. D., Scotland, G., Pooley, L., Spence, S., Wilkinson, I., McCallum, F., Julien, P., Rena, N. G., Michie, A. M., Erdogan, S., Zeng, L., Oconnell, J.

- C., Tobias, E. S., & Macphee, I. (1995) *Biochemical Society Transactions* 23, 393-398.
- Houslay, M. D. (1996) *Biochemical Society Transactions* 24, 980-986.
- Houslay, M. D., Sullivan, M., & Bolger, G. B. (1997) *manuscript submitted*.
- Houslay, M. D., Scotland, G., Erdogan, S., Huston, E., MacKenzie, S. J., McCallum, J. F., McPhee, I., Pooley, L., Rena, G., Ross, A., Beard, M., Peden, A., Begg, F., Wilkinson, I., Yarwood, S., Ackerman, C., Houslay, E. S., Hoffman, R., Engels, P., Sullivan, M., & Bolger, G. (1997) *Biochemical Society Transactions* 25, 374-381.
- Hsueh, Y.-P., & Lai, M.-Z. (1995) *J. Biol. Chem.* 270, 18094-18098.
- Hurwitz, R. L., Hirsch, K. M., Clark, D. J., Holcombe, V. N., & Hurwitz, M. Y. (1990) *J. Biol. Chem.* 265, 8901-8907.
- Huston, E., Lumb, S., Annette, R., Catterall, C., Ross, A. H., Steele, M. R., Bolger, G. B., Perry, M., Owens, R., & Houslay, M. D. (1997) *in press*.
- Huston, E., Pooley, L., Julien, P., Scotland, G., McPhee, I., Sullivan, M., Bolger, G., & Houslay, M. (1996) *J. Biol. Chem.* 271, 31334-31344.
- Ichimura, M., & Kase, H. (1993) *Biochem Biophys Res Commun* 193, 985-990.
- Ishikawa, Y., Katsushika, S., Chen, L., Halnon, N. J., Kawaba, J., & Homcy, C. J. (1992) *J. Biol. Chem.* 267, 13553-13557.
- Iwami, G., Kawabe, J.-i., Ebina, T., Cannon, P. J., Homcy, C. J., & Ishikawa, Y. (1995) *J. Biol. Chem.* 270, 12481-12484.
- Jacobitz, S., McLaughlin, M. M., Livi, G. P., Burman, M., & Torphy, T. J. (1996) *Molecular Pharmacology* 50, 891-899.
- Jacobowitz, O., Chen, J., Premont, R. T., & Ivengar, R. (1993) *J. Biol. Chem.* 268, 3829-3832.
- Jard, S., Roy, C., Barth, T., Rajerison, R., & Bockaert, J. (1975) *Adv. Cycl. Nucl. Res.* 5, 31-52.
- Jiang, X., Li, J., Paskind, M., & Epstein, P. M. (1996) *Proc. Natl. Acad. Sci.* 93, 11236-11241.
- Jin, S.-L., Swinnen, J. V., & Conti, M. (1992) *J. Biol. Chem.* 267, 18929-18939.
- Kakiuchi, S., & Yamazaki, R. (1970) *Biochem. Biophys. Res. Commun.* 41, 1104-1110.
- Kakiuchi, S., Yamazaki, R., & Nakajima, H. (1970) *Proc. Jpn. Acad.* 46, 587-592.
- Kammer, G. M. (1988) *Immunol Today* 9, 222-229.
- Kaneko, T., Alvarez, R., Ueki, I. F., & Nadel, J. A. (1995) *Cellular Signalling* 7, 527-534.

- Kasuya, J., Goko, H., & Yamaguchi, Y. F. (1995) *J. Biol. Chem.* 270, 14305-14312.
- Katada, T., Bokoch, G. M., Smigel, M. D., Ui, M., & Gilman, A. G. (1984) *J. Biol. Chem.* 259, 3589-3595.
- Kawabe, J., Iwami, G., Ebina, T., Ohno, S., Katao, T., Veda, Y., Homcy, C. J., & Ishikawa, Y. (1994) *J. Biol. Chem.* 269, 16554-16558.
- Kaye, J., & Ellenberger, D. L. (1992) *Cell* 71, 423-435.
- Kelley, L. L., Blackmore, P. F., Graber, S. E., & Steward, S. J. (1990) *J. Biol. Chem.* 256, 17657-17664.
- Kelly, J. J., Barnes, P. J., & Giembycz, M. A. (1996) *Biochem. J.* 318, 425-436.
- Kilgour, E., Anderson, N. G., & Houslay, M. D. (1989) *Biochem. J.* 260, 27-36.
- Kishihara, K., Penninger, J., Wallace, V. A., Kundig, T. M., Kawai, K., Wakeham, A., Timms, E., Pfeffer, K., Ohashi, P. S., Thomas, T. L., Furlonger, C., Paige, C. J., & Mak, T. W. (1993) *Cell* 74, 143-156.
- Klauck, T. M., Faux, M. C., Labudda, K., Langeberg, L. K., Jaken, S., & Scott, J. D. (1996) *Science* 270, 1210-1213.
- Klausner, R. D., O'Shea, J. J., Luong, H., Ross, P., Bluestone, J. A., & Samelson, L. E. (1987) *J. Biol. Chem.* 262, 12654-12659.
- Krause, D. S., & Deutsch, C. (1991) *J. Immunol.* 146, 2285-2294.
- Krause, W., Kuhne, G., & Sauerbrey, N. (1990) *Eur. J. Clin. Pharmacol.* 38, 71-75.
- Kvanta, A., Gerwins, P., Jondal, M., & Fredholm, B. B. (1990) *Cellular Signalling* 2, 461-470.
- Laemmli, U. K. (1970) *Nature* 227, 680-685.
- Lalli, E., & Sassone-Corsi, P. (1994) *J. Biol. Chem.* 269, 17359-17362.
- Laoide, B. M., Foulkes, N. S., Schlotter, F., & Sassone-Corsi, P. (1993) *EMBO J.* 12, 1179-1191.
- Lavan, B. E., Lakey, T., & Houslay, M. D. (1989) *Biochemical Pharmacology* 38, 4123-4136.
- Lee, C. Q., Yun, Y. D., Hoeffler, J. P., & Habener, J. F. (1990) *EMBO J.* 9, 4455-4465.
- Lenhard, J. M., Kassel, D. B., Rocque, W. J., Hamacher, L., Holmes, W. D., Patel, I., Hoffman, C., & Luther, M. (1996) *Biochem. J.* 316, 751-758.
- Lerner, A., Jacobson, B., & Miller, R. A. (1988) *J. Immunology* 140, 936-940.
- Levin, L. R., Han, P.-L., Hwang, P. M., Feinstein, P. G., Davis, R. L., & Reed, R. R. (1988) *Cell* 68, 479-489.
- Ling, D. S., Chan, M. A., & Gelfand, E. W. (1990) *J. Immunol.* 145, 449-455.

- Lipkin, V. M., Khrantsov, N. V., Vasilevskaya, I. A., Atabekova, N. V., Muradov, K. G., & Gubanov, V. V. (1990) *J. Biol. Chem.* 265, 12955-12959.
- Livi, G. P., Kmetz, P., Mchale, M. M., Cieslinski, L. B., Sathe, G. M., Taylor, D. P., Davis, R. L., Torphy, T. J., & Balcarek, J. M. (1990) *Mol. Cell. Biol.* 10, 2678-2686.
- Lobban, M., Shakur, Y., Beattie, J., & Houslay, M. D. (1994) *Biochem. J.* 304, 399-406.
- Loughney, K., Martins, T. J., Harris, E. A. S., Sadhu, K., Hicks, J. B., Sonnenburg, W. K., Beavo, J. A., & Ferguson, K. (1996) *J. Biol. Chem.* 271, 796-806.
- Luo, Z., Shafit-Zagardo, B., & Erlichman, J. (1990) *J. Biol. Chem.* 265, 21804-21810.
- Macphee, C. H., Reifsnnyder, D. H., Moore, T. A., Lerea, K. M., & Beavo, J. A. (1988) *J. Biol. Chem.* 263, 10353-10358.
- Manganiello, V. C., Murata, T., Taira, M., Belfrage, P., & Degerman, E. (1995a) *Archives of Biochemistry and Biophysics* 322, 1-13.
- Manganiello, V. C., Smith, C. J., Degerman, E., & Belfrage, P. (1990a) *Molecular Pharmacology of Cell Regulation* 2, 87-116.
- Manganiello, V. C., Taira, M., Degerman, E., & Belfrage, P. (1995b) *Cellular Signalling* 7, 445-455.
- Manganiello, V. C., Tanaka, T., & Murashima, S. (1990b) *Molecular Pharmacology of Cell Regulation* 2, 61-85.
- Manning, C. D., McLaughlin, M. M., Livi, G. P., Cieslinski, L. B., Torphy, T. J., & Barnette, M. S. (1996) *The Journal of Pharmacology and Experimental Therapeutics* 276, 810-818.
- Marchmont, R. J., Ayad, S. R., & Houslay, M. D. (1981) *Biochem. J.* 195, 645-652.
- Marchmont, R. J., & Houslay, M. D. (1980a) *Nature* 286, 904-906.
- Marchmont, R. J., & Houslay, M. D. (1980b) *Biochem. J.* 187, 381-392.
- Marcoz, P., Nemoz, G., Prigent, A. F., & Lagarde, M. (1993a) *Biochim. Biophys. Acta* 1176, 129-136.
- Marcoz, P., Prigent, A. F., Lagarde, M., & Nemoz, G. (1993b) *Mol. Pharmacol.* 44, 1027-1035.
- Martins, T. J., Mumby, M. C., & Beavo, J. A. (1982) *J. Biol. Chem.* 257, 1973-1979.
- Mary, D., Peyron, J.-F., Auberge, P., Aussel, C., & Fehlmann, M. (1989) *J. Biol. Chem.* 264, 14498-14502.
- Mayer, J. B., & Baltimore, D. (1993) *Trends Cell Biol.* 3, 8-13.

- McAllister, L. L. M., Sonenburg, W. K., Kadlcek, A., Seger, D., Trong, H. L., Colbran, J. L., Thomas, M. K., Walsh, K. A., Francis, S. H., Corbin, J. D., & Beavo, J. A. (1993) *J. Biol. Chem.* 268, 22863-22873.
- Mchala, M. M., Cieslinksi, L. B., Eng, W. K., Johnson, R. K., Torphy, T. J., & Livi, G. P. (1990) *Molecular Pharmacology* 39, 109-113.
- McLaughlin, M. M., Ciesliski, L. B., Burman, M., Torphy, T. J., & Livi, G. P. (1993) *J. Biol. Chem.* 268, 6470-6476.
- McPhee, I., Pooley, L., Lobban, M., Bolger, G., & Houslay, M. D. (1995) *Biochem. J.* 310, 965-974.
- Meacci, E., Taira, M., Moos, M. J., Smith, C. J., Movseian, M. A., Degerman, E., Belfrage, P., & Manganiello, V. C. (1992) *Proc. Natl. Acad. Sci. USA* 89, 3721-3725.
- Meinkoth, J. L., Ji, Y., Taylor, S. S., & Feramisco, J. R. (1990) *Proc. Natl. Acad. Sci. USA* 87, 9595-9599.
- Mery, P.-F., Pavione, C., Pecker, F., & Fischmeister, R. (1995) *Mol. Pharmacol.* 48, 121-130.
- Meyer, T. E., & Habener, J. F. (1993) *Endocr. Rev.* 14, 269-290.
- Michaeli, T., Bloom, T. J., Martins, T., Loughney, K., Ferguson, K., Riggs, M., Rodgers, L., Beavo, J. A., & Wigler, M. (1993) *J. Biol. Chem.* 268, 12925-12932.
- Michie, A. M. (1995), *Ph.D. Thesis*, University of Glasgow, Glasgow.
- Michie, A. M., Lobban, M., Muller, T., Harnett, M. M., & Houslay, M. D. (1996) *Cellular Signalling* 8, 97-110.
- Miki, N., Baraban, J. M., Keirns, J. J., Boyce, J. J., & Bitensky, M. W. (1975) *J. Biol. Chem.* 250, 6320-6327.
- Milatovich, A., Bolger, G., Michaeli, T., & Francke, U. (1994) *Somatic Cell and Molecular Genetics* 20, 75-86.
- Milligan, G. (1995) *Adn. Pharmacol.* 32, 1-29.
- Milligan, G., & Green, A. (1991) *TIPS* 12, 207-209.
- Monaco, L., Vicini, E., & Conti, M. (1994) *J. Biol. Chem.* 269, 347-357.
- Montminy, M. R., Sevarino, K. A., Wagner, J. A., Mandel, G., & Goodman, R. H. (1986) *Proc. Natl. Acad. Sci. USA* 83, 6682-6686.
- Moss, J., Manganiello, V., C., & Vaughan, M. (1977) *J. Biol. Chem.* 252, 5211-5215.
- Muir, J. G., & Murray, A. W. (1987) *J. Cell. Physiol.* 130, 382-391.
- Muller, T., Engels, P., & Fozard, J. R. (1996) *Trends in Pharmacological Sciences* 17, 294-298.
- Murad, F. (1973) *Adv. Cycl. Nucl. Res.* 3, 355.

- Murashima, S., Tanaka, T., Hockman, S., & Manganiello, V. (1990) *Biochemistry* 29, 5285-5292.
- Musacchio, A., Gibson, T., Lehto, V. P., & Saraste, M. (1992) *FEBS Letter* 307, 55-61.
- Nakashima, S., Mizutani, T., Nakamura, Y., Takemura, M., Miyata, H., Katagiri, Y., & Nozawa, Y. (1995) *Comparative Biochemistry and Physiology - Pharmacology Toxicology and Endocrinology* 112, 137-143.
- Neer, E. (1995) *Cell* 80, 249-257.
- Nel, A. E., & Daniels, J. (1988) *Biochem. J.* 256, 383-390.
- Nemoz, G., Zhang, R., Sette, C., & Conti, M. (1996) *FEBS Letter* 384, 97-102.
- Nicholson, C. D., Challis, R. A. C., & Shahid, M. (1991) *TIPS* 12, 19-27.
- Nielson, C. P. (1987) *J. Immunol.* 139, 2392-2397.
- Nielson, C. P., Vestal, R. E., Sturm, R. J., & Heaslip, R. (1990) *J. Allergy Clin. Immunol.* 86, 801-808.
- Nigg, E. A., Schafer, G., Hiltz, H., & Eppenberger, H. (1985) *Cell* 41, 1039-1051.
- Nighorn, A., Healy, M. J., & Davis, R. L. (1991) *Neuron* 6, 455-467.
- Nishimura, A., Morita, M., Nishimura, Y., & Sugino, Y. (1990) *Nucleic Acids Res.* 18, 6169.
- Novack, J. B., Charbonneau, H., Bently, J. K., Walsh, K. A., & Beavo, J. A. (1991) *Biochemistry* 30, 7940-7947.
- Novak, T. J., & Rothenberg, E. V. (1990) *Proc. Natl. Acad. Sci. U.S.A.* 87, 9353-9357.
- O'Connell, J. C., McCallum, J. F., McPhee, I., Wakefield, J., Houslay, E. S., Wishart, W., Bolger, G., Frame, M., & Houslay, M. D. (1996) *Biochem. J.* 318, 255-261.
- O'Shea, J. J., Urdahl, K. B., Luong, H. T., Chused, T. M., Samelson, L. E., & Klausner, R. D. (1987) *J. Immunol.* 139, 3463-3469.
- Oberholte, R., Ratzliff, J., Baecker, P. A., Daniels, D. V., Zuppan, P., Jarnagin, K., & Shelton, E. R. (1997) *Biochem. J.*, in press
- Omburo, G. A., Torphy, T. J., Scott, G., Susanne, J., Colman, R. F., & Colman, R. W. (1997) *Blood* 89, 1019-1026.
- Owens, R. J., Lumb, S., Rees-Milton, K., Russell, A., Baldock, D., Lang, V., Crabbe, T., Ballesteros, M., & Perry, M. (1997) in press.
- Oyen, O., Myklebust, F., Scott, J. D., Hansson, V., & Jahnsen, T. (1989) *FEBS Lett.* 246, 57-64.
- Palfreyman, M. N., & Souness, J. E. (1996) *Prog. Med. Chem.* 33, 1-52.
- Paliogianni, F., Kincaid, R. L., & Boumpas, D. T. (1993) *J. Exp. Med.* 178, 1813-1817.

- Pan, X., Arauz, E., Krzanowski, J. J., Fitzpatrick, D. F., & Polson, J. B. (1994) *Biochemical Pharmacology* 48, 827-835.
- Pawson, T., & Gish, G. D. (1992) *Cell* 71, 359-362.
- Payet, M. D., & Dupuis, G. (1992) *J. Biol. Chem.* 267, 18270-18273.
- Peachell, P. T., Udem, B. J., Schleimer, R. P., MacGlashan, D., Jr., Lichtenstein, L. M., Cieslinski, L. B., & Torphy, T. J. (1992) *Journal of Immunology* 148, 2503-2510.
- Phillips, R. J., Harnett, M. M., & Klaus, G. G. (1991) *Int. Immunol.* 3, 617-621.
- Pieroni, J. P., Jacobowitz, O., Chen, J., & Iyengar, R. (1993) *Current Opinion in Neurobiology* 3, 345-351.
- Pitt, G. S., Milona, M., Borleis, J., Lin, K. C., Reed, R. R., & Devreotes, P. N. (1992) *Cell* 69, 305-315.
- Pittler, S. J., Baehr, W., Wasmuth, J. J., McConnell, D. G., Champagne, M. S., VanTuinen, P., Ledbetter, D., & Davis, R. L. (1990) *Genomics* 6, 272-283.
- Podzuweit, T., Nennsteil, P., & Muller, A. (1995) *Cellular Signalling* 7, 733-738.
- Polli, J. W., & Kincaid, R. L. (1992) *Proc. Natl. Acad. Sci. USA* 89, 11079-11083.
- Polson, J. B., & Strada, S. J. (1996) *Annual Review of Pharmacology and Toxicology* 36, 403-427.
- Premont, R. T., Jacobowitz, O., & Iyengar, R. (1992) *Endocrinology* 131, 2774-2783.
- Pyne, N. J., Arshavsky, V., & Lochhead, A. (1996) *Biochemical Society Transactions* 24, 1019-1022.
- Pyne, N. J., Cooper, M. E., & Houslay, M. D. (1986) *Biochem. J.* 234, 325-334.
- Pyne, N. J., Cooper, M. E., & Houslay, M. D. (1987) *Biochem. J.* 242, 33-42.
- Pyne, N. J., Cushley, W., Nimmo, H. G., & Houslay, M. D. (1989) *Biochem. J.* 261, 897-901.
- Qiu, Y., & Davis, R. L. (1993) *Genes Devel.* 7, 1447-1458.
- Qui, Y. H., Chen, C. N., Malone, T., Richter, L., Beckendorf, S. K., & Davis, R. L. (1991) *J. Mol. Biol.* 222, 553-565.
- Rahn, T., Ridderstrale, M., Tornqvist, H., Manganiello, V., Fredrikson, G., Belfrage, P., & Degerman, E. (1994) *FEBS Letter* 350, 314-318.
- Rascon, A., Lindgren, S., Stavenow, L., Belfrage, P., Anderson, K. E., Manganiello, V. C., & Degerman, E. (1992) *Biochem. Biophys. Acta.* 1134, 149-156.

- Reeves, M. L., & England, P. J. (1990) in *Molecular Pharmacology of Cell Regulation* (Beavo, J. A., & Houslay, M. D., Eds.) pp 299-316, John Wiley & Sons Ltd., Chichester.
- Reinhardt, R. R., Chin, E., Zhou, J., Taira, M., Murata, T., & Manganiello, V. C. (1995) *The Journal of Clinical Investigation* 95, 1528-1538.
- Repaske, D. R., Corbin, J. G., Conti, M., & Goy, M. F. (1993) *Neuroscience* 56, 673-686.
- Repaske, D. R., Swinnen, J. V., Catherinejin, S. L., Vanwyk, J. J., & Conti, M. (1992) *J. Biol. Chem.* 267, 18683-18688.
- Rincon, M., Tugores, A., Lopez-Rivas, A., Silva, A., Alonso, M., Delandazuri, M. O., & Lopez-Botet, M. (1988) *Eur. J. Immunol.* 18, 1791-1796.
- Rochette-Egly, C., & Kempf, J. (1981) *J. Physiol. (Paris)* 77, 721-725.
- Rubin, C. S., Erlichman, J., & Rosen, O. R. (1972) *J. Biol. Chem.* 247, 6135-6139.
- Rutten, W. J., Shoot, B. M., & De Pont, J. J. H. H. M. (1973) *Biochim. Biophys. Acta* 315, 378-383.
- Rybalkin, S. D., & Beavo, J. A. (1996) *Biochemical Society Transactions* 24, 1005-1009.
- Salavatori, S., Damiani, E., Barhanin, J., Furlan, S., Giovanni, S., & Margreth, A. (1990) *Biochem J.* 267, 679-687.
- Savany, A., Abriat, C., Nemoz, G., Lgarde, M., & Prigent, A. F. (1996) *Cellular Signalling* 8, 511-516.
- Scheid, C. R., Honeyman, T. W., & Fay, F. S. (1979) *Nature (London)* 277, 32+36.
- Schmitz, W., Scholz, H., & Erdmann, E. (1987) *TIPS* 8, 447-450.
- Schneider, H. H., Schmiechen, R., Brezenski, M., & Seidler, J. (1986) *European Journal of Pharmacology* 127, 105-115.
- Schultz, J. E., Klumpp, S., Benz, R., Schurhoff-Goeters, W. S. J. C., & Schmid, A. (1992) *Science* 255, 600-603.
- Scotland, G., & Houslay, M. D. (1995) *Biochem. J.* 308, 673-681.
- Scott, A. I., Perini, A. F., Shering, P. A., & Whalley, L. J. (1991) *Eur. J. Clin. Pharmacol.* 40, 127-129.
- Scott, J. D. (1991) *Pharmacology and Therapeutics* 50, 123-145.
- Scott, J. D., & Carr, D. W. (1992) *NIPS* 7, 143-148.
- Seamon, K. B., Padgett, W., & Daly, J. W. (1981) *Proc. Natl. Acad. Sci. USA* 78, 3363-3367.
- Sekut, L., Yarnall, D., Stimpson, S. A., Noel, L. S., Batemanfite, R., Clarke, R. L., Brackeen, M. F., Menius, L. A., & Connolly, K. M. (1995) *Clin. Exp. Immunology* 100, 126-132.

- Sette, C., & Conti, M. (1996) *J. Biol. Chem.* 271, 16526-16534.
- Sette, C., Iona, S., & Conti, M. (1994a) *J. Biol. Chem.* 269, 9245-9252.
- Sette, C., Vincini, E., & Conti, M. (1994b) *J. Biol. Chem.* 269, 18271-18274.
- Shakur, Y., Pryde, J. G. M., & Houslay, M. D. (1993) *Biochem. J.* 292, 677-686.
- Shakur, Y., Wilson, M., Pooley, L., Lobban, M., Griffiths, S., Campbell, A. M., Beattie, J., Daly, C., & Houslay, M. D. (1995) *Biochem. J.* 306, 801-809.
- Sharma, R. K., Adachi, A. M., Adachi, K., & Wang, J. H. (1984) *J. Biol. Chem.* 259, 9248-9254.
- Sharma, R. K., & Kalra, J. (1994) *Biochem. J.* 299, 97-100.
- Sharma, R. K., & Wang, J. H. (1985) *Proc. Natl. Acad. Sci. USA* 82, 2603-2607.
- Sharma, R. K., & Wang, J. H. (1986) *J. Biol. Chem.* 261, 1322-1328.
- Smith, C. J., Krail, J., Manganiello, V. C., & Movsesian, M. (1993) *Biochem. Biophys. Res. Commun.* 190, 516-521.
- Smith, C. J., & Manganiello, V. C. (1989) *Mol. Pharmacol.* 35, 381-386.
- Smith, C. J., Vasta, V., Degerman, E., Belfrage, P., & Manganiello, V. C. (1991) *J. Biol. Chem.* 266, 13385-13390.
- Smith, K. J., Scotland, G., Beattie, J., Trayer, I. P., & Houslay, M. D. (1996) *J. Biological Chemistry* 271, 16703-16711.
- Snijdewint, F. G., Kalinski, P., Wierenga, E. A., Bos, J. D., & Kapsenberg, M. L. (1993) *J. Immunol.* 150, 5321-5329.
- Sommermeier, H., Schwinzer, R., Kaefer, V., Behl, B., & Resch, K. (1990) *Eur. J. Immunol.* 20, 1881-1886.
- Sonnenburg, W. K., Mullaney, P. J., & Beavo, J. A. (1991) *J. Biol. Chem.* 266, 17655-17661.
- Sonnenburg, W. K., Seger, D., & Beavo, J. A. (1993) *J. Biol. Chem.* 268, 645-652.
- Sonnenburg, W. K., Seger, D., Kwak, K. S., Huang, J., Charbonneau, H., & Beavo, J. A. (1995) *J. Biol. Chem.* 270, 30989-31000.
- Souness, J. E., Griffin, M., Maslen, C., Ebsworth, K., Scott, L. C., Pollock, K., Palfreyman, M. N., & Karlsson, J. A. (1996) *Br. J. Pharmacol.* 118, 649-658.
- Souness, J. E., Maslen, C., Griffin, M., Webber, S., Foster, F., Raeburn, D., Palfreyman, M. N., Ashton, M. J., & Karlsson, J. A. (1995) *Br. J. Pharmacol.* 115, 39-46.
- Souness, J. E., & Scott, L. C. (1993) *Biochem. J.* 291, 389-395.
- Souness, J. E., Villamil, M. E., Scott, L. S., Tomkinson, A., Giembycz, M. A., & Raeburn, D. (1994) *Br. J. Pharmacol.* 111, 1081-1088.

- Spence, S., Rena, G., Sullivan, M., Erdogan, S., & Houslay, M. D. (1997) *Biochem. J.* 321, 157-163.
- Spence, S., Rena, G., Sweeney, G., & Houslay, M. D. (1995) *Biochem. J.* 310, 975-982.
- Stralfors, P., Bjorgell, P., & Belfrage, P. (1984) *Proc. Natl. Acad. Sci. U.S.A.* 81, 3317-3321.
- Stroop, S. D., & Beavo, J. A. (1991) *J. Biol. Chem.* 266, 23802-23809.
- Stroop, S. D., & Beavo, J. A. (1992) *Adv. Second Messenger and Phosphoprotein Res.* 25, 55-71.
- Stroop, S. D., Charbonneau, H., & Beavo, J. A. (1989) *J. Biol. Chem.* 264, 13718-13725.
- Stryer, L. (1986) *Annu. Rev. Neurosci.* 9, 87-119.
- Su, B., Jacinto, E., Hibi, M., Kallunki, T., Karin, M., & Ben-Neriah, Y. (1994) *Cell* 77, 727-736.
- Sullivan, M., Egerton, M., Shakur, Y., Marquardsen, A., & Houslay, M. D. (1994) *Cellular Signalling* 6, 793-812.
- Sullivan, M., Erdogan, S., Wilson, M., & Houslay, M. D. (1997) *Biochem. J.* in press.
- Sunahara, R. K., Dessauer, C. W., & Gilman, A. G. (1996) *Annu. Rev. Pharmacol. Toxicol.* 36, 461-480.
- Sutherland, E. W., Robinson, G. A., & Butcher, R. W. (1968) *Circulation* 37, 279-306.
- Swinnen, J. V., D'Souza, B., Conti, M., & Ascoli, M. (1991a) *J. Biol. Chem.* 266, 14383-14389.
- Swinnen, J. V., Joseph, D. R., & Conti, M. (1989a) *Proc. Natl. Sci. Acad. USA* 86, 5325-5329.
- Swinnen, J. V., Joseph, D. R., & Conti, M. (1989b) *Proc. Natl. Acad. Sci. USA* 86, 8197-8201.
- Swinnen, J. V., Tsikalas, K. E., & Conti, M. (1991b) *J. Biol. Chem.* 266, 18370-18377.
- Szpirer, C., Szpirer, J., Riviere, M., Swinnen, J., Vicini, E., & Conti, M. (1995) *Cytogenet Cell Genet* 69, 11-14.
- Taira, M., Hockman, S. C., Calvo, J. C., Belfrage, P., & Manganiello, V. C. (1993) *J. Biol. Chem.* 268, 18573-18579.
- Takayama, H., Trenn, G., & Sitkovsky, M. V. (1988) *J. Biol. Chem.* 263, 2330-2336.
- Tamir, A., Granot, Y., & Isakov, N. (1996) *J. Immunol.* 157, 1514-1522.
- Tang, W.-J., & Gilman, A. G. (1991) *Science* 254, 1500-1503.
- Tang, W.-J., & Gilman, A. G. (1992) *Cell* 70, 869-872.

- Taussig, R., & Gilman, A. G. (1995) *J. Biol. Chem* 270, 1-4.
- Taylor, M. V., Metcalf, J. C., Hesketh, T. R., Smith, G. A., & Moore, J. P. (1984) *Nature* 312, 462-464.
- Taylor, S. S., Buechler, J. A., & Yonemoto, W. (1990) *Ann. Rev. Biochem.* 59, 971-1005.
- Teixeira, M. M., Rossi, A. G., Giembycz, M. A., & Hellewell, P. G. (1996) *British Journal of Pharmacology* 118, 2099-2106.
- Tenor, H., Staniciu, L., Schudt, C., Hatzelmann, A., Wendel, A., Djukanovic, R., Church, M. K., & Shute, J. K. (1995) *Clinical and Experimental Allergy* 25, 616-624.
- Teo, T. S., Wang, T. H., & Wang, J. H. (1973) *J. Biol. Chem.* 248, 588-595.
- Thomas, M. K., Francis, S. H., & Corbin, J. D. (1990) *J. Biol. Chem.* 265, 14971-14978.
- Thompson, W. J. (1991) *Pharmacol. Ther.* 51, 13-33.
- Thompson, W. J., & Appleman, M. M. (1971) *Biochemistry* 10, 311-316.
- Thompson, W. J., Ross, C. P., Pledger, W. J., Strada, S. J., Banner, R. L., & Hersh, E. M. (1976) *J. Biol. Chem.* 251, 4922-4929.
- Thompson, W. J., Terasaki, W. L., Epstein, P. M., & Strada, S. J. (1979) in *Advances in Cyclic Nucleotide Research* (G. Brooker, P. G., G.A. Robison, Ed.) pp 69-92, Raven Press, New York.
- Torphy, T. J., & Cieslinski, L. B. (1989) *Mol. Pharmacol.* 37, 206-214.
- Torphy, T. J., Stadel, J. M., Burman, M., Cieslinski, L. B., McLaughlin, M. M., White, J. R., & Livi, G. P. (1992) *J. Biol. Chem.* 267, 1798-1804.
- Torphy, T. J., & Udem, B. J. (1991) *Thorax* 46, 512-523.
- Torphy, T. J., Zhou, H.-L., Foley, J. J., Sarau, H. M., Manning, C. D., & Barnette, M. S. (1995) *J. Biol. Chem.* 270, 23598-23604.
- Tracey, K. J., & Cerami, A. (1993) *Ann. Rev. Cell. Biol.* 9, 317-343.
- Tsuboi, S., Matsumoto, H., & Yamazaki, E. (1994) *J. Biol. Chem.* 269, 15016-15023.
- Tulley, T., & Quinn, W. (1986) *Mol. Cell. Biol.* 6, 1464-1470.
- Udovichenko, I. P., Cunnick, J., Gonzales, K., & Takemoto, D. J. (1993) *Biochem. J.* 295, 49-55.
- Udovichenko, I. P., Cunnick, J., Gonzales, K., & Takemoto, D. J. (1994) *J. Biol. Chem.* 269, 9850-9856.
- Underwood, D. C., Osborn, R. R., Novak, L. B., Matthews, J. K., Newsholme, J. J., Udem, B. J., & Hand, J. M. (1993) *J. Pharmacol. Exp. Ther.* 266, 306-313.
- Vercammen, C., & Ceuppens, J. L. (1987) *Cell. Immunol.* 104, 24-36.

- Verghese, M. W., McConnel, R. T., Lenhard, J. M., Hamarcher, L., & Jin, S.-L. (1995) *Molecular Pharmacology* 47, 1164-1171.
- Wacholtz, M. C., Minakuchi, R., & Lipsky, P. E. (1991) *Cell. Immunol.* 135, 285-298.
- Wachtel, H. (1983) *Neuropharmacology* 22, 267-272.
- Wada, H., Osborne, J. C., & Manganiello, V. C. (1987) *J. Biol. Chem.* 262, 5139-5144.
- Wang, J. H., Sharma, R. K., & Mooibroek, M. J. (1990) in *Molecular Pharmacology of Cell Regulation* (Beavo, J. A., & Houslay, M. D., Eds.) pp 19-59, John Wiley & Sons Ltd., Chichester.
- Wang, P., Myers, J. G., Wu, P., Cheewatrakoolpong, B., Egan, R. W., & Billah, M. M. (1997) *Biochem. Biophys. Res. Commun.* 234, 320-324.
- Wang, T., Sheppard, J. R., & Foker, J. E. (1978) *Science* 201, 155-157.
- Weiss, A., Imboden, J. B., Hardy, K., Manger, B., Terhorst, C., & Stobo, J. D. (1986) *Ann. Rev. Immunol.* 4, 593-598.
- Weng, Z., Taylor, J. A., Turner, C. E., Brugge, J. S., & Seidel-Dugan, C. (1993) *J. Biol. Chem.* 268, 14956-14963.
- Wetzel, B., & Hael, N. (1988) *TIPS* 9, 166-170.
- Whalin, M. E., Strada, S. J., & Thompson, W. J. (1988) *Biochim. Biophys. Acta* 972, 79-94.
- Whitehurst, C. E., Owaki, H., Bruder, J. T., Rapp, U. R., & Geppert, T. D. (1995) *J. Biol. Chem.* 270, 5594-5599.
- Wilson, M. A. (1995), *Ph.D. Thesis*, University of Glasgow, Glasgow.
- Wilson, M., Sullivan, M., Brown, N., & Houslay, M. D. (1994) *Biochem. J.* 304, 407-415.
- Woods, M., & Houslay, M. D. (1991) *Biochem. Pharmacol.* 41, 385-394.
- Wu, J., Dent, P., Jelinek, T., Wolfman, A., Weber, M. J., & Sturgill, T. W. (1993) *Science* 262, 1065-1069.
- Yamamoto, K. K., Gonzales, G. A., Briggs, W. H., & Montminy, M. R. (1988) *Nature* 334, 494-498.
- Yamamoto, K. K., Gonzales, G. A., Menzel, P., Rivier, J., & Montminy, M. R. (1990) *Cell* 60, 611-617.
- Yamamoto, T., Manganiello, V. C., & Vaughan, M. (1983a) *J. Biol. Chem.* 258, 12526-12533.
- Yamamoto, T., Tamamoto, S., Osborne, J. C., Manganiello, V. C., & Vaughan, M. (1983b) *J. Biol. Chem.* 258, 14173-14177.
- Yan, C., Zhao, A. Z., Bentley, J. K., Loughney, K., Ferguson, K., & Beavo, J. A. (1995) *Proc. Nat. Acad. Sci. U.S.A.* 92, 9677-9681.

- Yan, C., Zhao, A. Z., Bently, J. K., & Beavo, J. A. (1996) *J. Biol. Chem.* 271, 25699-25706.
- Yang, Q., Paskin, M., Salfeld, J., Bolger, G., Thompson, W. J., Repaske, D. R., Cutler, L. S., & Epstein, P. (1994) *Biochem. Biophys. Res. Commun.* 205, 1850-1858.
- Yoshimura, M., & Cooper, D. M. F. (1992) *Proc. Natl. Acad. Sci. USA* 89, 6716-6720.
- Zhang, G. Y., Wang, J. H., & Sharma, R. K. (1993) *Mol. Cell. Biochem.* 122, 159-169.

PUBLICATIONS

(a) Research Papers

- 1- Erdogan, S., & Houslay, M. D. (1997). Challenge of human Jurkat T-cells with the adenylate cyclase activator forskolin elicits major changes in cAMP phosphodiesterase (PDE) expression by up-regulating PDE3 and inducing PDE4D1 and PDE4D2 splice variants as well as down-regulating a novel PDE4A splice variant. *Biochem. J.* 321, 165-175.
- 2- Spence, S., Rena, G., Sullivan, M., Erdogan, S., & Houslay, M. D. (1997). Receptor-mediated stimulation of lipid signalling pathways in CHO cells elicits the rapid transient induction of the PDE1B isoform of Ca²⁺/calmodulin-stimulated cyclic AMP phosphodiesterase. *Biochem. J.* 321, 157-163.
- 3- Bolger, G. B., Erdogan, S., Jones, R. E., Loughney, K., Wilkinson, I., Farrel, C., & Houslay, M. D. (1997). Characterisation of 5 different proteins produced by alternatively spliced mRNAs from the human cAMP-specific phosphodiesterase PDE4D gene. *Biochem. J.* in press.
- 4- Sullivan, M., Erdogan, S., Wilson, M., & Houslay, M. D. (1997). Generation of an active chimeric cyclic AMP phosphodiesterase, HYB1 by replacement of the C-terminal domain of the inactive human PDE4A splice variant 2EL (HSPDE4A7). *Biochem. J.* in press.

(b) Review Papers

- a. Houslay, M. D., Scotland, G., Erdogan, S., Huston, E., MacKenzie, S. J., McCallum, J. F., McPhee, I., Pooley, L., Rena, G., Ross, A., Beard, M., Peden, A., Begg, F., Wilkinson, I., Yarwood, S., Ackerman, C., Houslay, E. S., Hoffman, R., Engels, P., Sullivan, M., & Bolger, G. (1997). Intracellular targeting, interaction with Src homology 3 (SH3) domains and rolipram-detected conformational switches in cyclic AMP-specific PDE4A phosphodiesterase. *Biochemical Society Transactions* 25, 374-381.
- b. Houslay, M. D., Scotland, G., Pooley, L., Spence, S., Wilkinson, I., McCallum, F., Julien, P., Rena, N. G., Michie, A. M., Erdogan, S., Zeng, L., Oconnell, J. C., Tobias, E. S., & Macphee, I. (1995). Alternative splicing of the type-IVA cyclic-AMP phosphodiesterase gene provides isoform variants with distinct N-terminal domains fused to a common, soluble catalytic unit-designer changes in V_{max} , stability and membrane association. *Biochemical Society Transactions* 23, 393-398.